2014 年度　　博 士 論 文

Keggin 型および Dawson 型ポリ酸塩の チタン(IV)置換単量体の合成と展開

Synthesis and Development of Monomeric, Titanium(IV)-Substituted Keggin and Dawson-type Polyoxometalates

神奈川大学大学院　理学研究科　化学専攻

201270201 番　松木 悠介

指導教授　野宮 健司

2015 年 1 月 16 日 提出

Abstract

Keggin 型および Dawson 型ポリ酸塩のチタン(IV)置換単量体の合成と展開

Keggin 型ポリ酸塩$[\alpha\text{-}PW_{12}O_{40}]^{3-}$および Dawson 型ポリ酸塩$[\alpha\text{-}P_2W_{18}O_{62}]^{6-}$はその欠損種($[\alpha\text{-}PW_{11}O_{39}]^{7-}$, $[\alpha\text{-}P_2W_{15}O_{56}]^{12-}$ etc)と異種金属 M を反応させることで、位置選択的に異種金属で置換したポリ酸塩($[\alpha\text{-}PW_{11}MO_{40}]^{n-}$, $[\alpha\text{-}P_2W_{15}M_3O_{62}]^{n-}$ etc)の合成が可能である。これらの異種金属置換型ポリ酸塩は無置換型ポリ酸塩には見られない構造を形成する点や特異な触媒活性を発現する点で興味が持たれている。

特に Ti^{IV} はイオン半径が 0.75 Å であり W^{VI} のイオン半径(0.74 Å)に近く、チタン(IV)置換ポリ酸塩は容易に形成される。また、Keggin 型や Dawson 型のポリ酸塩は MO_6 八面体が稜共有と頂点共有を繰り返してできた構造であるため、その骨格金属 M (M = W^{VI} etc)を Ti^{IV} に置換すれば、ポリ酸塩が Rutile 型や Perovskite 型のフラグメントを持つことになり、光酸化触媒などの触媒としての利用が期待できる。

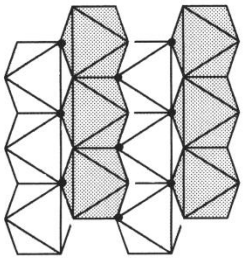
Rutile-type TiO_2

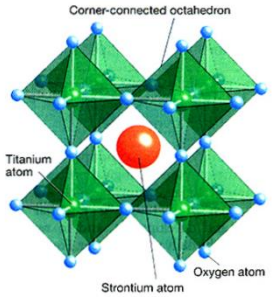

Perovskite-type $SrTiO_3$

チタン(IV)一置換 Keggin 型ポリ酸塩は O. A. Kholdeeva らによって合成され、単量体と二量体種の平衡が報告されている。[1-3] しかし、二量体種(μ-OH で Keggin unit が連結された二量体$[(\alpha\text{-}PW_{11}TiO_{39})_2OH]^{7-}$および μ-O で Keggin unit が連結された二量体$[(\alpha\text{-}PW_{11}TiO_{39})_2O]^{8-}$)の X 線構造解析は行われていない。これはおそらく一度粉体として単離した二量体からは結晶化せず、粉体が析出するためと思われる。第一章ではこのチタン(IV)一置換 Keggin 型ポリ酸塩二量体が単量体から二量体を誘導する過程で結晶化することを明らかにし、二量体の Keggin unit 間の連結様式が μ-OH ではなくて、μ-O であることを確認した。

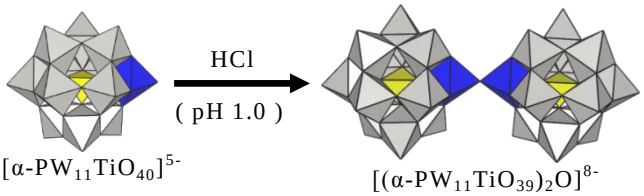

$[\alpha\text{-}PW_{11}TiO_{40}]^{5-}$ $[(\alpha\text{-}PW_{11}TiO_{39})_2O]^{8-}$

チタン(IV)三置換 Dawson 型ポリ酸塩については当研究室の Y. Sakai らによって詳細な研究が行われている。[4a-c] Dawson 型ポリ酸塩三欠損種と Ti^{IV} の反応から直接チタン(IV)三置換単量体は得られないが、二種類のテトラポッド型チタン(IV)三置換 Dawson 型ポリ酸塩四量体(架橋あり、架橋なし)が合成、構造解析されている。架橋あり四量体は Dawson unit が架橋チタンを介して縮合した四量体$[\{\alpha\text{-}P_2W_{15}Ti_3O_{59}(OH)_3\}_4\{\mu_3\text{-}Ti(OH_2)_3\}_4X]^{21-}$ (X = Cl, Br, I, NO_3)であり、一方架橋なし四量体は Dawson unit が直接縮合した四量体$[\{\alpha\text{-}P_2W_{15}Ti_3O_{57.5}(OH)_3\}_4Cl]^{25-}$であり、これらの四量体はいずれも中心空間にアニオンをカプセル化していた。また、架橋あり四量体と H_2O_2 との反応からペルオキソ配位チタン(IV)三置換 Dawson 型ポリ酸塩単量体$[\alpha\text{-}P_2W_{15}(TiO_2)_3O_{56}(OH)_3]^{9-}$が得られている。[5] このペルオ

キソ配位単量体は熱によりペルオキソ基が容易に分解し、それをビルディングブロックとしてNH_4^+カチオンがカプセル化された架橋なし四量体$[(\alpha\text{-}P_2W_{15}Ti_3O_{60.5})_4(NH_4)]^{35-}$が合成され、構造が決定されている。[6]このカチオンカプセル化架橋なし四量体はアニオンカプセル化架橋なし四量体の中心空間の 12 個の Ti-OH-Ti 結合のH^+を塩基で脱プロトン化することでも誘導できる。さらに最近になって架橋あり四量体と塩基の反応から、チタン(IV)三置換 Dawson 型ポリ酸塩単量体"$[P_2W_{15}Ti_3O_{62}]^{12-}$"が得られることが見出された。[6] このチタン(IV)三置換単量体は三欠損種とチタンの直接反応および架橋なし四量体の加水分解からは得られなかった。またペルオキソ配位単量体と同様に、この単量体からカチオンをカプセル化した架橋なし四量体の形成が期待できる。第二章ではこのチタン(IV)三置換単量体をビルディングブロックとしてNH_4^+カチオンがカプセル化された架橋なし四量体$[(\alpha\text{-}P_2W_{15}Ti_3O_{60.5})_4(NH_4)]^{35-}$の形成を明らかにした。

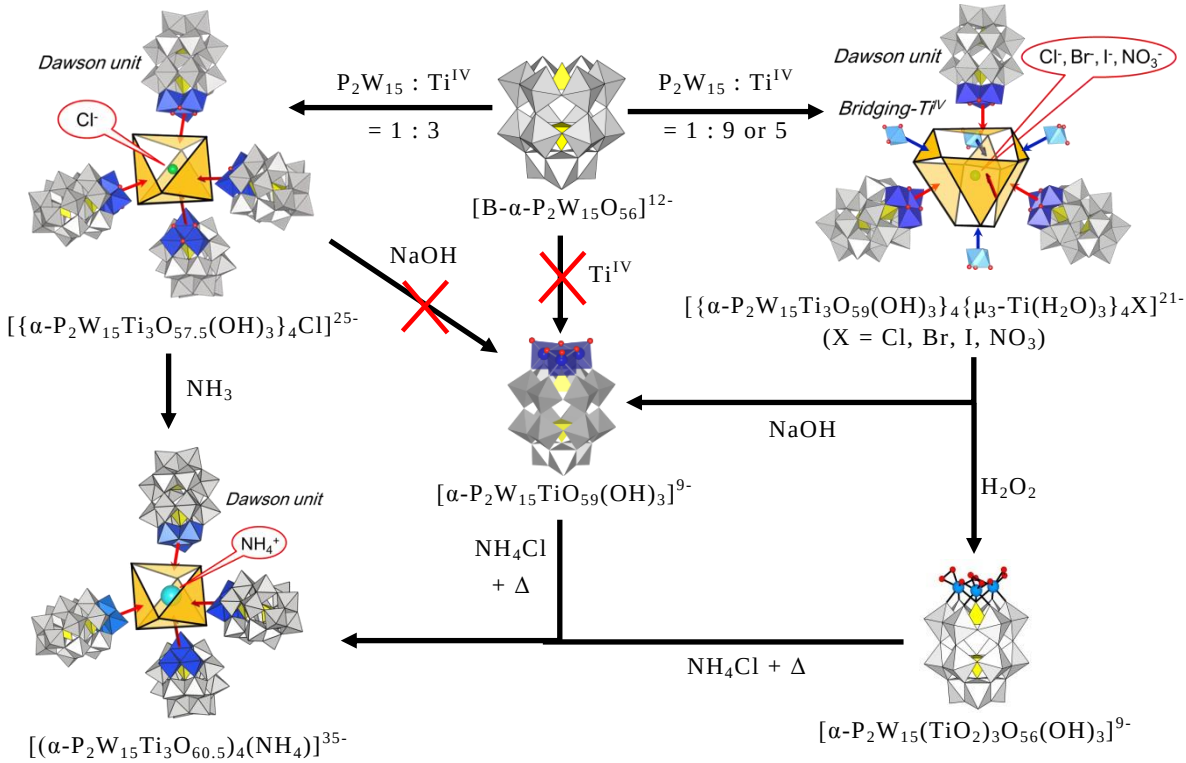

Nb^V,V^V 三置換 Dawson 型ポリ酸塩($[\alpha\text{-}P_2W_{15}Nb_3O_{62}]^{9-}$，$[\alpha\text{-}P_2W_{15}V_3O_{62}]^{9-}$)は置換表面の負電荷とカチオン性有機金属種が作用するため、有機金属種担持ポリ酸塩を形成することが知られている。例えばバナジウム(V)三置換 Dawson 型ポリ酸塩単量体$[\alpha\text{-}P_2W_{15}V_3O_{62}]^{9-}$は$[(C_6H_6)RuCl_2]_2$と反応して、担持位置の異なる二種類の$(C_6H_6)Ru$基担持ポリ酸塩$[(C_6H_6)RuP_2W_{15}V_3O_{62}]^{5-}$を形成する。[7] チタン(IV)三置換 Dawson 型ポリ酸単量体"$[\alpha\text{-}P_2W_{15}Ti_3O_{62}]^{12-}$"はこれまでの M 三置換 Dawson 型ポリ酸塩単量体$[\alpha\text{-}P_2W_{15}M_3O_{62}]^{9-}$に比べて負電荷密度が増大しており、今までにない構造や組成の有機金属種担持ポリ酸塩の形成が期待できる。

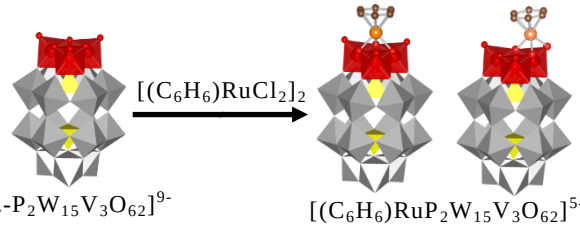

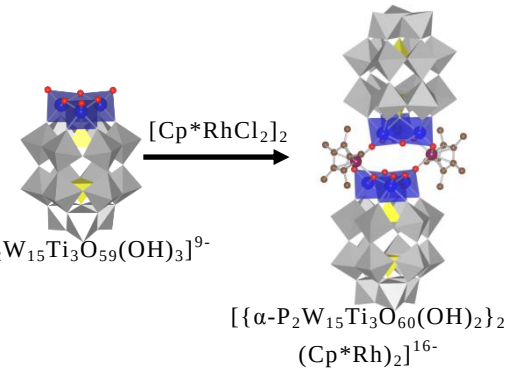

しかし、チタン(IV)三置換 Dawson 型ポリ酸塩単量体は中性、酸性条件で架橋なし四量体を形成しやすいので、塩基性条件で扱う必要があることや、この単量体は水に可溶なアルカリ金属塩でしか得られない(有機溶媒に可溶な四級アンモニウム塩に変換できない)ことから、非常に限定された条件でしか利用できないことが分かった。

そのような制限の中で第三章では、チタン(IV)三置換単量体$[\alpha\text{-}P_2W_{15}Ti_3O_{59}(OH)_3]^{9-}$と$[Cp^*RhCl_2]_2$の反応を行い 2 つの Dawson unit $[\alpha\text{-}P_2W_{15}Ti_3O_{60}(OH)_2]^{10-}$を 2 つの Cp*Rh で架橋した 2 : 2 型二量体$[\{\alpha\text{-}P_2W_{15}Ti_3O_{60}(OH)_2\}_2(Cp^*Rh)_2]^{16-}$の合成と構造解析を行った。

チタン(IV)含有ポリ酸塩に関する研究を主に行ってきたが、その他にも共同研究として同族のジルコニウム(IV)/ハフニウム(IV)含有 Keggin 型シリコタングステン酸塩 2 : 2 型面共有/稜共有錯体($[(SiW_{11}O_{39}M)_2(\mu\text{-}OH)_2]^{10-}$, $[(SiW_{11}O_{39}M)_2(\mu\text{-}OH)_3]^{11-}$)の構造解析に関する研究にも携わっている。Appendix として担当した X 線構造解析の部分について記述した。

第一章

チタン(IV)一置換 Keggin 型ポリ酸塩単量体および二量体の合成と構造解析

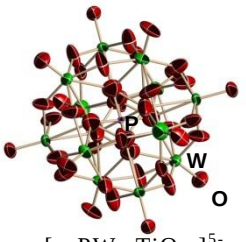

$[\alpha\text{-}PW_{11}TiO_{40}]^{5-}$

別途合成した Keggin 型ポリ酸塩一欠損種 $K_7[\alpha\text{-}PW_{11}O_{39}]\cdot 8H_2O$ (PW_{11})を水に溶解し、NaOAc 存在下で $TiCl_4$ とモル比 PW_{11} : $TiCl_4$ = 1 : 1、80 ºC で反応させ過剰量の Et_2NH_2Cl (DEACl)を加えることで粉体を得た。この粉体を水に溶解し、NaOAc 存在下で slow evaporation することで単量体 $DEA_5[\alpha\text{-}PW_{11}TiO_{40}]\cdot 0.6H_2O$ の無色透明柱状結晶を収率 80.3 %で得た。また、塩酸酸性下で slow evaporation することで二量体 $DEA_8[(\alpha\text{-}PW_{11}TiO_{39})_2O]\cdot 6H_2O$ の無色透明板状結晶を収率 65.3 %で得た。ここ十数年間にわたって二量体の X 線構造解析が無かった理由は、一度粉体として単離した二量体からは結晶化せず、粉体が析出するためと思われる。本実験では単量体から二量体を誘導する過程で二量体が結晶化することを初めて明らかにした。単結晶 X 線構造解析の結果、二量体は Keggin unit 間を μ-O で連結した二量体構造であり、BVS 計算から架橋酸素はプロトネーションしていなかった。単量体は disorder しており、チタン(IV)置換部位を決めることは出来なかったが、単量体構造であることを確認した。H_2O/DMSO (10/1)混合溶媒中の pH を変えた ^{31}P NMR 測定で、pH 3.2 (未調整)では-13.72 ppm に単量体のピークが観測され、pH 2.0 で-13.79 ppm に二量体のピークが観測され始め、pH 0.5 で二量体のみとなった。チタン(IV)一置換 Dawson 型ポリ酸塩では見られたような二量体プロトネーション種の生成は確認できなかった。

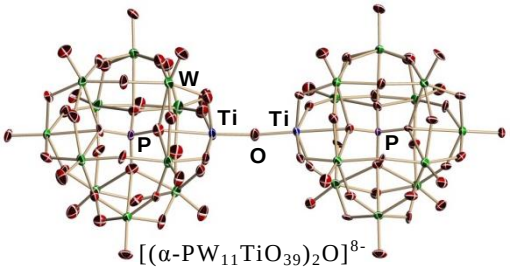

$[(\alpha\text{-}PW_{11}TiO_{39})_2O]^{8-}$

第二章

チタン(IV)三置換 Dawson 型ポリ酸塩単量体の合成とそれをビルディングブロックとした NH_4^+カチオンをカプセル化した架橋なし四量体の合成

別途合成した架橋あり四量体 $Na_{19}H_2[\{\alpha\text{-}P_2W_{15}Ti_3O_{59}(OH)_3\}_4\{\mu_3\text{-}Ti(H_2O)_3\}_4Cl]\cdot 124H_2O$ を水に溶解し、1 M NaOH *aq.*で pH = 9.0 に調整後、NaCl を加えることで単量体 "$Na_{12}[\alpha\text{-}P_2W_{15}Ti_3O_{62}]\cdot 22H_2O$"の白色粉体を収率 41.7 %で得た。この単量体を水に溶解し NH_4Cl を加え、0.1 M HCl で pH = 6.0 に調整し 80 ºC で加熱し、エバポレーターで濃縮し、純水を加え湯浴上(35 ºC)で室温まで徐々に放冷することで NH_4^+カプセル化架橋なし四量体$(NH_4)_{21}Na_{14}[(\alpha\text{-}P_2W_{15}Ti_3O_{60.5})_4(NH_4)]\cdot 70H_2O$ の無色透明針状結晶を収率 14.3 %で得た。この針状結晶は単結晶 X 線構造解析に適しておらず、X 線構造解析は行えなかった。FT-IR では得られた白色粉体は Dawson unit 間の Ti-O-Ti 結合に基づく振動バンドが観測されなかったことから、単量体構造と考えられる。^{31}P NMR ではこれまで合成されてきたどの四量体種の化学シフト(Cl⁻カプセル化架橋なし四量体; -7.65, -13.90 ppm/ Cl⁻カプセル化架橋あり四量体; -7.04, -13.77 ppm)とも一致しなかった。またペルオキソ基配位チタン(IV)三置換単量体の化学シフト(-3.95, -14.43 ppm)に近いことから単量体構造が示唆された。ペルオキソ基配位単量体をビルディングブロックとして誘導した NH_4^+カプセル化種の X 線構造解析では中心空間に NH_4^+がカプセル化されていることが確認されている。その ^{31}P NMR は-7.15, -14.23 ppm に一対の二本線ピークで観測される。これらのピークが単量体から誘導された NH_4^+カプセル化種のピーク(-7.21, -14.20 ppm)と一致していることから、単量体からも NH_4^+カプセル化種が誘導できることが分かった。

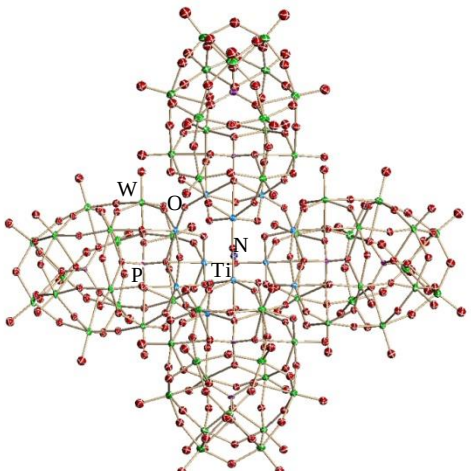

$[(\alpha\text{-}P_2W_{15}Ti_3O_{60.5})_4(NH_4)]^{35-}$ 6)

第三章

二つの Cp*Rh 基で架橋されたチタン(IV)三置換 Dawson 型ポリ酸塩二量体の合成と X 線構造解析

別途合成したチタン(IV)三置換単量体 $Na_8Cs[P_2W_{15}Ti_3O_{59}(OH)_3]\cdot TiO_2\cdot 20H_2O$ を水に溶解し 0.1 M LiOH *aq.*を単量体 : LiOH = 1 : 3 で加えた。この溶液に別途調製した $Cp^*Rh(BF_4)_2$ *aq.*を単量体 : Cp*Rh = 1 : 1 で加え 90 ºC で反応させ、濃縮後エタノールに再沈殿し得られた黄橙色粉体を水から再結晶することで Cp*Rh 架橋二量体 $Na_{14}Cs_2[\{\alpha\text{-}P_2W_{15}Ti_3O_{60}(OH)_2\}_2(Cp^*Rh)_2]\cdot 37H_2O\cdot 2TiO_2$ の橙色柱状結晶を収率 80.1 %で得た。X 線構造解析の結果、2 つの Dawson unit を 2 つの Cp*Rh 基で架橋した二量体構造であり、Dawson unit 内の稜共有 Ti-O-Ti 結合がプロトネーションしていた。このような二量体構造はこれまでの

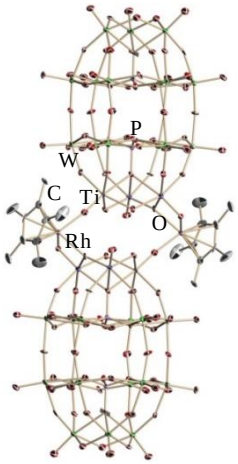

$[\{\alpha\text{-}P_2W_{15}Ti_3O_{60}(OH)_2\}_2(Cp^*Rh)_2]^{16-}$

有機金属種担持 Nb^{V}, V^{V} 三置換 Dawson 型ポリ酸塩には見られない非常に珍しい構造であった。溶液中の ^{31}P NMR で-5.20, -14.61 ppm に一対の二本線ピークが観測された。単量体のピーク(-4.97, -14.65 ppm)と比較して特にチタン置換サイトの P 共鳴が大きくシフトしているのは、チタン(IV)置換サイト周辺に担持された Cp*Rh 基の効果によるものであり、溶液中でも二量体構造が保持されていると思われる。

Appendix

ジルコニウム(IV)/ハフニウム(IV)含有 Keggin 型シリコタングステン酸塩 2 : 2 型錯体の X 線構造解析

二つの Zr^{IV}, Hf^{IV}、又は(M)をヘテロ原子 Si の Keggin 型ポリ酸塩一欠損種でサンドイッチした錯体について、二つの M を二本の μ-OH で架橋した稜共有錯体 $[(SiW_{11}O_{39}M)_2(\mu\text{-}OH)_2]^{10-}$ と、二つの M を三本の μ-OH で架橋した面共有錯体 $[(SiW_{11}O_{39}M)_2(\mu\text{-}OH)_3]^{11-}$ の構造解析を行った。二核錯体で稜共有はよくみられるが、面共有というのは非常に珍しい構造であった。これはヘテロ原子が Si や Ge のときに初めて実現され、ヘテロ原子 P のポリ酸塩では同じ pH では安定に存在できないため実現できない。

総括と展望

チタン(IV)置換 Keggin 型および Dawson 型ポリ酸塩の化学において、単量体から多量体の形成は pH が重要な鍵になっている。チタン(IV)置換体は二量体や四量体などオリゴマーが安定形であり、単量体を直接誘導するのは難しいといわれていた。本研究では Keggin 型チタン(IV)一置換体および Dawson 型チタン(IV)三置換体の単量体の合成条件を明らかにし、それから種々の化合物を誘導した。これによりチタン(IV)置換ポリ酸塩の合成化学の大きな展開が開けた。

reference

1) O. A. Kholdeeva et al, *Inorg. Chem*. **2000**, *39*, 3828.

2) O. A. Kholdeeva et al, *Inorg. Chem.* **2005**, *44*, 1635.

3) G. M. Maksimov et al, *J. Struct. Chem.* **2009**, *50*, 618-627.

4a) Y. Sakai et al, *Dalton Trans.***2003**, 3581.

4b) Y. Sakai et al, *Chem. Eur. J.* **2003**, *9*, 4077.

4c) Y. Sakai et al, *Bull. Chem. Soc. Jpn*. **2007**, *80*, 1965.

5) Y. Sakai et al, *Eur. J. Inorg. Chem*. **2004**, 4646.

6) Y. Sakai et al, *Inorg. Chem.* **2011**, *50*, 6575.

7) K. Nomiya et al, *Inorg. Chim. Acta* **2007**, *360*, 2313.

8) S. Yoshida et al, *Dalton Trans.* **2008**, 4630.

Original Paper (Peer Reviewed)

1. Monomer and Dimer of Mono-titanium(IV)-Containing α-Keggin Polyoxometalates: Synthesis, Molecular Structures, and pH-Dependent Monomer-Dimer Interconversion in Solution
   Y. Matsuki, Y. Mouri, Y. Sakai, S. Matsunaga, K. Nomiya, *Eur. J. Inorg. Chem.* **2013**, 1754-1761.
2. Encapsulation of Anion/Cation in the Central Cavity of Tetrameric Polyoxometalate, Composed of Four Trititanium(IV)-Substituted α-Dawson Subunits, Initiated by Protonation/Deprotonation of the Bridging Oxygen Atoms on the Intramolecular Surface
   Y. Sakai, S. Ohta, Y. Shintoyo, S. Yoshida, Y. Taguchi, Y. Matsuki, S. Matsunaga, K. Nomiya, *Inorg. Chem.*

2011, *50*, 1754-1761.

3. Synthesis and molecular structure of dimeric tri-titanium(IV)-substituted Dawson polyoxometalate bridged by two Cp^*Rh^{2+} groups

   Y. Matsuki, S, Takaku, T. Hoshino, S. Matsunaga, K. Nomiya, *Manuscript in preparation*.

4. 2:2-Type complexes of zirconium(IV)/hafnium(IV) centers with mono-lacunary Keggin polyoxometalates: Syntheses and molecular structures of $[(\alpha\text{-}SiW_{11}O_{39}M)_2(\mu\text{-}OH)_2]^{10-}$ (M = Zr, Hf) with edge-sharing octahedral units and $[(\alpha\text{-}SiW_{11}O_{39}M)_2(\mu\text{-}OH)_3]^{11-}$ with face-sharing octahedral units

   H. Osada, A. Ishikawa, Y. Saku, Y. Sakai, Y. Matsuki, S. Matsunaga, K. Nomiya, *Polyhedron*, **2013**, 52, 389-397.

Original Paper (Non-Peer Reviewed)

1. チタン(IV)三置換 Dawson 型ポリ酸塩単量体とそれを用いた NH_4^+内包テトラポッド型四量体の合成

   松木悠介, 星野貴弘, 増田佳奈, 松井敬祐, 力石紀子, 松永諭, 野宮健司, *Science Jornal of Kanagawa University*, **2014**, *25*, 69-72.

International Conference

1. Synthesis of monomeric, tri-titanium(IV)-substituted Dawson polyoxometalate and derivation of its non-bridging tetramer with encapsulated Br^--ion in the central cavity

   The 9th International Symposium on the Kanagawa University-National Taiwan University Exchange Program 2013, March 15, **2014**.

Meeting and Conference

1. チタン(IV)三置換 Dawson 型ポリ酸塩単量体の合成およびそれをビルディングブロックとした中心空間にカチオンをカプセル化した四量体の誘導

   松木悠介 et al, 第 61 回錯体化学討論会, 岡山理科大学, 2011 年 9 月, Abstr., **1PA-15**.

2. チタン(IV)三置換 Dawson 型ポリ酸塩単量体の合成および中心空間にアニオンをカプセル化した架橋なし四量体の誘導

   松木悠介 et al, 第 64 回錯体化学討論会, 中央大学後楽園キャンパス, 2014 年 9 月 Abstr. **1PA-026**.

3. チタン(IV)三置換 Dawson 型ポリ酸塩単量体の合成とそれをビルディングブロックとした中心空間にカチオンをカプセル化した架橋なし四量体の誘導

   松木悠介 et al, 第 92 回日本化学会春季年会, 慶応義塾大学日吉キャンパス, 2012 年 3 月, Abstr. **1PB-006**.

4. チタン(IV)一置換 Keggin 型ポリ酸塩単量体および二量体の合成、分子構造と単量体-未量体の pH に依存した相互変換

   松木悠介 et al, 第 93 回日本化学会春季年会, 立命館大学びわこ・くさつキャンパス, 2013 年 3 月, Abstr. **1B3-14**.

5. チタン(IV)一置換 α-Keggin 型ポリ酸塩単量体および二量体の合成、分子構造と pH に依存する単量体-二量体の平衡

   松木悠介 et al, 第 2 回 CSJ 化学フェスタ, 東京工業大学大岡山キャンパス, 2012 年 10 月, Abstr. **P1-28**.

6. チタン(IV)三置換 Dawson 型ポリ酸塩単量体から中心空間に Br^-を内包した架橋なし四量体の合成

   松木悠介 et al, 第 4 回 CSJ 化学フェスタ, タワーホール船堀, 2014 年 10 月 Abstr. **P3-060**.

Contents

Introduction

Background

ポリ酸塩

分子性の金属酸化物クラスターであるポリ酸塩(polyoxometalate ; POM)は金属 M (Mo^{VI}, W^{VI}, V^{V}, Nb^{V} etc)を中心とした MO_6 八面体が稜共有や頂点共有を繰り返すことで、対称性の良い多核構造を形成したオキソ酸の縮合体である。その中心はヘテロ原子と呼ばれる異種原子 X (X = Al^{III}, Si^{IV}, P^{V}, S^{VI} etc)を中心とした XO_4 四面体が存在する。MO_6 八面体を基本単位とするポリ酸塩の構造は 1929 年に L. Pauling によって提案され、[1] 1933 年に J. F. Keggin が T_d 対称の Keggin 型ポリ酸塩 free acid 型 $H_3[PW_{12}O_{40}]\cdot 6H_2O$ の粉末 X 線回折データを用いた構造解析を行い、その構造を明らかにした。[2]以来、数多くのポリ酸塩に関する物性やその構造が研究されてきた。

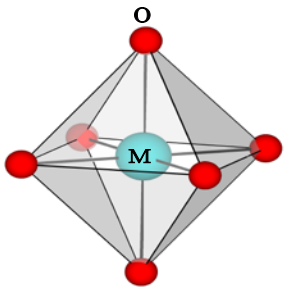

MO_6 の多面体表示


α-Keggin-Type[2)]
$[\alpha\text{-}XM_{12}O_{40}]^{n-}$

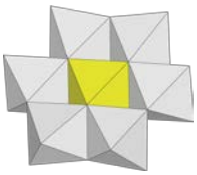
Anderson-Type[3)]
$[XM_6O_{24}H_6]^{n-}$

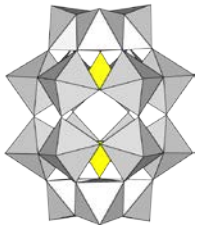
α-Dawson-Type[4)]
$[\alpha\text{-}X_2M_{18}O_{62}]^{n-}$

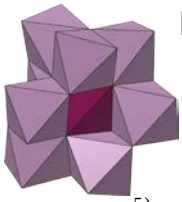
Waugh-Type[5)]
$[XMo_9O_{32}]^{6-}$

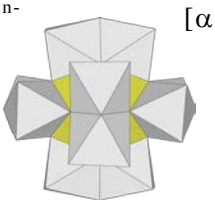
Dexter-Silverton-Type[6)]
$[XMo_{12}O_{42}]^{8-}$

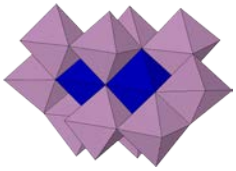
Evans-Showell-Type[7)]
$[Co_2Mo_{10}O_{38}H_4]^{6-}$

ポリ酸塩は特定の分子量を持つ分子性の化合物であり、カウンターカチオンに依存して、水や様々な有機溶媒に溶解性を示す。また、不均一系触媒担体である固体金属酸化物をミクロサイズまで切り刻んだ分子断片とみなすこともできる。そのため不均一系触媒担体の分子モデルとして興味が持たれている。さらに現在では、構成金属の一部を酸化数の異なる異種金属で置換できるという性質や、固体金属酸化物とは異なり溶液中でも固体状態でも各種分光学的手法により characterization できるという特徴を生かし、多核構造を有する種々の修飾型ポリ酸塩について分子設計を導入した無機合成化学的研究がされている。

Keggin 型ポリ酸塩の幾何異性体

Keggin 型ポリ酸塩は 1 つの XO_4 四面体(X = Si^{IV}, P^{V} etc)を MO_6 八面体(M = Mo^{VI}, W^{VI} etc) 3 つが稜共有した M_3O_{13} unit (B-site) 4 つで取り囲んだ構造をしている。

この Keggin 型ポリ酸塩にはα型(T_d 対称)に対して、B-site を 1 つ 60° 回転させたβ型(C_{3v} 対称)、2 つ 60° 回転させたγ型(C_{2v} 対称)、3 つ 60° 回転させたδ型(C_{3v} 対称)、全て 60° 回転させたε型(T_d 対称)の合計 5 つの幾何異性体が多面体モデルの上では存在する。なお、MO_6 八面体 3 つが頂点共有し合った M_3O_{15} unit は A-site と呼ばれている。これらの異性体は全て単結晶 X 線構造解析がされており、この内δ型、ε型に関してはアルミニウムのポリカチオン $[Al_{13}O_4(OH)_{24}(H_2O)_{12}]^{7+}$ として合成されている。[8-11)]

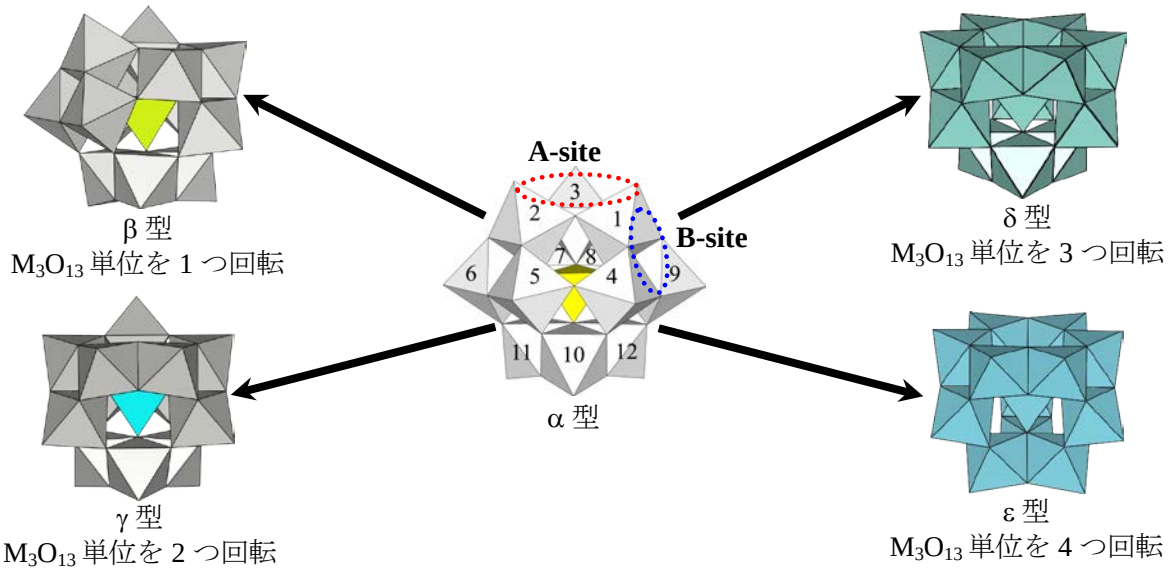

Dawson 型ポリ酸塩の幾何異性体

Dawson 型ポリ酸塩は 2 つのヘテロ原子の XO_4 四面体(X = Si^{IV}, P^{V} etc)を MO_6 八面体(M = Mo^{VI}, W^{VI} etc) 3 つが稜共有し合った M_3O_{13} unit (α_2-位と呼ばれる cap 部分) 2 つと、MO_6 八面体がリング状に稜共有と頂点共有し合った M_6O_{27} unit (α_1-位と呼ばれる belt 部分) 2 つで取り囲んだ構造をしている。

この Dawson 型ポリ酸塩にはα型(D_{3h} 対称)に対して、cap 部分の M_3O_{13} 単位の回転に基づく幾何異性体として、M_3O_{13} unit 1 つが 60° 回転したβ型(C_{3v} 対称)、上下 2 つが 60° 回転したγ型(D_{3h} 対称)が存在し、これら 3 つの異性体は全て X 線構造解析がなされている。ただしγ型に関しては$[\gamma\text{-}As_2W_{18}O_{62}]^{6-}$ についてのみである。その他に Dawson 型ポリ酸塩にはα型、β型、γ型についてそれぞれ下半分の $XO_4M_9O_{30}$ unit (A-site 三欠損 Keggin 型)が C_3 軸に関して 60° 回転した異性体α*型(D_{3d} 対称)、β*型(C_{3V} 対称)、γ*型(D_{3d} 対称)も存在する。近年ではヘテロ原子 S のγ*型タングストポリ酸塩$[\gamma^*\text{-}S_2W_{18}O_{62}]^{4-}$ やヘテロ原子 S のγ型、γ*型混合モリブドポリ酸塩$[\gamma, \gamma^*\text{-}S_2Mo_{18}O_{62}]^{4-}$ などの構造解析が行われている。[4,12-14)]

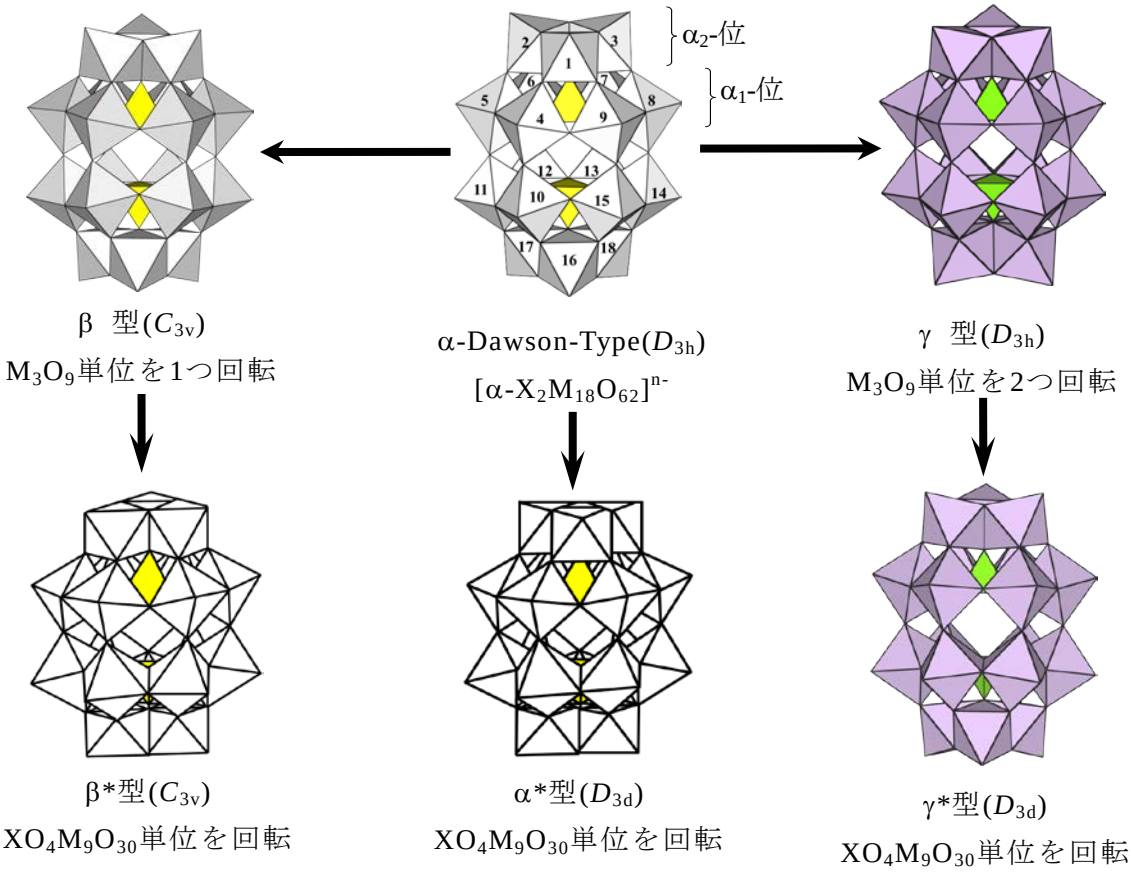

欠損型ポリ酸塩

幾何異性体と同様に基本骨格の一部が欠損した欠損型ポリ酸塩の研究も行われてきた。ポリ酸塩は基本骨格の一部を位置選択的に欠損させることが可能であり、これまでに多くの欠損種が合成されてきた。例えば、ヘテロ原子 Si の Keggin 型タングストポリ酸塩$[SiW_{12}O_{40}]^{4-}$では溶液の pH に依存して様々な欠損種が存在し、それらは電気化学的に存在が確認されている。[15)]

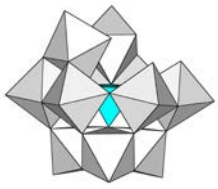

$[\alpha\text{-}SiW_{11}O_{39}]^{8-}$

$[A\text{-}\beta\text{-}SiW_{9}O_{34}]^{10-}$

$[\gamma\text{-}SiW_{10}O_{36}]^{8-}$

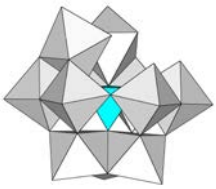

$[\beta_1\text{-}SiW_{11}O_{39}]^{8-}$

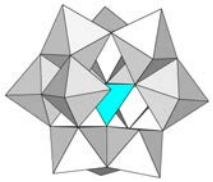

$[\beta_2\text{-}SiW_{11}O_{39}]^{8-}$

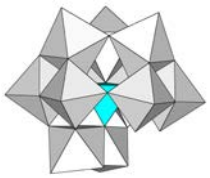

$[\beta_3\text{-}SiW_{11}O_{39}]^{8-}$

ヘテロ原子 P の Keggin 型タングストポリ酸塩$[\alpha\text{-}PW_{12}O_{40}]^{3-}$では 1 つあるいは 3 つの W^{VI} が欠損した一欠損種$[\alpha\text{-}PW_{11}O_{39}]^{7-}$、A-site 三欠損種$[A\text{-}PW_9O_{34}]^{9-}$、B-site 三欠損種$[B\text{-}PW_9O_{34}]^{9-}$[16)]が存在する。また、ヘテロ原子 P の Dawson 型タングストポリ酸塩$[\alpha\text{-}P_2W_{18}O_{62}]^{6-}$では cap 部分の 1 つあるいは 3 つの W^{VI} が欠損した α_2 一欠損種$[\alpha_2\text{-}P_2W_{17}O_{61}]^{10-}$[17)]、B-site 三欠損種$[B\text{-}\alpha\text{-}P_2W_{15}O_{56}]^{12-}$[17, 18)]、また belt 部分の 1 つあるいは 6 つが欠損した α_1 一欠損種$[\alpha_1\text{-}P_2W_{17}O_{61}]^{10-}$[17)]、六欠損種$[\alpha\text{-}H_2P_2W_{12}O_{48}]^{12-}$[17)]などが存在する。

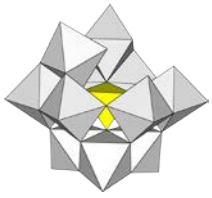

$[\alpha\text{-}PW_{11}O_{39}]^{7-}$

$[A\text{-}PW_9O_{34}]^{9-}$

$[B\text{-}PW_9O_{34}]^{9-}$

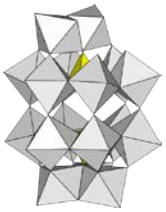

$[\alpha_2\text{-}P_2W_{17}O_{61}]^{10-}$

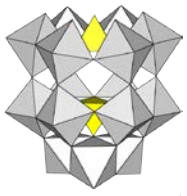

$[B\text{-}\alpha\text{-}P_2W_{15}O_{56}]^{12-}$

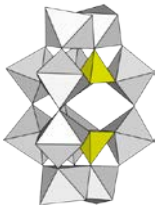

$[\alpha\text{-}H_2P_2W_{12}O_{48}]^{12-}$

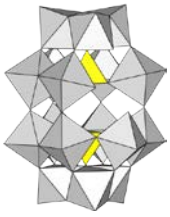

$[\alpha_1\text{-}P_2W_{17}O_{61}]^{10-}$

置換型ポリ酸塩

ポリ酸塩を構成する MO_6 八面体の中心金属 M は最高酸化数(d 電子数= 0)をとっている。このためポリ酸塩は電子を受け取りやすく、強力な酸化剤として作用する。電子を受け取ったポリ酸塩は特徴的な青色を呈し還元型ポリ酸塩と呼ばれ、この青色は Heteropoly blue として知られており、古くからリン酸イオンなどの定量分析などに用いられている。[8,19-20)]

従来の Keggin 型及び Dawson 型ポリ酸塩無置換体の負電荷は内部の XO_4 四面体の電荷に由来するものであり、ポリ酸塩表面の負電荷密度は極めて低い。

Keggin 型無置換体　$[SiW_{12}O_{40}]^{4-} = [(SiO_4^{4-})(W_{12}O_{36}^{0})]$

$[PW_{12}O_{40}]^{3-} = [(PO_4^{3-})(W_{12}O_{36}^{0})]$

Dawson 型無置換体　$[P_2W_{18}O_{62}]^{6-} = [(PO_4^{3-})_2(W_{18}O_{54}^{0})]$

しかし、これらのポリ酸塩は骨格金属の W^{VI} をより酸化数の低い金属 M (M = Nb^{V}, V^{V}, Ti^{IV} etc)に置換することで、分子表面上の負電荷密度を高めることができる。例えば、Dawson 型無置換体 $[P_2W_{18}O_{62}]^{6-}$ の B-site の W^{VI} 3 つを V^{V} 3 つで置換すれば、表面上に 3-の負電荷が生じる。さらに中心の 2 つの PO_4^{3-} に由来する 6-の負電荷を加えれば、全体で 9-の負電荷を持つようになる。

バナジウム(V)三置換 Dawson 型ポリ酸塩　$[P_2W_{15}V_3O_{62}]^{9-} = [(PO_4^{3-})_2(W_{15}V_3O_{54}^{3-})]$

また、Keggin 型無置換体 $[SiW_{12}O_{40}]^{4-}$ の A-site の W^{VI} 3 つを Nb^{V} 3 つで置換すれば、表面上に 3-の負電荷が生じる。さらに中心の 1 つの SiO_4^{4-} に由来する 4-の負電荷を加えれば、全体で 7-の負電荷を持つようになる。

ニオブ(V)三置換 Keggin 型ポリ酸塩　$[SiW_9Nb_3O_{40}]^{7-} \equiv [(SiO_4^{4-})(W_9Nb_3O_{36}^{3-})]$

このように置換型ポリ酸塩は無置換型ポリ酸塩よりも分子表面の負電荷密度が増大している。そのため無置換型には無い多中心活性部位が形成され、新たな触媒活性や生理活性を示すことが多い。

$[SiW_9Nb_3O_{40}]^{7-}$

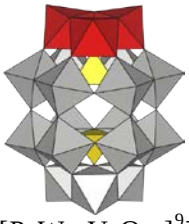

$[P_2W_{15}V_3O_{62}]^{9-}$

チタン(IV)置換ポリ酸塩

チタン(IV)酸化物である Rutile 型の酸化チタン TiO_2 や Perovskite 型のチタン酸ストロンチウム $SrTiO_3$ は従来から光半導体や光触媒として知られている。[21–26)]

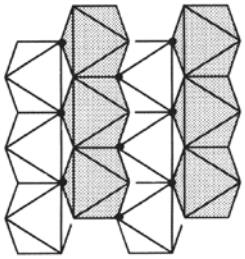

Rutile-type TiO_2

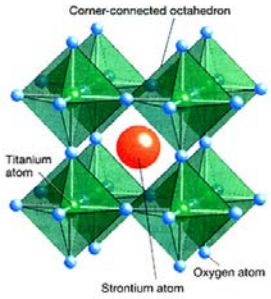

Perovskite-type $SrTiO_3$

上図のように Rutile 型の酸化チタン TiO_2 は TiO_6 八面体が稜共有を繰り返した構造で、Peroveskite 型のチタン酸ストロンチウム $SrTiO_3$ は TiO_6 八面体が頂点共有を繰り返した構造である。

また、Keggin 型や Dawson 型のポリ酸塩は MO_6 八面体が稜共有と頂点共有を繰り返してできた分子性の酸化物クラスターである。そのため、ポリ酸塩の骨格金属 M (M = Mo^{VI}, W^{VI} etc)を Ti^{IV} に置換すれば、ポリ酸塩が Rutile 型や Perovskite 型のフラグメントを持つことになり、光酸化触媒としての利用が期待できる。[27-29)]また、N. Serpone らによって TiO_2 の抗菌作用や染色汚染物質(Erythrosine, Rhodamine)の分解作用も報告されており、チタン(IV)置換ポリ酸塩の水系での抗菌作用や環境浄化作用についても非常に興味深い。[30)]

Ti^{IV} のイオン半径(0.75 Å)は W^{VI} のイオン半径(0.74 Å)とほぼ等しいため、チタン(IV)置換ポリ酸塩の形成は比較的に容易である。ヘテロ原子 P の Keggin 型ポリ酸塩では一置換単量体[α-$PW_{11}TiO_{40}$]$^{5-}$ [31,32)]、α-1,5-二置換単量体 [α-1,5-$PW_{10}Ti_2O_{40}$]$^{7-}$ [33,34)]、二置換二量体[(α-$PW_{10}Ti_2O_{38}$)$_2O_2$]$^{10-}$ [35,36)]、三置換二量体[(α-$PW_9Ti_3O_{37}$)$_2O_3$]$^{12-}$ [35,36)]について合成及び構造解析が報告されている。

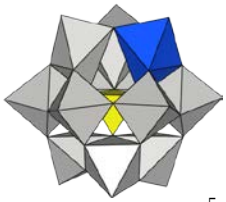

[α-$PW_{11}TiO_{40}$]$^{5-}$

[α-1,5-$PW_{10}Ti_2O_{40}$]$^{7-}$

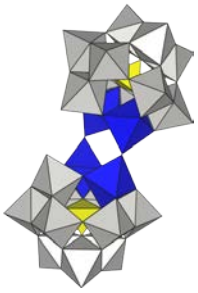

[(α-$PW_{10}Ti_2O_{38}$)$_2O_2$]$^{10-}$

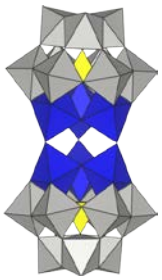

[(α-$PW_9Ti_3O_{37}$)$_2O_3$]$^{12-}$

また、一置換二量体は、水酸基によって分子間の Ti-O-Ti 結合が切断され monomer-dimer の平衡があると考えられているものの、その単結晶 X 線構造解析は未だされていない。[37-39)]

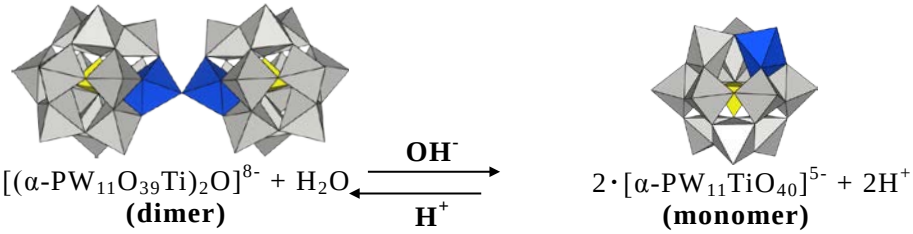

ヘテロ原子 P の Dawson 型ポリ酸塩では、2 つのα-二置換体が 2 つのμ-$Ti(ox)_2$ で架橋された二量体$[(P_2W_{16}Ti_2O_{62})_2\{\mu\text{-}Ti(ox)_2\}_2]^{20-}$ [27)]、チタン(IV)八面体 2 つが Dawson 型三欠損種 2 つで上下から挟まれた sandwich 型置換体 NH_4 塩$[(TiP_2W_{15}O_{55}OH)_2]^{14-}$ [40)] そのフリーアシッド型 $H_8[P_2W_{15}O_{54}Ti(OH_2)_2]_2\cdot 31H_2O$ [41)]、α-三置換四量体(中心空間カプセル化なし、架橋なし) $[\{P_2W_{15}Ti_3O_{57.5}(OH)_3\}_4]^{24-}$ [40)] が合成、構造解析されている。

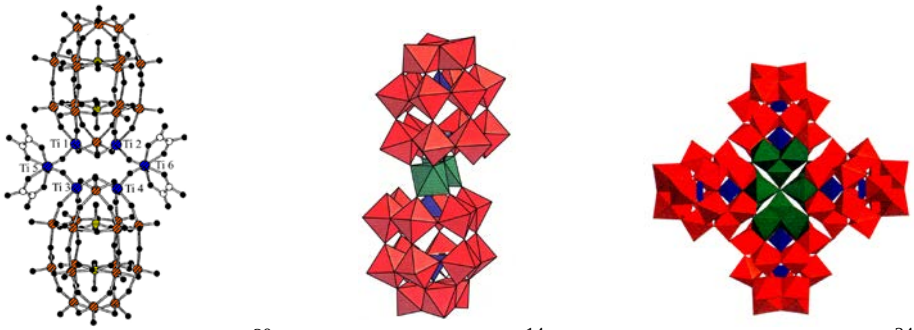

$[P_2W_{16}Ti_2O_{62}\{\mu\text{-}Ti(C_2O_4)_2\}]_2^{20-}$ $[(TiP_2W_{15}O_{55}OH)_2]^{14-}$ $[\{P_2W_{15}Ti_3O_{57.5}(OH)_3\}_4]^{24-}$

またα_2-一置換二量体は溶液中の pH に依存して単量体-二量体-二量体プロトネーション種の平衡が存在することが確認され。二量体 $K_{14}[(\alpha_2\text{-}P_2W_{17}TiO_{61})_2(\mu\text{-}O)]\cdot 17H_2O$、二量体プロトネーション種 $H_{13}[(\alpha_2\text{-}P_2W_{17}TiO_{61})(\alpha_2\text{-}P_2W_{17}TiO_{61}H)(\mu\text{-}O)]\cdot ca.50H_2O$ の構造解析が行われている。[42)]

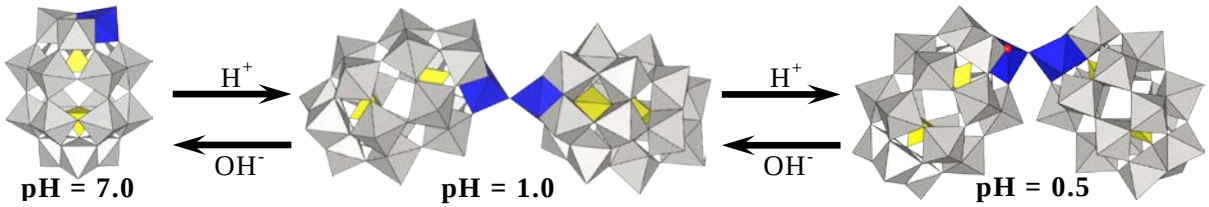

チタン(IV)三置換 Dawson 型ポリ酸塩の化学 [43, 44, 45)]

チタン(IV)三置換 Dawson 型ポリ酸塩は Dawson 型ポリ酸塩三欠損種 $[B\text{-}\alpha\text{-}P_2W_{15}O_{56}]^{12-}$とチタン($Ti^{IV}$)を反応させることで形成される。その際、単量体は形成されず自己縮合によって二種類のテトラポッド型四量体が形成される。Dawson unit が架橋チタン$\mu_3\text{-}Ti(H_2O)_3$を介してされた構造のものを架橋あり四量体といい、中心空間にアニオン X^- (X = Cl, Br, I, NO_3)をカプセル化した化合物が構造解析されている。Dawson unit が直接連結したものを架橋なし四量体といい、中心空間に Cl^-をカプセル化した化合物が構造解析されている。また架橋あり四量体は H_2O_2 と反応しペルオキソチタン(IV)三置換 Dawson 型ポリ酸塩単量体$[\alpha\text{-}P_2W_{15}(TiO_2)_3O_{56}(OH)_3]^{9-}$を形成する。このペルオキソチタン単量体は熱により容易にペルオキソ基が分解する。このペルオキソ基が分解した単量体は NH_4^+イオン存在下で自己縮合し、NH_4^+をカプセル化した架橋なし四量体が形成される。さらにアニオンをカプセル化した架橋なし四量体は中心空間の 12 個の Ti-OH-Ti 結合の H^+を塩基で脱プロトン化させることでカチオンをカプセル化した架橋なし四量体を形成する。

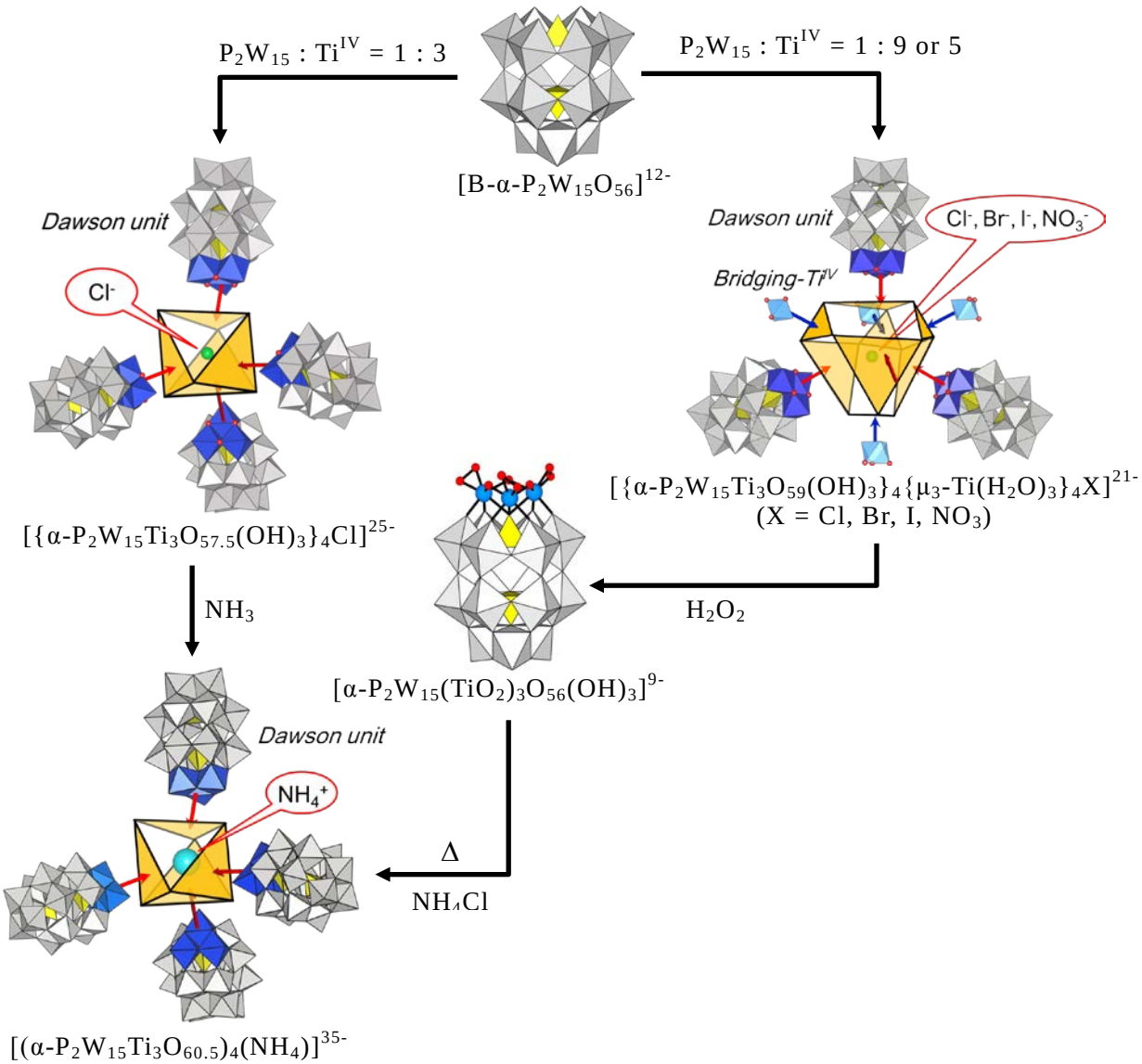

カチオン性有機金属種が担持された置換型ポリ酸塩

V^{V} や Nb^{V} 三置換ポリ酸塩の置換表面は負電荷密度が増大しており、カチオン性有機金属種がポリ酸塩の置換表面上に担持された化合物を形成する。実際に Bu_4N 塩として合成された有機金属種担持ポリ酸塩は、有機金属錯体と無機化合物の高次複合化した錯体として錯体化学的な意味で興味が持たれている。

これまでにヘテロ原子 P の Nb^{V} 三置換 Dawson 型ポリ酸塩単量体に担持された有機金属種は、$(cod)M^{+}$ (cod = 1,5-cyclooctadiene = 1,5-C_8H_{12}, M = Ir, Rh) [46, 47], $(C_6H_6)Ru^{2+}$ [48], $Cp^{*}Rh^{2+}$ (Cp^{*} = pentamethyl cyclopentadienyl = C_5Me_5) [48-50], $(CO)_3Re^{+}$, $(CO)_2Ir^{+}$ [51]などがある。この有機金属種担持ポリ酸塩は、不均一系触媒種の分子モデル的な構造を有しているため、ポリ酸塩を触媒担体とした有機溶媒中での均一系酸化触媒作用について期待できる。実際、$(cod)Ir^{+}$基を担持した$(Bu_4N)_5Na_3[\{(cod)Ir\}P_2W_{15}Nb_3O_{62}]$は、ジクロロエタン中で分子状酸素によるシクロヘキセンの自動酸化反応に対する良好な触媒作用を示す。[52]

また遷移金属錯体$[(CH_3CN)_xM]^{n+}$ (M = Mn^{II}, Fe^{II}, Co^{II}, Ni^{II}, Cu^{I}, Zn^{II})を担持した化合物は、ポリ酸塩担体に遷移金属錯体が一つ担持された 1 : 1 型だけでなく複数担持された化合物も単離されている。[52]

有機金属種担持ポリ酸塩は、固体金属酸化物を用いる触媒反応の解明やポリ酸塩を触媒担体とした新しい反応系の触媒設計にも利用されている。特に、触媒作用が一般に単離できない他の遷移状態を経て行われる kinetic な現象であることから、単離可能で反応性があり原子レベルで characterization できるこれらのポリ酸塩は、触媒化学的にも重要である。

さらに、$(cod)M^{+}$ (M = Ir, Rh)基担持ポリ酸塩は、アセトン溶液中でシクロヘキセンの水添反応に対する良好な触媒作用を示す金属ナノクラスター ($Ir^{0}_{\sim 300}$, $Rh^{0}_{\sim 2400}$)の出発化合物としても用いることができる。Finke らは、このナノクラスターを、“可溶性の不均一系金属クラスター触媒”として提案しており、ポリオキソアニオンは、クラスターの安定化と単離可能な性質に寄与している。[53]

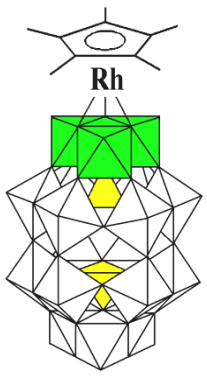

$[(Cp^{*}Rh)P_2W_{15}Nb_3O_{62}]^{7-}$

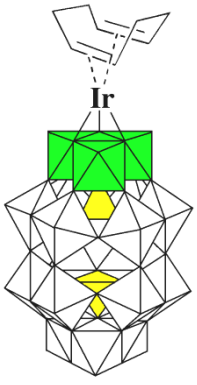

$[\{(cod)Ir\}P_2W_{15}Nb_3O_{62}]^{8-}$

一方、ヘテロ原子 P のバナジウム(V)三置換 Dawson 型ポリ酸塩単量体に担持されたカチオン性有機金属種は、$CpTi^{3+}$ [54], Cp^*Rh^{2+} [55], $(cod)Pt^{2+}$ [56], $(C_6H_6)Ru^{2+}$ [57]などがある。このうち Cp^*Rh^{2+} 基担持ポリ酸塩は Cp^*Rh^{2+} 基が二つ担持された 2 : 1 型錯体 $[(Cp^*Rh)_2P_2W_{15}V_3O_{62}]^{5-}$を形成し、バナジウム(V)三置換体とニオブ(V)三置換体では形成される有機金属種担持ポリ酸塩に違いが現れることがわかった。また、$(C_6H_6)Ru^{2+}$基担持バナジウム(V)三置換単量体では室温で *C*s 対称の 1 : 1 型錯体が形成され、さらに熱による異性化で C_{3v} 対称の 1 : 1 型錯体が形成されることが ^{51}V NMR により確認されている。

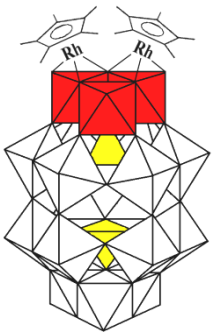

$[(Cp^*Rh)_2P_2W_{15}V_3O_{62}]^{5-}$

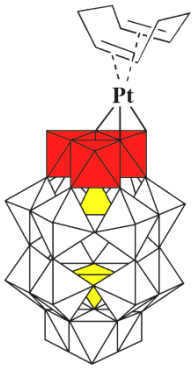

$[\{(cod)Pt\}P_2W_{15}V_3O_{62}]^{7-}$

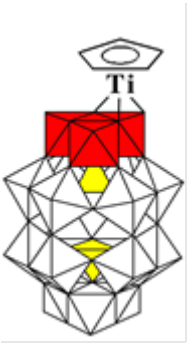

$[(CpTi)P_2W_{15}V_3O_{62}]^{6-}$

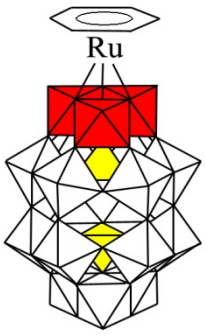

reflux 有り (C_{3v})

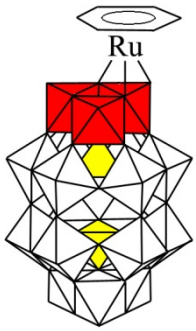

reflux 無し (C_S)

$[\{(C_6H_6)Ru\}P_2W_{15}V_3O_{62}]^{7-}$

Objective

本研究では、Keggin 型ポリ酸塩および Dawson 型ポリ酸塩のチタン(IV)置換体の合成と展開を目的としている。本論文の構成は以下の通りになっている。

十数年にわたってチタン(IV)一置換 Keggin 型ポリ酸塩二量体$[(\alpha\text{-}PW_{11}TiO_{39})_2O]^{8-}$は研究が行われてきた化合物である。C. L. Hill や O. A. Kholdeeva らによって二種類の推定構造 (μ-O 架橋二量体 $[(\alpha\text{-}PW_{11}TiO_{39})_2O]^{8-}$、μ-OH 架橋二量体$[(\alpha\text{-}PW_{11}TiO_{39})_2O]^{7-}$)が提案されているが、誰もその結晶化には成功せず X 線構造解析が行われていない。これまでは一度粉体として単離した二量体から結晶化方法の探索を行ってきたが結晶化には至らなかった。しかし、単量体$[\alpha\text{-}PW_{11}TiO_{40}]^{5-}$から二量体を誘導する過程で二量体が結晶化する可能性を見出した。そこで第一章ではチタン(IV)一置換 Keggin 型ポリ酸塩二量体の結晶化条件を明らかにし、構造解析により二量体の Keggin unit 間の連結様式が μ-OH ではなくて μ-O であることを決定した。

既に当研究室では、ペルオキソ基配位チタン(IV)三置換単量体$[\alpha\text{-}P_2W_{15}(TiO_2)_3O_{56}(OH)_3]^{9-}$から NH_4^+カチオンがカプセル化された架橋なし四量体$[\{\alpha\text{-}P_2W_{15}Ti_3O_{60.5}\}_4(NH_4)]^{35-}$が合成され、構造解析が行われている。最近新たにチタン(IV)三置換単量体“$[\alpha\text{-}P_2W_{15}Ti_3O_{62}]^{12-}$”が架橋あり四量体$[\{\alpha\text{-}P_2W_{15}Ti_3O_{59}(OH)_3\}_4\{\mu\text{-}Ti(OH_2)_3\}_4Cl]^{21-}$の加水分解から形成されることが見出され、この単量体をビルディングブロックとした場合でもカチオンカプセル化架橋なし四量体の形成が期待できる。そこで第二章ではチタン(IV)三置換単量体“$[\alpha\text{-}P_2W_{15}Ti_3O_{62}]^{12-}$”をビルディングブロックとして NH_4^+カチオンがカプセル化された架橋なし四量体$[\{\alpha\text{-}P_2W_{15}Ti_3O_{60.5}\}_4(NH_4)]^{35-}$の合成を行った。

バナジウム(V)やニオブ(V)三置換単量体$[\alpha\text{-}P_2W_{15}M_3O_{62}]^{9-}$ ($M = V^V, Nb^V$)は、その表面負電荷密度が未置換体に比べて増大しているのでカチオン性有機金属種と直接相互作用して、有機金属種担持ポリ酸塩が形成されることが分かっている。最近見出されたチタン(IV)三置換単量体$[\alpha\text{-}P_2W_{15}Ti_3O_{59}(OH)_3]^{9-}$は表面負電荷密度がバナジウム(V)やニオブ(V)三置換単量体よりもさらに増大おり、これまで報告されてきた有機金属種担持ポリ酸塩とは違った性質や構造を有するポリ酸塩の形成が期待できる。そこで第三章では、チタン(IV)三置換単量体$[\alpha\text{-}P_2W_{15}Ti_3O_{59}(OH)_3]^{9-}$と$[Cp^*RhCl_2]_2$の反応を行い、2 つの Dawson unit $[\alpha\text{-}P_2W_{15}Ti_3O_{60}(OH)_2]^{10-}$を 2 つの Cp*Rh で架橋した新規化合物の 2 : 2 型二量体$[\{\alpha\text{-}P_2W_{15}Ti_3O_{60}(OH)_2\}_2(Cp^*Rh)_2]^{16-}$の合成と構造解析を行った。

またチタン(IV)置換体ではないが、関連化合物としてジルコニウム(IV)/ハフニウム(IV)含有ポリ酸塩の構造についても成果が得られているので、Appendix に加えた。

Chapter 1

Synthesis and Structure of Mono-titanium(IV)-substituted Keggin-type Polyoxometalates

この章は、論文

"Monomer and Dimer of Mono-titanium(IV)-Containing α-Keggin Polyoxometalates: Synthesis, Molecular Structures, and pH-Dependent Monomer-Dimer Interconversion in Solution"

Y. Matsuki, Y. Mouri, Y. Sakai, S. Matsunaga, K. Nomiya, *Eur. J. Inorg. Chem.* **2013**, 1754-1761.

に記述された内容を中心に構成されている。

Abstract

チタン(IV)一置換 Keggin 型ポリ酸塩は C. L. Hill、O. A. Kholdeeva らによって合成され、単量体と二量体種の平衡が報告されている。[37-39] その中で二量体は μ-OH で Keggin unit が連結された構造$[(\alpha\text{-}PW_{11}TiO_{39})_2OH]^{7-}$と μ-O で Keggin unit が連結された構造$[(\alpha\text{-}PW_{11}TiO_{39})_2O]^{8-}$を報告している。しかし、いずれの二量体も X 線構造解析は行われておらず、その構造の確証は得られていない。

一方、α_2-チタン(IV)一置換 Dawson 型ポリ酸塩は当研究室の S. Yoshida らによって合成され、単量体と二量体種の平衡が報告されている。[42] その中で二量体は μ-O で Dawson unit が連結された構造$[(\alpha_2\text{-}P_2W_{17}TiO_{61})_2O]^{14-}$とさらに稜共有 Ti-O-W の酸素にプロトネーションした構造$[(\alpha_2\text{-}P_2W_{17}TiO_{61})(\alpha_2\text{-}P_2W_{17}TiO_{61}H)O]^{13-}$の二種類が X 線構造解析されている。

本章では Keggin 型ポリ酸塩一欠損種$[\alpha\text{-}PW_{11}O_{39}]^{7-}$と $TiCl_4$ との反応を行い、チタン(IV)一置換 Keggin 型ポリ酸塩単量体および二量体を合成し、X 線構造解析により構造を決めた。その合成法、各種キャラクタリゼーションの結果について報告する。

1-1. Reagents / Analytical Procedures

Reagents

ISOTEC

Deuterium oxide	D_2O
Acetonitrile-d_3	CD_3CN

Wako:

Titanium(IV) Chloride	$TiCl_4$
Diethylammonium Chloride	Et_2NH_2Cl
Sodium Acetate	CH_3COONa
Methanol	CH_3OH
Ethanol	EtOH
Diethyl ether	Et_2O
Dimethyl sulfoxide	$(CH_3)_2SO$
1 mol/L Hydrochloric Acid	HCl
6 mol/L Hydrochloric Acid	HCl

$K_7[\alpha\text{-}PW_{11}O_{39}]\cdot 8H_2O$ は文献 [58)]を参考に合成した。

Analytical Procedures

CHN elemental Analysis:

PerkinElmer 2400 Series II CHNS/O Elemental Analyzer

TG/DTA:

Rigaku Thermo Plus 2 Series TG/DTA TG 8120

under air, room temperature to 500 ºC, 4 ºC/min.

FT-IR:

Jasco FT/IR-4100 Spectrometer

KBr disks, under air, room temperature

Solid-state Cross-Polarization Magic-Angle-Spinning (CPMAS) NMR:

JEOL JNM-ECP 300 FT-NMR spectrometer

^{31}P (121.00 MHz) 6 mm o.d. rotors, $(NH_4)_2HPO_4$ (δ = 1.6, external standerd)

Solution NMR:

JEOL JNM-ECS 400 FT-NMR spectrometer

^{31}P (160.00 MHz) 5 mm o. d. tubes, 25 % H_3PO_4 *aq*. (δ = 0, external standerd)

JEOL JNM-ECP 500 FT-NMR spectrometer

^{183}W (20.00 MHz) 10 mm o. d. tubes, a saturated Na_2WO_4/D_2O solution. (δ = 0, external standerd)

X-ray Crystallography:

Bruker AXS SMART APEX CCD diffractometer (Mo-Kα, λ = 0.701069 Å)

mounted on cryoloop using liquid paraffin, cooled by N_2 gas

direct methods (SHELXS-97), full-matrix least-squares procedure on F^2 (SHELXL-97)

1-2. Synthesis

1-2-1. $(Et_2NH_2)_5[\alpha\text{-}PW_{11}TiO_{40}]\cdot 2H_2O$

Procedure:

① $K_7[\alpha\text{-}PW_{11}O_{39}]\cdot 8H_2O$ (M.W. = 3076.95) 2.0 g (0.65 mmol)を H_2O 20 mL に溶解した。
(無色透明溶液)

② NaOAc (M.W. = 82.03) 0.11 g (1.34 mmol)を加えた。 (無色透明溶液)

③ 氷浴で 15 min 撹拌し $TiCl_4$ 0.08 mL (*ca* 0.7 mmol)を 1 drop/2sec で加えた。
(無色透明溶液)

④ 湯浴上(80 ºC)で 1 hr 撹拌した。 (白色微懸濁溶液)

⑤ メンブランフィルター(JG 0.2 μm)でろ過した。 (無色透明溶液)

⑥ Et_2NH_2Cl (M.W. = 109.60) 3.0 g (27.4 mmol)をゆっくり加えた。 (白色粉体析出)

⑦ ガラスフィルター(P 40)で粉体を回収し、十分吸引乾燥した。 (白色粉体)

⑧ エタノール 10 mL、エーテル 10 mL で各三回洗浄した。

⑨ 凍結乾燥機で 2 hr 真空乾燥した。 (白色粉体: *powder sample*)

Crystallization

⑩ Et_2NH_2Cl (M.W. = 109.60) 0.2 g (1.82 mmol)、NaOAc (M.W. = 82.03) 0.15 g (1.83 mmol)を H_2O 30mL に溶解した。 (無色透明溶液)

⑪ $(Et_2NH_2)_5[\alpha\text{-}PW_{11}TiO_{40}]\cdot 2H_2O$ (M.W. = 3147.83) 2.0 g (0.64 mmol)を加えた。
(無色透明溶液)

⑫ 室温で slow evaporation した。 (3 日後、無色透明柱状結晶析出)

⑬ ガラスフィルター(P16)で結晶を回収し、十分吸引乾燥した。
(結晶性を失い、白色粉体)

⑭ エタノール、エーテル 10 mL で各 2 回洗浄した。

⑮ 凍結乾燥機で 2 hr 真空乾燥した。 (白色粉体: *crystal sample*)

Properties: 白色粉体
H_2O/DMSO (10/1)、H_2O/MeCN (1/3)混合溶媒、H_2O に易溶。MeOH に可溶。EtOH に微溶。E_2O に不溶。

Yield: 1.59 g (77.7 %) (*powder sample*) / 1.42 g (71.3 %) (*crystal sample*)
$(Et_2NH_2)_5[\alpha\text{-}PW_{11}TiO_{40}]\cdot 2H_2O$ (M.W. = 3147.83)(*powder sample*) /
$(Et_2NH_2)_5[\alpha\text{-}PW_{11}TiO_{40}]\cdot 0.4H_2O$ (M.W. = 3119.01)(*powder sample*)での計算値。

Characterization

CHN Elemental Analysis: (*powder sample*)

	C	H	N	P	W	Ti	O	Total
Calc.	7.63	2.05	2.22	0.98	64.24	1.52	21.35	100.00
Found	7.70	1.83	2.15					

Calc. $(Et_2NH_2)_5[\alpha\text{-}PW_{11}TiO_{40}]\cdot 2H_2O = C_{20}H_{64}N_5PW_{11}TiO_{42}$

(*crystal sample*)

	C	H	N	P	W	Ti	O	Total
Calc.	7.70	1.96	2.25	0.99	64.84	1.54	20.72	100.00
Found	7.80	1.87	2.22					

Calc. $(Et_2NH_2)_5[\alpha\text{-}PW_{11}TiO_{40}]\cdot 0.4H_2O = C_{20}H_{60.8}N_5PW_{11}TiO_{40.4}$

TG/DTA: (*powder sample*)

R.T.-199.3 ºC までに 2 個の H_2O に基づく 1.15 %の重量減。

$(Et_2NH_2)_5[\alpha\text{-}PW_{11}TiO_{40}]\cdot 2H_2O$: 1.14 %

(*crystal sample*)

R.T.-57.5 ºC までに 0.4 個の H_2O に基づく 0.23 %の重量減。

$(Et_2NH_2)_5[\alpha\text{-}PW_{11}TiO_{40}]\cdot 0.4H_2O$: 0.23 %

FT-IR: (*powder sample*)

1635(w), 1576(w), 1472(w), 1456(w), 1428(w), 1396(w), 1388(w), 1362(vw), 1307(vw), 1275(vw), 1192(vw), 1159(vw), 1090(m), 1062(m), 964(s), 886(m), 801(vs), 699(m), 656(m), 594(m), 515(m), 492(m) cm^{-1}

(*crystal sample*)

1630(w), 1603(w), 1573(w), 1472(w), 1453(w), 1427(w), 1389(w), 1362(vw), 1327(vw), 1306(vw), 1275(vw), 1192(vw), 1159(vw), 1090(m), 1062(m), 964(s), 886(m), 799(vs), 700(m), 655(m), 594(m), 515(m), 491(m) cm^{-1}

Solid-state CPMAS ^{31}P NMR (R.T.): (*powder sample*)

δ -12.96 ppm

Solution ^{31}P NMR (D_2O/DMSO (10:1 v/v), 23.2 ºC): (*powder sample*)

δ -13.71 ppm

(D_2O/DMSO (10:1 v/v), 23.3 ºC): (*crystal sample*)

δ -13.70 ppm

Solution ^{183}W NMR (D_2O/CD_3CN (1:3 v/v), R.T.): (*powder sample*)

δ -69.51, -69.59 (2W), -101.34 (2W), -110.08, -110.14 (1W), -114.31 (2W), -117.89 (2W), -124.53 (2W) ppm

X-ray Crystallography:

Crystal data and structure refinement for $(Et_2NH_2)_5[\alpha\text{-}PW_{11}TiO_{40}]\cdot 0.4H_2O$

Empirical formula	C0 H0 N0 O44 P Ti0 W12	
Formula weight	2941.17	
Temperature	100(2) K	
Wavelength	0.71073 Å	
Crystal system	Triclinic	
Space group	P-1	
Unit cell dimensions	a = 11.8449(14) Å	α= 104.547(2)°.
	b = 11.8552(14) Å	β= 104.450(2)°.
	c = 13.0038(15) Å	γ = 116.313(2)°.
Volume	1440.8(3) $Å^3$	
Z	1	
Density (calculated)	3.390 Mg/m^3	
Absorption coefficient	23.947 mm^{-1}	
F(000)	1255	
Crystal size	0.28 x 0.07 x 0.05 mm^3	
Theta range for data collection	1.78 to 28.35°.	
Index ranges	-15<=h<=15, -15<=k<=15, -17<=l<=17	
Reflections collected	19883	
Independent reflections	7148 [R(int) = 0.0385]	
Completeness to theta = 28.35°	99.2 %	
Absorption correction	Empirical	
Max. and min. transmission	0.3806 and 0.0570	
Refinement method	Full-matrix least-squares on F^2	
Data / restraints / parameters	7148 / 0 / 259	
Goodness-of-fit on F^2	1.074	
Final R indices [I>2sigma(I)]	R1 = 0.0675, wR2 = 0.2073	
R indices (all data)	R1 = 0.0897, wR2 = 0.2297	
Largest diff. peak and hole	5.650 and -7.119 e.$Å^{-3}$	

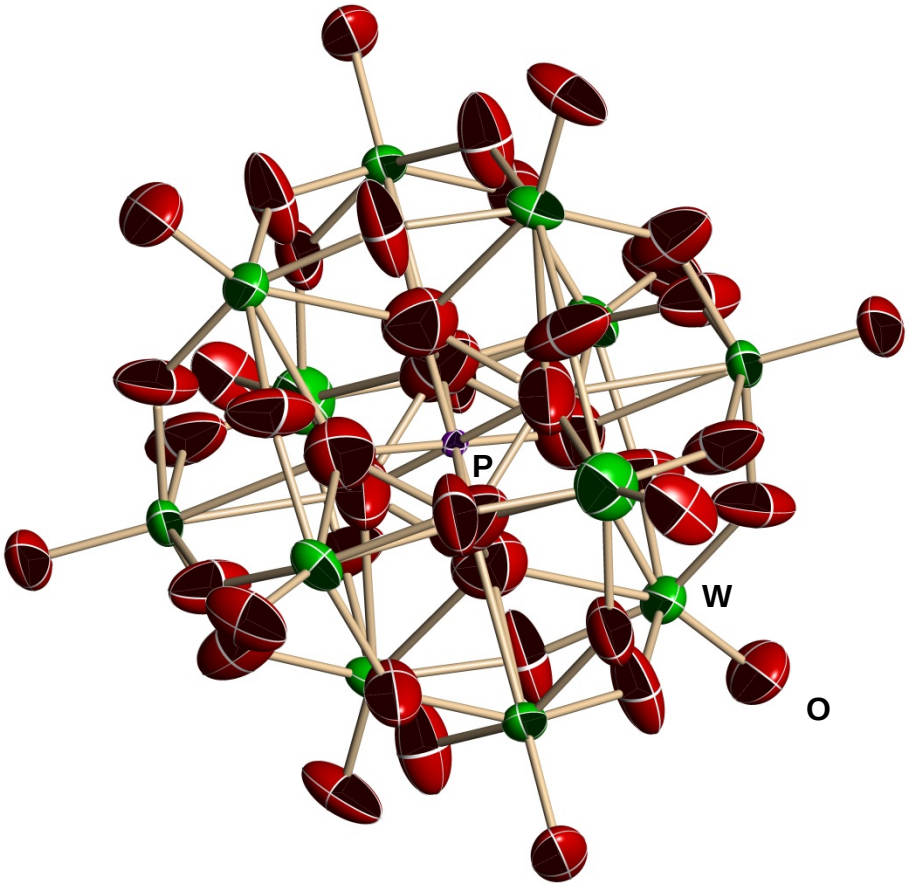

Disorder model of the polyoxoanion $[\alpha\text{-}PW_{11}TiO_{40}]^{5-}$

1-2-2. $(Et_2NH_2)_8[(\alpha\text{-}PW_{11}TiO_{39})_2O]\cdot 6H_2O$

Procedure:

① $(Et_2NH_2)_5[PW_{11}TiO_{40}]\cdot 2H_2O$ (M.W. = 3147.83) 0.5 g (0.16 mmol)を MeOH : H_2O = 1 : 1 混合溶媒 10 mL に溶解した。（無色透明溶液 pH = 4.9 ～ 5.3）

② 1M HCl *aq*. で pH = 1.0 に調整し、2 日間撹拌した。(白色微懸濁溶液)

③ メンブランフィルター(JG 0.2 μm)でろ過した。(無色透明溶液)

④ 室温で slow evaporation した。(3 日後、無色透明板状結晶析出)

⑤ ガラスフィルター(P 16)で結晶を回収し十分吸引乾燥した。(結晶性を失い、白色粉体)

⑥ エタノール、エーテル 10 mL で各 2 回洗浄した。

⑦ 凍結乾燥機で 2 hr 真空乾燥した。(白色粉体)

Properties: 白色粉体

H_2O/DMSO (10/1), H_2O/MeCN (1/3)混合溶媒に易溶。H_2O に微溶。EtOH、Et_2O に不溶。

Yield: 0.32 g (65.3 %)

$(Et_2NH_2)_8[(\alpha\text{-}PW_{11}TiO_{39})_2O]\cdot 6H_2O$ (M.W. = 6167.40)での計算値。

Characterization

CHN Elemental Analysis:

	C	H	N	P	W	Ti	O	Total
Calc.	6.23	1.77	1.82	1.00	65.58	1.55	22.05	100.00
Found	6.31	2.28	1.78					

Calc. $DEA_8[(\alpha\text{-}PW_{11}TiO_{39})_2O]\cdot 6H_2O = C_{32}H_{108}N_8P_2W_{22}Ti_2O_{85}$

TG/DTA:

R.T.-122.5 ºC までに 6 個の H_2O に基づく 1.84 %の重量減。

$(Et_2NH_2)_5[\alpha\text{-}PW_{11}TiO_{40}]\cdot 2H_2O$: 1.75 %

FT-IR:

1620(w), 1469(w), 1451(w), 1389(w), 1205(vw), 1158(vw), 1075(m), 968(s), 889(m), 807(vs), 654(s) , 594(m), 520(m), 499(m) cm^{-1}

Solid-state CPMAS ^{31}P NMR (R.T.):

δ -13.21 ppm

Solution ^{31}P NMR (D_2O/DMSO (10:1 v/v), 23.2 ºC):

δ -13.72, -13.79 ppm

(D_2O/DMSO (10:1 v/v), 23.0 ºC): (after addition of 1 M HCl aq. (0.05 mL, 50 μmol))

δ -13.78 ppm

Solution ^{183}W NMR (D_2O/CD_3CN (1:3 v/v), R.T.):

δ -99.20 (2W), -99.36 (2W), -101.30 (1W), -105.81 (2W), -116.74 (2W), -117.16 (2W) ppm

X-ray Crystallography:

Crystal data and structure refinement for $(Et_2NH_2)_8[(\alpha\text{-}PW_{11}TiO_{39})_2O]\cdot 6H_2O$

Empirical formula	C20 H60 N5 O82 P2 Ti2 W22	
Formula weight	5885.17	
Temperature	100(2) K	
Wavelength	0.71073 Å	
Crystal system	Triclinic	
Space group	P-1	
Unit cell dimensions	a = 11.6856(11) Å	α= 86.9960(10)°.
	b = 21.196(2) Å	β= 79.4420(10)°.
	c = 21.463(2) Å	γ = 78.1580(10)°.
Volume	5114.2(8) $Å^3$	
Z	2	
Density (calculated)	3.822 Mg/m^3	
Absorption coefficient	24.902 mm^{-1}	
F(000)	5146	
Crystal size	0.20 x 0.10 x 0.04 mm^3	
Theta range for data collection	1.81 to 27.50°.	
Index ranges	-15<=h<=15, -27<=k<=27, -27<=l<=27	
Reflections collected	60352	
Independent reflections	23161 [R(int) = 0.0658]	
Completeness to theta = 27.50°	98.6 %	
Absorption correction	Empirical	
Max. and min. transmission	0.4358 and 0.0825	
Refinement method	Full-matrix least-squares on F^2	
Data / restraints / parameters	23161 / 0 / 1158	
Goodness-of-fit on F^2	1.052	
Final R indices [I>2sigma(I)]	R1 = 0.0565, wR2 = 0.1358	
R indices (all data)	R1 = 0.0781, wR2 = 0.1475	
Largest diff. peak and hole	5.604 and -3.024 e.$Å^{-3}$	

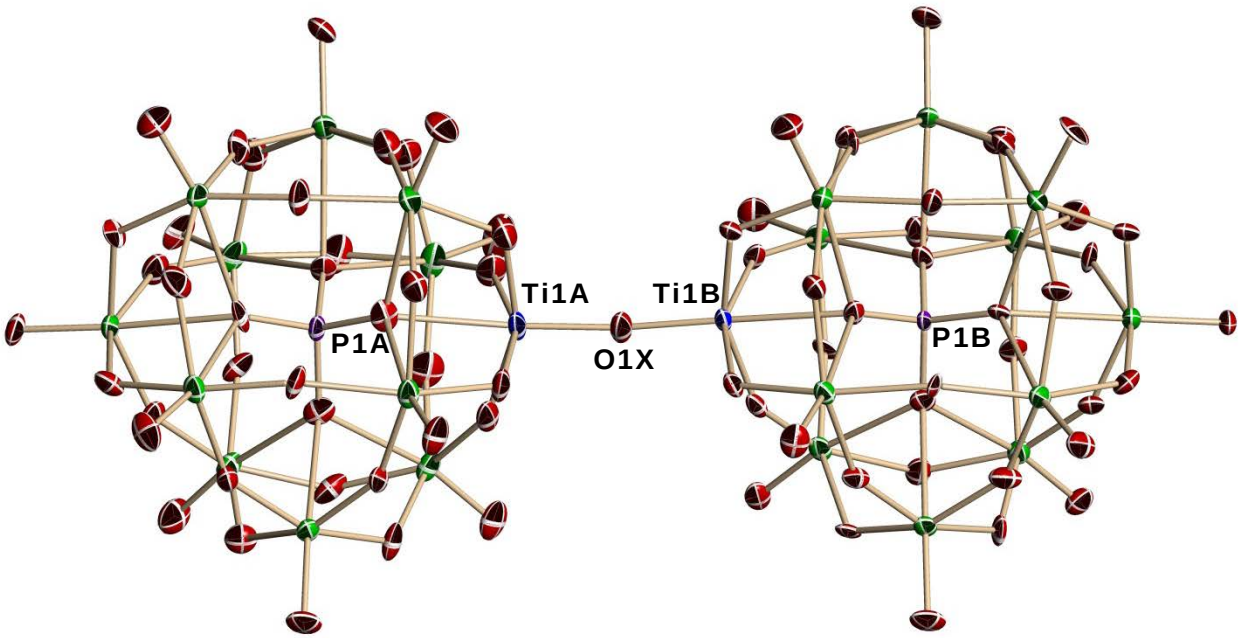

Molecular structure of the polyoxoanion $[(\alpha\text{-}PW_{11}TiO_{39})_2O]^{8-}$

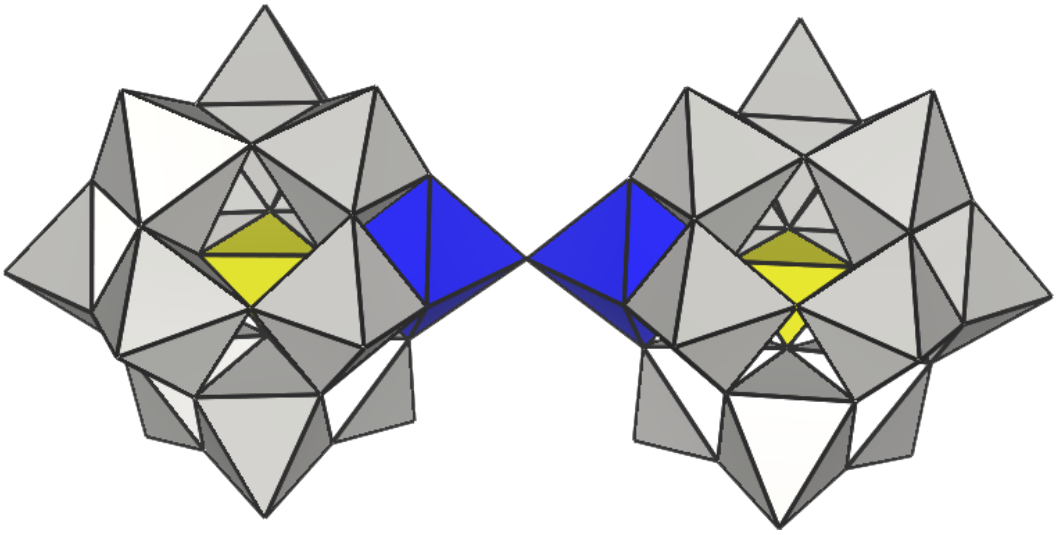

Polyhedral of the polyoxoanion $[(\alpha\text{-}PW_{11}TiO_{39})_2O]^{8-}$

1-3. pH-Varied ^{31}P NMR

Experiment:

① $(Et_2NH_2)_5[PW_{11}TiO_{40}]\cdot 2H_2O$ (M.W. = 3147.83) 0.6 g (0.19 mmol)を H_2O/DMSO (10/1) 混合溶媒 9.9 mL に溶解した。 (無色透明溶液 pH 3.2)

② 1M, 6M HCl *aq.*を用いて pH = X(X = 3.2(未調整), 2.0, 1.5, 1.0, 0.5)に調整した反応溶液の ^{31}P NMR を測定した。

pH	3.2	2.0	1.5	1.0	0.5
溶液の色	無色透明	無色透明	無色透明	無色透明	白色微懸濁

Characterization

Solution ^{31}P NMR (H_2O/DMSO (10:1 v/v), 23.1 ºC): *pH 3.2*

δ -13.72 ppm

(H_2O/DMSO (10:1 v/v), 23.9 ºC): *pH 2.0*

δ -13.72, -13.79 ppm

(H_2O/DMSO (10:1 v/v), 23.5 ºC): *pH 1.5*

δ -13.74, -13.79 ppm

(H_2O/DMSO (10:1 v/v), 23.7 ºC): *pH 1.0*

δ -13.76, -13.78 ppm

(H_2O/DMSO (10:1 v/v), 22.8 ºC): *pH 0.5*

δ -13.78 ppm

1-4. Result and Discussion

Abbreviation:

$(Et_2NH_2)_5[\alpha\text{-}PW_{11}TiO_{40}]\cdot nH_2O$ (n = 0.4, 2) (**EtN-1**)

$(Et_2NH_2)_8[(\alpha\text{-}PW_{11}TiO_{39})_2O]\cdot 6H_2O$ (**EtN-2**)

Experiment

$(Et_2NH_2)_5[\alpha\text{-}PW_{11}TiO_{40}]\cdot nH_2O$ (n = 0.4, 2):

純水中 NaOAc 存在下で Keggin 型ポリ酸塩一欠損種 $K_7[\alpha\text{-}PW_{11}O_{39}]\cdot 8H_2O$ と $TiCl_4$ をモル比 1 : 1 で反応させ、過剰量の Et_2NH_2Cl を加えることで白色粉体を得た(収率 77.7 %)。さらに NaOAc と Et_2NH_2Cl 存在下から slow evaporation することで無色透明柱状結晶を得た(収率 71.3 %)。

$$[\alpha\text{-}PW_{11}O_{39}]^{7-} + Ti^{4+} + H_2O + 2OAc^- \rightarrow [\alpha\text{-}PW_{11}TiO_{40}]^{5-} + 2HOAc$$

$(Et_2NH_2)_8[(\alpha\text{-}PW_{11}TiO_{39})_2O]\cdot 6H_2O$:

純水:メタノール= 1 : 1 混合溶媒にチタン(IV)一置換 Keggin 型ポリ酸塩単量体 $(Et_2NH_2)_5[\alpha\text{-}PW_{11}TiO_{40}]\cdot 2H_2O$ を溶解し、1 M HCl *aq.*で pH = 1.0 に調整し slow evaporation することで無色透明板状結晶を得た(収率 65.3 %)。

$$2[\alpha\text{-}PW_{11}TiO_{40}]^{5-} + 2H^+ \rightarrow [(\alpha\text{-}PW_{11}TiO_{39})_2O]^{8-} + H_2O$$

X-ray Crystallography

$(Et_2NH_2)_5[\alpha\text{-}PW_{11}TiO_{40}]\cdot 0.4H_2O$ (CCDC 906701):

分子構造全体が disorder しているため Ti^{IV} 置換サイトを特定することは出来なかった。しかし、このことから二量体ではなく単量体構造であると考えられる。また、カウンターカチオンおよび結晶水は disorder のためアサインできなかった。

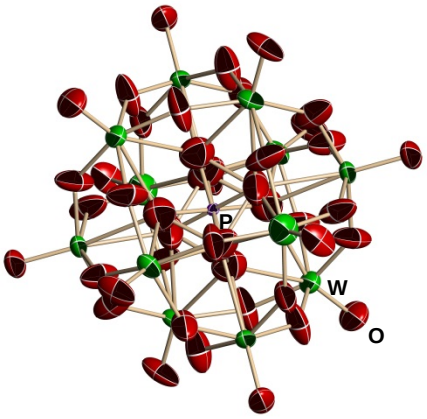

Disorder model of the polyoxoanion $[\alpha\text{-}PW_{11}TiO_{40}]^{5-}$

$(Et_2NH_2)_8[(\alpha\text{-}PW_{11}TiO_{39})_2O]\cdot 6H_2O$ (CCDC 906699):

2 つの Keggin unit が分子間の Ti-O-Ti 結合を介して連結した二量体構造であった。また Keggin unit にわずかな捻じれ(3.85°)がみられ単位格子中にエナンチオマー対が存在した。BVS 計算から架橋酸素原子(O1X)は計算値(2.152)が 2 に近いことから O^{2-} と考えられプロトネーションはしていなかった。また、結晶水とカウンターカチオンは disorder しており、$Et_2NH_2^+$カチオン 5 個と結晶水 3 個をアサインした。

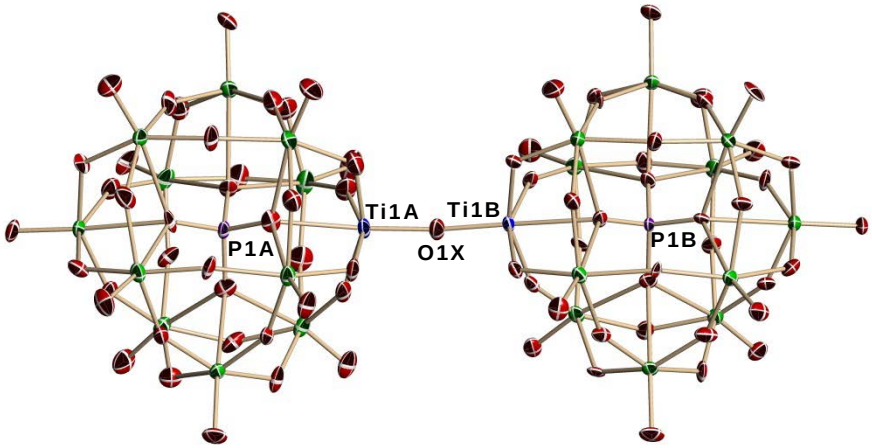

Molecular structure of the polyoxoanion $[(\alpha\text{-}PW_{11}TiO_{39})_2O]^{8-}$

CHN Elemental Analysis and TG/DTA

$(Et_2NH_2)_5[\alpha\text{-}PW_{11}TiO_{40}]\cdot 0.4H_2O$:

ポリ酸アニオン 1 つに $Et_2NH_2^+$カチオン 5 つ、TG/DTA で観測された結晶水 0.4 個を加えた組成で計算値と実測値が一致した。このことから Ti^{IV} の末端酸素は OH^-ではなく O^{2-}であると考えられる。

	C	H	N	P	W	Ti	O	Total
Calc.	7.70	1.96	2.25	0.99	64.84	1.54	20.72	100.00
Found	7.80	1.87	2.22					
Calc.	$(Et_2NH_2)_5[\alpha\text{-}PW_{11}TiO_{40}]\cdot 0.4H_2O = C_{20}H_{60.8}N_5PW_{11}TiO_{40.4}$							

Weight loss	0.23 % below 57.5 °C
Calcd.	0.23 % for $0.4H_2O$

$(Et_2NH_2)_8[(\alpha\text{-}PW_{11}TiO_{39})_2O]\cdot 6H_2O$:

単結晶 X 線構造解析で確認されたポリ酸アニオン 1 つに $Et_2NH_2^+$カチオン 8 つ、TG/DTA で観測された結晶水 6 個を加えた組成で計算値と実測値が一致した。このことからも Keggin unit 間の架橋酸素は OH^-ではなく O^{2-}であると考えられる。

	C	H	N	P	W	Ti	O	Total
Calc.	6.23	1.77	1.82	1.00	65.58	1.55	22.05	100.00
Found	6.31	2.28	1.78					
Calc.	$DEA_8[(\alpha\text{-}PW_{11}TiO_{39})_2O]\cdot 6H_2O = C_{32}H_{108}N_8P_2W_{22}Ti_2O_{85}$							

Weight loss	1.84 % below 122.5 °C
Calcd.	1.75 % for $6H_2O$

Solid-State CPMAS ^{31}P NMR and Solution ^{31}P NMR

固体状態で **EtN-1** は-12.96 ppm に一本線ピークで観測され、**EtN-2** は-13.21 ppm に一本線ピークで観測された。**EtN-2** は **EtN-1** よりも高磁場側に観測された。

D_2O/DMSO (10/1)混合溶媒中で **EtN-1** は-13.70 ppm に一本線ピークで観測され、**EtN-2** は-13.72, -13.79 ppm に二本線でピークが観測され、そこへ HCl を添加すると -13.78 ppm に一本線ピークが観測された。固体状態で **EtN-2** が一本線で観測されていることから H_2O による加水分解が起きており、pH に依存した平衡があると考えられる。さらに HCl を添加することで一本線で観測されたことから、酸によって平衡が二量体側に偏ったものと考えられる。

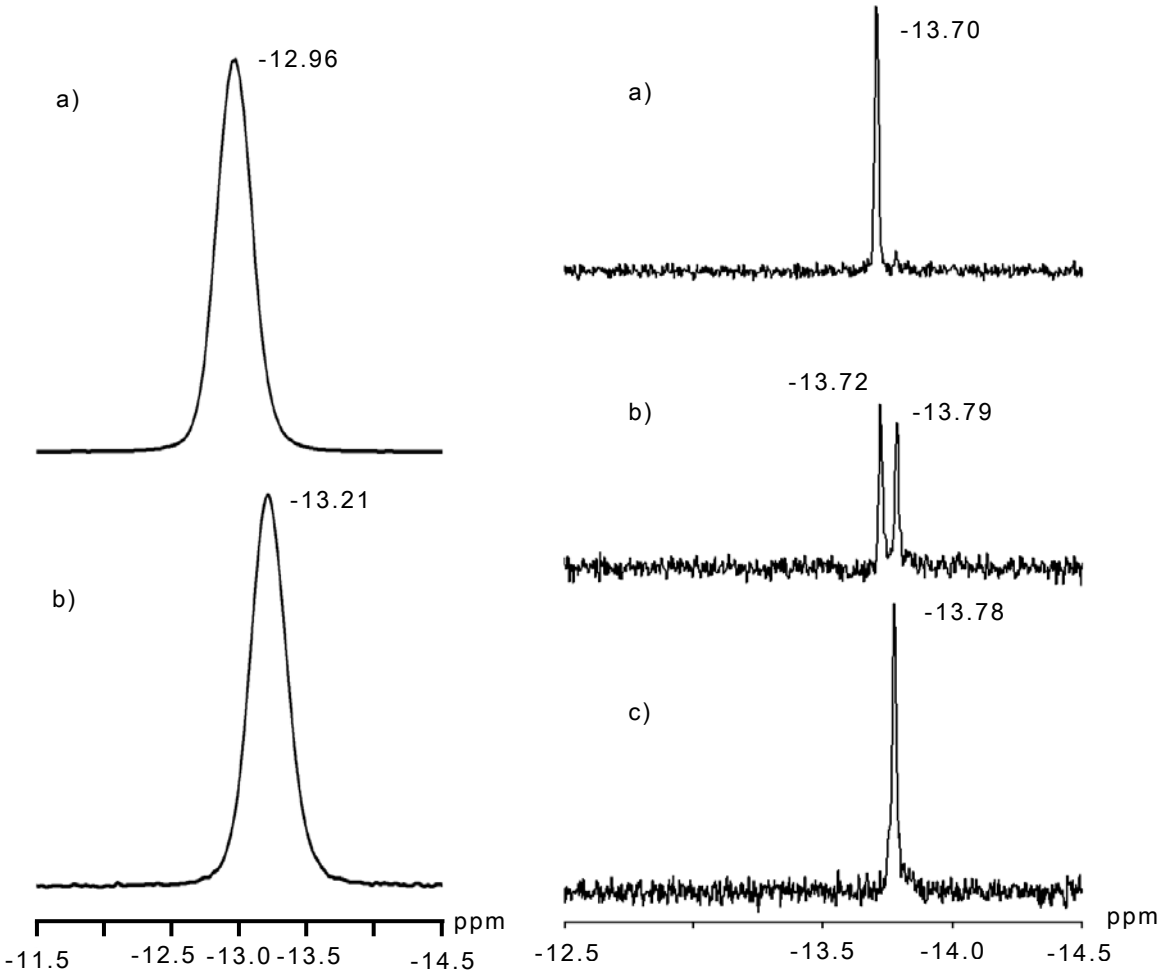

Solid-state CPMAS ^{31}P (left) and Solution ^{31}P (right) NMR spectra a) **EtN-1**, b) **EtN-2**, c) **EtN-2** + 1M HCl *aq*. (50 μL)

Solution ^{183}W NMR

D_2O/CD_3CN (1/3)混合溶媒中で **EtN-1** は単量体の対称性(*C*s)に基づく 2 : 2 : 1 : 2 : 2 : 2 の六本線ピークで観測された。一方 **EtN-2** は二量体の対称性(C_{2V})に基づく 2 : 2 : 1 : 2 : 2 : 2 の六本線ピークで観測された。D_2O/CD_3CN (1/3)混合溶媒中では **EtN-1** と **EtN-2** はそれぞれ固体構造を維持しているものと考えられる。

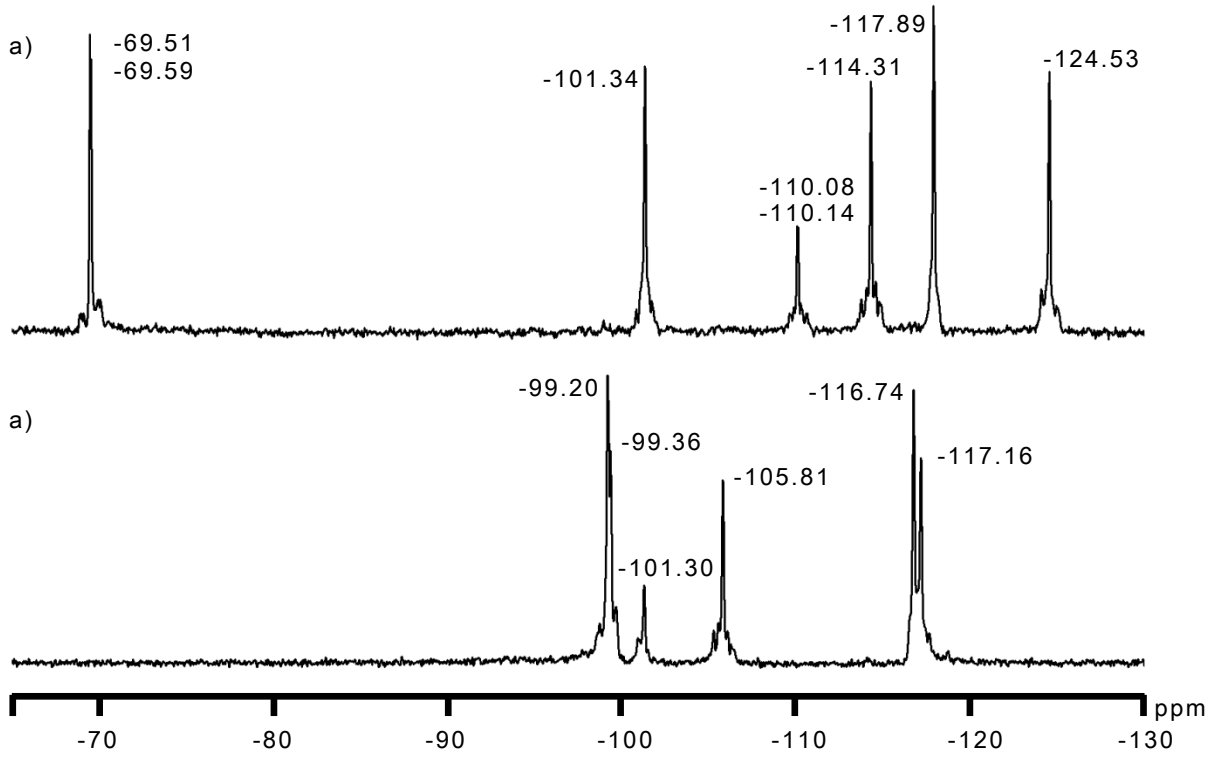

Solution ^{31}P NMR spectra a) **EtN-1**, b) **EtN-2**

FT-IR

EtN-1 は P-O に基づく振動バンドが二本線で観測され、Keggin unit 間の Ti-O-Ti 結合に基づく振動バンドが観測されなかった。一方で **EtN-2** は P-O に基づく振動バンドが一本線で観測され、Keggin unit 間の Ti-O-Ti 結合に基づく振動バンドが観測された。このことから **EtN-1** は単量体構造であり、**EtN-2** は二量体構造であると考えられる。

	P-O	W-O	Ti-O-Ti
EtN-1	1090, 1062	964, 886, 801	—
EtN-2	1075	968, 889, 807	654

pH-Varied ^{31}P NMR

H_2O/DMSO (10/1)混合溶媒中で pH 3.2 (未調整)では **EtN-1** は-13.72 ppm に一本線で観測され、pH 2.0 で-13.79 ppm に二量体のピークが観測され始め、pH 0.5 で二量体のみとなった。しかし、α_2-チタン(IV)一置換 Dawson 型ポリ酸塩とは異なり [1d]、pH 0.5 で二量体プロトネーション種の生成は確認できなかった。

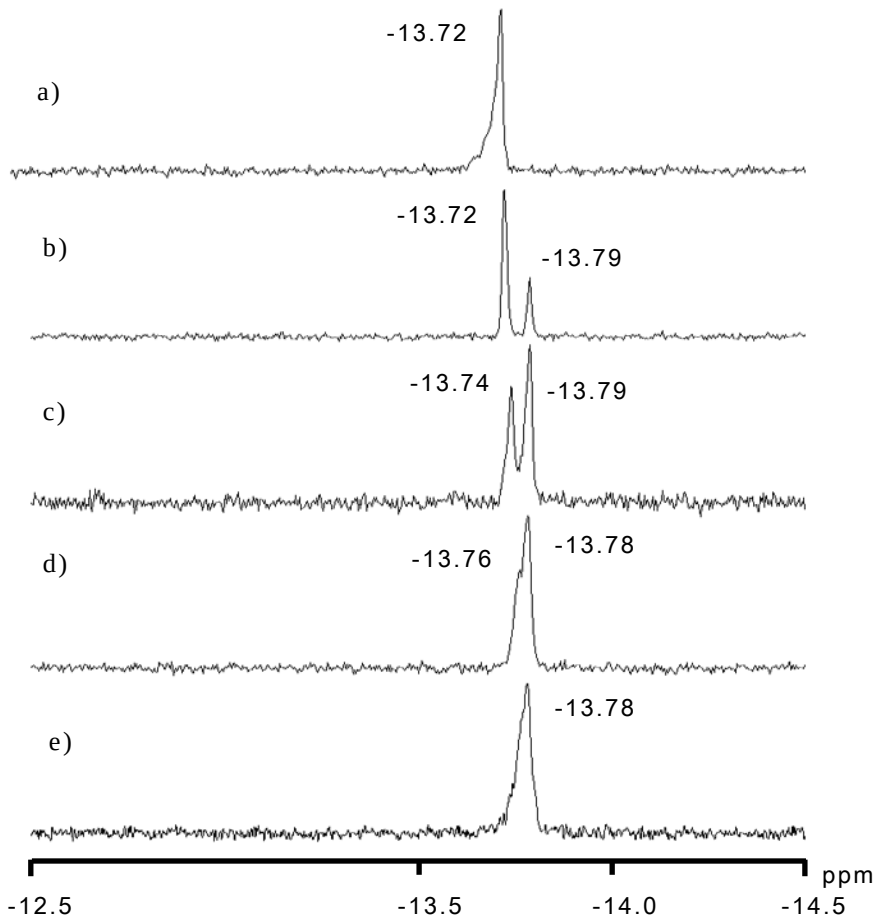

pH-varied ^{31}P NMR of **EtN-1** in H_2O/DMSO (10/1); pH (a) 3.2 (unadjusted); (b) 2.0; (c) 1.5; (d) 1.0; (e) 0.5

1-5. Conclusion

NaOAc 存在下で Keggin 型ポリ酸塩一欠損種$[\alpha\text{-}PW_{11}O_{39}]^{7-}$と Ti^{4+}の反応からチタン(IV)一置換 Keggin 型ポリ酸塩単量体$[\alpha\text{-}PW_{11}TiO_{40}]^{5-}$を合成し、この単量体から二量体$[(\alpha\text{-}PW_{11}TiO_{39})_2O]^{8-}$を誘導する過程で、世界で初めて二量体の結晶化に成功し、単結晶 X 線構造解析を行った。一度粉体で単離した二量体を結晶化させることは出来ないので、この方法に originality がある。また単量体についても結晶化条件を見つけ単結晶 X 線構造解析を行った。

X 線構造解析で単量体は disorder しておりチタン(IV)置換サイトを決めることは出来なかったが、単量体構造であることを確認した。一方、二量体は Keggin unit 間を Ti-O-Ti 結合で連結した構造であり、BVS 計算から Keggin unit 間の架橋酸素原子が O^{2-}であり μ-OH ではないことを確認した。

pH を変えた ^{31}P NMR 測定から pH 3.2 で単量体、pH 0.5 で二量体に変換されることが分かった。また、α_2-チタン(IV)一置換 Dawson 型ポリ酸塩とは異なり、pH 0.5 でも二量体のプロトネーション種の生成は確認できなかった。

Chapter 2

Synthesis of monomeric, tri-titanium(IV)-substituted Dawson polyoxometalate and derivation of its non-bridging tetrameric species with encapsulated NH_4^+ in the central cavity

この章は、論文
"Encapsulation of Anion/Cation in the Central Cavity of Tetrameric Polyoxometalate, Composed of Four Trititanium(IV)-Substituted α-Dawson Subunits, Initiated by Protonation/Deprotonation of the Bridging Oxygen Atoms on the Intramolecular Surface"
Y. Sakai, S. Ohta, Y. Shintoyo, S. Yoshida, Y. Taguchi, Y. Matsuki, S. Matsunaga, K. Nomiya, *Inorg. Chem.* **2011**, *50*, 1754-1761.
に記述された内容を中心に構成されている。

Abstract

Dawson 型ポリ酸塩三欠損種と Ti^{IV} の反応から直接チタン(IV)三置換単量体は得られないが、二種類のテトラポッド型チタン(IV)三置換 Dawson 型ポリ酸塩四量体 (架橋あり、架橋なし) が合成され、構造解析が行われている。[43] 架橋あり四量体は Dawson unit が架橋チタンを介して縮合した構造 $[\{\alpha\text{-}P_2W_{15}Ti_3O_{59}(OH)_3\}_4\{\mu_3\text{-}Ti(OH_2)_3\}_4X]^{21-}$ (X = Cl, Br, I, NO_3) で、架橋なし四量体は Dawson unit が直接縮合した構造 $[\{\alpha\text{-}P_2W_{15}Ti_3O_{57.5}(OH)_3\}_4Cl]^{25-}$ であり、これらの四量体は中心空間にアニオンをカプセル化している。また、Cl^-カプセル化架橋あり四量体と H_2O_2 との反応からペルオキソ配位チタン(IV)三置換 Dawson 型ポリ酸塩単量体 $[\alpha\text{-}P_2W_{15}(TiO_2)_3O_{56}(OH)_3]^{9-}$ が得られることが分かった。[44] このペルオキソ配位単量体は熱によりペルオキソ基が容易に分解し、それをビルディングブロックとして NH_4^+カチオンがカプセル化した架橋なし四量体 $[(\alpha\text{-}P_2W_{15}Ti_3O_{60.5})_4(NH_4)]^{35-}$ を形成することが分かった。[45] さらに、このカチオンカプセル化架橋なし四量体はアニオンカプセル化架橋なし四量体の中心空間の 12 個の Ti-OH-Ti 結合の H^+を塩基で脱プロトン化することでも誘導できる。

本章では Cl^-カプセル化架橋あり四量体と NaOH の反応からペルオキソ基の配位していないチタン(IV)三置換 Dawson 型ポリ酸塩単量体"$[\alpha\text{-}P_2W_{15}Ti_3O_{62}]^{12-}$"を得て、それをビルディングブロックとして NH_4^+カチオンがカプセル化した架橋なし四量体の誘導を行なった。その方法と各種キャラクタリゼーションの結果について報告する。

本研究は坂井、太田らとの共同研究の一部として行われた。

2-1. Reagents / Analytical Procedures

Reagents

ISOTEC

Deuterium oxide	D_2O

Wako:

Sodium Chloride	NaCl
Ammonium Chloride	NH_4Cl
Ethanol	EtOH
Diethyl ether	Et_2O
1 mol/L Sodium Hydroxide Solution	NaOH
0.1 mol/L Hydrochloric Acid	HCl

$Na_{19}H_2[\{\alpha\text{-}P_2W_{15}Ti_3O_{59}(OH)_3\}_4\{\mu_3\text{-}Ti(H_2O)_3\}_4Cl]\cdot 124H_2O$ は文献[43b)]を参考に合成した。

Analytical Procedures

CHN elemental Analysis:

PerkinElmer 2400 Series II CHNS/O Elemental Analyzer

TG/DTA:

Rigaku Thermo Plus 2 Series TG/DTA TG 8120

under air, room temperature to 500 ºC, 4 ºC/min.

FT-IR:

Jasco FT/IR-4100 Spectrometer

KBr disks, under air, room temperature

Solution NMR:

JEOL JNM-EX 400 FT-NMR spectrometer

^{31}P (161.70 MHz) 5 mm o. d. tubes, 25 % H_3PO_4 *aq*. (δ = 0, external standerd)

2-2. Synthesis

2-2-1. "$Na_{12}[\alpha\text{-}P_2W_{15}Ti_3O_{62}]\cdot 28H_2O$"

Procedure:

① $Na_{19}H_2[\{\alpha\text{-}P_2W_{15}Ti_3O_{59}(OH)_3\}_4\{\mu_3\text{-}Ti(H_2O)_3\}_4Cl]\cdot 124H_2O$ (M.W. = 18947.91) 4.8 g (0.253 mmol) を H_2O 20 mL に溶解した。 (無色透明溶液)

② この溶液に 1 M NaOH *aq.*を加えて pH 9.0 に調整した。[#1)] (無色透明溶液)

③ NaCl (MW : 58.44) 8.0 g (0.137 mol)を加え、1 hr 撹拌した。 (白色粉体析出)

④ メンブランフィルター(JG 0.2 μm)で回収し EtOH 30 mL、Et_2O 50 mL で各 3 回洗浄した。 (白色粉体)

⑤ 凍結乾燥機で 2 hr 乾燥した。 (白色粉体)

Note

#1) pH 9.0 で安定するまで、*ca.* 3 hr かかった。

Properties: 白色粉体

H_2O に可溶。EtOH、E_2O に不溶。

Yield: 2.0 g (41.7 %)

"$Na_{12}[\alpha\text{-}P_2W_{15}Ti_3O_{62}]\cdot 28H_2O$" (M.W. = 4735.46)での計算値。

Characterization

TG/DTA:

R.T.-307.6 ºC までに 28 個の H_2O に基づく 10.75 %の重量減。

“$Na_{12}[\alpha\text{-}P_2W_{15}Ti_3O_{62}]\cdot 28H_2O$”: 10.65 %

FT-IR:

1631(s), 1088(s), 1051(m), 1014(m), 941(vs), 914(vs), 825(vs), 742(vs), 599(s), 562(s), 525(s), 463(s) cm^{-1}

Solution ^{31}P NMR (D_2O, 22.9 ºC):

δ -4.94, -14.61 ppm

2-2-2. $(NH_4)_{21}Na_{14}[(P_2W_{15}Ti_3O_{60.5})_4(NH_4)]\cdot 70\ H_2O$

Procedure:

① "$Na_{12}[\alpha\text{-}P_2W_{15}Ti_3O_{62}]\cdot 22H_2O$" (M.W. = 4627.25) 0.5 g (0.11 mmol)を H_2O 12 mL に溶解し、30 min 撹拌した。 (pH 9.9 , 無色透明溶液)

② NH_4Cl (M.W. = 53.49) 0.06 g (1.12 mmol)を加えた。(pH 8.4 , 無色透明溶液)

③ 0.1 M HCl *aq.*で pH 6.0 に調整した。 (無色透明溶液)

④ 湯浴上(80 ºC)で 30 min 撹拌した。 (無色透明溶液)

⑤ evaporator (30 ºC)で粉体が析出するまで濃縮した。 (白色粉体析出)

⑥ H_2O 1 mL を加え、湯浴上(35 ºC)で撹拌した。 (無色透明溶液)

⑦ 35 ºC から室温までゆっくりと放冷した。 (無色透明針状結晶析出)

⑧ メンブランフィルター(JG 0.2 μm)で回収し EtOH 10 mL、Et_2O 50 mL で各 3 回洗浄した。 (結晶性を失い白色粉体)

⑨ 凍結乾燥機で 2 hr 乾燥した。 (白色粉体)

Properties: 白色粉体

H_2O に可溶。EtOH、Et_2O に不溶。

Yield: 0.067 g (14.3 %)

$(NH_4)_{21}Na_{14}[(\alpha\text{-}P_2W_{15}Ti_3O_{60.5})_4(NH_4)]\cdot 70\ H_2O$ (M.W. = 17704.38)での計算値。

Characterization

CHN Elemental Analysis:

	C	H	N	Na	P	W	Ti	O	Total
Calc.	0	1.30	1.74	1.82	1.40	62.30	3.25	28.20	100.01
Found	0.16	0.72	1.75						

Calc. $(NH_4)_{21}Na_{14}[(\alpha\text{-}P_2W_{15}Ti_3O_{60.5})_4(NH_4)]\cdot 70\ H_2O = H_{228}N_{22}P_8W_{60}Ti_{12}O_{312}$

TG/DTA:

R.T.-500.0 ºC までに 70 個の H_2O と 22 個の NH_4 に基づく 9.70 %の重量減。

$(NH_4)_{21}Na_{14}[(\alpha\text{-}P_2W_{15}Ti_3O_{60.5})_4(NH_4)]\cdot 70\ H_2O$: 9.71 % = (2.46 ($NH_4$) + 7.25 ($H_2O$))

FT-IR:

1620(w), 1469(w), 1451(w), 1389(w), 1205(vw), 1158(vw), 1075(m), 968(s), 889(m), 807(vs), 654(s) , 594(m), 520(m), 499(m) cm^{-1}

Solution ^{31}P NMR (D_2O, 21.5 ºC):

δ -7.21, -14.20 ppm

2-3. Result and Discussion

Abbreviation:

"$Na_{12}[\alpha\text{-}P_2W_{15}Ti_3O_{62}]\cdot 28H_2O$" (**Na-1**)

$(NH_4)_{21}Na_{14}[(\alpha\text{-}P_2W_{15}Ti_3O_{60.5})_4(NH_4)]\cdot 70\ H_2O$ (**NH_4Na-2**)

$(NH_4)_{27}Na_8[(\alpha\text{-}P_2W_{15}Ti_3O_{60.5})_4(NH_4)]\cdot ca.\ 90\ H_2O$ (**NH_4Na-2^P**)

(**NH_4Na-2^P** was synthesized from $[\alpha\text{-}P_2W_{15}(TiO_2)_3O_{56}(OH)_3]^{9-}$ as reference work)

Experiment

"$Na_{12}[\alpha\text{-}P_2W_{15}Ti_3O_{62}]\cdot 28H_2O$":

純水中で Cl^-カプセル化チタン(IV)三置換 Dawson 型ポリ酸塩架橋あり四量体 $Na_{19}H_2[\{\alpha\text{-}P_2W_{15}Ti_3O_{59}(OH)_3\}_4\{\mu_3\text{-}Ti(H_2O)_3\}_4Cl]\cdot 124H_2O$ を NaOH で加水分解させ、過剰量の NaCl を加えることで白色粉体を得た(収率 41.7 %)。

$$[\{\alpha\text{-}P_2W_{15}Ti_3O_{59}(OH)_3\}_4\{\mu_3\text{-}Ti(H_2O)_3\}_4Cl]^{21-} + 12OH^- \rightarrow 4\ "[\alpha\text{-}P_2W_{15}Ti_3O_{62}]^{12-}" + 4[Ti(H_2O)_6]^{4+} + Cl^-$$

$(NH_4)_{21}Na_{14}[(\alpha\text{-}P_2W_{15}Ti_3O_{60.5})_4(NH_4)]\cdot 70\ H_2O$:

純水中で NH_4^+存在下、チタン(IV)三置換 Dawson 型ポリ酸塩単量体 "$Na_{12}[\alpha\text{-}P_2W_{15}Ti_3O_{62}]\cdot 22H_2O$"を HCl で脱水縮合させ、加熱濃縮することで無色透明針状結晶を得た(収率 14.3 %)。

$$4"[\alpha\text{-}P_2W_{15}Ti_3O_{62}]^{12-}" + NH_4^+ + 12H^+ \rightarrow [(\alpha\text{-}P_2W_{15}Ti_3O_{60.5})_4(NH_4)]^{35-} + 6H_2O$$

CHN Elemental Analysis and TG/DTA

$(NH_4)_{21}Na_{14}[(\alpha\text{-}P_2W_{15}Ti_3O_{60.5})_4(NH_4)]\cdot 70\ H_2O$:

ポリ酸アニオン 1 つに NH_4^+カチオン 21 個、TG/DTA で観測された結晶水 70 個を加えた組成で計算値と実測値が一致した。

	C	H	N	Na	P	W	Ti	O	Total
Calc.	0	1.30	1.74	1.82	1.40	62.30	3.25	28.20	100.01
Found	0.16	0.72	1.75						

Calc. $(NH_4)_{21}Na_{14}[(\alpha\text{-}P_2W_{15}Ti_3O_{60.5})_4(NH_4)]\cdot 70\ H_2O = H_{228}N_{22}P_8W_{60}Ti_{12}O_{312}$

Weight loss	9.70 % below 500.0 °C
Calcd.	9.71 % for $70H_2O$ and $21NH_4$

FT-IR

Na-1 は P-O に基づく振動バンドが二本線で観測され、Dawson unit 間の Ti-O-Ti 結合に基づく振動バンドが観測されず、単量体構造であると考えられる。一方で **NH_4Na-2** は P-O に基づく振動バンドが一本線で観測され、Dawson unit 間の Ti-O-Ti 結合に基づく振動バンドが観測され、オリゴマー構造であると考えられる。また前駆体にペルオキソ配位単量体を用いて合成されたものと比較して、ほぼ変わらない振動バンドのパターンで観測されたことから、四量体構造であると考えられる。

	P-O	W-O	Ti-O-Ti
Na-1	1087, 1050	942, 913, 823, 741	—
NH_4Na-2	1086	944, 914, 892, 829, 779	683
NH_4Na-2^P	1086	943, 912, 831, 785	687

Solution ^{31}P NMR

D_2O 中で **Na-1** は-4.94, -14.61 ppm に二本線ピークで観測された。四量体種の化学シフトと比較して、低磁場側のピークが低磁場側へ大きく離れた位置に観測されており、O_2^{2-}配位単量体のピークに近いことから **Na-1** は単量体構造と考えられる。**NH_4Na-2** は-7.21, -14.20 ppm に二本線ピークで観測され、O_2^{2-}配位単量体から合成したものとほぼ同じ位置に観測された。このことから **NH_4Na-2** は NH_4^+カチオンをカプセル化した架橋なし四量体と考えられる。

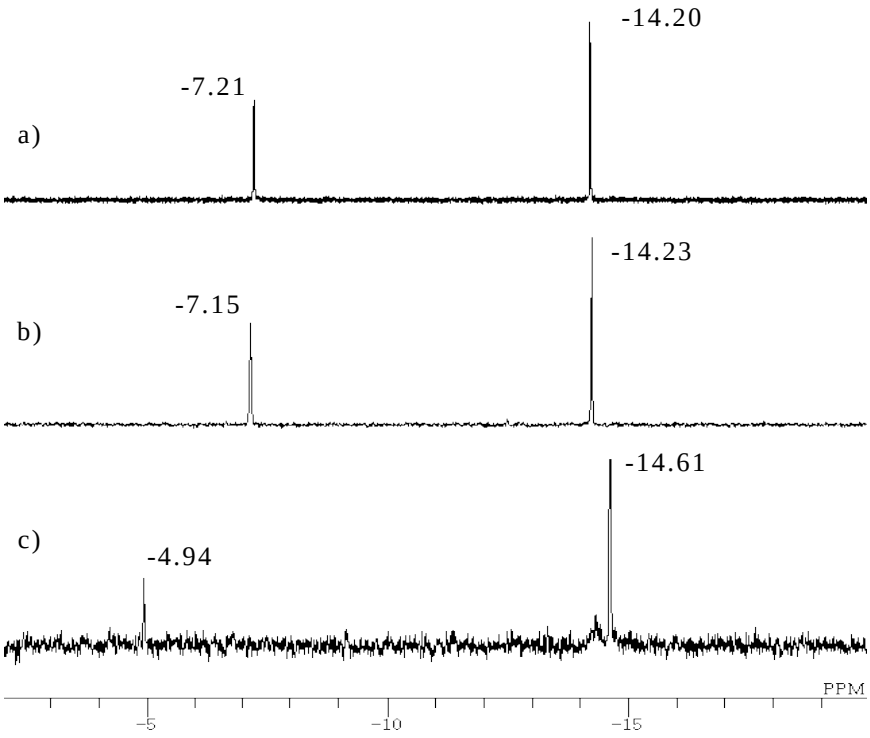

Solution ^{31}P NMR spectra a) **NH_4Na-2**, b) **NH_4Na-2^P**, c) **Na-1**

	P (low)	P (high)
架橋あり(Cl)	-7.04	-13.77
架橋なし(Cl)	-7.65	-13.90
O_2^{2-}配位単量体	-3.95	-14.43

X-ray crysrallography[45)]

Crystal data and structure refinement for $(NH_4)_{27}Na_8[(\alpha\text{-}P_2W_{15}Ti_3O_{60.5})_4(NH_4)]\cdot ca.\ 90H_2O$ (**$NH_4Na\text{-}2^P$**)

Empirical formula	H203 N19 O297 P8 Ti12 W60	
Formula weight	17076.38	
Temperature	273(2) K	
Wavelength	0.71073 Å	
Crystal system	Triclinic	
Space group	P-1	
Unit cell dimensions	a = 24.894(7) Å	α = 79.227(5)°.
	b = 38.246(11) Å	β = 88.597(5)°.
	c = 38.981(11) Å	γ = 87.413(5)°.
Volume	36418(18) $Å^3$	
Z	4	
Density (calculated)	3.114 Mg/m^3	
Absorption coefficient	19.240 mm^{-1}	
F(000)	30144	
Crystal size	0.22 x 0.08 x 0.06 mm^3	
Theta range for data collection	0.97 to 28.47°.	
Index ranges	-31<=h<=33, -50<=k<=46, -51<=l<=51	
Reflections collected	353666	
Independent reflections	166997 [R(int) = 0.0856]	
Completeness to theta = 28.47°	90.7 %	
Absorption correction	Empirical	
Refinement method	Full-matrix-block least-squares on F^2	
Data / restraints / parameters	166997 / 21990 / 6265	
Goodness-of-fit on F^2	1.041	
Final R indices [I>2sigma(I)]	R1 = 0.0830, wR2 = 0.1917	
R indices (all data)	R1 = 0.1587, wR2 = 0.2311	
Largest diff. peak and hole	11.717 and -6.005 e. $Å^{-3}$	

チタン(IV)三置換 Dawson 型ポリ酸塩単量体“$[\alpha\text{-}P_2W_{15}Ti_3O_{62}]^{12-}$”から合成した NH_4^+ カプセル化チタン(IV)三置換 Dawson 型ポリ酸単架橋なし四量体 $[(P_2W_{15}Ti_3O_{60.5})_4(NH_4)]^{35-}$ の結晶は X 線構造解析に適していなかった。しかし、ペルオキソチタン(IV)三置換 Dawson 型ポリ酸塩単量体 $[P_2W_{15}(TiO_2)_3O_{56}(OH)_3]^{9-}$ から合成した NH_4^+ カプセル化種(**$NH_4Na\text{-}2^P$**)の X 線構造解析には成功している。構造はチタン(IV)三置換 Dawson 型タングストポリ酸“$[P_2W_{15}Ti_3O_{62}]^{12-}$” unit 四つが Ti-O-Ti 結合により直接縮合した四量体構造(架橋なし四量体)になっており、四量体の中心空間に N 原子(NH_4^+)を一つアサインした。

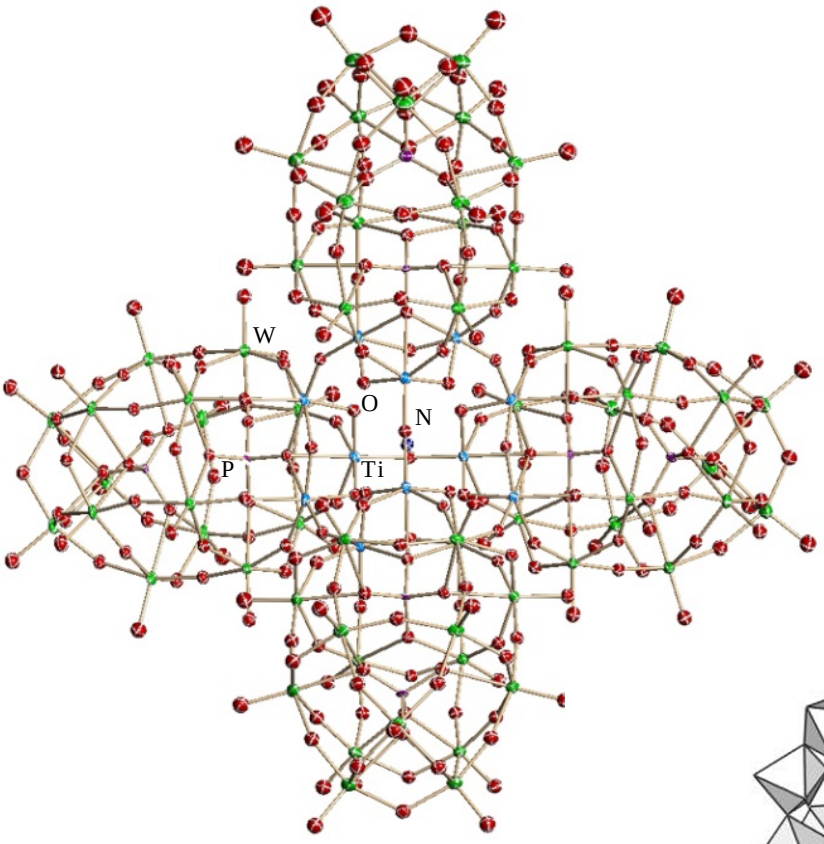

Molecular structure of polyoxoanion
$[(P_2W_{15}Ti_3O_{60.5})_4(NH_4)]^{35-}$

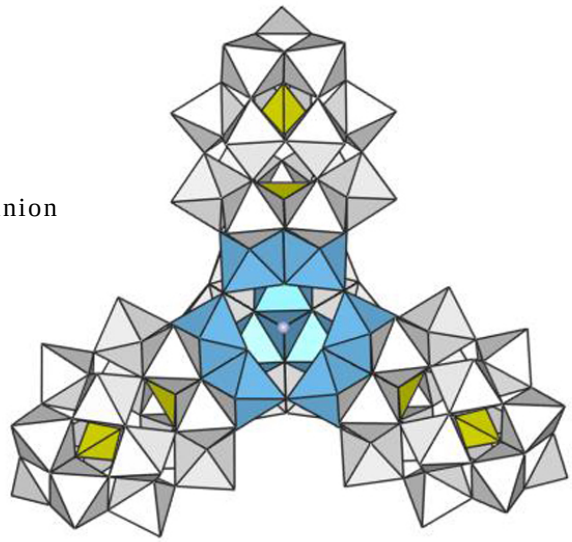

Polyhedral of the polyoxoanion
$[(P_2W_{15}Ti_3O_{60.5})_4(NH_4)]^{35-}$

2-4. Conclusion

純水中で Cl^-カプセル化チタン(IV)三置換 Dawson 型ポリ酸塩架橋あり四量体 $[\{\alpha\text{-}P_2W_{15}Ti_3O_{59}(OH)_3\}_4\{\mu_3\text{-}Ti(H_2O)_3\}_4Cl]^{21-}$を NaOH で加水分解させることで、チタン(IV)三置換 Dawson 型ポリ酸塩単量体"$[\alpha\text{-}P_2W_{15}Ti_3O_{62}]^{12-}$"が形成されることを見出した。また、この単量体をビルディングブロックとして NH_4^+をカプセル化した架橋なし四量体$[(\alpha\text{-}P_2W_{15}Ti_3O_{60.5})_4(NH_4)]^{35-}$の誘導を行った。

FT-IR や ^{31}P NMR から **Na-1** は単量体構造であると考えられる。**NH_4Na-2^P** は X 線構造解析により架橋なし四量体構造であり、中心空間に NH_4^+をカプセル化していることを確認している。**NH_4Na-2** は FT-IR や ^{31}P NMR のデータが **NH_4Na-2^P** のデータとほぼ一致していることから、NH_4^+をカプセル化した架橋なし四量体であると考えられる。このことから架橋あり四量体の加水分解によって初めてチタン(IV)三置換 Dawson 型ポリ酸塩単量体の合成に成功し、この単量体をビルディングブロックとしたカチオンカプセル化種の合成が可能であることが分かった。

Chapter 3

*Synthesis and molecular structure of dimeric tri-titanium(IV)-substituted Dawson polyoxometalate bridged by two Cp*Rh^{2+} groups*

この章は、投稿予定の論文
"Synthesis and molecular structure of dimeric tri-titanium(IV)-substituted Dawson polyoxometalate bridged by two Cp*Rh^{2+} groups"
Y. Matsuki, S, Takaku, T. Hoshino, S. Matsunaga, K. Nomiya, *Manuscript in preparation.*
の内容を中心に構成されている。

Abstract

チタン(IV)三置換 Dawson 型ポリ酸塩四量体は二種類のテトラポッド型四量体(架橋あり、架橋なし)として合成、構造解析が行われている。[43] 二種類の四量体の内、架橋あり四量体の加水分解からのみチタン(IV)三置換単量体[α-$P_2W_{15}Ti_3O_{59}(OH)_3$]$^{9-}$が形成されることが見出されている。$V^{5+}$や Nb^{5+}による金属三置換 Dawson 型ポリ酸塩([α-$P_2W_{15}V_3O_{62}$]$^{9-}$, [α-$P_2W_{15}Nb_3O_{62}$]$^{9-}$ など)は置換表面の負電荷密度が大きいのでとカチオン性有機金属種と直接相互作用が可能であり、有機金属種担持ポリ酸塩を形成することが知られている。[46-57] 一方チタン(IV)三置換 Dawson 型ポリ酸単量体"[α-$P_2W_{15}Ti_3O_{62}$]$^{12-}$"はこれまでの M (= Nb^V, V^V)三置換 Dawson 型ポリ酸塩単量体[$P_2W_{15}M_3O_{62}$]$^{9-}$に比べて負電荷密度がさらに増大しており、今までにない構造や組成の有機金属種担持ポリ酸塩の形成が期待できる。

しかし、チタン(IV)三置換 Dawson 型ポリ酸塩単量体は従来のニオブ(V)三置換体やバナジウム(V)三置換体とまるで性質が違っていた。チタン(IV)三置換体は①中性、酸性条件で架橋なし四量体を形成しやすいので、塩基性条件で扱う必要がある、②この単量体は水に可溶なアルカリ金属塩でしか得られない(有機溶媒に可溶な四級アンモニウム塩に変換できない)、③架橋あり四量体から誘導された単量体には必ずチタン(IV)化合物が *contamination* として含まれている、④稜共有 Ti-O-Ti サイトはプロトネーションしやすく、カチオン性有機金属種の結合の妨げになりやすいなど、非常に限定された条件でしか利用できないことが分かった。

そのような制限の中で本章では、単量体と[Cp^*RhCl_2]$_2$ の反応を行い 2 つの Dawson unit [α-$P_2W_{15}Ti_3O_{60}(OH)_2$]$^{10-}$ を 2 つの Cp*Rh で架橋した 2 : 2 型二量体[{α-$P_2W_{15}Ti_3O_{60}(OH)_2$}$_2$($Cp^*Rh$)$_2$]$^{16-}$を合成した。その合成法、各種キャラクタリゼーションの結果について報告する。

本研究は高久、星野らとの共同研究の一部として行われた。

3-1. Reagents / Analytical Procedures

Reagents

ISOTEC

Deuterium oxide	D_2O

Wako:

Cesium Chloride	CsCl
Sodium Acetate	CH_3COONa
Lithium Hydroxide Monohydrate	$LiOH \cdot H_2O$
Methanol	CH_3OH
Ethanol	EtOH
Diethyl ether	Et_2O
1 mol/L Sodium Hydroxide Solution	NaOH
Silver Tetrafluorborate	$AgBF_4$

Aldrich:

Rhodium Chloride Trihydrate	$RhCl_3 \cdot 3H_2O$
Cyclopentadiene	Cp*H
3-(Trimethylsilyl)-1-Propanesulfonic Acid Sodium Salt	DSS

$[Cp^*RhCl_2]_2$ は文献 [59, 60]を参考に合成した。

$Na_{19}H_2[\{\alpha\text{-}P_2W_{15}Ti_3O_{59}(OH)_3\}_4\{\mu_3\text{-}Ti(H_2O)_3\}_4Cl] \cdot 127\ H_2O$ は文献 [43b)]を参考に合成した。

Analytical Procedures

Complete Elemental Analysis:

Mikroanalytisches Labor Pascher (Remagen, Germany)

CHN elemental Analysis:

PerkinElmer 2400 Series II CHNS/O Elemental Analyzer

TG/DTA:

Rigaku Thermo Plus 2 Series TG/DTA TG 8120

under air, room temperature to 500 ºC, 4 ºC/min.

FT-IR:

Jasco FT/IR-4100 Spectrometer

KBr disks, under air, room temperature

Solution NMR:

JEOL JNM-ECS 400 FT-NMR spectrometer

^{31}P (160.00 MHz) 5 mm o. d. tubes, 25 % H_3PO_4 *aq*. (δ = 0, external standerd)

JEOL JNM-ECS 400 FT-NMR spectrometer

^{1}H (400.00 MHz) 5 mm o. d. tubes, DSS (δ = 0, internal standerd)

JEOL JNM-ECP 500 FT-NMR spectrometer

^{13}C (125.00 MHz) 5 mm o. d. tubes, DSS (δ = 0, internal standerd)

X-ray Crystallography:

Bruker AXS SMART APEX CCD diffractometer (Mo-Kα, λ = 0.701069 Å)

mounted on cryoloop using liquid paraffin, cooled by N_2 gas

direct methods (SHELXS-97), full-matrix least-squares procedure on F^2 (SHELXL-97)

3-2. Synthesis

3-2-1. $Na_8Cs[\alpha\text{-}P_2W_{15}Ti_3O_{59}(OH)_3]\cdot TiO_2\cdot 20H_2O$

Procedure:

① $Na_{19}H_2[\{\alpha\text{-}P_2W_{15}Ti_3O_{59}(OH)_3\}_4\{\mu_3\text{-}Ti(H_2O)_3\}_4Cl]\cdot 127\ H_2O$ (M.W. = 19002.62) 7.6 g (0.40 mmol) を H_2O 60 mL に溶解した。 (無色透明溶液)

② この溶液に 0.1M NaOH *aq*. 97.6 mL を 2hr かけて加え、10 min 撹拌した。 (無色透明溶液)

③ 湯浴上(60 ºC)で 20 min 撹拌した。 (無色透明溶液)

④ evaporator(35 ºC)で 50 mL まで濃縮した。 (無色透明溶液)

⑤ 0.2M CsCl *aq*. 8 mL を滴々加え、3 min 攪拌した。 (無色透明溶液)

⑥ NaOAc (M.W. = 82.03) 10.0 g (122 mmol) を一度に加え、1 min 攪拌した。 (白色懸濁溶液)

⑦ 氷浴で 15 min 攪拌した。 (白色懸濁溶液)

⑧ メンブランフィルター(JG 0.2 μm)で回収した。 (白色粉体)

⑨ 冷却した MeOH 10 mL で 3 回、冷却した EtOH 10 mL で 1 回、Et_2O 10 mL で 1 回洗浄した。 (白色粉体)

⑩ 凍結乾燥機で 2hr 凍結乾燥した。 (白色粉体)

Properties: 白色粉体

H_2O に易溶。MeOH に微溶。$(CH_3)_2CO$、CH_3CN、EtOH、Et_2O に不溶。

Yield: 5.92 g (74.8 %)

$Na_8Cs[\alpha\text{-}P_2W_{15}Ti_3O_{59}(OH)_3]\cdot TiO_2\cdot 20H_2O$ (M.W. = 4715.18)での計算値。

Characterization

Complete Elemental Analysis:

	H	Na	Cs	O	P	W	Ti	Total
Calc.	0.30	4.14	2.99	24.84	1.39	62.04	4.31	100.00
Found	0.29	4.38	2.96	22.9	1.41	61.4	4.38	97.72

Calc. $Na_8Cs_5[\alpha\text{-}P_2W_{15}Ti_3O_{59}(OH)_3]\cdot TiO_2\cdot 5H_2O = Na_8CsH_{13}P_2W_{15}Ti_4O_{69}$

(5.91 % weight loss at R.T. at 10-3-10-4 Torr overnight, Calcd. for $15H_2O$)

TG/DTA:

R.T.-296.8 ºC までに 26 個の H_2O に基づく 9.73 %の重量減。

$Na_8Cs_5[\alpha\text{-}P_2W_{15}Ti_3O_{59}(OH)_3]\cdot TiO_2\cdot 26H_2O$: 9.71 %

FT-IR:

1620(m), 1087(vs), 1052(m), 1014(m), 941(vs), 914(vs), 741(vs), 718(vs), 598(s), 562(s), 523(vs), 462(s) cm^{-1}

Solution ^{31}P NMR (D_2O, 23.2 ºC):

δ -4.97, -14.65 ppm

Solution ^{183}W NMR (D_2O, R.T.):

δ -158.11 (3W), -193.46, -193.54 (6W), -233.85, -233.93 (6W) ppm

3-2-2. $Na_{14}Cs_2[\{\alpha\text{-}P_2W_{15}Ti_3O_{60}(OH)_2\}_2(Cp^*Rh)_2]\cdot 37H_2O\cdot 2TiO_2$

Procedure:

① $Na_8Cs[\alpha\text{-}P_2W_{15}Ti_3O_{59}(OH)_3]\cdot TiO_2\cdot 26H_2O$ (M.W. = 4957.44) 0.49 g (0.1 mmol)を H_2O 6mL に溶解した。 (無色透明溶液)

② 0.1M LiOH *aq*. 3mL をゆっくり加え、1 hr 攪拌した。 (無色透明溶液)

③ 別途、MeOH 10 mL に $AgBF_4$ (M.W. = 194.67) 0.039 g (0.2 mmol)を溶解し、$[Cp^*RhCl_2]_2$ (M.W. = 618.08) 0.031 g (0.05 mmol)を加えた。 (橙色透明溶液→白色粉体析出)

④ 30 min.攪拌後、ろ過した。 (黄色透明溶液)

⑤ ④のろ液に H_2O 6mL を加え、evaporator(40 ºC) で MeOH を除き②に加えた。 (黄橙色透明溶液)

⑥ 湯浴上 (90 ºC) で 1 hr 加熱した。 (黄橙色透明溶液)

⑦ evaporator (40 ºC) で 5 mL まで濃縮し、EtOH 75 mL 加えた。(黄橙色粉体析出)

⑧ メンブランフィルター (JG 0.2 μm) で回収し、Et_2O 10 mL で 3 回洗浄した。 (黄橙色粉体)

⑨ 2 hr 凍結乾燥した。 (黄橙色粉体: *powder sample*)

crystallization

① 回収した粉体 0.30 g を H_2O 6mL に溶解し、slow evaporation した。 (2 日後、黄橙色粉体及び橙色柱状結晶析出)

② 上澄み液を分取し、slow evaporation した。 (1 日後、橙色柱状結晶析出)

③ メンブランフィルター (JV 0.1 μm)で回収し、EtOH 10 mL, Et_2O 10mL で各 3 回洗浄した。 (結晶性を失い、黄橙色粉体)

④ 2 hr 凍結乾燥した。 (黄橙色粉体: *crystal sample*)

Properties: **黄橙色粉体**

H_2O に易溶。MeOH に難溶。CH_3CN、EtOH、Et_2O に不溶

Yield: 0.41 g (85.4 %) (*powder sample*)/0.27 g (91.5 %) (*crystal sample*)

$Na_{14}Cs_2[\{\alpha\text{-}P_2W_{15}Ti_3O_{60}(OH)_2\}_2(Cp^*Rh)_2]\cdot 37H_2O\cdot 2TiO_2$ での計算値。

Characterization

Complete Elemental Analysis: (*powder sample*)

	H	C	Na	Cs	O	P	W	Ti	Rh	Total
Calc.	0.46	2.61	3.49	2.89	22.93	1.35	59.88	4.16	2.23	100.00
Found	0.54	2.56	3.56	2.56	20.80	1.30	57.70	4.97	1.92	95.91

Calc. $Na_{14}Cs_2[\{\alpha\text{-}P_2W_{15}Ti_3O_{60}(OH)_2\}_2(Cp^*Rh)_2]\cdot 37H_2O\cdot 2TiO_2$ =
$Na_{14}Cs_2C_{20}H_{42}O_{132}P_4W_{30}Ti_8Rh_2$
(6.44 % weight loss at R.T. at 10-3-10-4 Torr overnight, Calcd. for $35H_2O$)

TG/DTA:
R.T.-255.6 ºC までに 29 個の H_2O に基づく 5.45 %の重量減。
$Na_{14}Cs_2[\{\alpha\text{-}P_2W_{15}Ti_3O_{60}(OH)_2\}_2(Cp^*Rh)_2]\cdot 37H_2O\cdot 2TiO_2$: 5.38 %

FT-IR:
1623(m), 1473(w), 1376(vw), 1085(s), 1053(w), 1011(m), 939(vs), 915(vs), 742(vs), 599(m), 563(m), 521(vs), 459(m) cm^{-1}

Solution ^{31}P NMR (D_2O, 23.2 ºC):
δ -5.20, -14.61 ppm

Solution ^{1}H NMR (D_2O, 24.0 ºC):
δ 1.92 ppm

Solution ^{13}C NMR (D_2O, 27.3 ºC):
δ 11.34, 96.00 ppm

X-ray Crystallography:

Crystal data and structure refinement for $Na_{14}Cs_2[\{\alpha\text{-}P_2W_{15}Ti_3O_{60}(OH)_2\}_2(Cp^*Rh)_2]\cdot 37H_2O\cdot 2TiO_2$

Empirical formula	C20 H0 Cs7 K0 Na8 O154 P4 Rh2 Ti6 W30	
Formula weight	9951.09	
Temperature	100(2) K	
Wavelength	0.71073 Å	
Crystal system	Triclinic	
Space group	P-1	
Unit cell dimensions	a = 15.7416(14) Å	α= 102.514(2)°.
	b = 17.1112(15) Å	β= 93.555(2)°.
	c = 20.1302(18) Å	γ = 111.0420(10)°.
Volume	4881.9(7) $Å^3$	
Z	1	
Density (calculated)	3.385 Mg/m^3	
Absorption coefficient	19.415 mm^{-1}	
F(000)	4327	
Crystal size	0.10 x 0.04 x 0.03 mm^3	
Theta range for data collection	1.05 to 28.35°.	
Index ranges	-20<=h<=21, -22<=k<=22, -26<=l<=26	
Reflections collected	66934	
Independent reflections	24185 [R(int) = 0.0583]	
Completeness to theta = 28.35°	99.2 %	
Absorption correction	Empirical	
Max. and min. transmission	0.5935 and 0.2470	
Refinement method	Full-matrix least-squares on F^2	
Data / restraints / parameters	24185 / 714 / 1042	
Goodness-of-fit on F^2	1.026	
Final R indices [I>2sigma(I)]	R1 = 0.0626, wR2 = 0.1755	
R indices (all data)	R1 = 0.0958, wR2 = 0.1988	
Largest diff. peak and hole	13.854 and -7.746 $e.Å^{-3}$	

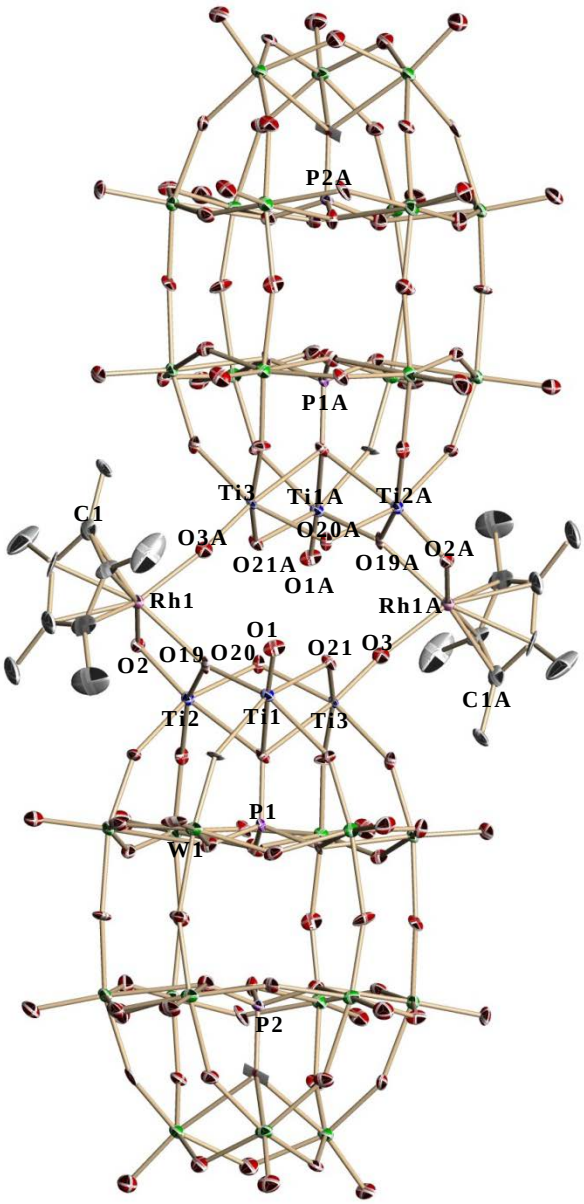

Molecular structure of the polyoxoanion $[\{\alpha\text{-}P_2W_{15}Ti_3O_{60}(OH)_2\}_2(Cp^*Rh)_2]^{16-}$

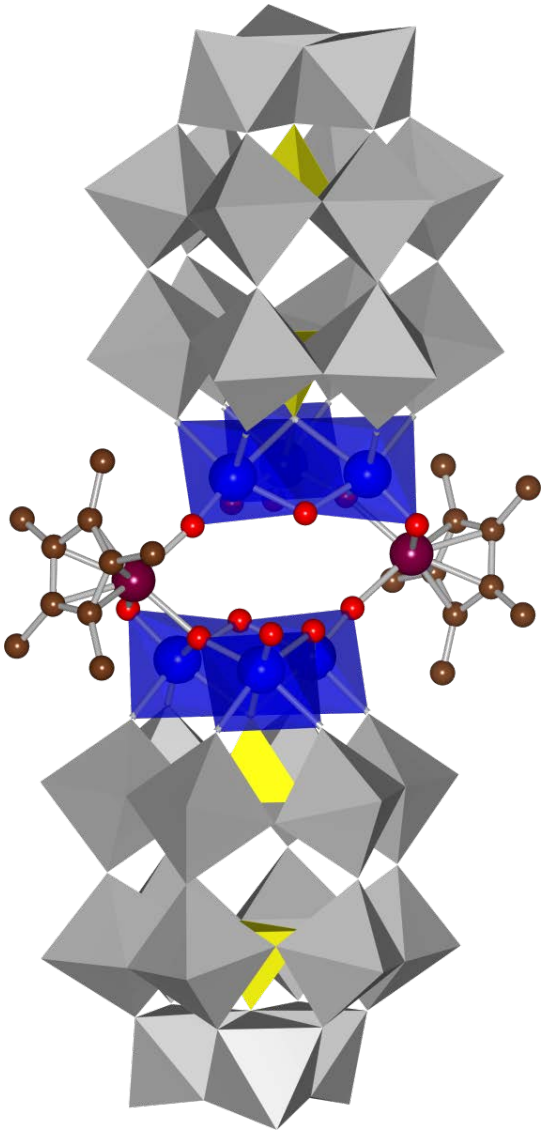

Polyhedral of the polyoxoanion $[\{\alpha\text{-}P_2W_{15}Ti_3O_{60}(OH)_2\}_2(Cp^*Rh)_2]^{16-}$

3-3. Result and Discussion

Abbreviation:

$Na_8Cs[\alpha\text{-}P_2W_{15}Ti_3O_{59}(OH)_3]\cdot TiO_2\cdot 20H_2O$ (**NaCs-M-1**)

$Na_{14}Cs_2[\{\alpha\text{-}P_2W_{15}Ti_3O_{60}(OH)_2\}_2(Cp^*Rh)_2]\cdot 37H_2O\cdot 2TiO_2$ (**NaCs-D-1**)

Experiment

$Na_{14}Cs_2[\{\alpha\text{-}P_2W_{15}Ti_3O_{60}(OH)_2\}_2(Cp^*Rh)_2]\cdot 37H_2O\cdot 2TiO_2$:

純水中で LiOH によって一部脱プロトン化したチタン(IV)三置換 Dawson 型ポリ酸塩単量体 $[P_2W_{15}Ti_3O_{60}(OH)_2]^{10-}$ と別途誘導した $Cp^*Rh(BF_4)_2$ を反応させ、slow evaporation することで無色透明柱状結晶を得た(収率 85.4 %)。

$$2[\alpha\text{-}P_2W_{15}Ti_3O_{59}(OH)_3]^{9-} + 2OH^- + 2Cp^*Rh^{2+} \rightarrow [\{\alpha\text{-}P_2W_{15}Ti_3O_{60}(OH)_2\}_2(Cp^*Rh)_2]^{16-} + 2H_2O$$

X-ray Crystallography

$Na_{14}Cs_2[\{\alpha\text{-}P_2W_{15}Ti_3O_{60}(OH)_2\}_2(Cp^*Rh)_2]\cdot 37H_2O\cdot 2TiO_2$ (CCDC 1033207):

2 つの Dawson unit が 2 つの Cp*Rh 基によって連結した二量体構造であることを確認した。このような二量体構造は有機金属種担持 M 三置換 Dawson 型ポリ酸塩単量体においては初めての例であり、非常に珍しい構造であった。また 2 つの末端酸素(Ti-O)および 1 つの稜共有酸素(Ti-O-Ti)が Rh に配位していた。BVS 計算の結果から 2 つ稜共有酸素(O20 (計算値 1.230), O21 (計算値 1.173))がプロトネーションしていることが分かった。また、カウンターカチオンおよび結晶水は disorder のためアサインできなかった。

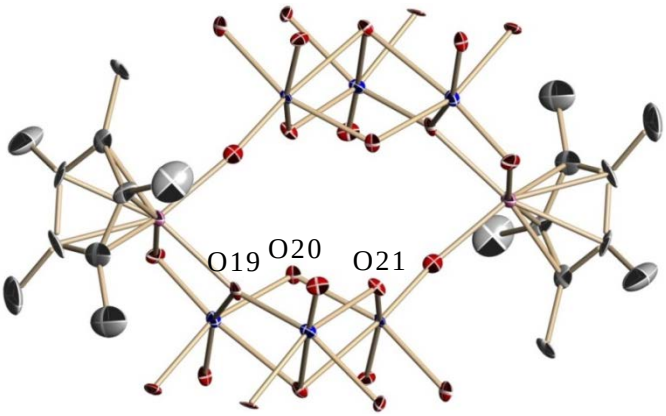

the partial structures around
the Ti and Rh center

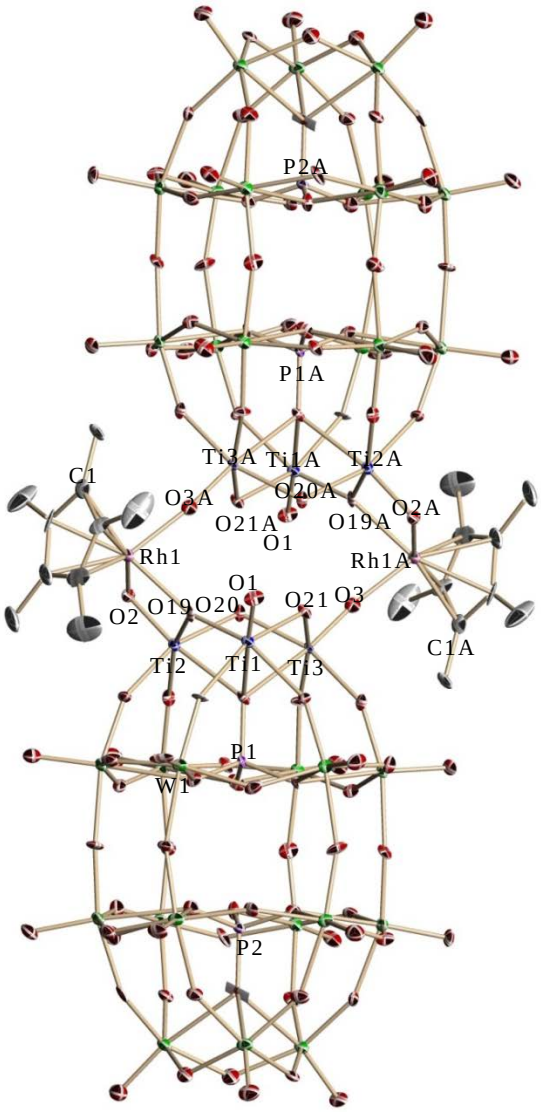

Polyhedral of the polyoxoanion
$[\{\alpha\text{-}P_2W_{15}Ti_3O_{60}(OH)_2\}_2(Cp^*Rh)_2]^{16-}$

Complete Elemental Analysis and TG/DTA: (*powder sample*)

$Na_{14}Cs_2[\{\alpha\text{-}P_2W_{15}Ti_3O_{60}(OH)_2\}_2(Cp^*Rh)_2]\cdot 37H_2O\cdot 2TiO_2$:

電荷バランスが釣り合う組成を考えると、ポリ酸アニオン 1 つに Na^+カチオン 14 個、Cs^+カチオン 2 個となる。このことからポリ酸アニオンには 2 か所プロトネーションしている可能性があり、X 線構造解析の結果を支持していた。

	H	C	Na	Cs	O	P	W	Ti	Rh	Total
Calc.	0.46	2.61	3.49	2.89	22.93	1.35	59.88	4.16	2.23	100.00
Found	0.54	2.56	3.56	2.56	20.80	1.30	57.70	4.97	1.92	95.91

Calc. $Na_{14}Cs_2[\{\alpha\text{-}P_2W_{15}Ti_3O_{60}(OH)_2\}_2(Cp^*Rh)_2]\cdot 2H_2O\cdot 2TiO$ =

$Na_{14}Cs_2C_{20}H_{42}O_{132}P_4W_{30}Ti_8Rh_2$

(6.44 % weight loss at R.T. at 10-3-10-4 Torr overnight, Calcd. for $35H_2O$)

Weight loss	5.54 % below 225.6 °C
Calcd.	5.38 % for $29H_2O$

Solution ^{31}P NMR

純水中で **NaCs-D-1** は-5.20, -14.61 ppm に二本線ピークで観測され、前駆体の **NaCs-M-1** と比較して低磁場側のピークが僅かに高磁場側へシフトしていた。

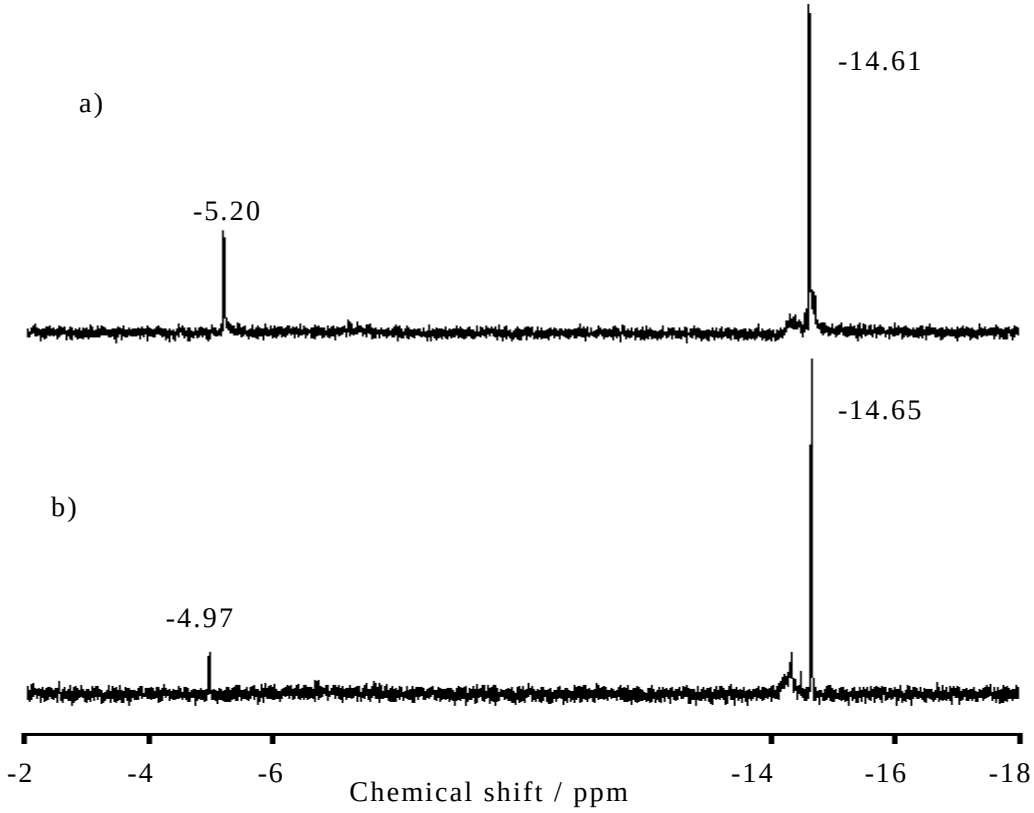

Solution ^{31}P NMR spectra a) **NaCs-D-1**, b) **NaCs-M-1**

Solution ^{1}H NMR and ^{13}C NMR

溶液中で **NaCs-D-1** は ^{1}H NMR で 1.92 ppm に観測され前駆体の$[Cp^*RhCl_2]_2$とは異なる位置に観測された。また ^{13}C NMR では 96.00, 11.34 ppm に二本線ピークで観測され前駆体の$[Cp^*RhCl_2]_2$とほぼ同じ位置に観測されていることから、水溶液中でも担持された Cp*Rh 基が分解しにくいと考えられる。

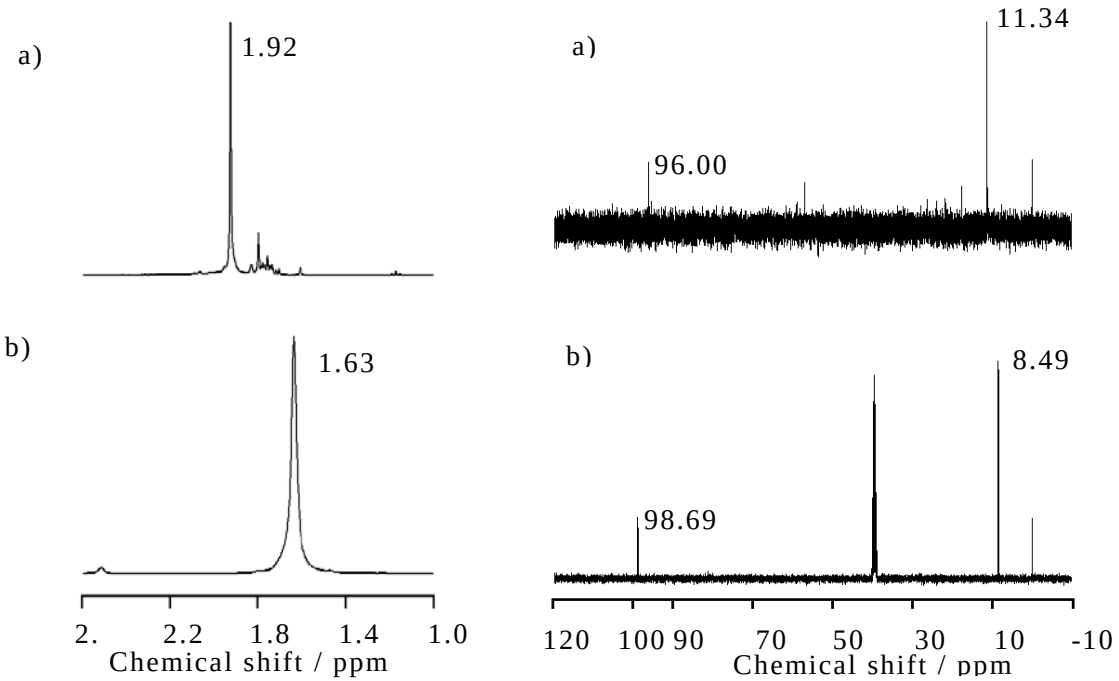

Solution ^{1}H (left) nad ^{13}C (right) NMR spectra a) **NaCs-D-1** in D_2O, b) $[Cp^*RhCl_2]_2$ in DMSO-d_6

FT-IR

NaCs-D-1 は P-O に基づく振動バンドが二本線で観測され、Dawson unit 間の Ti-O-Ti 結合に基づく振動バンドが観測されなかった。また Cp*Rh 基に基づく振動バンドが観測された。**NaCs-M-1** と比較してもポリ酸骨格に基づく振動バンドに大きな変化は見られなかった。

	P-O	W-O	Ti-O-Ti	Cp*Rh
NaCs-D-1	1085, 1053	939, 915, 742	—	1473, 1376
NaCs-M-1	1087, 1052	941, 914, 740	—	

3-4. Conclusion

純水中で LiOH によって一部脱プロトン化したチタン(IV)三置換 Dawson 型ポリ酸塩単量体$[P_2W_{15}Ti_3O_{60}(OH)_2]^{10-}$と別途誘導した $Cp^*Rh(BF_4)_2$ を反応させることで 2 つの Dawson unit が 2 つの Cp*Rh 基で架橋された二量体 $Na_{14}Cs_2[\{\alpha\text{-}P_2W_{15}Ti_3O_{60}(OH)_2\}_2(Cp^*Rh)_2]\cdot 37H_2O\cdot 2TiO_2$ を合成した。チタン(IV)三置換 Dawson 型ポリ酸塩はバナジウム(V)やニオブ(V)三置換体と比べて、非常に限られた条件でしか利用できないが、それでもカチオン性有機金属種を担持した化合物を誘導することができた。

単結晶 X 線構造解析から 2 つの Cp*Rh 基が 2 つの Dawson unit を連結した二量体構造であることが分かった。このような二量体構造は有機金属種担持 M 三置換 Dawson 型ポリ酸塩では初めての例で、珍しい構造だった。また BVS 計算から Dawson unit 内の 2 つの稜共有酸素がプロトネーションしていることが分かった。

溶液中の NMR からポリ酸に担持されている Cp*Rh 基は解離せず、二量体構造を保持していると思われる。

Appendix

Single crystal X-ray structure analysis of 2 : 2-type complexes of zirconium(IV)/hafnium(IV) centers with mono-lacunary Keggin polyoxosilicotungstate

付録として、論文

“2:2-Type complexes of zirconium(IV)/hafnium(IV) centers with mono-lacunary Keggin polyoxometalates: Syntheses and molecular structures of $[(\alpha\text{-}SiW_{11}O_{39}M)_2(\mu\text{-}OH)_2]^{10-}$ (M = Zr, Hf) with edge-sharing octahedral units and $[(\alpha\text{-}SiW_{11}O_{39}M)_2(\mu\text{-}OH)_3]^{11-}$ with face-sharing octahedral units”

H. Osada, A. Ishikawa, Y. Saku, Y. Sakai, Y. Matsuki, S. Matsunaga, K. Nomiya, *Polyhedron*, *52*, **2013**, 389-397.

に記述されている X 線構造解析に関する内容を記載する。

Abstract

チタン含有ポリ酸塩に関する研究を主に行ってきたが、その他にも共同研究者としてジルコニウム(IV)/ハフニウム(IV)含有 Keggin 型シリコタングステン酸 2 : 2 型面共有/稜共有錯体に関する研究にも携わっている。本章では担当した X 線構造解析の部分について記載する。

本研究は長田、石川らとの共同研究の一部として行われた。

Abbreviation:

$(Et_2NH_2)_{10}[(\alpha\text{-}SiW_{11}O_{39}Zr)_2(\mu\text{-}OH)_2]\cdot 4H_2O$	(**Zr-Edge**)
$(Et_2NH_2)_{11}[(\alpha\text{-}SiW_{11}O_{39}Zr)_2(\mu\text{-}OH)_3]\cdot 15H_2O$	(**Zr-Face**)
$(Et_2NH_2)_{10}[(\alpha\text{-}SiW_{11}O_{39}Hf)_2(\mu\text{-}OH)_2]\cdot 4H_2O$	(**Hf-Edge**)
$(Et_2NH_2)_{11}[(\alpha\text{-}SiW_{11}O_{39}Hf)_2(\mu\text{-}OH)_3]\cdot 15H_2O$	(**Hf-Face**)

X-ray Crystallography:

Crystal data and structure refinement for $(Et_2NH_2)_{10}[(\alpha\text{-}SiW_{11}O_{39}Zr)_2(\mu\text{-}OH)_2]\cdot 4H_2O$

Empirical formula	C40 H120 N10 O86 Si2 W22 Zr2	
Formula weight	6400.78	
Temperature	120(2) K	
Wavelength	0.71073 Å	
Crystal system	**Triclinic**	
Space group	**P-1**	
Unit cell dimensions	a = 12.2571(9) Å	α= 79.7940(10)°.
	b = 13.5084(10) Å	β= 86.3960(10)°.
	c = 20.1586(15) Å	γ = 65.7590(10)°.
Volume	2995.1(4) $Å^3$	
Z	1	
Density (calculated)	3.549 Mg/m^3	
Absorption coefficient	21.311 mm^{-1}	
F(000)	2854	
Crystal size	0.15 x 0.08 x 0.04 mm^3	
Theta range for data collection	1.03 to 28.34°.	
Index ranges	-16<=h<=16, -18<=k<=17, -26<=l<=26	
Reflections collected	23955	
Independent reflections	10690 [R(int) = 0.0581]	
Completeness to theta = 28.34°	71.5 %	
Absorption correction	Empirical	
Max. and min. transmission	0.4827 and 0.1423	
Refinement method	Full-matrix least-squares on F^2	
Data / restraints / parameters	10690 / 2376 / 740	
Goodness-of-fit on F^2	0.956	
Final R indices [I > 2sigma(I)]	R1 = **0.0443**, wR2 = 0.1123	
R indices (all data)	R1 = 0.0636, wR2 = 0.1288	
Largest diff. peak and hole	2.810 and -2.158 e. $Å^{-3}$	

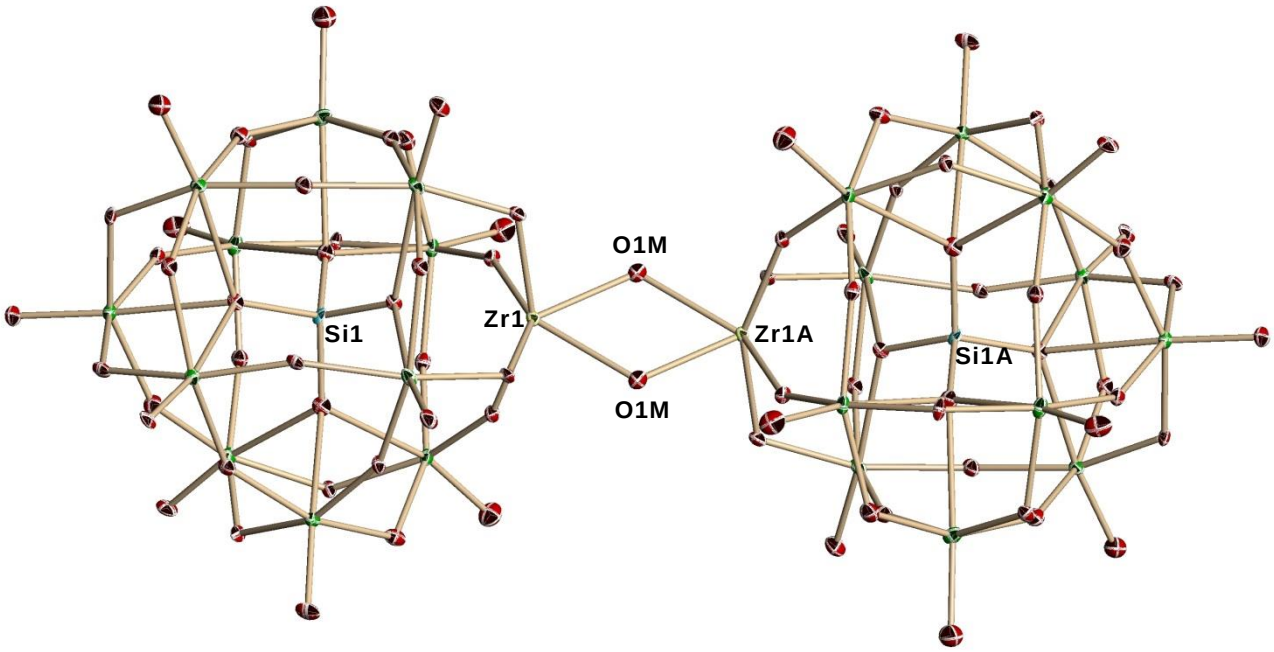

Molecular structure of the polyoxoanion $[(\alpha\text{-}SiW_{11}O_{39}Zr)_2(\mu\text{-}OH)_2]^{10-}$

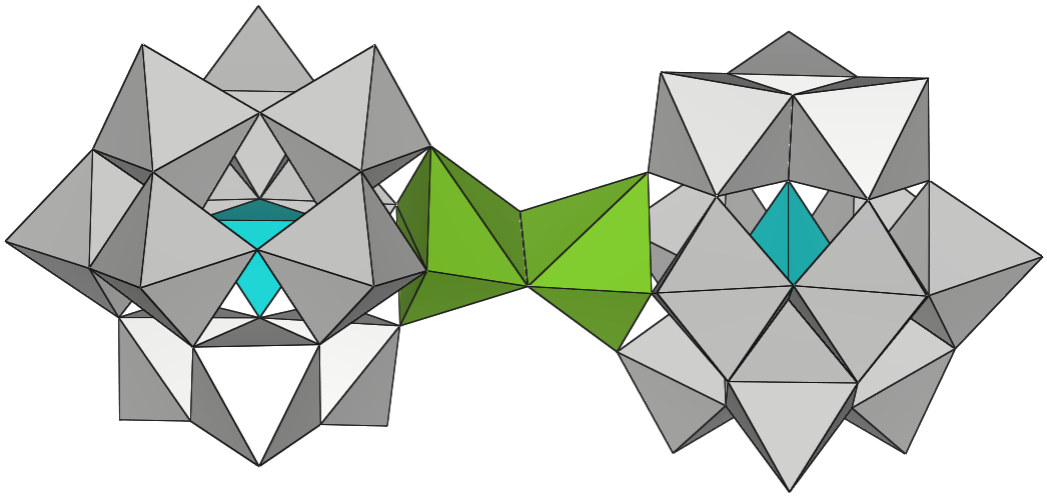

Polyhedral of the polyoxoanion $[(\alpha\text{-}SiW_{11}O_{39}Zr)_2(\mu\text{-}OH)_2]^{10-}$

Crystal data and structure refinement for $(Et_2NH_2)_{11}[(\alpha\text{-}SiW_{11}O_{39}Zr)_2(\mu\text{-}OH)_3]\cdot 15H_2O$

Empirical formula	C44 H132 N11 O94 Si2 W22 Zr2	
Formula weight	6602.93	
Temperature	90 K	
Wavelength	0.71073 Å	
Crystal system	**Monoclinic**	
Space group	**P2(1)/c**	
Unit cell dimensions	a = 13.5533(8) Å	α= 90°.
	b = 45.823(3) Å	β= 99.7050(10)°.
	c = 21.5559(13) Å	γ = 90°.
Volume	13195.8(14) $Å^3$	
Z	4	
Density (calculated)	3.324 Mg/m^3	
Absorption coefficient	19.358 mm^{-1}	
F (000)	11844	
Crystal size	0.28 x 0.08 x 0.04 mm^3	
Theta range for data collection	0.89 to 28.35°.	
Index ranges	-18<=h<=17, -61<=k<=61, -28<=l<=28	
Reflections collected	157067	
Independent reflections	32898 [R (int) = 0.0678]	
Completeness to theta = 28.35°	99.8 %	
Absorption correction	Empirical	
Max. and min. transmission	0.5115 and 0.0742	
Refinement method	Full-matrix least-squares on F^2	
Data / restraints / parameters	32898 / 4272 / 1208	
Goodness-of-fit on F^2	1.064	
Final R indices [I > 2sigma(I)]	R1 = **0.0457**, wR2 = 0.0960	
R indices (all data)	R1 = 0.0599, wR2 = 0.1026	
Largest diff. peak and hole	5.946 and -4.796 $e.Å^{-3}$	

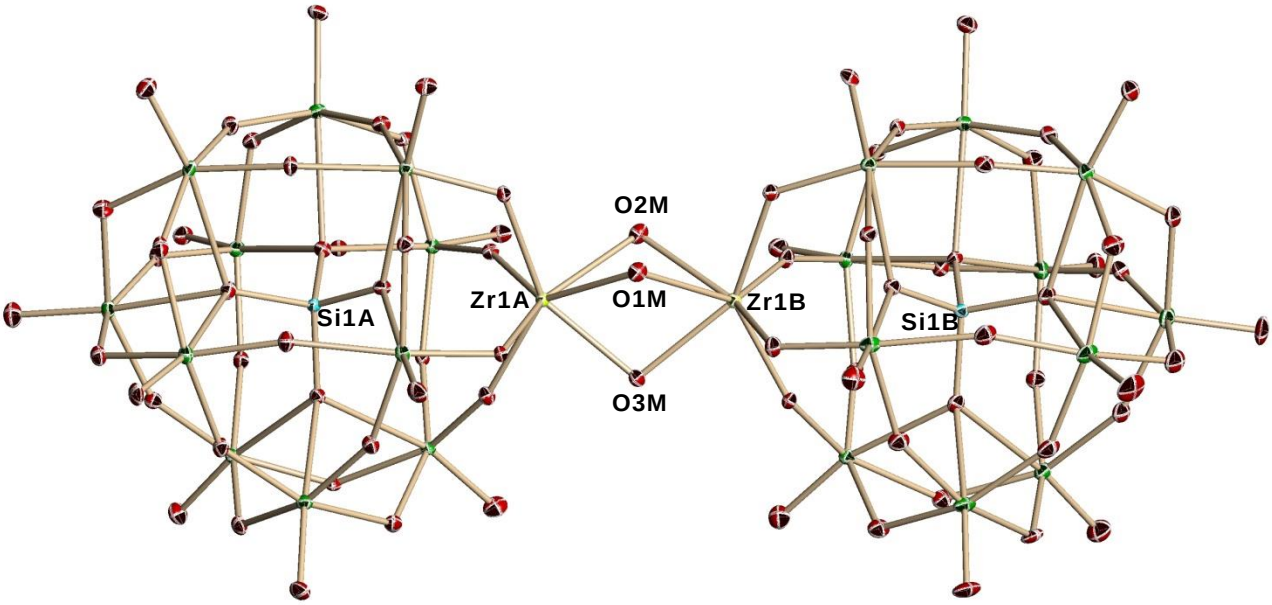

Molecular structure of the polyoxoanion $[(\alpha\text{-}SiW_{11}O_{39}Zr)_2(\mu\text{-}OH)_3]^{11-}$

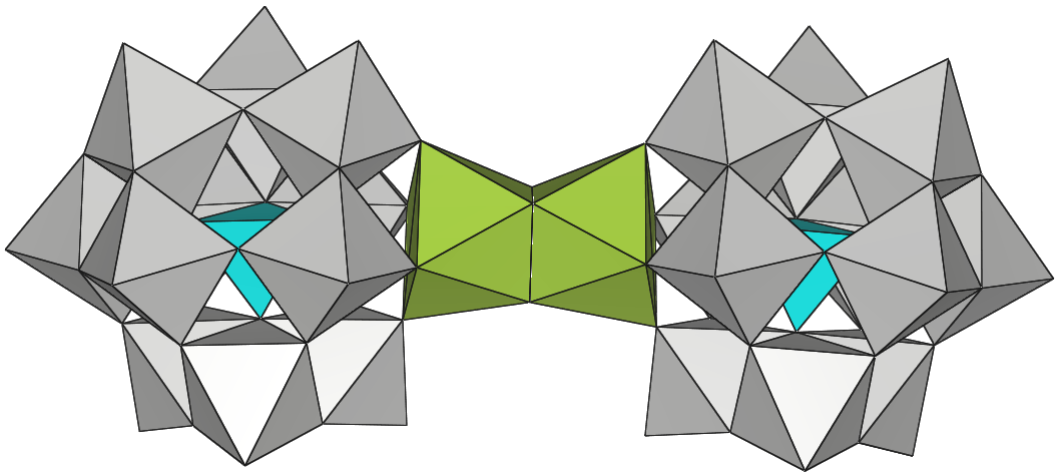

Polyhedral of the polyoxoanion $[(\alpha\text{-}SiW_{11}O_{39}Zr)_2(\mu\text{-}OH)_2]^{11-}$

Crystal data and structure refinement for $(Et_2NH_2)_{11}[(\alpha\text{-}SiW_{11}O_{39}Hf)_2(\mu\text{-}OH)_2]\cdot 4H_2O$

Empirical formula	C40 H120 Hf2 N10 O86 Si2 W22	
Formula weight	6575.32	
Temperature	120 K	
Wavelength	0.71073 Å	
Crystal system	**Triclinic**	
Space group	**P-1**	
Unit cell dimensions	a = 12.2527(11) Å	α = 79.7620(10)°.
	b = 13.4995(12) Å	β = 86.3360(10)°.
	c = 20.1314(18) Å	γ = 65.7310(10)°.
Volume	2987.1(5) $Å^3$	
Z	1	
Density (calculated)	3.655 Mg/m^3	
Absorption coefficient	22.930 mm^{-1}	
F(000)	2918	
Crystal size	0.20 x 0.19 x 0.03 mm^3	
Theta range for data collection	1.03 to 28.32°.	
Index ranges	-16<=h<=16, -18<=k<=17, -26<=l<=26	
Reflections collected	68566	
Independent reflections	14686 [R (int) = 0.0493]	
Completeness to theta = 28.32°	98.7 %	
Absorption correction	Empirical	
Max. and min. transmission	0.5462 and 0.0914	
Refinement method	Full-matrix least-squares on F^2	
Data / restraints / parameters	14686 / 1998 / 740	
Goodness-of-fit on F^2	1.059	
Final R indices [I > 2sigma(I)]	R1 = **0.0592**, wR2 = 0.1702	
R indices (all data)	R1 = 0.0623, wR2 = 0.1747	
Largest diff. peak and hole	7.543 and -4.921 $e.Å^{-3}$	

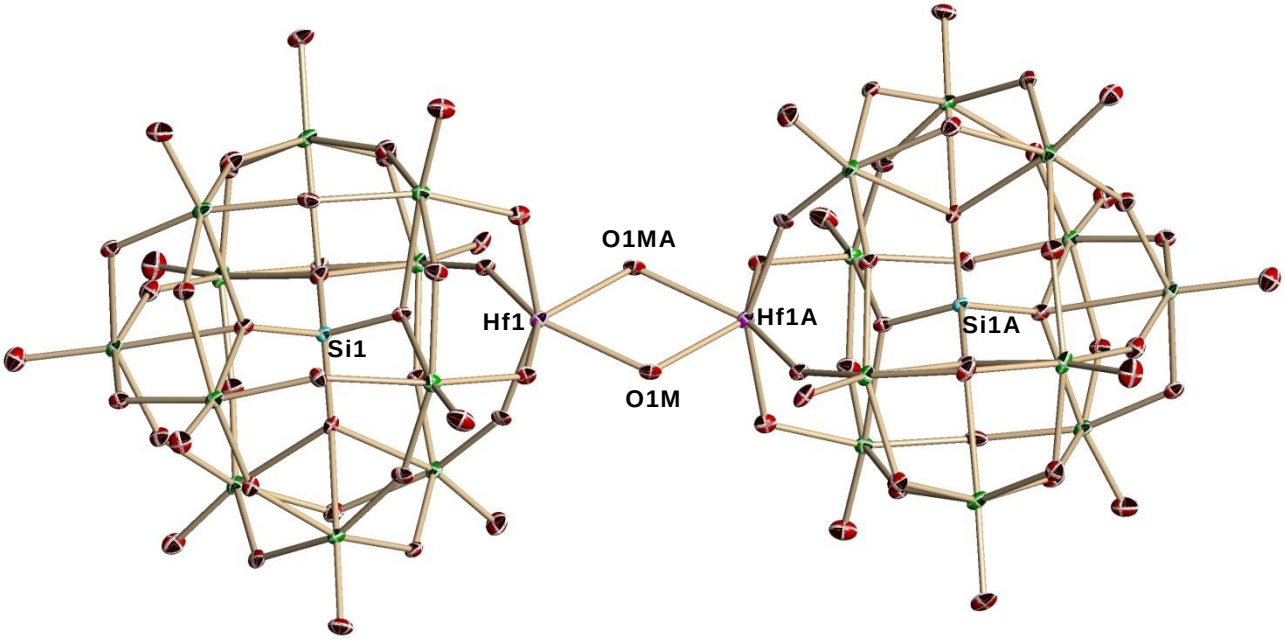

Molecular structure of the polyoxoanion $[(\alpha\text{-}SiW_{11}O_{39}Hf)_2(\mu\text{-}OH)_2]^{10-}$

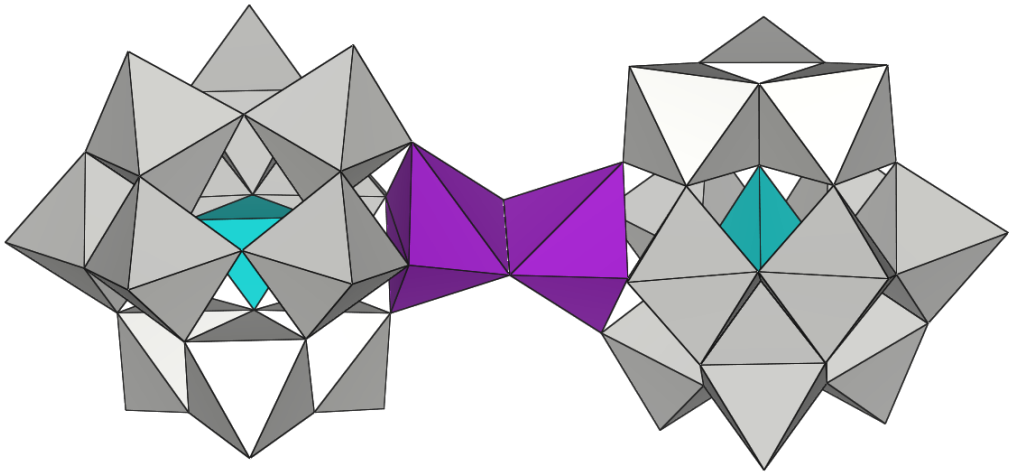

Polyhedral of the polyoxoanion $[(\alpha\text{-}SiW_{11}O_{39}Hf)_2(\mu\text{-}OH)_2]^{10-}$

Crystal data and structure refinement for $(Et_2NH_2)_{11}[(\alpha\text{-}SiW_{11}O_{39}Hf)_2(\mu\text{-}OH)_2]\cdot 15H_2O$

Empirical formula	C44 H132 Hf2 N11 O93 Si2 W22	
Formula weight	6761.47	
Temperature	120 K	
Wavelength	0.71073 Å	
Crystal system	**Monoclinic**	
Space group	**P2(1)/c**	
Unit cell dimensions	a = 13.6619(5) Å	α = 90°.
	b = 45.6954(17) Å	β = 99.6130(10)°.
	c = 21.5558(8) Å	γ = 90°.
Volume	13268.0(8) $Å^3$	
Z	4	
Density (calculated)	3.385 Mg/m^3	
Absorption coefficient	20.659 mm^{-1}	
F(000)	12068	
Crystal size	0.29 x 0.10 x 0.07 mm^3	
Theta range for data collection	0.89 to 28.33°.	
Index ranges	-18<=h<=9, -60<=k<=54, -26<=l<=28	
Reflections collected	90870	
Independent reflections	32517 [R (int) = 0.0687]	
Completeness to theta = 28.33°	98.2 %	
Absorption correction	Empirical	
Max. and min. transmission	0.3257 and 0.0655	
Refinement method	Full-matrix least-squares on F^2	
Data / restraints / parameters	32517 / 4914 / 1589	
Goodness-of-fit on F^2	1.050	
Final R indices [I > 2sigma(I)]	R1 = **0.0503**, wR2 = 0.1255	
R indices (all data)	R1 = 0.0700, wR2 = 0.1448	
Largest diff. peak and hole	6.453 and -3.306 e. $Å^{-3}$	

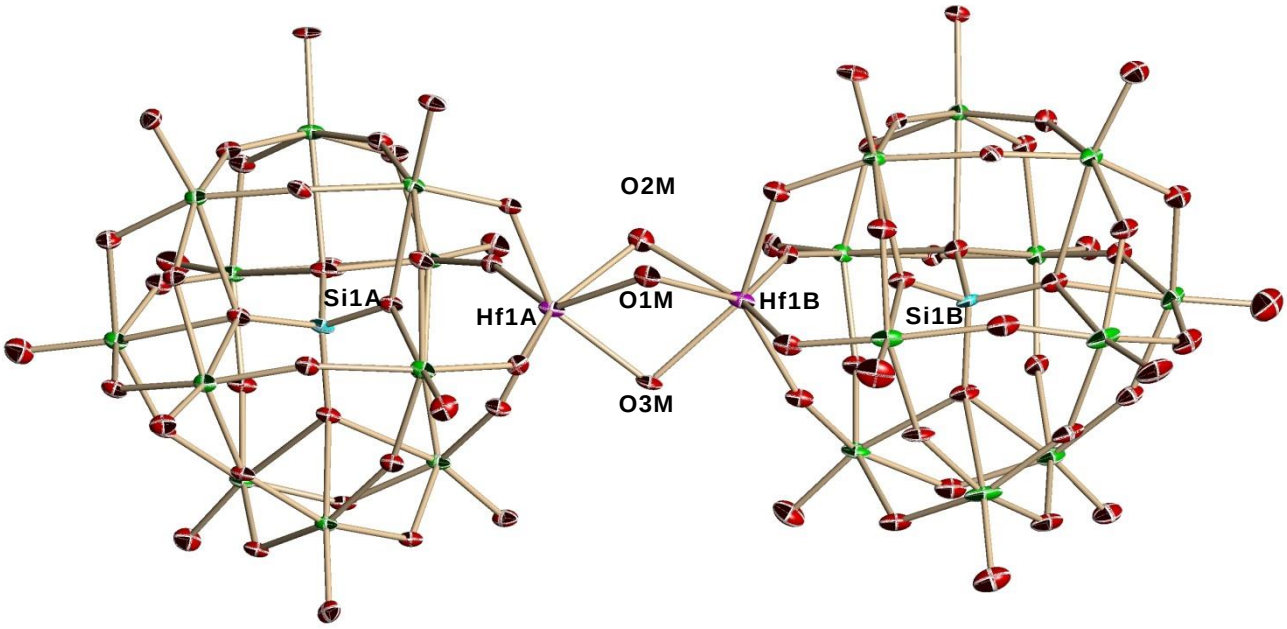

Molecular structure of the polyoxoanion $[(\alpha\text{-}SiW_{11}O_{39}Hf)_2(\mu\text{-}OH)_3]^{11-}$

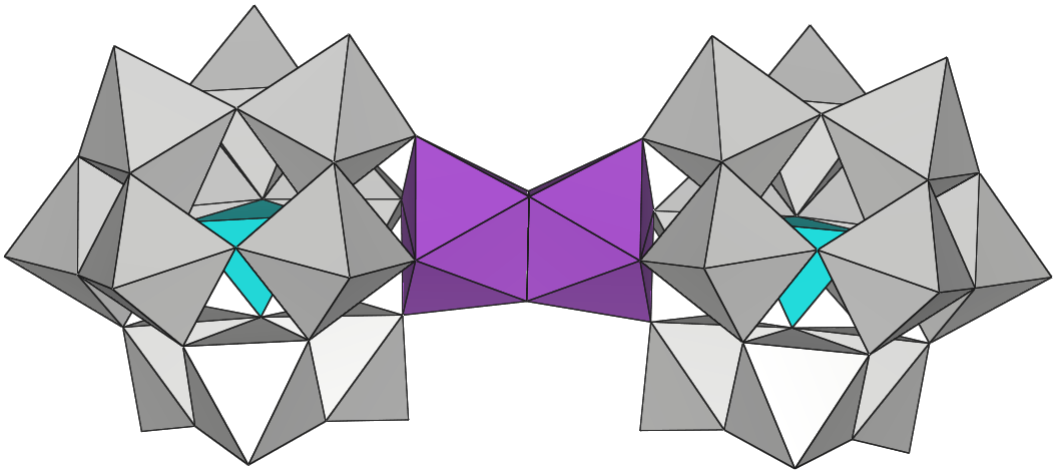

Polyhedral of the polyoxoanion $[(\alpha\text{-}SiW_{11}O_{39}Hf)_2(\mu\text{-}OH)_3]^{11-}$

Conclusion

単結晶 X 線構造解析から **Zr-Edge** および **Hf-Edge** は M (M = Zr^{IV}, Hf^{IV})を二本の μ-OH で架橋した稜共有構造であり、**Zr-Face** および **Hf-Face** は三本の μ-OH で架橋した面共有構造であった。BVS 計算(**Zr-Edge**; 1.160 / **Zr-Face**; 0.876, 0.947, 1.175 / **Hf-Edge**; 1.215 / **Hf-Face**; 0.979, 1.045, 1.272)からいずれの架橋酸素原子もプロトネーションしていることを確認した。二核錯体で稜共有はよくみられるが、面共有というのは非常に珍しい構造であった。これはヘテロ原子が Si や Ge のときに初めて実現され、ヘテロ原子 P のポリ酸塩では同じ pH では安定に存在できないので、面共有錯体は実現できない。

Conclusion

Chapter 1

一度粉体で単離した二量体$[(\alpha\text{-}PW_{11}TiO_{39})_2O]^{8-}$は結晶化せず、単量体$[\alpha\text{-}PW_{11}TiO_{40}]^{5-}$から二量体を誘導する過程で二量体が結晶化することを明らかにした。また単量体についても結晶化条件を見つけ単結晶 X 線構造解析を行った。

X 線構造解析で単量体は disorder しておりチタン(IV)置換サイトを決めることは出来なかったが、単量体構造であることを確認した。一方、二量体は Keggin unit 間を Ti-O-Ti 結合で連結した構造であり、BVS 計算から Keggin unit 間の架橋酸素原子が O^{2-}であり μ-OH ではないことを確認した。

Chapter 2

Dawson 型ポリ酸塩三欠損種と Ti^{IV} の直接反応および架橋なし四量体の加水分解からチタン(IV)三置換単量体"$[\alpha\text{-}P_2W_{15}Ti_3O_{62}]^{12-}$"は得られないが、架橋あり四量体の加水分解によって初めてチタン(IV)三置換 Dawson 型ポリ酸塩単量体が得られることを明らかにした。この単量体をビルディングブロックとしたカチオン(NH_4^+)カプセル化種$[(\alpha\text{-}P_2W_{15}Ti_3O_{60.5})_4(NH_4)]^{35-}$の合成が可能であることを明らかにした。

Chapter 3

2 つの Cp^*Rh^{2+}基で架橋されたチタン(IV)三置換 Dawson 型ポリ酸塩二量体$[\{\alpha\text{-}P_2W_{15}Ti_3O_{60}(OH)_2\}_2(Cp^*Rh)_2]^{16-}$を合成した。チタン(IV)三置換 Dawson 型ポリ酸塩単量体$[\alpha\text{-}P_2W_{15}Ti_3O_{59}(OH)_3]^{9-}$はバナジウム(V)やニオブ(V)三置換体と比べて、非常に限られた条件でしか利用できないが、それでもカチオン性有機金属種を担持した化合物を誘導することができた。

単結晶 X 線構造解析から 2 つの Cp*Rh 基が 2 つの Dawson unit を連結した二量体構造であることが分かった。このような二量体構造は有機金属種担持チタン(IV)三置換 Dawson 型ポリ酸塩では初めての例であり、非常に珍しい構造である。また BVS 計算から Dawson unit 内の 2 つの稜共有酸素がプロトネーションしていることが分かった。

Appendix

ヘテロ原子 Si の Keggin 型ポリ酸塩一欠損種で二つの M (M = Zr^{IV}, Hf^{IV})をサンドイッチしたポリ酸塩について、二つの M を二本の μ-OH で架橋した稜共有錯体 $[(\alpha\text{-}SiW_{11}O_{39}M)_2(\mu\text{-}OH)_2]^{10-}$と、二つの M を三本の μ-OH で架橋した面共有錯体 $[(\alpha\text{-}SiW_{11}O_{39}M)_2(\mu\text{-}OH)_3]^{11-}$の単結晶 X 線構造解析を行った。BVS 計算からいずれの架橋酸素原子もプロトネーションしていた。二核錯体で稜共有はよくみられるが、面共有というのは非常に珍しい構造であった。これはヘテロ原子が Si や Ge のときに初めて実現され、ヘテロ原子 P のポリ酸塩は同じ pH では安定に存在できないので、面共有錯体は実現できない。

References

1) L. Pauling, *J. Am. Chem. Soc*. **1929**, *51*, 2868.

2) J. F. Keggin, *Nature* **1933**, *131*, 908.

3) J. S. Anderson, *Nature* **1937**, *140*, 850.

4) B. Dawson, *Acta Cryst*. **1953**, *6*, 113.

5) J. L. T. Waugh, D. P. Shoemaker, L. Pauling, *Acta Cryst*. **1954**, *7*, 438.

6) D. D. Dexter, J. V. Silverton, *J. Am. Chem. Soc*. **1968**, *90*, 3589.

7) H. T. Evans, Jr., J. S. Showell, *J. Am. Chem. Soc*. **1969**, *91*, 6881.

8) M. T. Pope, Heteropoly, Isopoly Oxometalates, *Springer-Verlag* **1983**.

9) (a) G. Johansson, *Acta. Chem. Scand*. **1960**, *14*, 771.

(b) G. Johansson, *Arkiv. Kemi*. **1963**, *20*, 305.

(c) J. T. Gatlin, Z. L. Mensinger, L. N. Zakharov, D. Macinnes, D. W. Johnson, *Inorg. Chem*. **2008**, *47*, 1267.

10) A. Teze, E. Cadot, V. Bereau, G. Herve, *Inorg. Chem*. **2001**, *40*, 2000.

11) Y. U. Kwon, O. H. Han, J. H. Son, *Inorg. Chem*. **2003**, *42*, 4153-4159.

12) H. D' Amour, *Acta Crystallogr.* **1976**, *B32*, 729.

13) R. Contant, R. Thouvenot, *Inorg. Chim. Acta* **1993**, *212*, 41.

14) (a) P. J. S. Richardt, R. W. Gable, A. M. Bond, A. G. Wedd, *Inorg, Chem*. **2001**, *40*, 703.

(b) Y.-X. Sun, Z.-B. Zhang, Q. Sun, Y. Xu, *Wuji Huaxue Xuebao* **2011**, *27*, 556.

15) J. Canny, A. Teze, R. Thouvenot, G. Herve, *Inorg. Chem*. **1986**, *25*, 2114.

16) P. J. Domaille, *Inorg. Synth*. **1990**, *27*, 96.

17) R. Contant, *Inorg. Synth*. **1990**, *27*, 104.

18) K. Nomiya, M. Pohl, N. Mizuno, D. K. Lyon, R. G. Finke, *Inorg. Synth*. **1997**, *31*, 186.

19) V. W. Day, W. G. Klemperer, *Science* **1985**, *223*, 533.

20) 日本化学会編, 科学総論 ポリ酸の化学, 学会出版センター, 日本 **1993**.

21) U. Müller, *Inorganic Structural Chemistry*, Wiley, New York **1993**.

22) A. L. Linsenbigler, G. Lu, J. T. Yates, Jr., *Chem. Rev*. **1995**, *95*, 735.

23) T. Kawahara, Y. Konishi, H. Tada, N. Tohge, J. Nishii, S. Ito, *Angew. Chem. Int. Ed*. **2002**, *41*, 2811.

24) N. Erdman, K. R. Poeppelmeier, M. Asta, O. Warschkow, D. E. Ellis, L. D. Marks, *Nature* **2002**, *55*, 419.

25) A. Kudo, K. Domen, K. Maruya, T. Onishi, *J. Catal*. **1992**, *135*, 300.

26) D. Bao, X. Yao, N. Wakiya, K. Shinozaki, N. Mizutani, *Appl. Phys. Lett*. **2001**, *79*, 3767.

27) N. J. Crano, R. C. Chambers, V. M. Lynch, M. A. Fox, *J. Mol. Catal. A*, **1996**, *114*, 65.

28) M. A. Fox, M. T. Dulay, *Chem. Rev*. **1993**, *93*, 341.

29) R. C. Chamber, C. L. Hill, *Inorg. Chem*. **1991**, *30*, 2776.

30) F. Zhang, J. Zhao, L. Zang, T. Shen, H. Hidaka, N. Serpone, E. Pelizzetti, *J. Mol. Catal*. **1997**, *120*, 173.

31) W. H. Knoth, P. J. Domaille, D. C. Roe, *Inorg. Chem*. **1983**, *22*, 198.

32) T. Yamase, T. Ozeki, S. Motomura, *Bull. Chem. Soc. Jpn*. **1992**, *65*, 1453.

33) T. Yamase, T. Ozeki, *Acta. Cryst*. **1991**, *C47*, 693.

34) Y. Lin, T. J. R. Weakley, B. Rapko, R. G. Finke, *Inorg. Chem*. **1993**, *32*, 5095.

35) K. Nomiya, M. Takahashi, K. Ohsawa, J. A. Widegren, *J. Chem. Soc., Dalton Trans*. **2001**, 2872.

36) K. Nomiya, M. Takahashi, J. A. Widegren, T. Aizawa, Y. Sakai, N. C. Kasuga, *J. Chem. Soc., Dalton Trans*. **2002**, 3679.

37) O. A. Kholdeeva, G. M. Maksimov, R. I. Maksimovskaya, L. A. Kovaleva, M. A. Fedotov, V. A. Grigoriev, C. L. Hill, *Inorg. Chem*. **2000**, *39*, 3828.

38) O. A. Kholdeeva, T. A. Trubitsina, G. M. Maksimov, A. V. Golovin, R. I. Maksimovskaya, *Inorg. Chem*. **2005**, *44*, 1635-1642.

39) G. M. Maksimov, R. I. Maksimovskaya, O. A. Kholdeeva, M. A. Fedotov, V. I. Zaikovskii, V. G. Vasil'ev, S. S. Arzumanov. *J. Struct. Chem*. **2009**, *50*, 618-627.

40) U. Kortz, S. S. Hamzeh, A. Nasser, *Chem. Eur. J*. **2003**, *9*, 2945.

41) H. Murakami, K. Hayashi, I. Tsukada, T.Hasegawa, S. Yoshida, R. Miyano, C. N. Kato, K. Nomiya, *Bull. Chem. Soc. Jpn*. **2007**, *80*, 2161.

42) S. Yoshida, H. Murakami, Y. Sakai, K. Nomiya, *Dalton Trans*. **2008**, 4630.

43) (a) Y. Sakai, K. Yoza, C. N. Kato, K. Nomiya, *Dalton Trans*.**2003**, 3581.
(b) Y. Sakai, K. Yoza, C. N. Kato, K. Nomiya, *Chem. Eur. J*. **2003**, *9*, 4077.
(c) Y. Sakai, S. Yoshida, T. Hasegawa, H. Murakami, K. Nomiya, *Bull. Chem. Soc. Jpn*. **2007**, *80*, 1965.

44) Y. Sakai, Y. Kitakoga, K. Hayashi, K. Yoza, K. Nomiya, *Eur. J. Inorg. Chem*. **2004**, 4646.

45) S. Ohta, B. S. Thesis, Kanagawa University, Kanagawa, **2009**.

46) K. Nomiya, M. Pohl, N. Mizuno, D. K. Lyon, R. G. Finke, *Inorg. Chem*. **1995**, *34*, 1413.

47) (a) K. Lyon, R. G. Finke, *Inorg. Chem*. **1990**, *29*, 1787.
(b) R. G. Finke, D. K. Lyon, K. Nomiya, S. Sur, N. Mizuno, *Inorg. Synth*. **1997**, *31*, 186.
(c) A. Trovarelli, R. G. Finke, *Inorg. Chem*. **1993**, *32*, 6034.
(d) M. Pohl, R. G. Finke, *Organometallics* **1993**, *12*, 1453.
(e) M. Pohl, D. K. Lyon, N. Mizuno, K. Nomiya, M. Kaneko, H. Weiner, R. G. Finke, *Inorg. Chem*. **1995**, *34*, 1413-1429.

48) M. Pohl, Y. Lin, T. J. R. Weakley, K. Nomiya, M. Kaneko, H. Weiner, R. G. Finke, *Inorg. Chem*. **1995**, *34*, 767-777.

49) D. J. Edlund, R. J. Saxton, D. K. Lyon, R. G. Finke, *Organometallics* **1998**, ***7***, 1962.

50) K. Nomiya, C. Nozaki, M. Kaneko, R. G. Finke, M. Pohl, *J. Organometal. Chem*. **1995**, *505*, 23.

51) T. Nagata, M. Pohl, H. Weiner, R. G. Finke, *Inorg. Chem*. **1997**, *36*, 1366.

52) (a) N. Mizuno, D. K. Lyon, R. G. Finke, *J. Catal*. **1991**, *128*, 84.

(b) N. Mizuno, H. Weiner, R. G. Finke, *J. Mol. Catal.* **1996**, *A114*, 15.
53) H. Weiner, Y. Hayashi, R. G. Finke, *Inorg. Chem.* **1999** ,*38*, 2579.
54) B. M. Rapko, M. Pohl, R. G. Finke, *Inorg. Chem.* **1994**, *33*, 3625.
55) K. Nomiya and T. Hasegawa, *Chem. Lett.* **2000**,410.
56) K. Nomiya, H. Torii, C. N. Kato, Y. Sado, *Chem. Lett.* **2003**, *32*, 664.
57) Y. Kasahara, A. Shinohara, Y. Sado, K. Nomiya, *Inorg. Chim. Acta* **2007**, *360*, 2313-2320 .
58) S. Aoki, T. Kurashina, Y. Kasahara, T. Nishijima, K. Nomiya, *Dalton Trans.* **2011**, *40*, 1243-1253.
59) J. W. Kang, K. Moseley, P. M. Maitlis, *J. Am. Chem. Soc.* **1969**, *91*, 5970.
60) C. White, A. Yates, P. M. Maitlis, *Inorg. Synth.* **1992**, *29*, 228.

List of Publication

Original Paper (Peer Reviewed) (4 件)

1. Monomer and Dimer of Mono-titanium(IV)-Containing α-Keggin Polyoxometalates: Synthesis, Molecular Structures, and pH-Dependent Monomer-Dimer Interconversion in Solution
   Y. Matsuki, Y. Mouri, Y. Sakai, S. Matsunaga, K. Nomiya, *Eur. J. Inorg. Chem.* **2013**, 1754-1761.

2. Encapsulation of Anion/Cation in the Central Cavity of Tetrameric Polyoxometalate, Composed of Four Trititanium(IV)-Substituted α-Dawson Subunits, Initiated by Protonation/Deprotonation of the Bridging Oxygen Atoms on the Intramolecular Surface
   Y. Sakai, S. Ohta, Y. Shintoyo, S. Yoshida, Y. Taguchi, Y. Matsuki, S. Matsunaga, K. Nomiya, *Inorg. Chem.* **2011**, *50*, 1754-1761.

3. Synthesis and molecular structure of dimeric tri-titanium(IV)-substituted Dawson polyoxometalate bridged by two Cp^*Rh^{2+} groups
   Y. Matsuki, S, Takaku, T. Hoshino, S. Matsunaga, K. Nomiya, *Manuscript in preparation*.

4. 2:2-Type complexes of zirconium(IV)/hafnium(IV) centers with mono-lacunary Keggin polyoxometalates: Syntheses and molecular structures of $[(\alpha\text{-}SiW_{11}O_{39}M)_2(\mu\text{-}OH)_2]^{10-}$ (M = Zr, Hf) with edge-sharing octahedral units and $[(\alpha\text{-}SiW_{11}O_{39}M)_2(\mu\text{-}OH)_3]^{11-}$ with face-sharing octahedral units
   H. Osada, A. Ishikawa, Y. Saku, Y. Sakai, Y. Matsuki, S. Matsunaga, K. Nomiya, *Polyhedron*, *52*, **2013**, 389-397.

Original Paper (Non-Peer Reviewed) (1 件)

1. チタン(IV)三置換 Dawson 型ポリ酸塩単量体とそれを用いた NH_4^+内包テトラポッド型四量体の合成
   松木悠介, 星野貴弘, 増田佳奈, 松井敬祐, 力石紀子, 松永諭, 野宮健司, *Science Jornal of Kanagawa University*, **25**, 69-72, (2014).

International Conference (1 件)

1. Synthesis of monomeric, tri-titanium(IV)-substituted Dawson polyoxometalate and derivation of its non-bridging tetramer with encapsulated Br^--ion in the central cavity
   The 9th International Symposium on the Kanagawa University-National Taiwan University Exchange Program 2013, March 15, 2014

Meeting and Conference (11 件)

1. チタン(IV)三置換 Dawson 型ポリ酸塩単量体の合成およびそれをビルディングブロックとした中心空間にカチオンをカプセル化した四量体の誘導
   野宮健司, 松木悠介, 坂井善隆, 田口裕己, 髙久祥子, 第 61 回錯体化学討論会, 岡山理科大学, 2011 年 9 月, Abstr., **1PA-15**.

2. チタン(IV)三置換 Dawson 型ポリ酸塩単量体の合成および中心空間にアニオンをカプセル化した架橋なし四量体の誘導
   松木悠介, 坂井善隆, 星野貴弘, 野宮健司, 第 64 回錯体化学討論会, 中央大学後楽園キャンパス, 2014 年 9 月 Abstr. **1PA-026**.

3. チタン(IV)三置換 Dawson 型ポリ酸塩単量体の合成とそれをビルディングブロックとした中心空間にカチオンをカプセル化した架橋なし四量体の誘導
   野宮健司, 松木悠介, 髙久祥子, 第 92 回日本化学会春季年会, 慶応義塾大学日吉キャンパス, 2012 年 3 月, Abstr. **1PB-006**.

4. チタン(IV)一置換 Keggin 型ポリ酸塩単量体および二量体の合成、分子構造と単量体-未量体の pH に依存した相互変換
   松木悠介, 松永諭, 坂井善隆, 毛利有貴, 野宮健司, 第 93 回日本化学会春季年会, 立命館大学びわこ・くさつキャンパス, 2013 年 3 月, Abstr. **1B3-14**.

5. チタン(IV)一置換 α-Keggin 型ポリ酸塩単量体および二量体の合成、分子構造と pH に依存する単量体-二量体の平衡
   松木悠介, 坂井善隆, 松永諭, 毛利有貴, 野宮健司, 第 2 回 CSJ 化学フェスタ, 東京工業大学大岡山キャンパス, 2012 年 10 月, Abstr. **P1-28**.

6. チタン(IV)三置換 Dawson 型ポリ酸塩単量体から中心空間に Br^- を内包した架橋なし四量体の合成
   野宮健司, 松木悠介, 星野貴弘, 第 4 回 CSJ 化学フェスタ, タワーホール船堀, 2014 年 10 月, Abstr. **P3-060**.

7. Dawson 型ポリ酸塩チタン(IV)三置換体単量体にカチオン性有機金属種を担持した新規化合物の合成
   髙久祥子, 松木悠介, 松永諭, 野宮健司, 錯体化学会第 62 回討論会, 富山大学五福キャンパス, 2012 年 9 月, Abstr. **2PA-072**.

8. α-Keggin 型シリコタングステン酸塩一欠損種でサンドイッチされた Zr(IV)/Hf(IV)二核稜共有及び面共有型錯体の合成と分子構造
長田宏紀, 佐久惟, 松木悠介, 石川晃央, 松永諭, 野宮健司第 92 回日本化学会春季年会, 慶応義塾大学日吉キャンパス, 2012 年 3 月, Abstr. **1PB-005**.

9. α-Keggin 型シリコタングステート一欠損種でサンドイッチされた Zr(IV)/Hf(IV)二核稜共有及び面共有連結錯体の合成と分子構造
長田宏紀, 石川晃央, 佐久惟, 松木悠介, 松永諭, 野宮健司, 第 2 回 CSJ 化学フェスタ, 東京工業大学大岡山キャンパス, 2012 年 10 月, Abstr. **P5-19**.

10. チタン(IV)三置換 Dawson 型ポリ酸塩単量体とカチオン性有機金属種の反応生成物の構造
星野貴弘, 松木悠介, 野宮健司, 日本化学会第 94 春季年会, 2014 年 3 月, Abstr, **2PB-009**.

11. チタン(IV)三置換 Dawson 型ポリ酸塩単量体と $Cp^{*}Rh^{2+}$種の反応生成物の構造
星野貴弘, 松木悠介, 野宮健司, 第 4 回 CSJ 化学フェスタ, タワーホール船堀, 2014 年 10 月, Abstr. **P3-007**.

Acknowledgement

本論文は、神奈川大学理学部化学科野宮研究室における博士後期課程三年間の研究を中心に纏めたものです。論文を纏めるにあたり、お世話になりました全ての方々に感謝いたします。

神奈川大学理学部化学科卒業研究から六年間、長きに亘り数多くの御指導、御助言を頂いた指導教授の野宮健司教授に深く感謝いたします。

アドバイザーとして大変貴重なご助言を頂いた川本達也教授、山口和夫教授、堀久男教授に深く感謝致します。

投稿論文の作成や研究室のセミナーにおいて数多くの御助言を頂いた松永諭特別助教、力石紀子助教に深く感謝いたします。

NMR の測定に御指導、御助言を頂いた横山宙さんに深く感謝いたします。

卒業研究で一年間に亘り数多くの御助言を頂いた P.D.の坂井善隆さんに深く感謝いたします。

卒業研究から御世話になりました先輩の青木正太郎さん、桑名渉さん、毛利有貴さん、吉田拓也さん、高木由貴さんに心より感謝致します。

最後に、私と修士課程卒業までともに研究を行ってきた太田和明君、北村直己君、富樫欣洋君、吉川理絵さん、卒業研究生活を共に送った大沢裕美さん、神保郁美君、飯倉光君、口地哲平君、東浦諒君に感謝いたします。また私と共に研究を行ってきた田口裕己君、髙久祥子さん、長田宏紀君、齋藤和宏君、星野貴弘君を始め 18 期生 9 名、19 期生 12 名、20 期生 8 名、21 期生 9 名、22 期生 8 名に深く感謝いたします。

EurJIC European Journal of Inorganic Chemistry

ChemPubSoc Europe

FULL PAPER

DOI:10.1002/ejic.201201290

Monomer and Dimer of Mono-titanium(IV)-Containing α-Keggin Polyoxometalates: Synthesis, Molecular Structures, and pH-Dependent Monomer–Dimer Interconversion in Solution

CLUSTER ISSUE

Yusuke Matsuki,[a] Yuki Mouri,[a] Yoshitaka Sakai,[a] Satoshi Matsunaga,[a] and Kenji Nomiya*[a]

Dedicated to Professor Michael T. Pope on the occasion of his 80th birthday

Keywords: Polyoxometalates / Titanium / Tungsten

Powder and crystalline samples of the monomer $(Et_2NH_2)_5[\alpha\text{-}PW_{11}TiO_{40}]\cdot 2H_2O$ (EtN-**1**) and a crystalline sample of the μ-oxo dimer $(Et_2NH_2)_8[(\alpha\text{-}PW_{11}TiO_{39})_2O]\cdot 6H_2O$ (EtN-**2**) of mono-titanium(IV)-containing α-Keggin polyoxometalates (POMs) were prepared and characterized by elemental analysis, thermogravimetry/differential thermal analysis (TG/DTA), FTIR, single-crystal X-ray crystallography, and solid-state cross-polarization magic angle spinning (CPMAS) ^{31}P NMR and solution (^{31}P and ^{183}W) NMR spectroscopy. The molecular structure of the dimeric polyoxoanion with a μ-oxo group in **2** was determined for the first time. The monomer–dimer equilibrium in solution was clarified by pH-varied ^{31}P NMR spectroscopy.

Introduction

Polyoxometalates (POMs) are molecular metal oxide clusters that have attracted considerable attention in the fields of catalysis, medicine, surface science, materials science, and nanotechnology because POMs are often considered to be molecular analogues of metal oxides in terms of structural analogy.[1] The ionic radius of Ti^{IV} (0.75 Å) is close to that of W^{VI} (0.74 Å), which suggests that Ti^{IV} should fit nicely into the POM framework. Thus, site-selective substitution of W^{VI} atoms in POMs with Ti^{IV} atoms is particularly interesting because of the formation of multicenter active sites with corner- or edge-sharing TiO_6 octahedra and also the generation of oligomeric species through Ti–O–Ti bonds.[2–6] A number of catalytic reactions of titanium(IV)-containing POMs have also been reported so far.[1g,1m,3] Oxidation catalysis by peroxo and hydroperoxo species of Ti-containing Keggin POMs has been extensively studied.[3]

The dimerization process in Lindqvist and Keggin POMs (i.e., the mechanism of formation of the μ-oxo dimer) has been discussed by using DFT studies,[7] in which the most probable thermodynamic mechanism for the smaller clusters has been proposed: first, the formation of a protonated monomer, the protonation site of which is the O atom of a terminal M=O bond; second, the formation of di-μ-hydroxo intermediate from the M–OH species (this requires +28 kcal mol^{-1}); and the final step, formation of the μ-oxo dimer by loss of a water molecule from the di-μ-hydroxo intermediate.

The tri-titanium(IV)-substituted Dawson POM "$[P_2W_{15}Ti_3O_{62}]^{12-}$" has been realized through the formation of several tetrameric species[4] [e.g., the tetrameric Dawson Ti–O–Ti-bridged anhydride form without bridging μ_3-$Ti(H_2O)_3$ octahedral groups (the nonbridging Dawson tetramer)], which has an encapsulated Cl^- anion in the central cavity {i.e., $[\{\alpha\text{-}1,2,3\text{-}P_2W_{15}Ti_3O_{57.5}(OH)_3\}_4Cl]^{25-}$},[4b–4d] an encapsulated NH_4^+ cation species {i.e., $[(\alpha\text{-}1,2,3\text{-}P_2W_{15}Ti_3O_{60.5})_4(NH_4)]^{35-}$},[4g] and also the tetrameric Dawson species with bridging μ_3-$Ti(H_2O)_3$ groups (the bridging Dawson tetramer) with an encapsulated anion X $[\{\alpha\text{-}1,2,3\text{-}P_2W_{15}Ti_3O_{59}(OH)_3\}_4\{\mu_3\text{-}Ti(H_2O)_3\}_4X]^{21-}$ (X = Cl, Br, I, NO_3).[4a,4d,4e]

The dimeric mono-titanium(IV)-substituted Dawson POM {i.e., the μ-oxo Dawson dimer $[(\alpha_2\text{-}P_2W_{17}TiO_{61})_2(\mu\text{-}O)]^{14-}$ and its protonated species $[(\alpha_2\text{-}P_2W_{17}TiO_{61})(\alpha_2\text{-}P_2W_{17}TiO_{61}H)(\mu\text{-}O)]^{13-}$} has been structurally charac-

[a] Department of Chemistry, Faculty of Science, Kanagawa University, Hiratsuka, Kanagawa 259-1293, Japan
Homepage: http://professor.kanagawa-u.ac.jp/sci/chemistry/prof05.html

Supporting information for this article is available on the WWW under http://dx.doi.org/10.1002/ejic.201201290.

terized by single-crystal X-ray crystallography.[5] In the latter, the protonation site is the surface Ti–O–W site of one of the two Dawson units, but not the μ-oxo site, and therefore, two Dawson units became inequivalent. The monomeric form $K_8[\alpha_2\text{-}P_2W_{17}TiO_{62}]\cdot 18H_2O$ was also prepared. pH-varied ^{31}P NMR spectroscopic measurements showed the presence of monomer–dimer equilibrium in solution; that is, the predominant species in aqueous solutions are the monomeric species at pH 7.0, the μ-oxo dimer at pH 1.0–3.0, and the monoprotonated species at pH 0.5, the protonation site of which is the surface Ti–O–W site of one of the two Dawson units.

In terms of the Keggin derivatives, tri-titanium(IV)-1,2,3- and di-titanium(IV)-1,2-substituted Keggin POMs have been isolated as tri-μ-oxo dimers {e.g., $[(\beta\text{-}1,2,3\text{-}SiW_9Ti_3O_{37})_2O_3]^{14-}$,[2a] $[(\alpha\text{-}1,2,3\text{-}GeW_9Ti_3O_{37})_2O_3]^{14-}$,[2b] $[(\beta\text{-}1,2,3\text{-}GeW_9Ti_3O_{37})_2O_3]^{14-}$,[2c] and $[(\alpha\text{-}1,2,3\text{-}PW_9Ti_3O_{37})_2O_3]^{12-}$}[2e] and as a di-μ-oxo dimer {e.g., $[(\alpha\text{-}1,2\text{-}PW_{10}Ti_2O_{38})_2O_2]^{10-}$}.[2d] Furthermore, di-titanium(IV)-substituted γ-Keggin silicotungstate and germanotungstate {i.e., $[\{\gamma\text{-}SiTi_2W_{10}O_{36}(OH)_2\}_2O_2]^{8-}$[2f] and $[\{\gamma\text{-}GeTi_2W_{10}O_{36}(OH)_2\}_2O_2]^{8-}$}[2g] have also been prepared as a dimeric species, whereas a di-titanium(IV)-1,5-substituted β-Keggin POM has been isolated as a tetrameric species, $[\{\beta\text{-}Ti_2SiW_{10}O_{39}\}_4]^{24-}$.[2h] In addition, cyclic tri-titanium(IV)-substituted Keggin trimers such as $[(\alpha\text{-}Ti_3PW_9O_{38})_3(PO_4)]^{18-}$,[2i] $[(\alpha\text{-}Ti_3SiW_9O_{37}OH)_3\{TiO_3(OH_2)_3\}]^{17-}$,[2i] and $\{K[\{Ge(OH)O_3\}(GeW_9Ti_3O_{38}H_2)_3]\}^{14-}$[2j] have recently been reported.

As to the titanium(IV)-substituted Keggin POMs, however, it should be noted that no structural determination through X-ray crystallography of the mono-titanium(IV)-containing POMs has been reported. Concerned with such POMs, Kholdeeva's group has reported the preparation and characterization of the μ-hydroxo dimer $(Bu_4N)_7[(PTiW_{11}O_{39})_2(\mu\text{-}OH)]$ (H**1**) formed in acidic MeCN from the monomeric species Keggin POM $(Bu_4N)_5[PTiW_{11}O_{40}]$ (**2**), and pH-dependent interconversion between them.[6a] The same research group has also reported the μ-oxo dimer $(Bu_4N)_8[(PTiW_{11}O_{39})_2(\mu\text{-}O)]$ (μ-oxo dimer **1**) and three monomeric derivatives $(Bu_4N)_4[PTi(L)W_{11}O_{39}]$ {L = OH, OMe, and OAr [ArOH = 2,3,6-trimethylphenol (TMP)]}, which have been synthesized starting from the μ-hydroxo dimer $(Bu_4N)_7[(PTiW_{11}O_{39})_2(\mu\text{-}OH)]$ (H**1**) or the heteropolyacid $H_5PW_{11}TiO_{40}\cdot 12H_2O$.[6b] In these studies, however, the molecular structures of the μ-hydroxo dimer and the μ-oxo dimer have not been determined through X-ray crystallography.

In this work, we have prepared and characterized the monomeric Keggin POM $(Et_2NH_2)_5[\alpha\text{-}PW_{11}TiO_{40}]\cdot 2H_2O$ (EtN-**1**) and the μ-oxo Keggin dimer $(Et_2NH_2)_8[(\alpha\text{-}PW_{11}TiO_{39})_2O]\cdot 6H_2O$ (EtN-**2**), and also confirmed a monomer–dimer equilibrium in solution by pH-varied ^{31}P NMR spectroscopy. Furthermore, we have successfully determined the molecular structure of μ-oxo dimeric polyoxoanion **2** by X-ray crystallography. Herein, we report full details of the synthesis and characterization of EtN-**1** and EtN-**2**.

Results and Discussion

Synthesis and Characterization

The monomer and dimer of the titanium(IV)-substituted Keggin POM have been significantly discussed.[6] However, their X-ray structures have not been reported so far, because the crystals suitable for X-ray crystallography have never been obtained. In this work, we successfully prepared and crystallized the monomer in the presence of NaOAc. The dimer was also crystallized from the monomer under acidic conditions of pH 1.0 and the X-ray structure was determined.

In the presence of NaOAc, a 1:1 molar ratio reaction of mono-lacunary Keggin POM $K_7[PW_{11}O_{39}]\cdot 8H_2O$ with $TiCl_4$ in an aqueous solution and the addition of excess amounts of solid Et_2NH_2Cl produced the diethylammonium salt of the monomeric Keggin POM, $(Et_2NH_2)_5[\alpha\text{-}PW_{11}TiO_{40}]\cdot 2H_2O$ (EtN-**1**). Monomer EtN-**1** was dissolved in an H_2O/MeOH (1:1 v/v) mixed solvent, and the solution was adjusted to pH 1.0 with a 1 M aqueous HCl solution, followed by stirring for 2 days at room temperature. The solution was evaporated slowly, and after 3 days, colorless, clear plate crystals of the dimer Keggin POM, $(Et_2NH_2)_8[(\alpha\text{-}PW_{11}TiO_{39})_2O]\cdot 6H_2O$ (EtN-**2**), were obtained. These compounds were characterized by CHN elemental analysis, FTIR, thermogravimetry/differential thermal analysis (TG/DTA), X-ray crystallography, and solution and solid-state cross-polarization magic angle spinning (CPMAS) ^{31}P NMR and solution ^{183}W NMR spectroscopy.

The number of water molecules was determined by TG/DTA measurements under atmospheric conditions and elemental analysis. In the TG/DTA, weight losses of 1.15% observed at below 199.3 °C for EtN-**1** (Figure S1 in the Supporting Information) and 1.84% observed at below 122.5 °C for EtN-**2** (Figure S2 in the Supporting Information) corresponded to approximately two water molecules and approximately six water molecules, respectively, which were consistent with the data from elemental analyses.

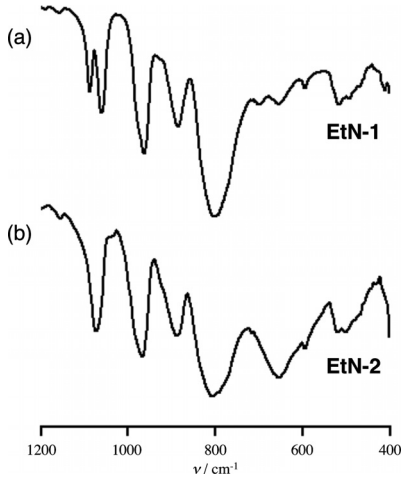

Figure 1. The FTIR spectra in the polyoxoanion region (1200–400 cm^{-1}), measured in KBr disks, of (a) $(Et_2NH_2)_5[\alpha\text{-}PW_{11}TiO_{40}]\cdot 2H_2O$ (EtN-**1**) and (b) $(Et_2NH_2)_8[(\alpha\text{-}PW_{11}TiO_{39})_2O]\cdot 6H_2O$ (EtN-**2**).

The solid FTIR spectrum of monomer EtN-**1** (Figure 1, a) measured in a KBr disk showed prominent bands in the polyoxometalate region (1200–400 cm^{-1}) at 1090, 1062, 964, 886, and 801 cm^{-1}, which originated from mono-lacunary Keggin POM, $[PW_{11}O_{39}]^{7-}$. These are the characteristic vibration bands of the Keggin-type "$PW_{12}O_{40}^{3-}$".[8] The Ti–O–Ti vibration band of the inter-Keggin units was not observed at around 650 cm^{-1}. The P–O vibration band was observed as split peaks at 1090 and 1062 cm^{-1}. The FTIR spectrum of dimer EtN-**2** measured in a KBr disk also showed prominent bands in the polyoxometalate region (1200–400 cm^{-1}) at 1075, 968, 889, 807, and 654 cm^{-1}. The Ti–O–Ti vibration band of the inter-Keggin units in EtN-**2** was observed at 654 cm^{-1}, which was consistent with the X-ray crystallography data (see below). The P–O vibration band of EtN-**2** was observed as a single peak at 1075 cm^{-1}.

Molecular Structures of Dimeric EtN-2 and Monomeric EtN-1

The molecular structure of polyoxoanion **2** in EtN-**2** and its polyhedral representation are shown in Figure 2 (a and b), respectively. Selected bond lengths [Å] and angles [°] around the titanium(IV) centers in **2** are listed in Table 1, whereas other bond lengths [Å] and angles [°] for the Keggin unit (Table S1) and bond valence sum (BVS) calculations (Table S2) are given in the Supporting Information.

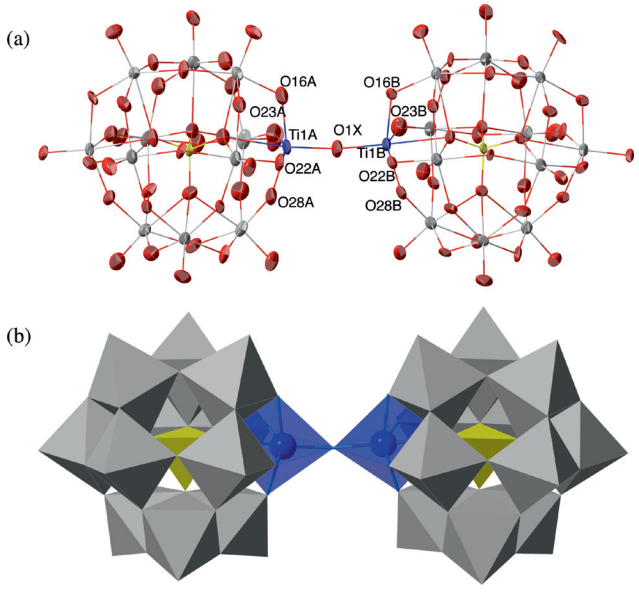

Figure 2. (a) Molecular structure of the polyoxoanion $[(\alpha\text{-}PW_{11}TiO_{39})_2O]^{8-}$ (**2**) in EtN-**2** and (b) its polyhedral representation.

The composition and formula of EtN-**2**, which contains eight diethylammonium countercations and six hydrated water molecules, were determined by CHN elemental analysis and TG/DTA analysis. In X-ray crystallography, one polyoxoanion that contained two Keggin units, five diethylammonium cations, and three hydrated water molecules per formula unit was identified in the crystal structure.

X-ray crystallography of EtN-**2** revealed that six-coordinate geometry around each Ti center was accomplished by bonding with five oxygen atoms in the mono-lacunary site of the Keggin POM and the bridging oxygen atom (μ-O). Here the bonding between the titanium atom and the oxygen atom coordinated to the P atom [O(36A)–Ti(1A) 2.361(12) Å, O(36B)–Ti(1B) 2.343(11) Å] is incorporated in the coordination. The two Keggin units are crystallographically independent due to the slight twist between each Keggin unit, thus resulting in the overall C_1 symmetry of the polyoxoanion molecule in the solid state. However, in solution, the twist was averaged, thus resulting in overall C_{2v} symmetry. Therefore, the six-line ^{183}W NMR spectrum in D_2O/CD_3CN (1:3 v/v) was observed with a relative intensity ratio of 2:2:1:2:2:2 (Figure 6; see below). The Ti–O–Ti bonding moiety and the eleven W atoms in the Keggin unit exhibited conventional octahedral coordination polyhedra (Figure 2, b). Structural analysis revealed that **2** was composed of two mono-titanium(IV)-substituted Keggin POM subunits "$[\alpha\text{-}PW_{11}TiO_{39}]^{3-}$" linked through one μ-oxo group. The bond angle of the Ti–O–Ti moiety [Ti(1A)–O(1X)–Ti(1B) 169.9(9)°] and the inter-Keggin unit Ti–Ti distance [Ti(1A)–Ti(1B) 3.562 Å] in **2** can be compared with those of the previously reported di- and tri-titanium(IV)-substituted dimeric Ti–O–Ti-bridged anhydride forms (Figure 3); that is, (i) the Ti–O–Ti angles between the two Keggin units (135.7, 136.3°) in the di-titanium(IV)-substituted dimer, $[(\alpha\text{-}1,2\text{-}PW_{10}Ti_2O_{38})_2O_2]^{10-}$ (Figure 3, b),[2d] and (ii) the Ti–O–Ti angles between the two Keggin units (130.2, 130.9, 131.3°) in the tri-titanium(IV)-substituted dimer, $[(\alpha\text{-}1,2,3\text{-}PW_9Ti_3O_{37})_2O_3]^{12-}$ (Figure 3, c).[2e] The angle of the intermolecular Ti–O–Ti moiety of **2** was more of a linear alignment, and the inter-Keggin unit Ti–Ti distance of **2** was longer than those of the previously reported di- and tri-Ti^{IV}-substituted Keggin dimers. The bond lengths of the Ti–O–Ti moiety [O(1X)–Ti(1A) 1.794(12) Å, O(1X)–Ti(1B) 1.782(11) Å] in **2** were slightly shorter than those of di- and tri-titanium(IV)-substituted Keggin dimers {1.80(2)–1.84(2) Å for $[(\alpha\text{-}1,2\text{-}PW_{10}Ti_2O_{38})_2O_2]^{10-}$, 1.80(1)–1.86(1) Å for $[(\alpha\text{-}1,2,3\text{-}PW_9Ti_3O_{37})_2O_3]^{12-}$}.

The bond valence sum (BVS) value of the bridging oxygen atom [O(1X)], which was calculated on the basis of the observed bond lengths in **2** (Table S2 in the Supporting Information), strongly suggested that the bridging oxygen atom [O(1X)] was not protonated (i.e., ascribed to O^{2-}). As for the other oxygen atoms in the Keggin units of **2**, there

Table 1. Selected bond lengths [Å] and angles [°] around the Ti^{IV} center in $[(\alpha\text{-}PW_{11}TiO_{39})_2O]^{8-}$ (**2**).

Ti–O bond lengths			
Ti(1A)–O(1X)	1.794(12)	Ti(1B–O(1X)	1.782(11)
Ti(1A)–O(16A)	1.934(14)	Ti(1A)–O(23A)	1.912(13)
Ti(1A)–O(22A)	1.943(12)	Ti(1A)–O(28A)	1.904(13)
Ti(1B)–O(16B)	1.933(11)	Ti(1B)–O(23B)	1.893(10)
Ti(1B)–O(22B)	1.947(11)	Ti(1B)–O(28B)	1.906(12)
Ti(1A)–O(36A)	2.361(12)	Ti(1B)–O(36B)	2.343(11)
Ti–O–Ti angle			
Ti(1A)–O(1X)–Ti(1B)	169.9(9)		

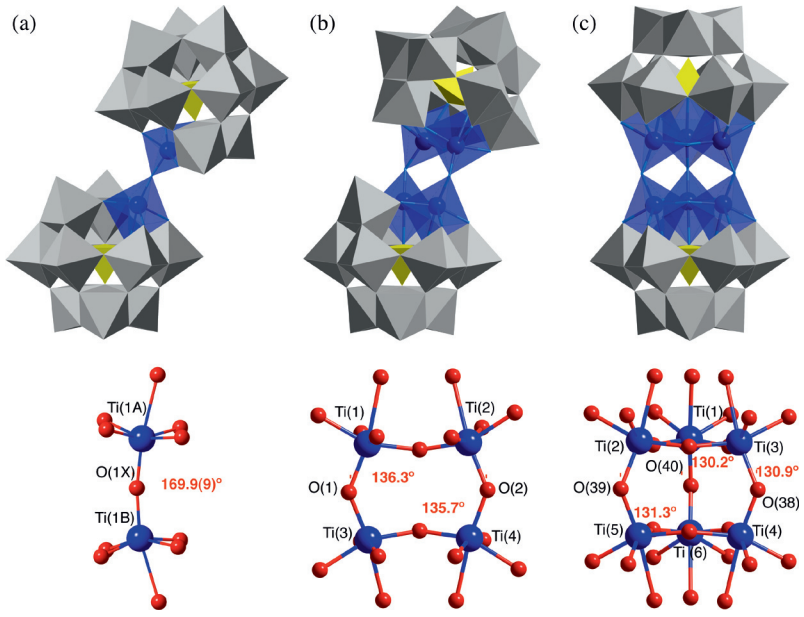

Figure 3. Structures and partial structures around the Ti center of (a) mono-titanium(IV)-substituted dimer, $[(\alpha\text{-}PW_{11}TiO_{39})_2O]^{8-}$ (this work), (b) di-titanium(IV)-substituted dimer, $[(\alpha\text{-}1,2\text{-}PW_{10}Ti_2O_{38})_2O_2]^{10-}$,[2d] and (c) tri-titanium(IV)-substituted dimer, $[(\alpha\text{-}1,2,3\text{-}PW_9Ti_3O_{37})_2O_3]^{12-}$.[2e]

was also no protonation in any of them. The BVS values of other elements in **2** reasonably corresponded to the formal valences of O^{2-}, Ti^{4+}, W^{6+}, and P^{5+} (Table S2 in the Supporting Information).

The crystal structure of **1** in EtN-**1** was successfully determined (Figure S3 in the Supporting Information) and had the same structure as the saturated Keggin POM. However, it was not possible to determine the mono-Ti^{IV} site due to the high symmetry of the Keggin structure. Nevertheless, from this X-ray structural analysis, we were able to confirm that **1** was not a dimeric structure but rather a monomeric structure.

Solid-State ^{31}P CPMAS NMR Spectroscopy

Solid-state ^{31}P CPMAS NMR spectroscopy of EtN-**1** and EtN-**2** showed a single broad signal due to Keggin units at δ = –12.96 and –13.21 ppm, respectively (Figure 4), which should be consistent with X-ray crystallography. Solid-state ^{31}P NMR spectra of EtN-**1** and EtN-**2** corresponded to solution ^{31}P NMR spectra in D_2O/DMSO (10:1 v/v) in a similar region.

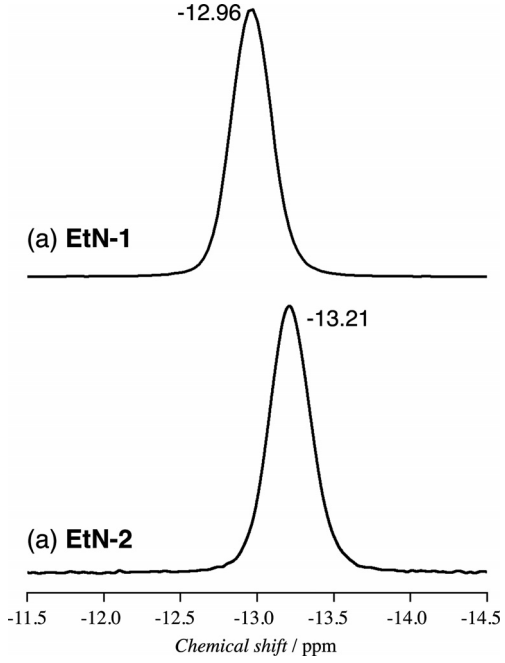

Figure 4. Solid-state ^{31}P CPMAS NMR spectra of (a) $(Et_2NH_2)_5[\alpha\text{-}PW_{11}TiO_{40}]\cdot 2H_2O$ (EtN-**1**), and (b) $(Et_2NH_2)_8[(\alpha\text{-}PW_{11}TiO_{39})_2O]\cdot 6H_2O$ (EtN-**2**).

Solution (^{31}P and ^{183}W) NMR and pH-Varied ^{31}P NMR Spectroscopy

The ^{31}P NMR spectrum of EtN-**1** in D_2O/DMSO (10:1 v/v; Figure 5, a) showed only one resonance at δ = –13.71 ppm, thus showing the formation of a single phosphorus-containing species and that the molecular structure of **1** in the solid state was maintained in solution. On the other hand, the ^{31}P NMR spectrum of EtN-**2** in D_2O/DMSO (10:1 v/v; Figure 5, b) showed two peaks at δ = –13.72 and –13.79 ppm, in which the downfield resonance was assigned to monomeric species **1**, and the upfield resonance was assigned to dimeric species **2**. When 1 M aqueous HCl (50 μL) was added to this NMR spectroscopy sample tube, only one resonance due to dimer **2** was observed at δ = –13.78 ppm (Figure 5, c). These ^{31}P NMR spectra indicate that monomer **1** and dimer EtN-**2** in solution are strongly dependent on pH.

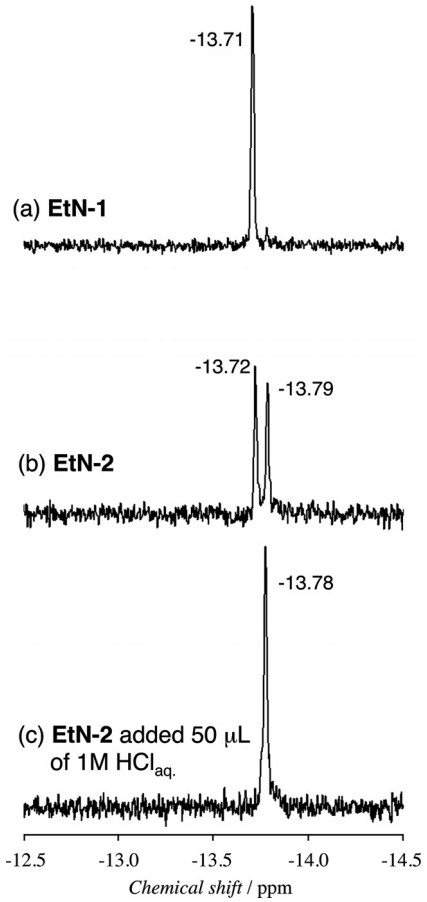

Figure 5. Solution ^{31}P NMR spectra of (a) $(Et_2NH_2)_5[\alpha\text{-}PW_{11}TiO_{40}]\cdot 2H_2O$ (EtN-**1**), and (b) $(Et_2NH_2)_8[(\alpha\text{-}PW_{11}TiO_{39})_2O]\cdot 6H_2O$ (EtN-**2**) dissolved in a solvent mixture of D_2O/DMSO (10:1 v/v), and (c) the solution of (b) to where 50 µL of 1 M aqueous HCl were added.

The ^{183}W NMR spectrum of EtN-**1** measured in D_2O/CD_3CN (1:3 v/v) (Figure 6, a) showed a six-line spectrum at δ = –69.55 (2 W), –101.34 (2 W), –110.11 (1 W), –114.31 (2 W), –117.89 (2 W) and –124.53 (2 W) ppm. The peaks at around δ = –69.55 and –110.11 ppm were observed as doublets due to ^{183}W-^{31}P coupling.[9] This NMR spectrum, consistent with a C_s symmetric compound, indicates that the solid-state structure of **1** is maintained in solution. The ^{183}W NMR spectrum of EtN-**2** in D_2O/CD_3CN (1:3 v/v) (Figure 6, b) showed a six-line spectrum at δ = –99.20 (2 W), –99.36 (2 W), –101.30 (1 W), –105.81 (2 W), –116.74 (2 W) and –117.16 (2 W) ppm. In the solid state, the whole symmetry of the molecule is shown with approximate C_1 symmetry. However, the six-line ^{183}W NMR spectrum indicated the overall C_{2v} symmetry in solution, because the twist between each Keggin unit was averaged.

The pH-varied ^{31}P NMR spectra were also measured using monomeric species EtN-**1** as the starting material. The pH of the H_2O/DMSO (10:1 v/v) solution (pH 3.2) of monomer EtN-**1** was adjusted to 2.0, 1.5, 1.0, and finally to 0.5 by 6 and 1 M aqueous HCl solutions, and the ^{31}P NMR spectra were measured (Figure 7). ^{31}P NMR spectra in the unadjusted sample (pH 3.2) showed a single signal at

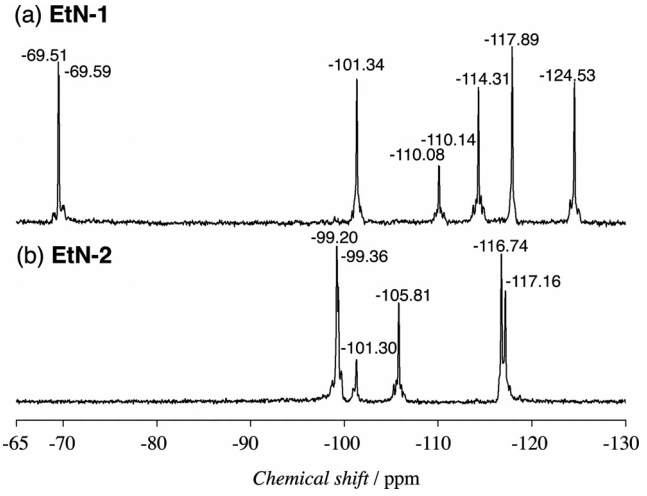

Figure 6. Solution ^{183}W NMR spectra in D_2O/CD_3CN (1:3 v/v) of (a) $(Et_2NH_2)_5[\alpha\text{-}PW_{11}TiO_{40}]\cdot 2H_2O$ (EtN-**1**) and (b) $(Et_2NH_2)_8[(\alpha\text{-}PW_{11}TiO_{39})_2O]\cdot 6H_2O$ (EtN-**2**).

δ = –13.72 ppm, which can be assigned to the monomeric Ti-containing Keggin POM **1**. In the pH range of 2.0–1.0, the signal of dimeric Ti-containing Keggin POM **2** was observed in addition to the signal of monomer **1**. At pH 0.5,

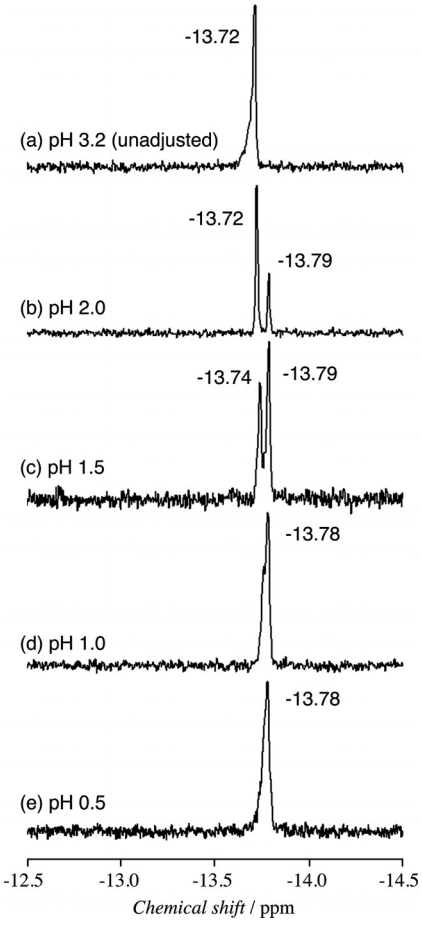

Figure 7. pH-varied ^{31}P NMR spectra of $(Et_2NH_2)_5[\alpha\text{-}PW_{11}TiO_{40}]\cdot 2H_2O$ (EtN-**1**) in H_2O/DMSO (10:1 v/v); pH (a) 3.2 (unadjusted); (b) 2.0; (c) 1.5; (d) 1.0; (e) 0.5 ppm.

the signal of only dimer **2** was observed. Therefore, dimeric species **2** was the predominant species in solution. The tendency for the ^{31}P NMR spectroscopic resonances of monomeric **1** to appear in a higher field than that of dimer **2** is consistent with the solid-state ^{31}P CPMAS NMR spectra of EtN-**1** and EtN-**2**. Thus, interconversion between the monomer and the dimer can be controlled by the pH of the solutions. The pH-varied ^{31}P NMR spectra of the mono-Ti^{IV}-substituted Dawson analogues reported previously[5] {i.e., $K_{14}[(\alpha_2\text{-}P_2W_{17}TiO_{61})_2(\mu\text{-}O)]\cdot 55H_2O$} in aqueous solutions showed that the monomer at pH 7.0, the dimer at pH 1.0–3.0, and the mono-protonated species of the dimer at pH 0.5 were the predominant species in the solutions. The present mono-Ti^{IV}-substituted Keggin POM denoted the same tendency as the Dawson analogue, that is, the mono-Ti^{IV}-substituted POM was present as a dimeric form under acidic conditions, but as a monomeric form under less acidic conditions. Unlike the Dawson analogues, the mono-protonated species of the dimer was not found in the pH range of 3.2–0.5.

Conclusion

In this work, we prepared and characterized the monomer Keggin POM $(Et_2NH_2)_5[\alpha\text{-}PW_{11}TiO_{40}]\cdot 2H_2O$ (EtN-**1**) and the μ-oxo Keggin dimer $(Et_2NH_2)_8[(\alpha\text{-}PW_{11}TiO_{39})_2O]\cdot 6H_2O$ (EtN-**2**). The molecular structure of μ-oxo dimeric polyoxoanion **2** was successfully determined for the first time by single-crystal X-ray crystallography. Structural analysis revealed that **2** was composed of two mono-titanium(IV)-substituted Keggin POM subunits "$[\alpha\text{-}PW_{11}TiO_{39}]^{3-}$" linked through one μ-oxo group. The BVS value of the bridging oxygen atom [O(1X)] of **2** has strongly suggested that it is not protonated. The pH-varied ^{31}P NMR spectra revealed that monomer **1** and dimer **2** in solution were strongly dependent upon pH, and therefore, the interconversion between them can be controlled by the pH of the solutions. Unlike the Dawson analogues, the mono-protonated species of the dimer was not found in the pH range of 3.2–0.5. These facts also provide significant information about acid catalysis by the Keggin mono-titanium(IV)-substituted POMs.

Experimental Section

Materials: The following reactants were used as received: NaOAc, Et_2NH_2Cl, MeOH, EtOH, Et_2O, DMSO, CH_3CN, $TiCl_4$ (Wako); D_2O, CD_3CN (Isotec). The precursor $K_7[\alpha\text{-}PW_{11}O_{39}]\cdot 8H_2O$ was prepared and identified by FTIR, TG/DTA, and ^{31}P NMR spectroscopy.[10]

Instrumentation/Analytical Procedures: CHN elemental analyses were carried out with a Perkin–Elmer 2400 CHNS Elemental Analyzer II. Infrared spectra were recorded with a JASCO 4100 FTIR spectrometer in KBr disks at room temperature. TG and DTA were acquired with a Rigaku Thermo Plus 2 series TG/DTA TG 8120 instrument. ^{31}P NMR (160 MHz) spectra in a D_2O solution were recorded in 5 mm outer diameter tubes with a JEOL JNM-ECS 400 FT-NMR spectrometer and a JEOL ECS-400 NMR spectroscopic data processing system and were referenced with an external standard of 25% H_3PO_4 in H_2O in a sealed capillary. The ^{31}P NMR spectroscopic signals with the usual 85% H_3PO_4 are shifted by +0.544 ppm from our data with 25% H_3PO_4. The ^{183}W NMR (20 MHz) spectra were recorded in 10 mm outer diameter tubes with a JEOL JNM-ECP 500 FT-NMR spectrometer equipped with a JEOL NM-50 T10L low-frequency tunable probe and a JEOL ECP-500 NMR spectroscopic data processing system. The ^{183}W NMR spectra measured in D_2O were referenced with an external standard of a saturated Na_2WO_4/D_2O solution. The ^{183}W NMR spectroscopic signals were shifted by –0.787 ppm by using a 2 M Na_2WO_4 solution as a reference instead of the saturated Na_2WO_4 solution. Solid-state CPMAS ^{31}P NMR (120 MHz) spectra were recorded in 6 mm outer diameter tubes with a JEOL JNM-ECP 300 FT-NMR spectrometer with a JEOL ECP-300 NMR spectroscopic data processing system and were referenced to an external standard of $(NH_4)_2HPO_4$. Chemical shifts are reported as negative for resonances upfield of $(NH_4)_2HPO_4$ (δ = 1.60).

Synthesis of the Monomeric POM, $(Et_2NH_2)_5[PW_{11}TiO_{40}]\cdot 2H_2O$ (EtN-1): NaOAc (0.11 g, 1.34 mmol) was added to a solution of $K_7[PW_{11}O_{39}]\cdot 8H_2O$ (2.0 g, 0.65 mmol) dissolved in water (20 mL). After stirring for 15 min in an ice bath, a colorless solution of $TiCl_4$ (ca. 0.08 mL, ca. 0.7 mmol) was added at a rate of one drop per 2 s. The solution was stirred for 1 h in a water bath at 80 °C, followed by filtration. Et_2NH_2Cl (3.0 g, 27.4 mmol) was added to the filtrate at once. The white powder formed was collected with a glass filter (P40, or G 4.0), washed with EtOH (10 mL three times) and Et_2O (10 mL three times), and then dried under vacuum for 2 h. At this stage, the white powder was obtained in a yield of 1.59 g {77.7% relative to $(Et_2NH_2)_5[PW_{11}TiO_{40}]\cdot 2H_2O$}, which was very soluble in water and a solvent mixture of water/DMSO (10:1 v/v) and water/CH_3CN (1:3 v/v), soluble in MeOH, sparingly soluble in EtOH, but insoluble in Et_2O. IR (KBr) (polyoxometalate region): $\tilde{\nu}$ = 1635 (w), 1576 (w), 1472 (w), 1456 (w), 1428 (w), 1396 (w), 1388 (w), 1362 (vw), 1307 (vw), 1275 (vw), 1192 (vw), 1159 (vw), 1090 (m), 1062 (m), 964 (s), 886 (m), 801 (vs), 699 (m), 656 (m), 594 (m), 515 (m), 492 (m) cm^{-1}. ^{31}P NMR [23.2 °C, D_2O/DMSO (10:1 v/v)]: δ = –13.71 ppm. Solid-state ^{31}P NMR: δ = –12.96 ppm. ^{183}W NMR [room temp., D_2O/CD_3CN (1:3 v/v)]: δ = –69.51, –69.59 (2 W), –101.34 (2 W), –110.08, –110.14 (1 W), –114.31 (2 W), –117.89 (2 W), –124.53 (2 W) ppm. TG/DTA under atmospheric conditions: a weight loss of 1.15%, due to dehydration of solvated water molecules, was observed at below 199.3 °C; calcd. 1.14% for x = 2 in $(Et_2NH_2)_5[PW_{11}TiO_{40}]\cdot xH_2O$. A weight loss of 10.98%, due to decomposition of Et_2NH_2 cations, was observed between 199.3 and 500 °C with an exothermic peak at 359.1 °C. Calcd. for $(Et_2NH_2)_5[PW_{11}TiO_{40}]\cdot 2H_2O$ or $C_{20}H_{64}N_5O_{42}P_1W_{11}Ti_1$: C 7.63, H 2.05, N 2.22; found: C 7.70, H 1.83, N 2.15.

pH-Varied ^{31}P NMR Spectroscopy: The monomeric powder sample of $(Et_2NH_2)_5[PW_{11}TiO_{40}]\cdot 2H_2O$ (EtN-**1**; 0.6 g, 0.19 mmol) was dissolved in a solvent mixture of water and DMSO (9.9 mL, 10:1 v/v). The pH of the solution (pH 3.2) was adjusted to 2.0, 1.5, 1.0, and 0.5, using 6 and 1 M aqueous HCl solutions and their ^{31}P NMR spectra were measured (Figure 7). The solutions of pH 3.2, 2.0, 1.5, and 1.0 were colorless and clear, but the solution of pH 0.5 was not clear (cloudy or a bit suspended).

Crystallization of the Monomeric Species (EtN-1): EtN-**1** (2.0 g, 0.64 mmol) was added to a solution of Et_2NH_2Cl (0.20 g, 1.82 mmol) and NaOAc (0.15 g, 1.83 mmol) dissolved in water (30 mL). The colorless, clear solution was slowly evaporated at room temperature. After 3 d, colorless, clear column crystals were deposited, which were collected by a glass frit (P16, or G 3.5),

washed with EtOH (20 mL two times) and Et_2O (20 mL two times), and dried under vacuum for 2 h. White powder, obtained in a yield of 1.42 g {71.3% relative to $(Et_2NH_2)_5[PW_{11}TiO_{40}]\cdot 0.4H_2O$}, was very soluble in water and a solvent mixture of water/CH_3CN (1:3 v/v), soluble in MeOH, sparingly soluble in EtOH, but insoluble in Et_2O. IR (KBr) (polyoxometalate region): $\tilde{\nu}$ = 1630 (w), 1603 (w), 1573 (w), 1472 (w), 1453 (w), 1427 (w), 1389 (w), 1362 (vw), 1327 (vw), 1306 (vw), 1275 (vw), 1192 (vw), 1159 (vw), 1090 (m), 1062 (m), 964 (s), 886 (m), 799 (vs), 700 (m), 655 (m), 594 (m), 515 (m), 491 (m) cm^{-1}. ^{31}P NMR [23.3 °C, D_2O/DMSO (10:1 v/v)]: δ = –13.70 ppm. TG/DTA under atmospheric conditions: a weight loss of 0.23%, due to dehydration of solvated water molecules, was observed at below 57.5 °C; calcd. 0.23% for x = 0.4 in $(Et_2NH_2)_5[PW_{11}TiO_{40}]\cdot xH_2O$. A weight loss of 10.22%, due to decomposition of Et_2NH_2 cations, was observed between 57.5 and 500 °C with exothermic peaks at 322.6 and 372.2 °C. Calcd. for $(Et_2NH_2)_5[PW_{11}TiO_{40}]\cdot 0.4H_2O$ or $C_{20}H_{60.8}N_5O_{40.4}P_1W_{11}Ti_1$: C 7.70, H 1.96, N 2.25; found C 7.80, H 1.87, N 2.22.

Crystallization of the Dimeric Species (EtN-2): The monomeric species $(Et_2NH_2)_5[PW_{11}TiO_{40}]\cdot 2H_2O$ (EtN-**1**; 0.5 g, 0.16 mmol) was dissolved in a solvent mixture of MeOH/water (10 mL, 1:1 v/v), with the pH of the solution being 4.9–5.3. The pH was adjusted to 1.0 by using 1 M aqueous HCl, followed by stirring for 2 d. The white suspension formed was filtered by a membrane filter (JG 0.2 μm). The colorless, clear filtrate was slowly evaporated at room temperature. After 3 d, colorless, clear plate crystals were deposited, which were collected by a glass frit (G 4.0), washed with EtOH (20 mL two times) and Et_2O (20 mL two times), and dried under vacuum for 2 h. The white powder, obtained in a yield of 0.32 g {65.3% relative to $(Et_2NH_2)_8[(PW_{11}TiO_{39})_2O]\cdot 6H_2O$}, was very soluble in a solvent mixture of water/DMSO (10:1 v/v) and water/CH_3CN (1:3 v/v), less soluble in water, and insoluble in EtOH and Et_2O. IR (KBr) (polyoxometalate region): $\tilde{\nu}$ = 1620 (w), 1469 (w), 1451 (w), 1389 (w), 1205 (vw), 1158 (vw), 1075 (m), 968 (s), 889 (m), 807 (vs), 654 (s) [intermolecular Ti–O–Ti], 594 (m), 520 (m), 499 (m) cm^{-1}. ^{31}P NMR [23.2 °C, D_2O/DMSO (10:1 v/v)]: δ = –13.72, –13.79 ppm. ^{31}P NMR [23.0 °C, D_2O/DMSO (10:1 v/v), after addition of 1 M aqueous HCl (0.05 mL, 50 μmol)]: δ = –13.78 ppm. Solid-state ^{31}P NMR: δ = –13.21 ppm. ^{183}W NMR [room temp., D_2O/CD_3CN (1:3 v/v)]: δ = –99.20 (2 W), –99.36 (2 W), –101.30 (1 W), –105.81 (2 W), –116.74 (2 W), –117.16 (2 W) ppm. TG/DTA under atmospheric conditions: a weight loss of 1.84%, due to dehydration of solvated water molecules, was observed at below 122.5 °C; calcd. 1.75% for x = 6 in $(Et_2NH_2)_8[(PW_{11}TiO_{39})_2O]\cdot xH_2O$. A weight loss of 9.40%, due to decomposition of Et_2NH_2 cations, was observed between 122.5 and 500 °C with endothermic peaks at 40.5 and 60.6 °C and an exothermic peak at 371.5 °C. Calcd. for $(Et_2NH_2)_8[(PW_{11}TiO_{39})_2O]\cdot 6H_2O$ or $C_{32}H_{108}N_8O_{85}P_2W_{22}Ti_2$: C 6.23, H 1.77, N 1.82; found C 6.31, H 2.28, N 1.78.

X-ray Crystallography: A colorless column crystal of EtN-**1** ($0.28\times0.07\times0.05$ mm^3) and a colorless plate crystal of EtN-**2** ($0.20\times0.10\times0.04$ mm^3) were surrounded by liquid paraffin (Paratone-N) to prevent its degradation. Data collection was carried out with a Bruker SMART APEX CCD diffractometer at 100 K in a range of $3.56° < 2\theta < 56.70°$ (EtN-**1**) and $3.62° < 2\theta < 55.00°$ (EtN-**2**). The intensity data were automatically corrected for Lorentz and polarization effects during integration. The structure was solved by direct methods (SHELXS-97[11a] for EtN-**1** and SIR2004[12] for EtN-**2**), followed by subsequent difference Fourier calculation and refined by a full-matrix least-squares procedure on F^2 (SHELXL-97).[11b] Absorption correction was performed with SADABS (empirical absorption correction).[11c] High-level alerts in the checkCIF report are due to the disorder of many hydrated water molecules and countercations. The compositions and formulae of the POMs that contained many countercations and many hydrated water molecules were determined by CHN elemental analysis and TG analysis. In general, it is not possible in X-ray crystallography to determine the location of the hydrogen atoms of hydrated water molecules due to extensive disorder of the countercations and the hydrate water molecules. Such features are frequently encountered and common in POM crystallography.

Crystal Data for EtN-1: $O_{44}PW_{12}$; M_r = 2941.17; triclinic, space group $P\bar{1}$; a = 11.8449(14) Å, b = 11.8552(14) Å, c = 13.0038(15) Å; α = 104.547(2)°, β = 104.450(2)°, γ = 116.313(2)°; V = 1440.8(3) $Å^3$; Z = 1; $D_{calcd.}$ = 3.390 $g\,cm^{-3}$; μ(Mo-K_α) = 23.947 mm^{-1}; $R1$ = 0.0897, $wR2$ = 0.2297 (for all data), R_{int} = 0.0385, $R1$ = 0.0675, $wR2$ = 0.2073; GOF = 1.074 {19883 total reflections, 7148 unique reflections [$I > 2\sigma(I)$]}.

Crystal Data for EtN-2: $C_{20}H_{60}N_5O_{82}P_2Ti_2W_{22}$; M_r = 5909.19; triclinic, space group $P\bar{1}$; a = 11.6856(11) Å, b = 21.196(2) Å, c = 21.463(2) Å; α = 86.9960(10)°, β = 79.4420(10)°, γ = 78.1580(10)°; V = 5114.2(8) $Å^3$; Z = 2; $D_{calcd.}$ = 3.837 $g\,cm^{-3}$; μ(Mo-K_α) = 24.903 mm^{-1}; $R1$ = 0.0781, $wR2$ = 0.1475 (for all data), R_{int} = 0.0658, $R1$ = 0.0565, $wR2$ = 0.1358; GOF = 1.052 {60352 total reflections, 23161 unique reflections [$I > 2\sigma(I)$]}.

CCDC-906701 (for EtN-**1**) and -906699 (for EtN-**2**) contain the supplementary crystallographic data for this paper. These data can be obtained free of charge from The Cambridge Crystallographic Data Centre via www.ccdc.cam.ac.uk/data_request/cif.

Supporting Information (see footnote on the first page of this article): TG/DTA data for EtN-**1** and EtN-**2** (Figures S1 and S2); the molecular structure and polyhedral representation of **1** in EtN-**1** (Figure S3); bond lengths and angles for **2** in EtN-**2** (Table S1); and BVS calculations of Ti and O around Ti for **2** in EtN-**2**.

Acknowledgments

This work was supported by the Japan Society for the Promotion of Science through a Grant-in-Aid for Scientific Research (C) (JSPS KAKENHI Grant Number 22550065) and by the Ministry of Education, Culture, Sports, Science and Technology of Japan (Strategic Research Base Development Program for Private Universities).

[1] a) M. T. Pope, A. Müller, *Angew. Chem.* **1991**, *103*, 56; *Angew. Chem. Int. Ed. Engl.* **1991**, *30*, 34–48; b) M. T. Pope, *Heteropoly and Isopoly Oxometalates*, Springer Verlag, New York, **1983**; c) V. W. Day, W. G. Klemperer, *Science* **1985**, *228*, 533–541; d) C. L. Hill (Ed.), *Chem. Rev.* **1998**, *98*, 1–390; e) T. Okuhara, N. Mizuno, M. Misono, *Adv. Catal.* **1996**, *41*, 113–252; f) C. L. Hill, C. M. Prosser-McCartha, *Coord. Chem. Rev.* **1995**, *143*, 407–455; g) a series of 34 papers in a volume devoted to polyoxoanions in catalysis: C. L. Hill (Ed.), *J. Mol. Catal. A* **1996**, *114*, 1–371; h) R. Neumann, *Prog. Inorg. Chem.* **1998**, *47*, 317–370; i) M. T. Pope, A. Müller Editors (Eds.), *Polyoxometalate Chemistry from Topology via Self-Assembly to Applications*, Kluwer Academic Publishers, The Netherlands, **2001**; j) T. Yamase, M. T. Pope (Eds.), *Polyoxometalate Chemistry for Nano-Composite Design*, Kluwer Academic Publishers, The Netherlands, **2002**; k) M. T. Pope, in: *Comprehensive Coordination Chemistry II* (Ed.: A. G. Wedd), Elsevier Science, New York, **2004**, vol. 4, p. 635; l) C. L. Hill in *Comprehensive Coordination Chemistry II* (Ed.: A. G. Wedd), Elsevier Science, New York, **2004**, vol. 4, p. 679; m) a series of 32 papers was published in a volume devoted to polyoxometalates in catalysis: C. L. Hill, *J. Mol. Catal. A* **2007**, *262*, 1; n) B. Hasenknopf, K. Micoine,

E. Lacôte, S. Thorimbert, M. Malacria, R. Thouvenot, *Eur. J. Inorg. Chem.* **2008**, 5001–5013; o) A. Proust, R. Thouvenot, P. Gouzerh, *Chem. Commun.* **2008**, 1837–1852; p) D. Laurencin, R. Thouvenot, K. Boubekeur, F. Villain, R. Villanneau, M.-M. Rohmer, M. Benard, A. Proust, *Organometallics* **2009**, *28*, 3140–3151; q) D.-L. Long, R. Tsunashima, L. Cronin, *Angew. Chem.* **2010**, *122*, 1780; *Angew. Chem. Int. Ed.* **2010**, *49*, 1736–1758; r) A. Dolbecq, E. Dumas, C. R. Mayer, P. Mialane, *Chem. Rev.* **2010**, *110*, 6009–6048; s) C. P. Pradeep, D.-L. Long, L. Cronin, *Dalton Trans.* **2010**, *39*, 9443–9457; t) K. Nomiya, Y. Sakai, S. Matsunaga, *Eur. J. Inorg. Chem.* **2011**, 179–196.

[2] a) Y. Lin, T. J. R. Weakley, B. Rapko, R. G. Finke, *Inorg. Chem.* **1993**, *32*, 5095–5101; b) T. Yamase, T. Ozeki, H. Sakamoto, S. Nishiya, A. Yamamoto, *Bull. Chem. Soc. Jpn.* **1993**, *66*, 103–108; c) T. Yamase, X. O. Cao, S. Yazaki, *J. Mol. Catal. A* **2007**, *262*, 119–127; d) K. Nomiya, M. Takahashi, J. A. Widegren, T. Aizawa, Y. Sakai, N. C. Kasuga, *J. Chem. Soc., Dalton Trans.* **2002**, 3679–3685; e) K. Nomiya, M. Takahashi, K. Ohsawa, J. A. Widegren, *J. Chem. Soc., Dalton Trans.* **2001**, 2872–2878; f) Y. Goto, K. Kamata, K. Yamaguchi, K. Uehara, S. Hikichi, N. Mizuno, *Inorg. Chem.* **2006**, *45*, 2347–2356; g) R. Tan, D. Li, H. Wu, C. Zhang, X. Wang, *Inorg. Chem. Commun.* **2008**, *11*, 835–836; h) F. Hussain, B. S. Bassil, L.-H. Bi, M. Reicke, U. Kortz, *Angew. Chem.* **2004**, *116*, 3567; *Angew. Chem. Int. Ed.* **2004**, *43*, 3485–3488; i) G. A. Al-Kadamany, F. Hussain, S. S. Mal, M. H. Dickman, N. Leclerc-Laronze, J. Marrot, E. Cadot, U. Kortz, *Inorg. Chem.* **2008**, *47*, 8574–8576; j) Y. H. Ren, S. X. Liu, R. G. Cao, X. Y. Zhao, J. F. Cao, C. Y. Gao, *Inorg. Chem. Commun.* **2008**, *11*, 1320–1322.

[3] a) K. Hayashi, C. N. Kato, A. Shinohara, Y. Sakai, K. Nomiya, *J. Mol. Catal. A* **2007**, *262*, 30–35; b) O. A. Kholdeeva, T. A. Trubitsina, R. I. Maksimovskaya, A. V. Golovin, W. A. Neiwert, B. A. Kolosov, X. López, J. M. Poblet, *Inorg. Chem.* **2004**, *43*, 2284–2292; c) C. N. Kato, K. Hayashi, S. Negishi, K. Nomiya, *J. Mol. Catal. A* **2007**, *262*, 25–29; d) C. N. Kato, S. Negishi, K. Yoshida, K. Hayashi, K. Nomiya, *Appl. Catal.* **2005**, *292*, 97–104; e) J. Gong, Q. J. Shan, D. R. Wang, R. N. Hua, L. Y. Qu, *J. Electroanal. Chem.* **1998**, *455*, 39–44; f) O. A. Kholdeeva, T. A. Trubitsina, M. N. Timofeeva, G. M. Maksimov, R. I. Maksimovskaya, V. Rogov, *J. Mol. Catal. A* **2005**, *232*, 173–178; g) O. A. Kholdeeva, *Top. Catal.* **2006**, *40*, 229–243.

[4] a) Y. Sakai, K. Yoza, C. N. Kato, K. Nomiya, *Chem. Eur. J.* **2003**, *9*, 4077–4083; b) Y. Sakai, K. Yoza, C. N. Kato, K. Nomiya, *Dalton Trans.* **2003**, 3581–3586; c) K. Nomiya, Y. Arai, Y. Shimizu, M. Takahashi, T. Takayama, H. Weiner, T. Nagata, J. A. Widegren, R. G. Finke, *Inorg. Chim. Acta* **2000**, *300–302*, 285–304; d) Y. Sakai, Y. Kitakoga, K. Hayashi, K. Yoza, K. Nomiya, *Eur. J. Inorg. Chem.* **2004**, 4646–4652; e) Y. Sakai, S. Yoshida, T. Hasegawa, H. Murakami, K. Nomiya, *Bull. Chem. Soc. Jpn.* **2007**, *80*, 1965–1974; f) U. Kortz, S. S. Hamzeh, N. A. Nasser, *Chem. Eur. J.* **2003**, *9*, 2945–2952; g) Y. Sakai, S. Ohta, Y. Shintoyo, S. Yoshida, Y. Taguchi, Y. Matsuki, S. Matsunaga, K. Nomiya, *Inorg. Chem.* **2011**, *50*, 6575–6583.

[5] S. Yoshida, H. Murakami, Y. Sakai, K. Nomiya, *Dalton Trans.* **2008**, 4630–4638.

[6] a) O. A. Kholdeeva, G. M. Maksimov, R. I. Maksimovskaya, L. A. Kovaleva, M. A. Fedotov, V. A. Grigoriev, C. L. Hill, *Inorg. Chem.* **2000**, *39*, 3828–3837; b) O. A. Kholdeeva, T. A. Trubitsina, G. M. Maksimov, A. V. Golovin, R. I. Maksimovskaya, *Inorg. Chem.* **2005**, *44*, 1635–1642; c) G. M. Maksimov, R. I. Maksimovskaya, O. A. Kholdeeva, M. A. Fedotov, V. I. Zaikovskii, V. G. Vasil'ev, S. S. Arzumanov, *J. Struct. Chem.* **2009**, *50*, 618–627.

[7] X. López, I. A. Weinstock, C. Bo, J. P. Sarasa, J. M. Poblet, *Inorg. Chem.* **2006**, *45*, 6467–6473.

[8] a) C. Rocchiccioli-Deltcheff, R. Thouvenot, R. Franck, *Spectrochim. Acta A* **1976**, *32*, 587–597; b) C. Rocchiccioli-Deltcheff, M. Fournier, R. Franck, *Inorg. Chem.* **1983**, *22*, 207–216; c) R. Thouvenot, M. Fournier, R. Franck, C. Rocchiccioli-Deltcheff, *Inorg. Chem.* **1984**, *23*, 598–605.

[9] G. Lenoble, B. Hasenknopf, R. Thouvenot, *J. Am. Chem. Soc.* **2006**, *128*, 5735–5744.

[10] S. Aoki, T. Kurashina, Y. Kasahara, T. Nishijima, K. Nomiya, *Dalton Trans.* **2011**, *40*, 1243–1253.

[11] a) G. M. Sheldrick, *Acta Crystallogr., Sect. A* **1990**, *46*, 467–473; b) G. M. Sheldrick, *SHELXL-97, Program for Crystal Structure Refinement*, University of Göttingen, Germany, **1997**; c) G. M. Sheldrick, *SADABS*, University of Göttingen, Germany, **1996**.

[12] M. C. Burla, R. Caliandro, M. Camalli, B. Carrozzini, G. L. Cascarano, L. De Caro, C. Giacovazzo, G. Polidori, R. Spagna, *J. Appl. Crystallogr.* **2005**, *38*, 381–388.

Received: October 24, 2012
Published Online: January 23, 2013

Inorganic Chemistry

ARTICLE

pubs.acs.org/IC

Encapsulation of Anion/Cation in the Central Cavity of Tetrameric Polyoxometalate, Composed of Four Trititanium(IV)-Substituted α-Dawson Subunits, Initiated by Protonation/Deprotonation of the Bridging Oxygen Atoms on the Intramolecular Surface

Yoshitaka Sakai, Shuji Ohta, Yukihiro Shintoyo, Shoko Yoshida, Yuhki Taguchi, Yusuke Matsuki, Satoshi Matsunaga, and Kenji Nomiya*

Department of Chemistry (old name Department of Materials Science), Faculty of Science, Kanagawa University, Hiratsuka, Kanagawa 259-1293, Japan

Supporting Information

ABSTRACT: Preparation and structural characterization of a novel polyoxometalate (POM), $[(P_2W_{15}Ti_3O_{60.5})_4(NH_4)]^{35-}$ **1**, i.e., an encapsulated NH_4^+ cation species in the central cavity of a tetramer (called the Dawson tetramer) constituted by trititanium(IV)-substituted α-Dawson POM substructure, are described. POM **1** was synthesized by several different methods and unequivocally characterized by complete elemental analysis, thermogravimetric and differential thermal analysis (TG/DTA), FTIR spectroscopy, solution ($^{15}N\{^1H\}$, ^{31}P, ^{183}W) NMR spectroscopy, and X-ray crystallography. First, POM **1** was synthesized by a reaction of NH_4Cl in aqueous solution with a precursor, which was derived by thermal treatment of a monomeric triperoxotitanium(IV)-substituted Dawson POM, $[\alpha\text{-}1,2,3\text{-}P_2W_{15}(TiO_2)_3O_{56}(OH)_3]^{9-}$ **2**, for 3 h in an electric furnace at 200 °C. The encapsulated NH_4^+ cation in **1** was confirmed by $^{15}N\{^1H\}$ NMR measurement and X-ray crystallography. As another synthesis of **1**, a direct exchange of the Cl^- anion encapsulated in $[\{\alpha\text{-}1,2,3\text{-}P_2W_{15}Ti_3O_{57.5}(OH)_3\}_4Cl]^{25-}$ **3** with the NH_4^+ cation was attained by neutralizing an aqueous solution containing **3** with the addition of aqueous NH_3 (the initial pH of ca. 2−2.5 was changed to 6.4), followed by adding NH_4Cl. It has been clarified that the conditions as to whether the anion or the cation is encapsulated in the central cavity of the Dawson tetramer were significantly related to the protonation/deprotonation of the bridging oxygen atoms on the intramolecular surface, Ti−O−Ti/Ti−OH−Ti sites constituting the Dawson subunits.

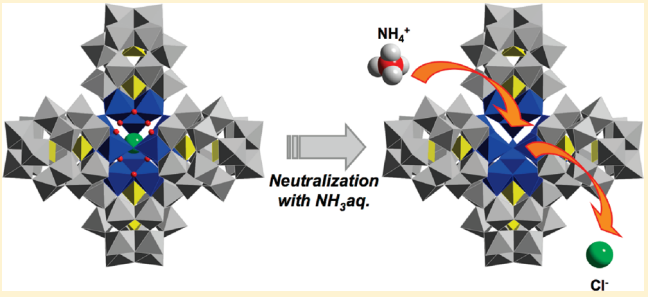

INTRODUCTION

Polyoxometalates (POMs) are molecular metal−oxide clusters, which have attracted considerable attention in the fields of catalysis, medicine, surface science, and materials science, since POMs are often considered to be molecular analogues of metal oxides in terms of structural analogy.[1] From a structural viewpoint, POM-based giant molecules have recently received much attention.[2] In fact, many POM-based giant molecules have been prepared, through self-assembly of Keggin or Dawson lacunary units or other substructure units, e.g., as $[As^{III}_{12}Ce^{III}_{16}(H_2O)_{36}W_{148}O_{524}]^{76-}$,[2a] $[\{Sn(CH_3)_2(H_2O)\}_{24}\{Sn(CH_3)_2\}_{12}(A\text{-}XW_9O_{34})_{12}]^{36-}$ (X = P, As),[2b] $[Gd_6As_6W_{65}O_{229}(OH)_4(H_2O)_{12}(OAc)_2]^{38-}$,[2c] $[Yb_{10}As_{10}W_{88}O_{308}(OH)_8(H_2O)_{28}(OAc)_4]^{40-}$,[2c] $[W_{72}Mn^{III}_{12}O_{268}X_7]^{40-}$ (X = Si, Ge),[2d,e] $[(H_2P_2W_{15}O_{56})_4\{Mo_2O_2S_2(H_2O)_2\}_4\{Mo_4S_4O_4(OH)_4(H_2O)\}_2]^{28-}$,[2f] $[(UO_2)_{12}(\mu_3\text{-}O)_4(\mu\text{-}H_2O)_{12}(P_2W_{15}O_{56})_4]^{32-}$,[2g] $[KFe_{12}(OH)_{18}(\alpha\text{-}1,2,3\text{-}P_2W_{15}O_{56})_4]^{29-}$,[2h] and $[Cu_{20}Cl(OH)_{24}(H_2O)_{12}(P_8W_{48}O_{184})]^{25-}$.[2i] The two compounds in refs 2g and 2h possess the tetrahedral structure based on the Dawson tetramer. A number of polyoxomolybdate-based giant molecules have also been reported as mixed valence molybdates by Müller's group,[1i,j] the formation of which has involved a reduction process of *a part* of molybdates in aqueous media.

Site-selective substitution of the W^{VI} atoms in POMs with Ti^{IV} atoms is particularly interesting, because of the formation of multicenter active sites with corner- or edge-sharing TiO_6 octahedra and, also, generation of oligomeric species through Ti−O−Ti bonds.[3,4] The ionic radius of Ti^{IV} (0.75 Å) is close to that of W^{VI} (0.74 Å), suggesting that Ti^{IV} should fit nicely into the POM framework. However, there is a significant consequence in terms of oligomeric Ti−O−Ti anhydride formation resulting from substitution by several Ti^{IV} atoms. As a matter of fact, many examples of Keggin POM-based oligomeric species are reported.[3e−r]

On the other hand, fewer examples of oligomeric species of Ti^{IV}-substituted Dawson POMs are reported. For example, the dimeric Dawson POM bridged by two $Ti(ox)_2$ groups

Received: February 18, 2011
Published: June 15, 2011

(H_2ox = oxalic acid), $[P_2W_{16}Ti_2O_{62}\{\mu\text{-}Ti(C_2O_4)_2\}]_2^{20-}$,[4a] dilacunary Dawson sandwich complex, $(NH_4)_{14}[P_2W_{15}O_{55}Ti(OH)]_2\cdot nH_2O$,[4b] and its free acid form, $H_8[Ti_2\{P_2W_{15}O_{54}(OH_2)_2\}_2]\cdot 31H_2O$,[4c] and the two mono-$Ti^{IV}$-substituted Dawson POM dimers, i.e., $K_{14}[(\alpha_2\text{-}P_2W_{17}TiO_{61})_2(\mu\text{-}O)]\cdot 17H_2O$[4d] and $H_{13}[(\alpha_2\text{-}P_2W_{17}TiO_{61})(\alpha_2\text{-}P_2W_{17}TiO_{61}H)(\mu\text{-}O)]\cdot 55H_2O$,[4d] have been reported. Furthermore, tetramers composed of tri-Ti^{IV}-substituted Dawson POM substructures have also been isolated as two giant "tetrapod"-shaped POMs, i.e., tetrameric Ti−O−Ti-bridged anhydride forms without bridging μ_3-Ti$(H_2O)_3$ octahedral groups (called the nonbridging Dawson tetramer) and the species with bridging μ_3-Ti$(H_2O)_3$ groups (called the bridging Dawson tetramer), both of which have an encapsulated Cl^- anion in the central cavity, such as $[\{\alpha\text{-}1,2,3\text{-}P_2W_{15}Ti_3O_{57.5}(OH)_3\}_4Cl]^{25-}$ (**3**)[5b−d] and $[\{\alpha\text{-}1,2,3\text{-}P_2W_{15}Ti_3O_{59}(OH)_3\}_4\{\mu_3\text{-}Ti(H_2O)_3\}_4Cl]^{21-}$ (**4**).[5a,d] As to **4**, we have recently obtained three bridging Dawson tetramers with different anions encapsulated, $[\{\alpha\text{-}1,2,3\text{-}P_2W_{15}Ti_3O_{59}(OH)_3\}_4\{\mu_3\text{-}Ti(H_2O)_3\}_4X]^{21-}$ (X = Br, I, NO_3).[5e] As a related compound, the monomeric triperoxotitanium(IV)-substituted Dawson POM $[\alpha\text{-}1,2,3\text{-}P_2W_{15}(TiO_2)_3O_{56}(OH)_3]^{9-}$ (**2**) has been derived from a reaction of **4** with aqueous hydrogen peroxide, but not from a reaction of **3**.[5d] Preliminary experiments have shown that the monomeric peroxo-compound **2** can be used as a building block for preparation of the two giant "tetrapod"-shaped POMs, **3** and **4**, by killing the coordinating peroxo group thermally or chemically using $NaHSO_3$.[5d] In this work, we first synthesized the encapsulated NH_4^+ cation species in the nonbridging Dawson tetramer, $[(\alpha\text{-}1,2,3\text{-}P_2W_{15}Ti_3O_{60.5})_4(NH_4)]^{35-}$ (**1**). The encapsulated NH_4^+ cation was confirmed by $^{15}N\{^1H\}$ NMR measurement and X-ray crystallography. Furthermore, using **3**, we also realized a direct exchange of the Cl^- anion encapsulated in the central cavity with the NH_4^+ cation. The conditions as to whether the anion or the cation was encapsulated therein were found to be significantly related to the protonation of the surface Ti−O−Ti sites within the Dawson subunits. The protonated species of the Ti−O−Ti sites resulted in encapsulation of the anion in the central cavity, while the deprotonated species led to encapsulation of the cation therein.

Herein, we report full details of the synthesis and structure of the novel nonbridging Dawson tetramer with an encapsulated NH_4^+ cation, $(NH_4)_{27}Na_8[(P_2W_{15}Ti_3O_{60.5})_4(NH_4)]\cdot$ca.$90H_2O$ (**NH_4Na-1**) and $(NH_4)_{24}Na_7K_4[(P_2W_{15}Ti_3O_{60.5})_4(NH_4)]\cdot$ca.$50H_2O$ (**NH_4NaK-1**). [Note: the polyoxoanion moiety in **NH_4Na-1** and **NH_4NaK-1** is abbreviated simply as **1**.]

EXPERIMENTAL SECTION

Materials. The following reactants were used as received: NH_4Cl, $^{15}NH_4Cl$ (Wako); D_2O (Isotec). The trilacunary Dawson POM, $Na_{12}[P_2W_{15}O_{56}]\cdot nH_2O$ (n = 19, 25), was synthesized via pure $K_6[\alpha\text{-}P_2W_{18}O_{62}]\cdot nH_2O$ (n = 13, 14) prepared by modification of the literature,[6a,b] and characterized by solid-state CPMAS ^{31}P and solution ^{31}P NMR, FTIR, and TG/DTA (see Supporting Information). Solution ^{31}P NMR of a freshly prepared D_2O solution was in excellent accord with the literature data.[6c−e] Syntheses and characterizations of the three POM precursors [the monomeric, peroxo-titanium(IV)-containing species $Na_9[P_2W_{15}(TiO_2)_3O_{56}(OH)_3]\cdot 14H_2O$ (**Na-2**), the nonbridging Dawson tetramer with an encapsulated Cl^- ion, $Na_{21}K_4[\{P_2W_{15}Ti_3O_{57.5}(OH)_3\}_4Cl]\cdot 70H_2O$ (**NaK-3**), and the bridging Dawson tetramer with an encapsulated Cl^- ion, $Na_{19}H_2[\{\alpha\text{-}1,2,3\text{-}P_2W_{15}Ti_3O_{59}(OH)_3\}_4\{\mu_3\text{-}Ti(H_2O)_3\}_4Cl]\cdot 124H_2O$ (**NaH-4**)] have been reported elsewhere.[5a,b,d]

Instrumentation/Analytical Procedures. Complete elemental analysis was carried out by Mikroanalytisches Labor Pascher (Remagen, Germany). A sample was dried at room temperature under 10^{-3}−10^{-4} Torr overnight before the complete elemental analysis. Infrared spectra were recorded on a Jasco 4100 FTIR spectrometer in KBr disks at room temperature. Thermogravimetric (TG) anaylses and differential thermal analyses (DTA) were acquired using a Rigaku Thermo Plus 2 series TG/DTA TG 8120 instrument. TG/DTA measurement was run under air with a temperature ramp of 4 °C/min between 20 and 500 °C.

^{31}P NMR (161.70 MHz) spectra in a D_2O solution were recorded in 5-mm outer diameter tubes on a JEOL JNM-EX 400 FT-NMR spectrometer with a JEOL EX-400 NMR data processing system. ^{31}P NMR spectra were measured in a D_2O solution with reference to an external standard of 25% H_3PO_4 in H_2O in a sealed capillary. The ^{31}P NMR data with the usual 85% H_3PO_4 reference were shifted to +0.544 ppm from our data. Chemical shifts were reported as negative for resonances upfield from 25% H_3PO_4 (δ 0). ^{183}W NMR (16.50 MHz) spectra were recorded in 10-mm outer diameter tubes on a JEOL NM40T10L low-frequency tunable probe and a JEOL EX 400 NMR data processing system. ^{183}W NMR spectra measured in D_2O were referenced to an external standard of a saturated Na_2WO_4−D_2O solution. The ^{183}W NMR signals were shifted to −0.787 ppm by using a 2 M Na_2WO_4 solution as a reference instead of a saturated Na_2WO_4 solution. Chemical shifts were reported as negative for resonances upfield from Na_2WO_4 (δ 0). $^{15}N\{^1H\}$ NMR (50.00 MHz) spectra in a D_2O solution were recorded in 5-mm outer diameter tubes on a JEOL ECP-500 FT-NMR spectrometer with a JEOL ECP-500 NMR data processing system. The $^{15}N\{^1H\}$ NMR spectrum was measured in a D_2O solution with reference to an external standard of NH_4NO_3 in a D_2O solution. Chemical shifts were reported as positive for resonances downfield from NH_4NO_3 (δ 30.0, NH_4^+).

Synthesis. $(NH_4)_{27}Na_8[(\alpha\text{-}1,2,3\text{-}P_2W_{15}Ti_3O_{60.5})_4(NH_4)]\cdot$ca.$90H_2O$ (NH_4Na-1). Solid $Na_9[P_2W_{15}(TiO_2)_3O_{56}(OH)_3]\cdot 14H_2O$ (**Na-2**) was treated for 3 h in an electric furnace at 200 °C. The resulting white yellow powder (0.5 g) was dissolved in 12 mL of water, and then stirred for 30 min. To the yellow clear solution was added 0.12 g (2.24 mmol) of NH_4Cl, followed by stirring for 30 min in a water bath at about 80 °C. The clear yellow solution was left to stand at 30 °C in a water bath for 1 day. Additionally, the solution was left to stand at 27 °C in a water bath for 1 day. The colorless needle crystals formed were collected on a membrane filter (JG 0.2 μm), washed with EtOH (10 mL × 3) and then Et_2O (50 mL × 3), and dried in vacuo for 2 h. The crystals obtained in 54.0% (0.27 g scale) yield were soluble in water and insoluble in EtOH and Et_2O. Found: H, 0.93; N, 2.26; Na, 1.08; P, 1.47; W, 66.1; Ti, 3.43; O, 24.7; Cl, <0.1; total 99.97%. Calcd for $H_{146}N_{28}Na_8P_8W_{60}Ti_{12}O_{259}$ or $(NH_4)_{27}Na_8[(P_2W_{15}Ti_3O_{60.5})_4(NH_4)]\cdot 17H_2O$: H, 0.88; N, 2.35; Na, 1.10; P, 1.48; W, 65.97; Ti, 3.44; O, 24.78%. A weight loss of 6.64% (weakly solvated or adsorbed water) was observed during the course of drying at room temperature at 10^{-3}−10^{-4} Torr overnight before analysis, suggesting the presence of 66 water molecules. TG/DTA under atmospheric conditions (Figure S1): a weight loss of 9.18% below 200 °C was observed with endothermic peaks at 40.7, 64.0, 98.0, 121.9, and 183.0 °C; calcd 9.17% for x = 92 in $(NH_4)_{27}Na_8[(P_2W_{15}Ti_3O_{60.5})_4(NH_4)]\cdot xH_2O$. IR(KBr) (polyoxometalate region): 1400 s, 1086 s, 1007 w, 943 s, 912 s, 831 s, 785 s, 687 vs, 600 m, 565 m, 526 m, 480 w, 465 w, 449 w, 403 w cm^{-1}. ^{31}P NMR (27.4 °C, D_2O): δ −7.15, −14.23. ^{31}P NMR (23.5 °C, 0.1 M HCl aq): δ −7.72, −14.05. ^{183}W NMR (14.0 °C, D_2O): δ −154.2 (3 W × 4), −184.3 (6 W × 4), −224.5 (6 W × 4). $^{15}N\{^1H\}$ NMR (35 °C, D_2O): δ 29.89 (countercation), 35.45 (encapsulated cation). $^{15}N\{^1H\}$ NMR measurement was performed for the ^{15}N-enriched sample prepared by using $^{15}NH_4Cl$ in the above synthesis.

Synthesis of $(NH_4)_{24}Na_7K_4[(\alpha\text{-}1,2,3\text{-}P_2W_{15}Ti_3O_{60.5})_4(NH_4)]\cdot$ca.$50H_2O$ (NH_4NaK-1) Using $Na_{21}K_4[\{\alpha\text{-}1,2,3\text{-}P_2W_{15}Ti_3O_{57.5}(OH)_3\}_4Cl]\cdot 70H_2O$ (NaK-3): Exchange of the Encapsulated Chloride Ion with an Ammonium Ion. The

dx.doi.org/10.1021/ic200355e |Inorg. Chem. 2011, 50, 6575–6583

pH of a solution (pH 2−2.5) of $Na_{21}K_4[\{P_2W_{15}Ti_3O_{57.5}(OH)_3\}_4Cl]\cdot 70H_2O$ (**NaK-3**, 2.0 g, 0.11 mmol) dissolved in 40 mL of water was adjusted to 6.4 by adding 3% aqueous NH_3. To the colorless clear solution, 0.48 g (8.97 mmol) of NH_4Cl was added, followed by stirring for 30 min in a water bath at 80 °C. The colorless clear solution was allowed to stand overnight at 35 °C. The white crystalline powder precipitated was collected on a membrane filter (JG 0.2 μm), washed with EtOH (30 mL × 3) and then Et_2O (50 mL × 3), and dried in vacuo for 2 h. The white powder obtained in 45.2% (0.89 g scale) yield was soluble in water and insoluble in EtOH and Et_2O. Found: H, 0.94; N, 1.62; Na, 0.78; K, 0.66; P, 1.53; W, 66.2; Ti, 3.40; O, 24.7; Cl, 0.016; total 99.85%. Calcd for $H_{130}N_{25}Na_7K_4P_8W_{60}Ti_{12}O_{257}$ or $(NH_4)_{24}Na_7K_4[(P_2W_{15}Ti_3O_{60.5})_4(NH_4)]\cdot 15H_2O$: H, 0.78; N, 2.09; Na, 0.96; K, 0.93; P, 1.48; W, 65.80; Ti, 3.43; O, 24.53%. A weight loss of 3.50% (weakly solvated or adsorbed water) was observed during the course of drying at room temperature at 10^{-3}−10^{-4} Torr overnight before analysis, suggesting the presence of 34 water molecules. TG/DTA under atmospheric conditions (Figure S2): a weight loss of 5.21% below 200 °C was observed with an endothermic peak at 57.1 °C; calcd 5.18% for x = 50 in $(NH_4)_{24}Na_7K_4[(P_2W_{15}Ti_3O_{60.5})_4(NH_4)]\cdot xH_2O$. IR(KBr) (polyoxometalate region): 1401 s, 1086 s, 1008 w, 944 s, 914 s, 831 s, 786 s, 688 vs, 598 m, 567 m, 526 m, 472 w, 405 w cm^{-1}. ^{31}P NMR (22.5 °C, D_2O): δ −7.12, −14.25.

We obtained the crystalline sample of **NH_4NaK-1** and tried a single crystal structural analysis. However, we have not obtained good data.

When NaOH, instead of aqueous NH_3, was used to deprotonate all sodium salt of **3** in the workup, Na^+ ion is surely encapsulated. [Note: Solid sample of such a compound was difficult to isolate because it was highly soluble in water.] However, there are some problems in the use of NaOH or KOH for the compounds with mixed counterions such as **NaK-3**, because encapsulation significantly depends upon the interaction between countercation and POM anion. The present workup using aqueous NH_3 and NH_4Cl is also concerned with the solubility in water.

Control Experiment 1: Preparation of 1 Using the Monomeric Trititanium(IV)-Substituted Dawson POM, [α-1,2,3-$P_2W_{15}Ti_3O_{62}]^{12-}$ (5), Prepared by Hydrolysis of the Bridging Dawson Tetramer with an Encapsulated Chloride Ion (4).

(1) For the synthesis of $Na_{12}[P_2W_{15}Ti_3O_{62}]\cdot 28H_2O$ (**Na-5**), the monomeric form **5** of the trititanium(IV)-substituted Dawson POM cannot be derived from a direct reaction of the trilacunary Dawson species $[P_2W_{15}O_{56}]^{12-}$ with Ti source, but it can be prepared by hydrolysis of the bridging Dawson tetramer with an encapsulated Cl^- ion **4**. The pH of a solution of $Na_{19}H_2[\{\alpha\text{-}1,2,3\text{-}P_2W_{15}Ti_3O_{59}(OH)_3\}_4\{\mu_3\text{-}Ti(H_2O)_3\}_4Cl]\cdot 124H_2O$ (**NaH-4**, 4.8 g, 0.253 mmol) dissolved in 20 mL of water was adjusted to 9.0 by adding 1 M NaOH aqueous solution. [Note: It took more than 3 h to stabilize and maintain the pH at 9.0 by adding 1 M NaOH aqueous solution.] To the colorless clear solution was added 8.0 g (0.137 mol) of NaCl, followed by stirring for 1 h. The white powder precipitated was collected on a membrane filter (JG 0.2 μm), washed with EtOH (30 mL × 3) and then Et_2O (50 mL × 3), and dried in vacuo for 2 h. The white powder obtained in 41.7% (2.0 g scale) yield was soluble in water and insoluble in EtOH and Et_2O. TG/DTA under atmospheric conditions: a weight loss of 10.75% below 307.6 °C was observed with endothermic peaks at 43.3 and 75.4 °C and an exothermic peak at 481.8 °C; calcd 10.65% for x = 28 in $Na_{12}[P_2W_{15}Ti_3O_{62}]\cdot xH_2O$. IR(KBr) (polyoxometalate region): 1631 s, 1088 s, 1051 m, 1014 m, 941 vs, 914 vs, 825 vs, 742 vs, 599 s, 562 s, 525 s, 463 s cm^{-1}. [Note: No Ti−O−Ti vibration band of inter-Dawson units, usually observed in the range 690−650 cm^{-1} as prominent bands in the Dawson tetramers, indicates that this compound is a monomer.] ^{31}P NMR (22.9 °C, D_2O): δ −4.94, −14.61.

(2) For the synthesis of the ammonium sodium salt of **1** from the monomer **Na-5**, NH_4Cl (0.06 g, 1.12 mmol) was added to a stirred solution (pH 9.9) of the monomer (**Na-5**, 0.50 g, 0.11 mmol) dissolved in 12 mL of water. The pH of the solution (pH 8.4) was adjusted to 6.0 using 0.1 M aqueous HCl, followed by stirring for 30 min in a water bath at 80 °C. The solution was evaporated until white powder deposited with a rotary evaporator at 30 °C. After adding 1 mL of water, the white powder was dissolved by further stirring in a water bath at 35 °C. On cooling gradually the solution from 35 °C to room temperature, colorless needle crystals deposited, which were collected on a membrane filter (JG 0.2 μm), washed with EtOH (10 mL × 3) and Et_2O (50 mL × 3), and dried in vacuo for 3 h. White powder of the ammonium sodium salt of **1**, obtained in 14.3% (0.067 g scale) yield, was soluble in water and insoluble in EtOH and Et_2O. TG/DTA under atmospheric conditions (Figure S3): a weight loss of 9.7% below 500 °C was observed with an endothermic peak at 48.4 °C. The formula of the ammonium sodium salt of **1** was tentatively determined on the basis of elemental analysis and TG/DTA as $(NH_4)_ySn_{35-y}[(\alpha\text{-}1,2,3\text{-}P_2W_{15}Ti_3O_{60.5})_4(NH_4)]\cdot 70H_2O$ (y = 20−22). IR(KBr) (polyoxometalate region): 1620 w, 1407 w, 1086 m, 1008 w, 944 s, 914 m, 892 m, 829 s, 779 s, 683 vs, 599 m, 566 m, 524 m, 468 m cm^{-1}. ^{31}P NMR (21.5 °C, D_2O): δ −7.21, −14.20.

Control Experiment 2: In-Situ-Generation of the Nonbridging Dawson Tetramer with an Encapsulated Sodium Ion. In a fume hood, ca. 0.1 mL (ca. 0.91 mmol) of $TiCl_4$ was added to 20 mL of water in an ice bath. To this mixture was added 1.25 g (0.29 mmol) of solid $Na_{12}[P_2W_{15}O_{56}]\cdot 19H_2O$[6] (see Materials), followed by stirring for 10 min. The pH of the solution was adjusted to 6.6 by adding solid Na_2CO_3, followed by stirring overnight. The ^{31}P NMR of the solution was measured: −7.45, −14.21 ppm (main peaks due to the encapsulated Na^+ species in the Dawson tetramer) and −4.98, −14.68 ppm (minor peaks due to the monomeric trititanium(IV)-substituted Dawson POM species). Solid sample of the sodium salt with the encapsulated Na^+ ion was not isolated because of its high solubility. Preliminary data have shown that the ^{31}P NMR in D_2O of the in-situ-generated and/or isolated nonbridging Dawson tetramers are significantly changed by encapsulated ions: for NH_4^+ ion (δ ca. −7.14, −14.21), Na^+ ion (δ ca. −7.42, −14.15), K^+ ion (δ −7.39, −14.15), Cl^- (δ −7.62, −13.93).

X-ray Crystallography. A colorless needle crystal of **NH_4Na-1** (0.22 × 0.08 × 0.06 mm^3) was surrounded by liquid paraffin (Paratone-N) to prevent its degradation. Data collection was done by a Bruker SMART APEX CCD diffractometer at 90 K in a range 1.94° < 2θ < 56.96°. The intensity data were automatically corrected for Lorentz and polarization effects during integration. The structure was solved by direct methods (program SHELXS-97)[7a] followed by subsequent difference Fourier calculation and refined by a full-matrix least-squares procedure on F^2 (program SHELXL-97).[7b] Absorption correction was performed with SADABS (empirical absorption correction).[7c] The composition and formula of the POM containing many counterions and many hydrated water molecules have been determined by complete elemental analysis and TG/DTA analysis. Refinements of the positions of many counterions and many solvent molecules in the POM are limited because of their disorder. We can reveal only the molecular structure of the POM, but not the crystal structure. These features are very common in the POM crystallography.[2−5]

Crystal Data for NH_4Na-1. $H_{292}N_{28}Na_8O_{332}P_8Ti_{12}W_{60}$: M = 18036.10; triclinic, space group $P\bar{1}$; a = 24.906(7) Å, b = 38.261(11) Å, c = 38.991(11) Å, α = 79.228(5)°, β = 88.604(5)°, γ = 87.418(5)°, V = 36460(18) Å^3, Z = 4, D_c = 3.286 g cm^{-3}, μ(Mo Kα) = 19.243 mm^{-1}. R1 = 0.1564, wR2 = 0.2240 (for all data). R_{int} = 0.0856, R1 = 0.0805, wR2 = 0.1846, GOF = 1.023 (353 990 total reflections, 167 191 unique reflections where $I > 2\sigma(I)$). The maximum and minimum residual density (+11.683 and −5.826 e Å^{-3}) holes were located at 1.01 Å from O6D and 0.26 Å from W1H, respectively.

The main features of the molecular structure of the polyoxoanion (60 tungsten atoms, 12 titanium atoms, 8 phosphorus atoms, 242 oxygen

dx.doi.org/10.1021/ic200355e |Inorg. Chem. 2011, 50, 6575–6583

atoms, and 1 encapsulated ammonium cation per formula unit) were clarified. CCDC identification number is 805 517.

RESULTS AND DISCUSSION

Synthesis and Compositional Characterization. A crystalline sample of the nonbridging Dawson tetramer with an encapsulated NH_4^+ cation, $(NH_4)_{27}Na_8[(P_2W_{15}Ti_3O_{60.5})_4(NH_4)]\cdot$ca.$90H_2O$ (**NH_4Na-1**), was obtained in 54% yield by a reaction with NH_4Cl in an aqueous solution at 80 °C for the POM precursor, which was derived by thermal treatment at 200 °C for monomeric triperoxotitanium(IV)-substituted Dawson POM **2**. The composition and molecular formula of **NH_4Na-1** were consistent with complete elemental analysis, including O and Cl analyses, TG/DTA, FTIR spectroscopy, ($^{15}N\{^1H\}$, ^{31}P, and ^{183}W) NMR spectroscopy, and X-ray crystallography. The formation of **1** can be represented in eqs 1 and 2. In eq 1, the actual reaction is based on the conversion of the peroxotitanium(IV) species in POM to the hydroxotitanium(IV) species (**Z**) by a reaction with water in an electric furnace at 200 °C and subsequent proton transfer from the Ti−OH−Ti bond in the intra-Dawson unit to the terminal Ti−O group. Equation 2 shows that 4 units of **Z** condense to form the nonbridging Dawson tetramer by encapsulating NH_4^+ cation.

$$[P_2W_{15}(TiO_2)_3O_{56}(OH)_3]^{9-}\ (\mathbf{2}) + 3H_2O \rightarrow$$
$$''[P_2W_{15}\{Ti(OH)\}_3O_{59}]^{9-''}\ (\mathbf{Z}) + 3H_2O_2 \quad (1)$$

$$4''[P_2W_{15}\{Ti(OH)\}_3O_{59}]^{9-''}\ (\mathbf{Z}) + NH_4Cl \rightarrow$$
$$[(\alpha\text{-}1,2,3\text{-}P_2W_{15}Ti_3O_{60.5})_4(NH_4)]^{35-}\ (\mathbf{1}) + Cl^- + 6H_2O \quad (2)$$

On the other hand, tetramer **1** was also synthesized by the direct exchange of the encapsulated Cl^- ion in the tetrameric POM **3** with the NH_4^+ ion; the ammonium potassium sodium salt of **1**, $(NH_4)_{24}Na_7K_4[(P_2W_{15}Ti_3O_{60.5})_4(NH_4)]\cdot$ca.$50H_2O$ (**NH_4NaK-1**), was obtained in 45.2% yield by neutralizing the aqueous solution containing **3** with aqueous NH_3 (the initial pH of ca. 2−2.5 was changed to 6.4). The **NH_4NaK-1** was also characterized by complete elemental analysis, TG/DTA, FTIR spectroscopy, and ^{31}P NMR spectroscopy. The formation of **1** from **3** can be represented in eq 3.

$$[\{P_2W_{15}Ti_3O_{57.5}(OH)_3\}_4Cl]^{25-}\ (\mathbf{3}) + NH_4^+ + 12OH^- \rightarrow$$
$$[(\alpha\text{-}1,2,3\text{-}P_2W_{15}Ti_3O_{60.5})_4(NH_4)]^{35-}\ (\mathbf{1}) + Cl^- + 12H_2O \quad (3)$$

Tetramer **1** was also synthesized from a monomeric form of the trititanium(IV)-substituted Dawson POM, $[\alpha\text{-}1,2,3\text{-}P_2W_{15}Ti_3O_{62}]^{12-}$ (**5**), in the presence of NH_4Cl under slightly acidic conditions (see Control Experiment 1). It should be noted that the monomeric form **5** of high purity can be derived in good yield only by hydrolysis of the bridging Dawson tetramer with an encapsulated Cl^- ion **4**, but not by any reactions of the nonbridging Dawson tetramer with Cl^- ion **3**. It should be also noted that the monomer **5** as a single species has never been derived from a direct reaction of the trilacunary Dawson species $[P_2W_{15}O_{56}]^{12-}$ with Ti source.[5c] IR and ^{31}P NMR suggest that the monomer **5** in aqueous solution would be substantially the same as the hydroxotitanium(IV) species **Z** in eq 1. Such a formation of **1** can be shown in eqs 4 and 5.

$$[\{\alpha\text{-}1,2,3\text{-}P_2W_{15}Ti_3O_{59}(OH)_3\}_4\{\mu_3\text{-}Ti(H_2O)_3\}_4Cl]^{21-}\ (\mathbf{4})$$
$$+ 12OH^- \rightarrow 4[\alpha\text{-}1,2,3\text{-}P_2W_{15}Ti_3O_{62}]^{12-}\ (\mathbf{5})$$
$$+ 4[Ti(H_2O)_6]^{4+} + Cl^- \quad (4)$$

$$4[\alpha\text{-}1,2,3\text{-}P_2W_{15}Ti_3O_{62}]^{12-}\ (\mathbf{5}) + NH_4^+ + 12H^+ \rightarrow$$
$$[(\alpha\text{-}1,2,3\text{-}P_2W_{15}Ti_3O_{60.5})_4(NH_4)]^{35-}\ (\mathbf{1}) + 6H_2O \quad (5)$$

Here, it is suggested that the nonbridging Dawson tetramer with an encapsulated Na^+ ion is in-situ-generated in aqueous solution (see Control Experiment 2). The pH-varied ^{31}P NMR spectra of **NaK-3** using aqueous NH_3 showed that some of the bridging oxygen atoms were still protonated in the pH range less than 5.0, but they were completely deprotonated in the pH range greater than 6.0 (up to 8.0). In the synthetic conditions at pH 6.6 using Na_2CO_3, the edge-sharing oxygen atoms of the Ti−O−Ti bonds are completely deprotonated, and the central cavity becomes highly anionic. The species with an encapsulated Na^+ cation should be formed, because any other cations are not present in this system. Furthermore, the ^{31}P NMR data in control experiment 2 (^{31}P NMR in D_2O, −7.45 and −14.21 ppm) strongly suggest the encapsulation of Na^+ ion.

The samples of **NH_4Na-1** and **NH_4NaK-1** for elemental analysis were dried at room temperature under a vacuum of 10^{-3}−10^{-4} Torr overnight before analyses. All elements (H, N, Na, P, W, Ti, and O for **NH_4Na-1**, and H, N, Na, K, P, W, Ti, and O for **NH_4NaK-1**) were observed for a total of 99.97% for **NH_4Na-1** and 99.85% for **NH_4NaK-1**, the data of which were consistent with the composition of $(NH_4)_{27}Na_8[(P_2W_{15}Ti_3O_{60.5})_4(NH_4)]\cdot 17H_2O$ and $(NH_4)_{24}Na_7K_4[(P_2W_{15}Ti_3O_{60.5})_4(NH_4)]\cdot 15H_2O$, respectively. Furthermore, it should be noted that Cl ions were not observed (found <0.1%), revealing that the Cl^- ions are not contained in these complexes. The weight losses observed during the drying before analysis were 6.64% for **NH_4Na-1** and 3.50% for **NH_4NaK-1**, both of which corresponded to ca. 66 and ca. 34 weakly solvated and/or adsorbed water molecules, respectively. Thus, elemental analysis showed a presence of a total of ca. 83 water molecules for **NH_4Na-1** and a total of ca. 49 water molecules for **NH_4NaK-1** under atmospheric conditions. On the other hand, in TG/DTA measurements carried out under atmospheric conditions, a weight loss of 9.18% for **NH_4Na-1** was observed at below 200 °C due to dehydration, with endothermic peaks at 40.7, 64.0, 98.0, 121.9, and 183.0 °C, while that of 5.21% for **NH_4NaK-1** was observed at below 200 °C with an endothermic peak at 57.1 °C (Figures S1 and S2). The former value corresponded to a total of 92 water molecules for **NH_4Na-1**, whereas the latter corresponded to a total of 50 water molecules for **NH_4NaK-1**. Thus, the results by TG/DTA measurements are approximately consistent with those of complete elemental analyses. The formulas were determined on the basis of TG/DTA data at ca. 90 water molecules for **NH_4Na-1** and ca. 50 water molecules for **NH_4NaK-1**.

Solid-state FTIR measurements (Figure 1) of **NH_4Na-1** and **NH_4NaK-1** showed spectral patterns characteristic of the Dawson-type "$[P_2W_{18}O_{62}]^{6-}$" POM framework.[8] The IR spectra of **NH_4Na-1** and **NH_4NaK-1** in the Dawson POM region (1200−400 cm^{-1}) were very similar to that of tetramer **3**, especially with regard to the prominent bands, such as P−O bands (1086 cm^{-1} for **NH_4Na-1**, 1086 cm^{-1} for **NH_4NaK-1**, and 1090 cm^{-1} for **3**),

dx.doi.org/10.1021/ic200355e |*Inorg. Chem.* 2011, 50, 6575–6583

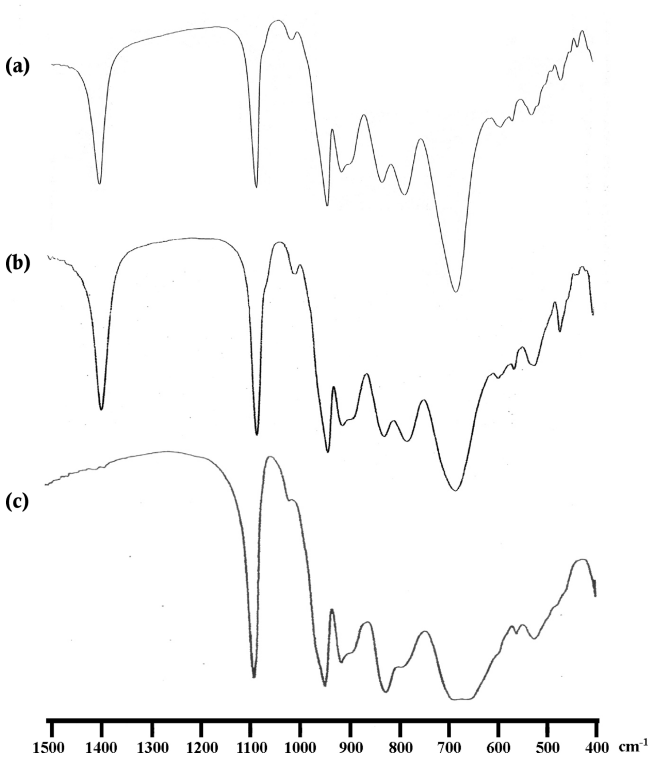

Figure 1. FTIR spectra in the polyoxoanion region (1500−400 cm^{-1}), measured in KBr disks, of (a) $(NH_4)_{27}Na_8[(P_2W_{15}Ti_3O_{60.5})_4(NH_4)]\cdot$ ca.$90H_2O$ (**NH_4Na-1**) and (b) $(NH_4)_{24}Na_7K_4[(P_2W_{15}Ti_3O_{60.5})_4(NH_4)]\cdot$ca.$50H_2O$ (**NH_4NaK-1**) that was obtained by exchange of the encapsulated chloride ion with the ammonium ion (see Experimental Section), and (c) $Na_{21}K_4[\{P_2W_{15}Ti_3O_{57.5}(OH)_3\}_4Cl]\cdot 70H_2O$ (**NaK-3**), which is the nonbridging Dawson tetramer with an encapsulated chloride ion, as a reference.

the bands assignable to $M-O_{terminal}$ bonds (943 cm^{-1} for **NH_4Na-1**, 944 cm^{-1} for **NH_4NaK-1**, and 952 cm^{-1} for **3**), the bands assignable to corner-sharing M−O−M bonds (912 cm^{-1} for **NH_4Na-1**, 914 cm^{-1} for **NH_4NaK-1**, and 918 cm^{-1} for **3**), and the bands assignable to edge-sharing M−O−M bonds (831, 785 cm^{-1} for **NH_4Na-1**; 831, 786 cm^{-1} for **NH_4NaK-1**; and 832 cm^{-1} for **3**). The Ti−O−Ti vibration bands of inter- and intra-Dawson units were also observed in close positions (687 cm^{-1} for **NH_4Na-1**, 688 cm^{-1} for **NH_4NaK-1**, and 689, 662 cm^{-1} for **3**). The Ti−O−Ti bands of **NH_4Na-1** and **NH_4NaK-1** were more sharply observed than that of **3**; the Ti−O−Ti bands of **NH_4Na-1** and **NH_4NaK-1** were observed as a single peak, while that of **3** was split. This splitting of Ti−O−Ti band in **3** would be attributable to coexistence of protonated and deprotonated Ti−O−Ti bonds, i.e., Ti−OH−Ti bond in the intra-Dawson unit and Ti−O−Ti bond of inter-Dawson units. As a matter of fact, the splitting has been observed in independent IR measurements of three different samples such as (689, 662 cm^{-3}), (689, 652 cm^{-3}), and (689, 656 cm^{-3}). On the other hand, all Ti−O−Ti bands in **NH_4Na-1** and **NH_4NaK-1** were not split because all Ti−O−Ti bonds were deprotonated.

Molecular Structure of 1. The molecular structure of polyoxoanion **1** in **NH_4Na-1**, its polyhedral representation, and the partial structure around the central octahedral cavity composed of the Ti−O−Ti bonding framework are shown in Figure 2a,b,c, respectively. Selected bond lengths (Å) and angles (deg) around the titanium(IV) centers for the Dawson POM unit A in **1** are given Table 1. Other bond lengths (Å) and angles (deg) in **1** (Table S1) and bond valence sum (BVS) calculations[9] of the W, P, Ti, and O atoms (Table S2) are shown in the Supporting Information.

The main features of the molecular structure of polyoxoanion **1**, i.e., 60 W atoms, 12 Ti atoms, 8 P atoms, 242 O atoms, and one encapsulated ammonium cation per formula unit, were identified by X-ray crystallography, but the location of some hydrated water molecules and countercations were not determined as the result of disorder. Therefore, the composition and formula of **NH_4Na-1** were determined by complete elemental analysis and TG/DTA analysis.

Structure analysis revealed that the molecular structure of **1** was composed of four "$P_2W_{15}Ti_3O_{62}$" Dawson units (designated as A, B, C, and D), which were linked through six intermolecular Ti−O−Ti bonds and arranged in approximately T_d symmetry, and one atom occupied the central octahedral cavity; the four Ti_3O_6 faces of the "$P_2W_{15}Ti_3O_{62}$" Dawson units occupied four alternate faces of an octahedron. The encapsulated atom was assigned to an N atom (NH_4^+ cation) due to the observed electron density. The encapsulated NH_4^+ cation was confirmed by $^{15}N\{^1H\}$ NMR signal at 35.45 ppm of **NH_4Na-1**, and the Cl^- ion-free sample was ascertained by complete elemental analysis. The nonbridging Dawson tetrameric structure of **1** was essentially the same as that of the tetramer **3**,[5b] but the Ti−O bond distances of the Ti−O−Ti bonds within the Dawson units in **1** were different from those of **3**. With respect to Dawson unit A, the Ti−O distances of the Ti−O−Ti bonds within the Dawson unit in **1** [1.83(2)−1.90(2) Å; average 1.87 Å] were shorter than those of **3** [1.888(15)−1.955(2) Å; average 1.934] (see Table 1 and ref 5b). Other bond distances and angles in **1** were in the normal range and were very similar to those in **3**.[5b] The bond valence sum (BVS) calculations (Table S2) have strongly suggested that all of the oxygen atoms of the Ti−O−Ti bonds within the Dawson units are not protonated, i.e., they are due to O^{2-}, but not OH^-. As a result, it appears that the central cavity of **1** becomes highly anionic, and thus, the NH_4^+ cation is encapsulated. On the contrary, all of the 12 oxygen atoms of the Ti−O−Ti bonds in **3**, which encapsulate the Cl^- anion, are protonated (see refs 5b and 5d), resulting in the fact that a highly cationic cavity in **3** is constructed and, therefore, the Cl^- anion is encapsulated.

The calculated bond valence sums (BVS),[9] based on the observed bond distances for Dawson units A, B, C, and D in **1**, were reasonably consistent with the formal valences of Ti^{4+} (4.020−4.300), W^{6+} (5.874−6.418), and P^{5+} (4.589−5.075). The BVS for the O atoms (1.488−2.182), including the oxygen atoms of the Ti−O−Ti bonds within the Dawson units (O49, O50, and O51 in each Dawson unit), were also consistent with the formal valence of O^{2-}, indicating that of the all O atoms were not protonated.

From the viewpoint of protonation/deprotonation of the briding oxygen atoms on the surface, the previously reported tetrameric POM $[(\alpha\text{-}1,2,3\text{-}P_2W_{15}Ti_3O_{57.5}(OH)_3)_4]^{24-}$[4b] is also discussed here. In 2003, Kortz and co-workers reported a tetrameric POM based on four trititanium(IV)-substituted Dawson subunits with the formula $K_4(NH_4)_{20}[\{P_2W_{15}Ti_3O_{57.5}(OH)_3\}_4]\cdot 77H_2O$.[4b] On the basis of BVS calculations, they indicated that the μ_2-oxo sites of all three Ti−O−Ti bridges within each Dawson fragment are protonated, whereas the μ_2-oxo sites of the six Ti−O−Ti bridges linking the four

dx.doi.org/10.1021/ic200355e |*Inorg. Chem.* 2011, 50, 6575–6583

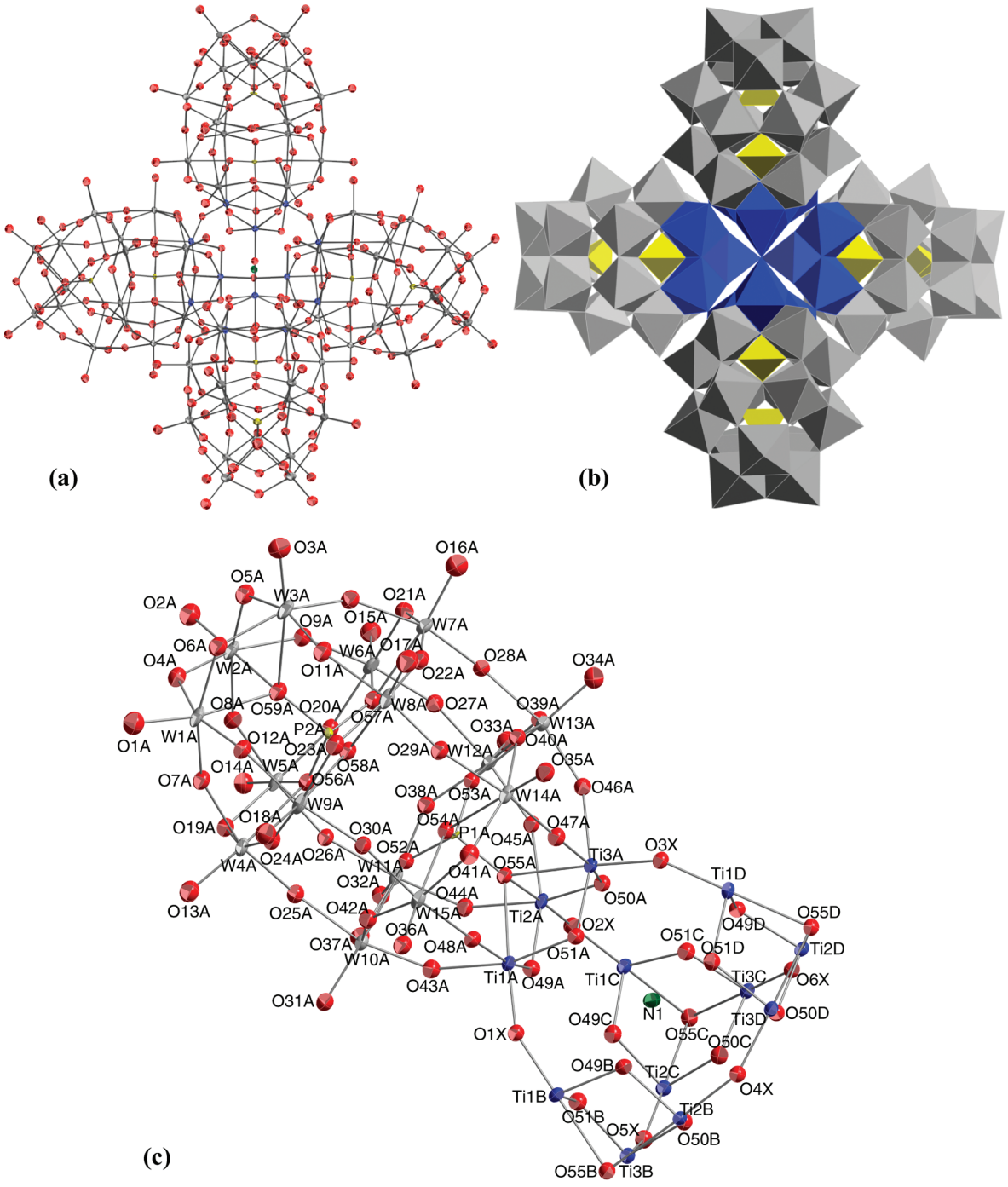

Figure 2. (a) Molecular structure of the polyoxoanion $[(\alpha\text{-}1,2,3\text{-}P_2W_{15}Ti_3O_{60.5})_4(NH_4)]^{35-}$ **1** in NH_4Na-**1**, (b) its polyhedral representation, and (c) the partial structure of the central moiety including the intramolecular and intermolecular Ti−O−Ti bonding framework. Polyhedral representation of the giant "tetrapod" polyoxoanion with approximately T_d symmetry, which is composed of the WO^6 octahedra (gray), the internal PO_4 tetrahedra (yellow), and the TiO_6 octahedra in the Ti_3 cap (blue). The encapsulated anion in the central cavity is hidden.

Dawson fragments to each other are not protonated. As to the protonation sites of the bridging oxygen atoms, their results are reasonable, and the same conclusion was also obtained in regard to our previous compounds, i.e., the nonbridging Dawson tetramer with one encapsulated Cl^- ion, i.e., $[(\alpha\text{-}1,2,3\text{-}P_2W_{15}Ti_3O_{57.5}(OH)_3)_4Cl]^{25-}$ $\mathbf{3}$[5b−d] and the bridging Dawson tetramer with different encapsulated X anions, i.e., $[\{\alpha\text{-}P_2W_{15}Ti_3O_{59}(OH)_3\}_4\{\mu_3\text{-}Ti(H_2O)_3\}_4X]^{21-}$ (X = Cl^- **4**, Br^-, I^-, and NO_3^-).[5]

However, the encapsulated ions in the central cavity are not indicated in the formula.[4b] *The formula apparently shows a compound without any encapsulated ions.* Thus, using the CIF file Kortz et al. have deposited, we rechecked the structure analysis and BVS calculation of the bridged oxygen atoms in all Ti−O−Ti bonds. It was confirmed that their compound was the nonbridging Dawson tetramer, but possessing one encapsulated ion in the central cavity. In fact, they analyzed the structure

dx.doi.org/10.1021/ic200355e |*Inorg. Chem.* 2011, 50, 6575–6583

Table 1. Selected Bond Lengths (Å) and Angles (deg) around the Titanium(IV) Centers for the Dawson-Polyoxoanion Unit A in 1

Ti−O−Ti distances (within Dawson units)		Ti−O−W distances (within Dawson units)			
Ti1A−O49A	1.88(2)	Ti1A−O43A	2.01(2)	W10A−O43A	1.83(2)
Ti2A−O49A	1.90(2)	Ti1A−O48A	1.96(2)	W15A−O48A	1.86(2)
Ti2A−O50A	1.83(2)	Ti2A−O44A	2.00(2)	W11A−O44A	1.85(2)
Ti3A−O50A	1.87(2)	Ti2A−O45A	2.00(2)	W12A−O45A	1.84(2)
Ti3A−O51A	1.86(2)	Ti3A−O46A	2.00(2)	W13A−O46A	1.84(2)
Ti1A−O51A	1.87(2)	Ti3A−O47A	2.02(2)	W14A−O47A	1.82(2)
Ti−O−Ti Distances					
Ti-Oa distances		between Dawson units			
Ti1A−O55A	2.27(2)	Ti1A−O1X	1.80(2)		
Ti2A−O55A	2.30(2)	Ti2A−O2X	1.81(2)		
Ti3A−O55A	2.26(2)	Ti3A−O3X	1.82(2)		
Angles					
Ti1A−O49A−Ti2A	116.1(12)	Ti2A−O45A−W12A	150.3(13)		
Ti2A−O50A−Ti3A	116.6(12)	Ti3A−O46A−W13A	150.7(13)		
Ti3A−O51A−Ti1A	114.8(12)	Ti3A−O47A−W14A	150.3(13)		
Ti1A−O43A−W10A	149.3(13)	Ti1A−O1X−Ti1B	150.0(14)		
Ti1A−O48A−W15A	150.4(13)	Ti2A−O2X−Ti1C	149.2(14)		
Ti2A−O44A−W11A	149.5(13)	Ti3A−O3X−Ti1D	148.3(13)		

of the compound with one atom (O(O32W)) placed in the central cavity. However, they state in the text of their paper that the atom (O32W) may be an ammonium ion (T_d symmetry) with the same symmetry as a tetrameric POM, although they did not assign an N atom to the structure analysis. In their compound, the description with regard to the central encapsulated ion is not consistent with the formula. Since all of the Ti−O−Ti sites within the Dawson fragments are protonated, the framework constructing the central cavity of the tetrameric POM should be cationic. Thus, the encapsulated ion would be an anionic species, most likely Cl^-, but not a cationic species such as NH_4^+.

Solution (^{31}P, ^{15}N{^{1}H}, ^{183}W) NMR of 1. The solution ^{31}P NMR spectra of **NH_4Na-1** in D_2O showed a clean two-line spectrum with signals at −7.15 and −14.23 ppm, confirming its purity and single-product nature (Figure 3a). The downfield resonance is assigned to the phosphorus atoms closest to the Ti_3 cap sites, whereas the upfield resonance is due to the phosphorus atoms closer to the W_3 cap in the Dawson units. These chemical shifts of **NH_4Na-1** are different from those of tetramer **3** containing the encapsulated Cl^- anion (−7.6 and −14.0 ppm) (Figure 3d). On the other hand, the ^{31}P NMR spectra of **NH_4Na-1** in 0.1 M HCl aq. (−7.7 and −14.1 ppm) were comparable to that of POM **3** measured in D_2O. The results have suggested that the bridging oxygen atoms on the surface of **NH_4Na-1** in D_2O are deprotonated, while they are protonated under 0.1 M HCl aq conditions. Thus, the encapsulated species in **NH_4Na-1** changes from the cation (NH_4^+) in D_2O to the anion (Cl^-) under HCl conditions. The ^{31}P NMR of **NH_4NaK-1** in D_2O (−7.12 and −14.25 ppm) (Figure 3c) was essentially the same as that of **NH_4Na-1** measured in D_2O.

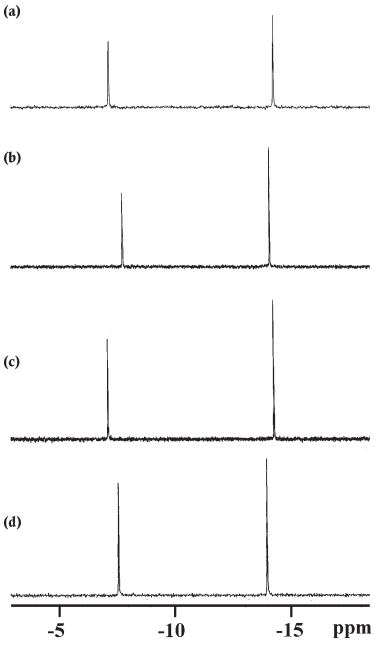

Figure 3. ^{31}P NMR spectra of (a) $(NH_4)_{27}Na_8[(P_2W_{15}Ti_3O_{60.5})_4(NH_4)]\cdot$ca.$90H_2O$ (**NH_4Na-1**) in D_2O and (b) in 0.1 M HCl aq, (c) $(NH_4)_{24}Na_7K_4[(P_2W_{15}Ti_3O_{60.5})_4(NH_4)]\cdot$ca.$50H_2O$ (**NH_4NaK-1**) in D_2O, and (d) $Na_{21}K_4[\{P_2W_{15}Ti_3O_{57.5}(OH)_3\}_4Cl]\cdot 70H_2O$ (**NaK-3**) in D_2O as a reference.

The solution ^{15}N{^{1}H} NMR spectrum of **NH_4Na-1** in D_2O (Figure 4a) was measured using a ^{15}N-enriched sample, which

dx.doi.org/10.1021/ic200355e |*Inorg. Chem.* 2011, 50, 6575–6583

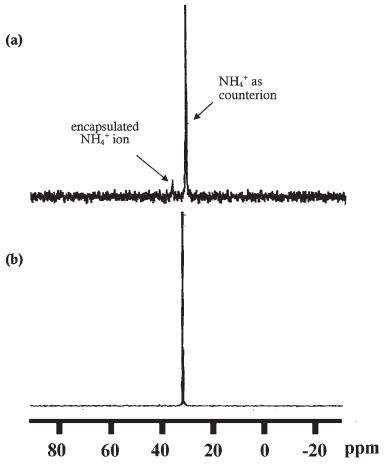

Figure 4. $^{15}N\{^1H\}$ NMR spectra in D_2O of (a) the ^{15}N-enriched sample of **NH_4Na-1** prepared using $^{15}NH_4Cl$ and (b) $^{15}NH_4Cl$ as a reference.

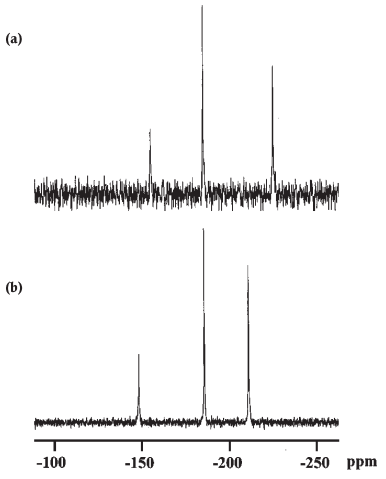

Figure 5. ^{183}W NMR spectra in D_2O of (a) $(NH_4)_{27}Na_8[(P_2W_{15}Ti_3O_{60.5})_4(NH_4)]\cdot ca.90H_2O$ (**NH_4Na-1**) and (b) $Na_{21}K_4[\{P_2W_{15}Ti_3O_{57.5}(OH)_3\}_4Cl]\cdot 70H_2O$ (**NaK-3**) as a reference.

was independently prepared using $^{15}NH_4Cl$. The $^{15}N\{^1H\}$ NMR spectrum of **NH_4Na-1** in D_2O showed a two-line spectrum of 29.89 and 35.45 ppm with integrated intensities of ca. 25:1, due to the counterions and the encapsulated ion, respectively, the larger signal of which should be compared with the $^{15}N\{^1H\}$ NMR spectrum in D_2O of the free $^{15}NH_4Cl$ alone showing only one peak at 31.56 ppm (Figure 4b). It should be noted that the ^{15}N NMR chemical shift of NH_4^+ as counterion of **1** is not superimposable with that of free NH_4Cl. It is due to the interaction of NH_4^+ counterion with the POM anion, but not from the error in the measurement by the substitution method. These results suggest that the NH_4^+ cation is encapsulated in the central cavity of **NH_4Na-1** in D_2O.

The ^{183}W NMR spectrum of **NH_4Na-1** measured in D_2O showed a three-line spectrum with signals at −154.2, −184.3, and −224.5 ppm with integrated intensities of 1:2:2 (Figure 5a) due to the Dawson substructure "$[\alpha$-1,2,3-$P_2W_{15}Ti_3O_{62}]^{12-}$". It should be noted that the most upfield resonance is much more shifted to a higher field, compared with that of the tetramer **3** (−148.3, −185.8, and −211.2 ppm). The difference in the ^{183}W NMR chemical shifts between **NH_4Na-1** and **3** is probably attributed to whether the oxygen atoms of the Ti−O−Ti bonds are protonated or not. A similar shifting to a higher field was also observed for the mono-Ti-substituted Keggin POM dimer, as previously reported by Kholdeeva et al.[3n]

Thus, solution (^{31}P, $^{15}N\{^1H\}$, ^{183}W) NMR in D_2O showed that NH_4^+ cation-encapsulating POM **1** is constructed with intramolecular Ti−(μ-O^{2-})−Ti bonds in Dawson subunits, which is consistent with the solid-state molecular structure revealed by X-ray crystallography. The encapsulating NH_4^+ ion in **1** in D_2O can be exchanged with the Cl^- ion under HCl conditions.

CONCLUSION

The chemistry of the Dawson tetramers composed of four trititanium(IV)-substituted Dawson subunits and their related compounds (**1**−**5**) has been exhaustively studied here. All ions so far encapsulated in the central cavities of the nonbridging Dawson tetramer and the bridging Dawson tetramer were only anions, i.e., a Cl^- ion for the former[5b] and Cl^-, Br^-, I^-, and NO_3^- ions for the latter.[5a,e] In this work, the nonbridging Dawson tetramer encapsulating the NH_4^+ cation, $[(P_2W_{15}Ti_3O_{60.5})_4(NH_4)]^{35-}$ **1**, was successfully synthesized by three different methods shown in eqs 1−5 (Results and Discussion), and unequivocally characterized. The possibility of other cation-encapsulating species was also indicated. X-ray crystallography revealed that the framework of the nonbridging tetramer encapsulating the NH_4^+ cation **1** was very similar to that of **3**. The factor determining whether the encapsulated ion in the central cavity is an anion or a cation depends on whether the edge-sharing oxygen atoms of the Ti−O−Ti bonds within the Dawson subunits are protonated or not. Thus, protonation/deprotonation of the μ-O atoms in the Ti−O−Ti bonds within the Dawson subunit results in encapsulation of anion/cation in the central cavity of the Dawson tetramer. That is to say, the formation of total $(Ti-OH-Ti)_{12}$ bonds in the Dawson tetramer leads to the cationic character of the central cavity, i.e., anion-encapsulation, while that of total $(Ti-O-Ti)_{12}$ bonds leads to the anionic property of the central cavity, i.e., cation-encapsulation. If a partial protonation such as $(Ti-OH-Ti)_6(Ti-O-Ti)_6$ is possible, the encapsulation of neutral molecules or the formation of an empty cavity may be realized.

The uptake/release of cations by POM-based capsule in solution and the potential of this phenomenon to extend a large variety of cation-transport phenomenon have been described by A. Müller et al.[10] Switching of the encapsulated anion/cation, based on the protonation/deprotonation of the edge-sharing oxygen atoms of the Ti−O−Ti bonds, can be controlled with the pH of the solution, and such a system may be considered as an inorganic model of the ion-transport and ion-channel systems driven by polarization/depolarization of membrane potential in the biological system.[11] Synthesis of the tetrameric POMs containing encapsulated cations other than NH_4^+ and Na^+ is in progress.

ASSOCIATED CONTENT

Supporting Information. Synthesis of the POM precursors. X-ray crystallographic data in CIF format. Selected bond lengths (Å) and angles (deg) around the titanium(IV) centers for the Dawson-POM units B, C, and D for **1**, and average bond lengths (Å) and angles (deg) for the Dawson-POM units in **1** (Table S1). Bond valence sum (BVS) calculations of W, P, Ti, and O atoms for **1** in **NH_4Na-1** (Table S2). TG/DTA of **NH_4Na-1**

(Figure S1), **NH_4NaK-1** (Figure S2), and the ammonium sodium salt of **1** derived from the monomer **Na-5** (Figure S3). This material is available free of charge via the Internet at http://pubs.acs.org.

AUTHOR INFORMATION

Corresponding Author
*E-mail: nomiya@kanagawa-u.ac.jp.

ACKNOWLEDGMENT

This work was supported by a Grant-in-Aid for Scientific Research (C) No. 22550065 from the Ministry of Education, Culture, Sports, Science and Technology, Japan.

REFERENCES

(1) (a) Pope, M. T.; Müller, A. *Angew. Chem., Int. Ed. Engl.* **1991**, *30*, 34–48. (b) Pope, M. T. *Heteropoly and Isopoly Oxometalates*; Springer-Verlag: New York, 1983. (c) Day, V. W.; Klemperer, W. G. *Science* **1985**, *228*, 533–541. (d) Hill, C. L. *Chem. Rev.* **1998**, *98*, 1–390. (e) Okuhara, T.; Mizuno, N.; Misono, M. *Adv. Catal.* **1996**, *41*, 113–252. (f) Hill, C. L.; Prosser-McCartha, C. M. *Coord. Chem. Rev.* **1995**, *143*, 407–455. (g) A series of 34 papers in a volume devoted to polyoxoanions in catalysis: Hill, C. L. *J. Mol. Catal.* **1996**, *114*, 1–359. (h) Neumann, R. *Prog. Inorg. Chem.* **1998**, *47*, 317–370. (i) *Polyoxometalate Chemistry from Topology via Self-Assembly to Applications*; Pope, M. T., Müller, A., Eds.; Kluwer Academic Publishers: Dordrecht, The Netherlands, 2001. (j) *Polyoxometalate Chemistry for Nano-Composite Design*; Yamase, T., Pope, M. T., Eds.; Kluwer Academic Publishers: Dordrecht, The Netherlands, 2002. (k) Pope, M. T. In *Comprehensive Coordination Chemistry II*; Wedd, A. G., Ed.; Elsevier Science: New York, 2004; Vol. 4, pp 635−678. (l) Hill, C. L. In *Comprehensive Coordination Chemistry II*; Wedd, A. G., Ed.; Elsevier Science: New York, 2004; Vol. 4, pp 679−759. (m) A series of 32 recent papers in a volume devoted to polyoxometalates in catalysis: Hill, C. L. *J. Mol. Catal. A: Chem.* **2007**, *262*, 1–242. (n) Proust, A.; Thouvenot, R.; Gouzerh, P. *Chem. Commun.* **2008**, 1837–1852. (o) Hasenknopf, B.; Micoine, K.; Lacôte, E.; Thorimbert, S.; Malacria, M.; Thouvenot, R. *Eur. J. Inorg. Chem.* **2008**, 5001–5013. (p) Laurencin, D.; Thouvenot, R.; Boubekeur, K.; Villain, F.; Villanneau, R.; Rohmer, M.-M.; Benard, M.; Proust, A. *Organometallics* **2009**, *28*, 3140–3151. (q) Long, D.-L.; Tsunashima, R.; Cronin, L. *Angew. Chem., Int. Ed.* **2010**, *49*, 1736–1758. (r) Dolbecq, A.; Dumas, E.; Mayer, C. R.; Mialane, P. *Chem. Rev.* **2010**, *110*, 6009–6048. (s) Pradeep, C. P.; Long, D.-L.; Cronin, L. *Dalton Trans.* **2010**, *39*, 9443–9457. (t) Nomiya, K.; Sakai, Y.; Matsunaga, S. *Eur. J. Inorg. Chem.* **2011**, 179–196.

(2) (a) Wassermann, K.; Dickman, M. H.; Pope, M. T. *Angew. Chem., Int. Ed.* **1997**, *36*, 1445–1448. (b) Kortz, U.; Hussain, F.; Reicke, M. *Angew. Chem., Int. Ed.* **2005**, *44*, 3773–3777. (c) Hussain, F.; Gable, R. W.; Speldrich, M.; Kogerler, P.; Boskovic, C. *Chem. Commun.* **2009**, 328–330. (d) Ritchie, C. I.; Streb, C.; Thiel, J.; Mitchell, S. G.; Miras, H. N.; Long, D. L.; Boyd, T.; Peacock, R. D.; McGlone, T.; Cronin, L. *Angew. Chem., Int. Ed.* **2008**, *47*, 6881–6884. (e) Thiel, J.; Ritchie, C.; Streb, C.; Long., D. L.; Cronin, L. *J. Am. Chem. Soc.* **2009**, *131*, 4180–4181. (f) Cadot, E.; Pilette, M.-A.; Marrot, J.; Secheresse, F. *Angew. Chem., Int. Ed.* **2003**, *42*, 2173–2176. (g) Gaunt, A. J.; May, I.; Collison, D.; Holman, K. T.; Pope, M. T. *J. Mol. Struct.* **2003**, *656*, 101–106. (h) Pradeep, C. P.; Long, D. L.; Kogerler, P.; Cronin, L. *Chem. Commun.* **2007**, 4254–4256. (i) Mal, S. S.; Kortz, U. *Angew. Chem., Int. Ed.* **2005**, *44*, 3777–3780. (j) Godin, B.; Chen, Y. G.; Vaissermann, J.; Ruhlmann, L.; Verdaguer, M.; Gouzerh, P. *Angew. Chem., Int. Ed.* **2005**, *44*, 3072–3075. (k) Kim, G.-S.; Zeng, H.; VanDerveer, D.; Hill, C. L. *Angew. Chem., Int. Ed.* **1999**, *38*, 3205–3207. (l) Zhao, J. W.; Zhang, J.; Zheng, S. T.; Yang, G. Y. *Inorg. Chem.* **2007**, *46*, 10944–10946.

(3) (a) Domaille, P. J.; Knoth, W. H. *Inorg. Chem.* **1983**, *22*, 818–822. (b) Ozeki, T.; Yamase, T. *Acta Crystallogr., Sect. C* **1991**, *47*, 693–696. (c) Knoth, W. H.; Domaille, P. J.; Roe, D. C. *Inorg. Chem.* **1983**, *22*, 198–201. (d) Yamase, T.; Ozeki, T.; Motomura, S. *Bull. Chem. Soc. Jpn.* **1992**, *65*, 1453–1459. (e) Lin, Y.; Weakley, T. J. R.; Rapko, B.; Finke, R. G. *Inorg. Chem.* **1993**, *32*, 5095–5101. (f) Yamase, T.; Ozeki, T.; Sakamoto, H.; Nishiya, S.; Yamamoto, A. *Bull. Chem. Soc. Jpn.* **1993**, *66*, 103–108. (g) Yamase, T.; Cao, X.; Yazaki, S. *J. Mol. Catal. A: Chem.* **2007**, *262*, 119–127. (h) Nomiya, K.; Takahashi, M.; Ohsawa, K.; Widegren, J. A. *J. Chem. Soc., Dalton Trans.* **2001**, 2872–2878. (i) Nomiya, K.; Takahashi, M.; Widegren, J. A.; Aizawa, T.; Sakai, Y.; Kasuga, N. C. *J. Chem. Soc., Dalton Trans.* **2002**, 3679–3685. (j) Goto, Y.; Kamata, K.; Yamaguchi, K.; Uehara, K.; Hikichi, S.; Mizuno, N. *Inorg. Chem.* **2006**, *45*, 2347–2356. (k) Tan, R. X.; Li, D. L.; Wu, H. B.; Zhang, C. L.; Wang, X. H. *Inorg. Chem. Commun.* **2008**, *11*, 835–836. (l) Hussain, F.; Bassil, B. S.; Bi, L.-H.; Reicke, M.; Kortz, U. *Angew. Chem., Int. Ed.* **2004**, *43*, 3485–3488. (m) Kholdeeva, O. A.; Maksimov, G. M.; Maksimovskaya, R. I.; Kovaleva, L. A.; Fedotov, M. A.; Grigoriev, V. A.; Hill, C. L. *Inorg. Chem.* **2000**, *39*, 3828–3837. (n) Kholdeeva, O. A.; Trubitsina, T. A.; Maksimov, G. M.; Golovin, A. V.; Maksimovskaya, R. I. *Inorg. Chem.* **2005**, *44*, 1635–1642. (o) Hussain, F.; Bassil, B. S.; Kortz, U.; Kholdeeva, O. A.; Timofeeva, M. N.; de Oliveira, P.; Keita, B.; Nadjo, L. *Chem.—Eur. J.* **2007**, *13*, 4733–4742. (p) Al-Kadamany, G. A.; Hussain, F.; Mal, S. S.; Dickman, M. H.; Leclerc-Laronze, N.; Marrot, J.; Cadot, E.; Kortz, U. *Inorg. Chem.* **2008**, *47*, 8574–8576. (q) Ren, Y. H.; Liu, S. X.; Cao, R. G.; Zhao, X. Y.; Cao, J. F.; Gao, C. Y. *Inorg. Chem. Commun.* **2008**, *11*, 1320–1322. (r) Mouri, Y.; Sakai, Y.; Kobayashi, Y.; Yoshida, S.; Nomiya, K. *Materials* **2010**, *3*, 503–518.

(4) (a) Crano, N. J.; Chambers, R. C.; Lynch, V. M.; Fox, M. A. *J. Mol. Catal. A: Chem.* **1996**, *114*, 65–75. (b) Kortz, U.; Hamzeh, S. S.; Nasser, A. *Chem.—Eur. J.* **2003**, *9*, 2945–2952. (c) Murakami, H.; Hayashi, K.; Tsukada, I.; Hasegawa, T.; Yoshida, S.; Miyano, R.; Kato, C. N.; Nomiya, K. *Bull. Chem. Soc. Jpn.* **2007**, *80*, 2161–2169. (d) Yoshida, S.; Murakami, H.; Sakai, Y.; Nomiya, K. *Dalton Trans.* **2008**, 4630–4638.

(5) (a) Sakai, Y.; Yoza, K.; Kato, C. N.; Nomiya, K. *Chem.—Eur. J.* **2003**, *9*, 4077–4083. As for the protonation sites within the tetrameic Dawson POMs found with BVS calculations of the oxygen atoms, see also ref 6 cited in ref 5d. (b) Sakai, Y.; Yoza, K.; Kato, C. N.; Nomiya, K. *Dalton Trans.* **2003**, 3581–3586. (c) Nomiya, K.; Arai, Y.; Shimizu, Y.; Takahashi, M.; Takayama, T.; Weiner, H.; Nagata, T.; Widegren, J. A.; Finke, R. G. *Inorg. Chim. Acta* **2000**, *300*−*302*, 285–304. (d) Sakai, Y.; Kitakoga, Y.; Hayashi, K.; Yoza, K.; Nomiya, K. *Eur. J. Inorg. Chem.* **2004**, 4646–4652. (e) Sakai, Y.; Yoshida, S.; Hasegawa, T.; Murakami, H.; Nomiya, K. *Bull. Chem. Soc. Jpn.* **2007**, *80*, 1965–1974.

(6) (a) Mbomekalle, I.-M.; Lu, Y. W.; Keita, B.; Nadjo, L. *Inorg. Chem. Commun.* **2004**, *7*, 86–90. (b) Graham, C. R.; Finke, R. G. *Inorg. Chem.* **2008**, *47*, 3679–3686. (c) Contant, R. *Inorg. Synth.* **1990**, *27*, 104–111. (d) Hornstein, B. J.; Finke, R. G. *Inorg. Chem.* **2002**, *41*, 2720–2721. (e) Randall, W. J.; Droege, M. W.; Mizuno, N.; Nomiya, K.; Weakley, T. J. R.; Finke, R. G. *Inorg. Synth.* **1997**, *31*, 167–185.

(7) (a) Sheldrick, G. M. *Acta Crystallogr., Sect. A* **1990**, *46*, 467–473. (b) Sheldrick, G. M. *SHELXL-97 Program for Crystal Structure Refinement*; University of Göttingen: Germany, 1997. (c) Sheldrick, G. M. *SADABS*; University of Göttingen: Germany, 1996.

(8) Rocchiccioli-Deltcheff, C.; Thouvenot, R. *Spectrosc. Lett.* **1979**, *12*, 127–138.

(9) (a) Brown, I. D.; Altermatt, D. *Acta Crystallogr., Sect. B* **1985**, *41*, 244–247. (b) Brown, I. D.; Shannon, R. D. *Acta Crystallogr., Sect. A* **1973**, *29*, 266–282. (c) Brown, I. D. *Acta Crystallogr., Sect. B* **1992**, *48*, 553–572. (d) Brown, I. D. *J. Appl. Crystallogr.* **1996**, *29*, 479–480.

(10) (a) Müller, A; Das, S. K.; Talismanov, S.; Roy, S.; Beckmann, E.; Bögge, H.; Schmidtmann, M; Merca, A; Berkle, A.; Allouche, L.; Zhou, Y.; Zhang, L. *Angew. Chem., Int. Ed.* **2003**, *42*, 5039–5044. (b) Müller, A.; Rehder, D.; Haupt, E. T. K.; Merca, A.; Bögge, H.; Schmidtmann, M.; Heinze-Brückner, G. *Angew. Chem., Int. Ed.* **2004**, *43*, 4466–4470. (c) Ziv, A.; Grego, A.; Kopilevich, S.; Zeiri, L.; Miro, P.; Bo, C.; Müller, A.; Weinstock, I. A. *J. Am. Chem. Soc.* **2009**, *131*, 6380–6382.

(11) Atkins, P.; Overton, T.; Rourke, J.; Weller, M.; Armstrong, F. *Shriver & Atkins Inorganic Chemistry*, 4th ed.; Oxford University Press: Oxford, U.K., 2006; p 719.

Ver. 1.01 (14-12-14)

Graphical abstract

A novel tri-titanium(IV)-substituted Dawson polyoxometalate (POM)-based dimeric complex with the two bridging Cp*Rh groups, $[\{\alpha\text{-}1,2,3\text{-}P_2W_{15}Ti_3O_{60}(OH)_2\}_2(Cp^*Rh)_2]^{16-}$ (**D-1**), was synthesized by the 1 : 2 molar ratio reaction of the organometallic precursor $[Cp^*RhCl_2]_2$ with the separately prepared, monomeric tri-titanium(IV)-substituted Dawson polyoxometalate, $[\alpha\text{-}1,2,3\text{-}P_2W_{15}Ti_3O_{59}(OH)_3]^{9-}$ (**M-1**), and characterized by complete elemental analysis, TG/DTA, FTIR, X-ray crystallography and solution (^1H, ^{13}C, ^{31}P) NMR spectroscopy.

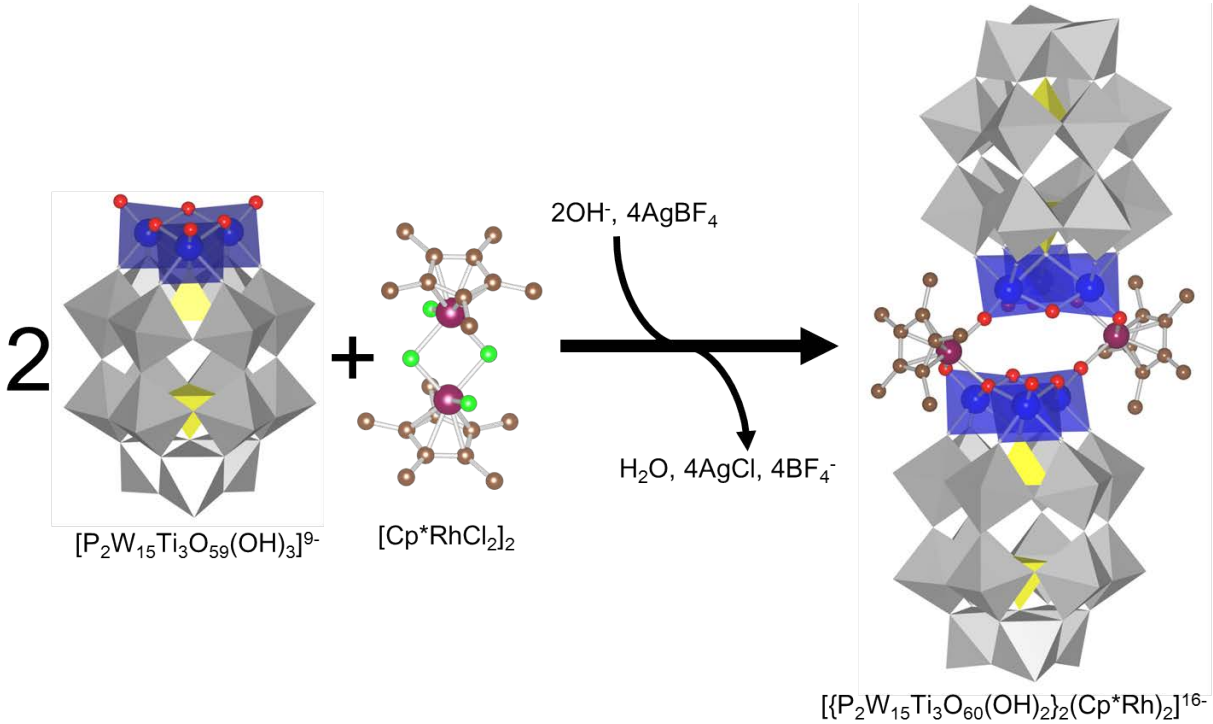

Ver. 0.10 (15-1-16)

Synthesis and molecular structure of dimeric tri-titanium(IV)-substituted Dawson polyoxometalate bridged by two Cp^*Rh^{2+} groups

Yusuke Matsuki, Shoko Takaku, Takahiro Hoshino, Satoshi Matsunaga and Kenji Nomiya*

Department of Chemistry, Faculty of Science, Kanagawa University, Hiratsuka, Kanagawa 259-1293, Japan.

Abstract

A novel tri-titanium(IV)-substituted Dawson polyoxometalate (POM)-based dimer with the two bridging Cp*Rh groups, $[\{\alpha\text{-}1,2,3\text{-}P_2W_{15}Ti_3O_{60}(OH)_2\}_2(Cp^*Rh)_2]^{16-}$ (**D-1**), was synthesized by the 1 : 2 molar ratio reaction of the organometallic precursor $[Cp^*RhCl_2]_2$ with the separately prepared, monomeric tri-titanium(IV)-substituted Dawson polyoxometalate, $[\alpha\text{-}1,2,3\text{-}P_2W_{15}Ti_3O_{59}(OH)_3]^{9-}$ (**M-1**). **D-1** was

characterized by complete elemental analysis, TG/DTA, FTIR, single-crystal X-ray structure analysis and solution (^{1}H, ^{13}C, ^{31}P) NMR spectroscopy. Single-crystal X-ray structure analysis revealed that the two tri-titanium-substituted Dawson units "$[P_2W_{15}Ti_3O_{62}]^{12-}$" are bridged by the two Cp^*Rh^{2+} groups, resulting in the overall C_i symmetry. The Cp^*Rh^{2+} groups were linked to two terminal oxygen atoms of the titanium sites and edge-sharing oxygen atom of the Ti-O-Ti bond. Tri-titanium-substituted Dawson POM-supported organometallic complex has not been reported so far and **D-1** is the first example of this type of complex.

Keywords: Dawson-type polyoxometalate; Tri-titanium (IV)-substitution; Organometallic complex; Cp^*Rh^{2+} group; X-ray crystallogrphy

1. Introduction

Polyoxometalates (POMs) are discrete metal-oxide clusters that are of current interest as soluble metal oxides. The coordination chemistry of POMs with transition metal cations (TMC) has been particularly well documented in the past few decades and for their applications in catalysis, medicine, and material science [1-12]. However, the lack of reactivity of bridging and terminal oxo ligands in a large number of POMs prevents the formation of TMC derivatives [11]. To improve the

nucleophilicity of the oxygen atoms, there are two synthetic routes: (i) the use of lacunary species of POMs in which the most nucleophilic oxygen atoms constitute the vacant sites; (ii) the increase of the overall negative charge of the POMs. The latter pathway can be achieved, for example, by replacement of one or several Mo^{VI} and W^{VI} centers by cations with a lower charge (V^{V}, Nb^{V}, Ti^{IV}, ...). In fact, Keggin and Dawson POM-supported organometallic and transition-metal complexes have been intensively studied [12] in the viewpoint of molecular modeling of metal-oxide-supported transition metal catalysts. For example, tri-M(V)-substituted Dawson POM-supported organometallic complexes (M = niobim(V), vanadium(V)) have been formed by covalently binding of cationic organometallic species utilizing the surface, three extra negative charge of the tri-M-substituted Dawson POM anion $[P_2W_{15}M_3O_{62}]^{9-}$, compared with the parent anion $[P_2W_{18}O_{62}]^{6-}$; for the case of M = niobium(V), such as $[(Cp^*Rh)P_2W_{15}Nb_3O_{62}]^{7-}$ [13-15], $[\{(C_6H_6)Ru\}P_2W_{15}Nb_3O_{62}]^{7-}$ [13,14], $[\{(cod)Y\}P_2W_{15}Nb_3O_{62}]^{8-}$ (Y = Rh^{I}, Ir^{I}) [16-19] and $[\{Z\}P_2W_{15}Nb_3O_{62}]^{8-}$ (Z = $Re(CO)_3^{+}$, $Ir(CO)_2^{+}$, $Rh(CO)_2^{+}$) [20], and for the case of M = vanadium(V), such as $[(CpTi)P_2W_{15}V_3O_{62}]^{6-}$ [21], $[(Cp^*Rh)_2P_2W_{15}V_3O_{62}]^{5-}$ [22], $[(Cp^*Rh)P_2W_{16}V_2O_{62}]^{6-}$ [23], $[\{(cod)Pt\}P_2W_{15}V_3O_{62}]^{7-}$ [24], $[\{(C_6H_6)Ru\}P_2W_{15}V_3O_{62}]^{7-}$ [25]. These complexes are the monomer-form with composition ratio of 1 : 1 or 1 : 2 to POM and organometallic fragment. On the other hand, only a few dimer-form complexes with

composition ratio of 2 : 1 or 2 : 2 to POM and organometallic fragment such as $[(PNbW_{11}O_{40})_2ZrCp_2]^{6-}$ [26] and $[\alpha\text{-}PW_{11}Al(OH)O_{39}ZrCp_2]_2^{6-}$ [27] have been also reported.

As for the tri-titanium(IV)-substituted Dawson POM, it has been reported as two stable tetrapod-shape tetramers by the reactions of tri-lacunary Dawson POM $[B\text{-}P_2W_{15}O_{56}]^{12-}$ with Ti^{IV} [10], but not as the monomeric form "$[P_2W_{15}Ti_3O_{62}]^{12-}$". One of the tetramers $[\{P_2W_{15}Ti_3O_{57.5}(OH)_3\}_4Cl]^{25-}$ (here called the non-bridging tetramer, i.e., the tetramer without the bridging Ti groups) is composed of four Dawson units, linked through intermolecular Ti-O-Ti bonds, and one encapsulated Cl^- ion [28]. The other tetramer, $[\{P_2W_{15}Ti_3O_{59}(OH)_3\}_4\{\mu_3\text{-}Ti(H_2O)_3\}_4Cl]^{21-}$ (**Tb-1**; here called the bridging tetramer, i.e., the tetramer with bridging Ti groups), is composed of four Dawson units, four $\mu_3\text{-}Ti(H_2O)_3$ groups and one encapsulated Cl^- ion [29, 30] These Dawson POM-based tetrapod-shaped tetramers are actually generated by self-assembly due to rapid formation of Ti-O-Ti bonds among the monomers "$[P_2W_{15}Ti_3O_{62}]^{12-}$". Nevertheless, the monomeric form of the tri-titanium(IV)-substituted Dawson POM has never been obtained by the reaction of tri-lacunary Dawson POM with Ti^{IV}. Thus, the organometallic complexes supported on the tri-titanium(IV)-sustituted Dawson POM have never been realized.

Recently we found that the monomeric, tri-titanium(IV)-substituted Dawson POM,

was formed by hydrolysis of the bridging tetramer (**Tb-1**) [31], but not of the non-bridging tetramer. In our prelimnary experiments, we first found that the monomeric form was formed as the protonated form $[P_2W_{15}Ti_3O_{59}(OH)_3]^{9-}$ (**M-1**). In this work, we isolated of the monomeric form **M-1** as sodium/caesium salt (**NaCs-M-1**) in the solid state by a hydrolysis of **Tb-1** by aqueous NaOH, and examined the reaction of **M-1** in water with $[Cp^*Rh]^{2+}$ species, which has been *in situ* generated by AgCl elimination by a reaction of $[Cp^*RhCl_2]_2$ and $AgBF_4$ in MeOH, forming the tri-titanium(IV)-substituted Dawson POM-based organometallic complex **D-1**.

Herein, we report full details of the synthesis and characterization of the dimer-form complex with a 2 : 2-ratio composition of the tri-titanium-substituted Dawson POM and Cp^*Rh^{2+} group, *i.e.*, $[\{\alpha\text{-}1,2,3\text{-}P_2W_{15}Ti_3O_{60}(OH)_2\}_2(Cp^*Rh)_2]^{16-}$ (**D-1**), by complete elemental analysis including oxygen, thermogravimetric (TG) and differential thermal analyses (DTA), FTIR, X-ray crystallography and solution (^1H, ^{13}C and ^{31}P) NMR spectroscopy.

2. Experimental

2.1. General

The following were used as received: NaOAc, CsCl, 1 M NaOH *aq*., $AgBF_4$, $LiOH\cdot H_2O$, MeOH, EtOH, Et_2O (Wako); D_2O (Isotec); $RhCl_3\cdot 3H_2O$, Cp*H, DSS

(Aldrich). The precursor $[Cp^*RhCl_2]_2$ was prepared according to literature methods [32, 33], and identified with elemental analysis, TG/DTA, FT-IR, ^1H and ^{13}C NMR. The precursor $Na_{19}H_2[\{\alpha\text{-}1,2,3\text{-}P_2W_{15}Ti_3O_{59}(OH)_3\}_4\{\mu_3\text{-}Ti(OH_2)_3\}_4Cl]\cdot 127H_2O$ (**Na-Tb-1**) was prepared and identified with elemental analysis, TG/DTA, FT-IR, ^{31}P NMR spectra in D_2O according to the literature [29, 30].

Complete elemental analysis was carried out by Mikroanalytisches Labor Pascher (Remagen, Germany). A sample was dried at room temperature under 10^{-3}-10^{-4} Torr overnight before analysis. CHN elemental analyses were carried out with a Perkin Elmer 2400 CHNS Elemental Analyzer II. Infrared spectra were recorded on a JASCO 4100 FTIR spectrometer in KBr disks at room temperature. TG and DTA were acquired using a Rigaku Thermo Plus 2 series TG/DTA TG 8120 instrument. ^{31}P NMR (160 MHz) and ^1H NMR (400 MHz) spectra in a D_2O solution were recorded in 5 mm outer diameter tubes on a JEOL JNM-ECS 400 FT-NMR spectrometer and a JEOL ECS-400 NMR data processing system. $^{13}C\{^1H\}$ NMR (125 MHz) spectra were recorded in 5 mm outer diameter tubes on a JEOL JNM-ECP 500 FT-NMR spectrometer and a JEOL ECP-500 NMR data processing system. The ^{31}P NMR spectra were referenced to an external standard of 25% H_3PO_4 in H_2O in a sealed capillary. The ^{31}P NMR signals with the usual 85% H_3PO_4 are shifted to +0.544 ppm from our data with 25% H_3PO_4. The ^1H NMR and ^{13}C NMR spectra were referenced to an internal

standard of DSS.

*2.2.1. Synthesis of precursor $Na_8Cs[\alpha\text{-}1,2,3\text{-}P_2W_{15}Ti_3O_{59}(OH)_3]\cdot TiO_2\cdot 20H_2O$ (**NaCs-M-1**)*

$Na_{19}H_2[\{\alpha\text{-}1,2,3\text{-}P_2W_{15}Ti_3O_{59}(OH)_3\}_4\{\mu_3\text{-}Ti(OH_2)_3\}_4Cl]\cdot 127H_2O$ (**Na-Tb-1**: 7.6 g, 0.40 mmol) was dissolved in water (60 mL). To the solution was added 0.1 M NaOH *aq*. (97.6 mL) for 2 hr, followed by stirring for 10 min. This solution was stirred for 20 min in a water-bath at 60 °C and evaporated to 50 mL by rotary evaporator at 35 °C. To the solution was added dropwise 0.2 M CsCl *aq*. (8 mL), followed by stirring for 3 min. To it NaOAc (10.0 g, 122 mmol) was added at once. After stirring for 1 min, the white suspension was stirred for 15 min in ice-bath. The white precipitate formed was collected on a membrane filter (JG 0.2 μm), washed with cooled MeOH (10 mL×3), cooled EtOH (10 mL) and Et_2O (10 mL), and dried *in vacuo* for 2 hr. The white powder was obtained in a yield of 5.92 g {78.4 % relative to $Na_8Cs[\alpha\text{-}1,2,3\text{-}P_2W_{15}Ti_3O_{59}(OH)_3]\cdot TiO_2\cdot 20H_2O$}, which was very soluble in water, but insoluble in Me_2CO, MeCN, EtOH and Et_2O. *Anal*. Calc. for $Na_8CsH_{13}O_{69}P_2W_{15}Ti_4$ or $Na_8Cs[\alpha\text{-}1,2,3\text{-}P_2W_{15}Ti_3O_{59}(OH)_3]\cdot TiO_2\cdot 5H_2O$: H, 0.30; Na, 4.14; Cs, 2.99; O, 24.84; P, 1.39; W, 62.04; Ti, 4.31 %. Found: H, 0.29; Na, 4.38; Cs, 2.96; O, 22.9; P, 1.41; W, 61.4; Ti, 4.38 %. A weight loss of 5.91 % (weakly solvated or adsorbed

water) was observed during the course of drying at room temperature at 10^{-3}-10^{-4} Torr overnight before analysis, suggesting the presence of 15 water molecules. TG/DTA under atmospheric conditions: a weight loss of 9.73 % at below 296.8 °C was observed with an endothermic peak at 85.1 °C; calc. 9.71 % for x = 26 in $Na_8Cs[\alpha\text{-}1,2,3\text{-}P_2W_{15}Ti_3O_{59}(OH)_3]\cdot TiO_2\cdot xH_2O$. (IR (KBr) (polyoxometalate region): 1620 (m), 1087 (vs), 1052 (m), 1014(m), 941 (vs), 914(vs), 822(vs), 787(vs), 741 (vs), 718(vs), 598 (s), 523 (vs), 462 (s) cm^{-1}. ^{31}P NMR [24.9 °C, D_2O]: δ = -4.97, -14.65 ppm.

*2.2.2. Synthesis of $Na_{14}Cs_2[\{\alpha\text{-}1,2,3\text{-}P_2W_{15}Ti_3O_{60}(OH)_2\}_2(Cp^*Rh)_2]\cdot 2TiO_2\cdot 37H_2O$ (**NaCs-D-1**)*

$Na_8Cs[\alpha\text{-}1,2,3\text{-}P_2W_{15}Ti_3O_{59}(OH)_3]\cdot TiO_2\cdot 26H_2O$ (**NaCs-M-1**: 0.49 g, 0.1 mmol) was dissolved in water (6 mL). To the solution was added 0.1 M LiOH *aq*. (3 mL) for 2 hr. and stirred for 1 hr. Separately, $AgBF_4$ (0.039 g, 0.2 mmol) was dissolved in MeOH (10 mL). $[Cp^*RhCl_2]_2$ (0.031 g, 0.05 mmol) was added to the $AgBF_4$ methanol solution, followed by stirring for 30 min. The resulting solution was filtered through a membrane filter (JG 0.2 μm). Water (6 mL) was added to the filtrate and removed MeOH by a rotary evaporator at 40 °C. The solution containing "$Cp^*Rh(BF_4)_2$ " was added to the POM solution, followed by stirring for 1 hr in a water-bath at 90 °C. The

solution was evaporated to 5 mL by a rotary evaporator at 40 °C, to the concentrate was added EtOH (75 mL). The yellow-orange precipitate formed was collected on a membrane filter (JG 0.2 μm), washed with cooled Et_2O (10 mL×3), and dried *in vacuo* for 2 hr. At this stage, sodium-cesium salt was obtained in a yield of 0.41 g.

Crystallyzation. The yellow-orange powder was dissolved in water (6 mL). The yellow-orange clear solution was slowly evaporated at room temperature. After 2 days, yellow-orange powder and a few orange clear rod crystals were deposited, followed by separating the supernatant liquid. The supernatant liquid was slowly evaporated at room temperature. After 1 day, orange clear rod crystals were deposited, which were collected by a membrane filter (JG 0.2 μm), washed with EtOH (10 mL×3) and Et_2O (10 mL×3), and dried *in vacuo* for 2 hr. The crystalline samples obtained in a yield of 0.27 g {80.1 % relative to $Na_{14}Cs_2[\{\alpha\text{-}1,2,3\text{-}P_2W_{15}Ti_3O_{60}(OH)_2\}_2(Cp^*Rh)_2]\cdot 37H_2O\cdot 2TiO_2$ (**NaCs-D-1**), were very soluble in water, less soluble in MeOH, but insoluble in MeCN, EtOH and Et_2O. *Anal*. Calc. for $Na_{14}Cs_2C_{20}H_{42}O_{132}P_4W_{30}Ti_8\ Rh_2$ or $Na_{14}Cs_2[\{\alpha\text{-}1,2,3\text{-}P_2W_{15}Ti_3O_{60}(OH)_2\}_2(Cp^*Rh)_2]\cdot 2TiO_2\cdot 2H_2O$: H, 0.46; C, 2.61; Na, 3.49; Cs, 2.89; O, 22.93; P, 1.35; W, 59.88; Ti, 4.16; Rh, 2.23 %. Found : H, 0.54; C, 2.56; Na, 3.56; Cs, 2.56; O, 20.80; P, 1.30; W, 57.70; Ti, 4.97; Rh, 1.92 %. A weight loss of 6.44 % (weakly solvated or adsorbed water) was observed during the course of

drying at room temperature at 10^{-3}-10^{-4} Torr overnight before analysis, suggesting the presence of 35 water molecules. TG/DTA under atmospheric conditions: a weight loss of 5.45 % at below 255.6 °C was observed ; calc. 5.38 % for x = 29 in $Na_{14}Cs_2[\{\alpha\text{-}1,2,3\text{-}P_2W_{15}Ti_3O_{60}(OH)_2\}_2(Cp^*Rh)_2]\cdot 2TiO_2\cdot xH_2O$. (IR (KBr) (polyoxometalate region): 1623 (m), 1473 (w), 1376 (vw), 1085 (s), 1053 (w), 1011 (m), 939 (vs), 915 (vs), 742 (vs), 599 (m), 563 (m), 521 (vs), 459 (m) cm^{-1}. ^{31}P NMR [23.8 °C, D_2O]: δ = -5.20, -14.61 ppm. ^{1}H NMR[24.8 °C, D_2O] δ = 1.92 ppm. ^{13}C NMR[27.3 °C, D_2O] δ = 11.34, 96.00 ppm.

2.3. X-ray crystallography

Orange clear rod crystals of **NaCs-D-1** (0.10×0.04×0.03 mm) were surrounded by liquid paraffin (Paraton-N) to prevent their degradation. Data collection was done by a Bruker SMART APEX CCD diffractometer at 100 K in the range of 1.05° < θ < 28.35°. The intensity data were automatically corrected for Lorentz and polarization effects during integration. The structure was solved by direct methods (program SHELXS-97) [34], followed by subsequent difference Fourier calculation and refined by a full-matrix least-squares procedure on F^2 (program SHELXS-97) [35]. Absorption correction was performed with SADABS (empirical absorption correction) [36]. The compositions and formulae of the POMs containing many countercations

and many hydrated water molecules were determined by complete elemental analysis and TG analysis. As with other structural investigations of crystals of highly hydrated large polyoxometalate complexes, it was not possible to locate every countercation and hydrated water molecule. This frequently encountered situation is attributed to extensive disorder of the cations and many of the hydrated water molecules.

Crystal data for **NaCs-D-1**: $C_{20}H_0Cs_7K_0Na_8O_{154}P_4Rh_2Ti_6W_{30}$; M = 9951.09; triclinic, space group P-1; a = 15.7416(14), b = 17.1112(15), c = 20.1302(18) Å, α = 102.514(2), β = 93.555(2), γ = 111.0420(10)^o, V = 4881.9(7) Å^3, Z = 1, D_c = 3.385 g cm^{-3}, μ(Mo-Kα) = 19.415 mm^{-1}. $R1$ = 0.0958, $wR2$ = 0.1988 (for all data). R_{int} = 0.0583, $R1$ = 0.0626, $wR2$ = 0.1755, GOF = 1.026 (66934 total reflections, 24185 unique reflections where $I > 2\sigma(I)$).

CCDC-1033207 contains the supplementary crystallographic data for **NaCs-D-1** in this paper. These data can be obtained free of charge from The Cambridge Crystallographic Data Centre via www.ccdc.cam.ac.uk/data_request/cif.

3. Result and Disscussion

3.1. Synthesis and compositional characterization

Tri-titanium(IV)-substituted Dawson POM monomer (**M-1**) was obtained as

water-soluble sodium/caesium salt (**NaCs-M-1**) in 78.4% yield by hydrolysis of the bridging tetramer (**Na-Tb-1**) by aqueous NaOH. Crystalline solid was obtained, but the crystal data were poor, although they suggested the monomeric nature of **M-1**. This compound in solution was readily converted to the tetramers under acidic/neutral aqueous conditions, i.e., it was stable only under basic conditions (pH 9-12 ??). In addition, this compound can not be converted to the organic solvent-soluble form such as Bu_4N^+ salt. These features are quite unusal in the usual POM chemistry and also seriously restrict formation of the Ti_3-POM-based organometallic complexes. Further, it was found by complete elemental analysis that the monomeric Ti_3-Dawson POM (**M-1**) was always contaminated with "water-soluble titanium species" or mixtures of "TiO_2" and "Na_2O", even in the three independently prepared samples, and it has never been obtained in the form without contamination of titanium species. Complete elemental analysis also suggested that this compound contained protonation of the Ti-O-Ti sites in the **M-1**. Solid IR spectrum showed that it is the monomeric species, because of no vibrational band based on the intermolecular Ti-O-Ti bonds around 660 cm^{-1} due to the tetramer. Solution ^{31}P NMR in D_2O showed the two-line spectrum at -4.97 and -14.65 ppm, which was quite different from those of the bridging tetramer (**Na-Tb-1**) at -7.04 and -13.77 ppm [29], and the non-bridiging tetramer at -7.59 and -13.97 ppm [28], both containing the encapsulated Cl^- ion.

The POM-supported organometallic complex, i.e., 2 : 2-type dimer (**D-1**), was formed by 2 : 2-molar ratio reaction of $[\alpha\text{-}1,2,3\text{-}P_2W_{15}Ti_3O_{59}(OH)_3]^{9-}$ (**M-1**), with the separately *in situ*-derived chloride-free $[Cp^*Rh]^{2+}$ in water. The solution was stirred at 90 °C. The sodium/caesium salts formed were crystallized by slow evaporation in water. The formation of polyoxoanion **D-1** can be represented in Eq. (1).

$$2\ [\alpha\text{-}1,2,3\text{-}P\ P_2W_{15}Ti_3O_{59}(OH)_3]^{9-}\ (\mathbf{M\text{-}1}) + 2\ OH^- + 2\ Cp^*Rh^{2+} \rightarrow [\{\alpha\text{-}1,2,3\text{-}P\ P_2W_{15}Ti_3O_{60}(OH)_2\}(Cp^*Rh)_2]^{16-}\ (\mathbf{D\text{-}1}) + 2\ H_2O \quad (1)$$

Sodium/caesium salts of the dimer-form complex with 2 : 2 ratio of tri-titanium-substituted Dawson POM and Cp^*Rh^{2+}, $Na_{14}Cs_2[\{\alpha\text{-}1,2,3\text{-}P_2W_{15}Ti_3O_{60}(OH)_2\}_2(Cp^*Rh)_2]\cdot 37H_2O\cdot 2TiO_2$ (**NaCs-D-1**) as crystalline samples, were obtained in 80.1 % yield. The crystalline samples were characterized by complete elemental analysis, *i.e.*, H, C, O, Na, Cs, P, W, Ti, Rh analysis, FTIR, TG/DTA, (^{31}P, ^{1}H, ^{13}C) NMR in a D_2O, X-ray crystallography.

NaCs-D-1 for elemental analysis was dried at room temperature under a vacuum of 10^{-3}-10^{-4} Torr overnight. The data we found were in accord with the calculated values for formulas with 14 sodium and 2 cesium cations, 2 Cp*Rh groups, 2 di-protonated tri-titanium-substituted Dawson polyoxoanions, 2 hydrated water molecules and 2 TiX.

TiX was contaminant, which cannot be removed even in the three independent samples of **M-1** and identified. In the case, the calculated values were led as X = O_2 from element analysis.

The number of water molecules was determined by TG/DTA measurements under atmospheric conditions and elemental analysis. In the TG/DTA, weight losses of 5.45 % observed at below 255.6 ºC for **NaCs-D-1** corresponded to ca. 29 water molecules, which were consistent with the elemental analyses data.

The solid FTIR spectrum (Fig. 1) of **NaCs-D-1** measured in a KBr disk showed prominent bands at 1085, 1053, 1011, 939, 915, and 742 cm^{-1}. The spectra showed the characteristic band of the Dawson-type "α-$P_2W_{18}O_{62}^{6-}$" POM framework in the polyoxometalate region (1200-400 cm^{-1}) at 1090, 957, 916 and 789 cm^{-1}. The Ti-O-Ti vibration band of the inter-Dawson units was not observed at around 650 cm^{-1} as same as precursor **NaCs-M-1**. The presence of Cp*Rh^{2+} groups was confirmed by IR band at 1473 and 1376 cm^{-1}.

*3.2. Molecular structures of **D-1***

The molecular structure of polyoxoanion in **D-1**, its polyhedral representation, and the partial structure around the Rh and Ti_3 centers are shown in Fig. 2a-c, respectively. Selected bond lengths (Å) and angles (º) around the Rh and Ti_3 centers in **D-1** are given

in Table 1, while other bond lengths (Å) in **D-1** (Table S1) and the bond valence sum (BVS) calculations of the W, Ti, O and P atoms (Table S2) are deposited in the Supplementary material.

The composition and formula of **NaCs-D-1** containing 14 sodium countercations and 37 water molecules were determined by complete elemental analysis and TG/DTA analysis. In X-ray crystallography, polyoxoanion **D-1**, 8 sodium cations, 7 cesium cations and 30 hydrated water molecules per formula unit were identified in the crystal structure (see Section 2.3), but the location of a cesium cation and 7 hydrated water molecules per formula unit were not determined as a result of disorder.

X-ray crystallography of **D-1** revealed that the two organometallic fragment $[Cp^*Rh]^{2+}$ was sandwiched between two tri-titanium-substituted Dawson POM units $[\alpha\text{-}1,2,3\text{-}P_2W_{15}Ti_3O_{60}(OH)_2]^{10-}$, resulting in C_i symmetry. One Cp*Rh groups is coordinated to 2 oxygen atoms (O2, O19) for Dawson unit and the other Cp*Rh groups is coordinated to 1 oxygen (O3)[Rh-O average 2.123 Å] (Fig. 2b and c). Each Rh center was bound to the terminal oxygen atoms of the Ti sites (O2, O3) and the edge-sharing (O19) of the Ti-O-Ti linkage. A similar polyoxometalate with bridging organometallic fragment was recently reported as the Keggin type POM, *i.e.*, $[(n\text{-}C_4H_9)_4N]_6[\alpha\text{-}PW_{11}Al(OH)O_{39}ZrCp_2]_2$ with approximate C_2 symmetry [27]. In the tri-titanium-substituted Dawson unit in **D-1**, the W-O bond lengths were in the normal

range [2]; W-Ot (terminal) [1.706(14)-1.741(14) Å; average 1.724 Å], W-Oc (corner-sharing) [1.780(11)-2.046(12) Å; average 1.899 Å], W-Oe (edge-sharing) [1.889(14)-1.964(14) Å; average 1.925 Å], W-Oa (coordinating to P atom) [2.387(14)-2.327(14) Å; average 2.353 Å] (Table S1).

The values of the bond valence sum (BVS) calculations (Table S2) for **D-1**, which were calculated based on the observed bond lengths, were in the range of 5.965-6.292 (average 6.170) for 15 W atoms, 4.931-4.972 (average 4.952) for 2 P atoms, 4.140-4.241 (average 4.193) for 3 Ti atoms, 1.391-2.120 (average 1.896) for 60 O atoms, excluding O20 and O21; these values were within reasonable agreement with the formal valences of W^{6+}, P^{5+}, Ti^{4+} and O^{2-}, respectively (Table S2). The calculated BVS values of O20 and O21 at the two edge-sharing Ti-O-Ti bonds were 1.173 and 1.230, respectively, suggesting that a proton was bound to each of the two edge-sharing oxygen atoms of the substituted-titanium site.

3.3. (^{31}P, ^{1}H and ^{13}C) NMR characterization

The ^{31}P NMR spectrum of **NaCs-D-1** in D_2O (Fig. 3a) showed a two-line signal at -5.20 and -14.61 ppm, indicating that two Dawson units in polyoxoanion **D-1** were equivalent in D_2O, consisted with the result of X-ray structure analysis. The lower field signal was assigned to the P atom closest to the titanium-substituted side.

Compared with **NaCs-M-1** in D_2O (-4.97, -14.65 ppm), the lower field signal was shifted to much a higher field, whereas the up field signal was somewhat shifted to a lower field.

The ^{1}H NMR spectrum of **NaCs-D-1** in D_2O (Fig. 4a) showed a single peak at 1.92 ppm, due to methyl groups of Cp*. Therefore, the two Cp*Rh fragments in polyoxoanion **D-1** were equivalent in D_2O and the solid state molecular structure is kept in solution.

The ^{13}C NMR (Fig. 5a) showed a two-line spectrum at 11.34 and 96.00 ppm due to the Cp* group. Therefore, the two Cp*Rh fragments in polyoxoanion **D-1** were equivalent and **D-1** is relatively stable in D_2O.

4. Conclusion

In this work, we realized synthesis of a novel tri-titanium(IV)-substituted Dawson POM-based dimer with two bridging Cp*Rh groups $[\{\alpha\text{-}1,2,3\text{-}P_2W_{15}Ti_3O_{60}(OH)_2\}_2(Cp^*Rh)_2]^{16-}$ (**D-1**), using the separately prepared, tri-titanium(IV)-substituted Dawson POM support (**M-1**) that has been isolated by a hydrolysis of the bridging tetramer (**Na-Tb-1**) with aqueous NaOH. Since tri-titanium-substituted Dawson POM-supported organometallic complexes have not been reported, **D-1** is the first example of this type of complex. This complex is

water-soluble and stable in water. The molecular structure, which was the dimer-form complex with the 2 : 2 ratio of the tri-metal-substituted Dawson POM and the organometallic groups, is no example of the previous samples, and therefore **D-1** is expected to evolve new physical properties. **D-1** is also expected as homogeneous catalyst precursors which show selective oxidation catalysis of various alcohols with molecular oxygen. Such works will be reported in due course.

Acknowledgements

This work was supported by JSPS KAKENHI Grant number 22550065 and also by the Strategic Research Base Development Program for Private University of the Ministry of Education, Culture, Sports, Science and Technology of Japan.

References

[1] M. T. Pope, A. Müller, Angew. Chem., Int. Ed. Engl. 30 (1991) 34.

[2] M. T. Pope, Heteropoly and Isopoly Oxometalates, Springer-Verlag, New York, 1983.

[3] V. W. Day, W. G. Klemperer, Science 228 (1985) 533.

[4] C. L. Hill (Ed.), Chem. Rev. 98 (1998) 1.

[5] C. L. Hill, C.M. Prosser-McCartha, Coord. Chem. Rev. 143 (1995) 407.

[6] M.T. Pope, A. Müller (Eds.), Polyoxometalate Chemistry from Topology via Self-Assembly to Applications, Kluwer Academic Publishers, The Netherlands, 2001.

[7] T. Yamase, M. T. Pope (Eds.), Polyoxometalate Chemistry for Nano-Composite Design, Kluwer Academic Publishers, The Netherlands, 2002.

[8] M. T. Pope, Polyoxo anions: synthesis and structure, Comprehensive Coordination Chemistry II, 4, Elsevier Science, New York, 2004, p. 635.

[9] C. L. Hill, Polyoxometalates: reactivity, Comprehensive Coordination Chemistry II, 4, Elsevier Science, New York, 2004, p. 679.

[10] K. Nomiya, Y. Sakai, S. Matsunaga, Eur. J. Inorg. Chem. (2011) 179.

[11] V. Artero, D. Laurencin, R. Villanneau, R. Thouvenot, P. Herson, P. Gouzerh, A. Proust, Inorg. Chem. 44 (2005) 2826.

[12] A. Dolbecq, E. Dumas, C. R. Mayer, P. Mialane, Chem. Rev. 110 (2010) 6009.

[13] M. Pohl, Y. Lin, T. J. R. Weakley, K. Nomiya, M. Kaneko, H. Weiner, R.G. Finke, Inorg. Chem. 34 (1995) 767.

[14] D. J. Edlund, R. J. Saxton, D. K. Lyon, R. G. Finke, Organometallics 7 (1988) 1692.

[15] K. Nomiya, C. Nozaki, M. Kaneko, R.G. Finke, M. Pohl, J. Organomet. Chem. 505 (1995) 23.

[16] M. Pohl, D.K. Lyon, N. Mizuno, K. Nomiya, R.G. Finke, Inorg. Chem. 34 (1995) 1413.

[17] K. Nomiya, M. Pohl, N. Mizuno, D.K. Lyon, R.G. Finke, Inorg. Synth. 31 (1997) 186.

[18] M. Pohl, R.G. Finke, Organometallics 12 (1993) 1453.

[19] H. Weiner, J.D. Aiken III, R.G. Finke, Inorg. Chem. 35 (1996) 7905.

[20] T. Nagata, M. Pohl, H. Weiner, R.G. Finke, Inorg. Chem. 36 (1997) 1366.

[21] B. M. Rapko, M. Pohl, R.G. Finke, Inorg. Chem. 33 (1994) 3625.

[22] K. Nomiya, T. Hasegawa, Chem. Lett. (2000) 410.

[23] K. Nomiya, Y. Sakai, T. Hasegawa, J. Chem. Soc., Dalton Trans. (2002) 252.

[24] K. Nomiya, H. Torii, C.N. Kato, Y. Sado, Chem. Lett. 32 (2003) 664.

[25] K. Nomiya, Y. Kasahara, Y. Sado, A. Shinohara, Inorg. Chim. Acta 360 (2007) 2313.

[26] E. V. Radkov, V. G. Young Jr., R. H. Beer, J. Am. Chem. Soc. 121 (1999) 8953.

[27] C. N. Nozaki, Y. Makino, W. Unno, H. Uno, Dalton Trans. 42 (2013) 1129.

[28] Y. Sakai, K. Yoza, C. N. Kato, K. Nomiya, Dalton Trans. (2003) 3581.

[29] Y. Sakai, K. Yoza, C. N. Kato, K. Nomiya, Chem. Eur. J. 9 **(**2003) 4077.

[30] Y. Sakai, S. Yoshida, T. Hasegawa, H. Murakami, K. Nomiya, Bull. Chem. Soc. Jpn. 80 (2007) 1965.

[31] Y. Sakai, S. Ohta, Y. Shintoyo, S. Yoshida, Y. Taguchi, Y. Matsuki, S. Matsunaga, K. Nomiya, Inorg. Chem. 50 (2011) 6575.

[32] J.W. Kang, K. Moseley, P.M. Maitlis, J. Am. Chem. Soc. 91 (1969) 5970.

[33] C. White, A. Yates, P.M. Maitlis, Inorg. Synth. 29 (1992) 228.

[34] G. M. Sheldrick, Acta Crystallogr., Sect. A 46 (1990) 467.

[35] G. M. Sheldrick, SHELXL-97, Program for Crystal Structure Refinement, University of Göttingen, Germany, 1997.

[36] G. M. Sheldrick, SADABS, University of Göttingen, Germany, 1996.

Table 1. Selected bond lengths (Å) and angles (º) around the Ti^{IV} and Rh^{III} center in $[\{\alpha\text{-}1,2,3\text{-}P_2W_{15}Ti_3O_{60}(OH)_2\}_2(Cp^*Rh)_2]^{16-}$ (**D-1**).

bond lengths (# : oxygen coordinating to Rh atom)

Rh-O		C-C (extra aromatic ring)		Ti-Ot (Ot : termnal oxygen)	
Rh(1)-O(2)	2.184(12)	C(1)-C(6)	1.46(3)	Ti(1)-O(1)	1.693(12)
Rh(1)-O(3A)	2.061(13)	C(2)-C(7)	1.52(3)	# Ti(2)-O(2)	1.741(12)
Rh(1)-O(19)	2.126(12)	C(3)-C(8)	1.58(4)	# Ti(3)-O(3)	1.665(13)
		C(4)-C(9)	1.51(4)		
Rh-C		C(5)-C(10)	1.58(4)	Ti-Oe (Oe : edge-sharing oxygen)	
Rh(1)-C(1)	2.154(19)			Ti(1)-O(21)	2.019(12)
Rh(1)-C(2)	2.115(17)	Ti-Oc (Oc : corner-sharing oxygen)		Ti(2)-O(20)	2.006(12)
Rh(1)-C(3)	2.122(19)	Ti(1)-O(22)	1.996(12)	Ti(3)-O(20)	1.984(12)
Rh(1)-C(4)	2.10(2)	Ti(1)-O(27)	2.044(12)	Ti(3)-O(21)	2.006(12)
Rh(1)-C(5)	2.082(18)	Ti(2)-O(23)	1.969(12)	# Ti(1)-O(19)	1.884(12)
		Ti(2)-O(24)	2.015(12)	# Ti(2)-O(19)	1.877(12)
C-C (intra aromatic ring)		Ti(3)-O(25)	1.999(12)		
C(1)-C(2)	1.43(3)	Ti(3)-O(26)	1.981(12)	Ti-Oa	
C(2)-C(3)	1.42(3)			(Oa : oxygen coordinating to P atom)	
C(3)-C(4)	1.41(4)			Ti(1)-O(55)	2.426(12)
C(4)-C(5)	1.39(3)			Ti(2)-O(55)	2.272(12)
C(5)-C(1)	1.41(3)			TI(3)-O(55)	2.307(12)

bond angles

Ti-Oe-Ti		O-Rh-O		Ti-Ot-Rh	
Ti(3)-O(20)-Ti(2)	113.5(6)	O(19)-Rh(1)-O(2)	77.7(4)	Ti(2)-O(2)-Rh(1)	93.3(5)
Ti(3)-O(21)-Ti(1)	115.9(6)	O(3A)-Rh(1)-O(19)	83.4(5)	Ti(3)-O(3)-Rh(1A)	171.8(8)
Ti(2)-O(19)-Ti(1)	119.8(6)	O(3A)-Rh(1)-O(2)	86.9(5)		

Figure captions

Fig. 1. The FTIR spectra in the polyoxoanion region (1800-400 cm^{-1}), measured in KBr disks, of (a) $Na_{14}Cs_2[\{\alpha\text{-}1,2,3\text{-}P_2W_{15}Ti_3O_{60}(OH)_2\}_2(Cp^*Rh)_2]\cdot 37H_2O\cdot 2TiO_2$ (**NaCs-D-1**) and (b) $Na_8Cs[\alpha\text{-}1,2,3\text{-}P_2W_{15}Ti_3O_{59}(OH)_3]\cdot TiO_2\cdot 20H_2O$ (**NaCs-M-1**).

Fig. 2. (a) Molecular structure of the polyoxoanion $[\{\alpha\text{-}1,2,3\text{-}P_2W_{15}Ti_3O_{60}(OH)_2\}_2(Cp^*Rh)_2]^{16-}$ in **D-1**, (b) its polyhedral representation and (c) the partial structures around the Ti and Rh center.

Fig. 3. ^{31}P NMR spectra of (a) $Na_{14}Cs_2[\{\alpha\text{-}1,2,3\text{-}P_2W_{15}Ti_3O_{60}(OH)_2\}_2(Cp^*Rh)_2]\cdot 37H_2O\cdot 2TiO_2$ (**NaCs-D-1**), and (b) $Na_8Cs[\alpha\text{-}1,2,3\text{-}P_2W_{15}Ti_3O_{59}(OH)_3]\cdot TiO_2\cdot 20H_2O$ (**NaCs-M-1**) dissolved in D_2O.

Fig. 4. ^{1}H NMR spectra of (a) $Na_{14}Cs_2[\{\alpha\text{-}1,2,3\text{-}P_2W_{15}Ti_3O_{60}(OH)_2\}_2(Cp^*Rh)_2]\cdot 37H_2O\cdot 2TiO_2$ (**NaCs-D-1**) dissolved in D_2O and (b) $[Cp^*RhCl_2]_2$ dissolved in DMSO.

Fig. 5. ^{13}C NMR spectra of (a) $Na_{14}Cs_2[\{\alpha\text{-}1,2,3\text{-}P_2W_{15}Ti_3O_{60}(OH)_2\}_2(Cp^*Rh)_2]\cdot 37H_2O\cdot 2TiO_2$ (**NaCs-D-1**) dissolved

in D_2O and (b) $[Cp^*RhCl_2]_2$ dissolved in DMSO. The carbon signals denoted by an asterisk in (a) are from the methylene groups of the DSS.

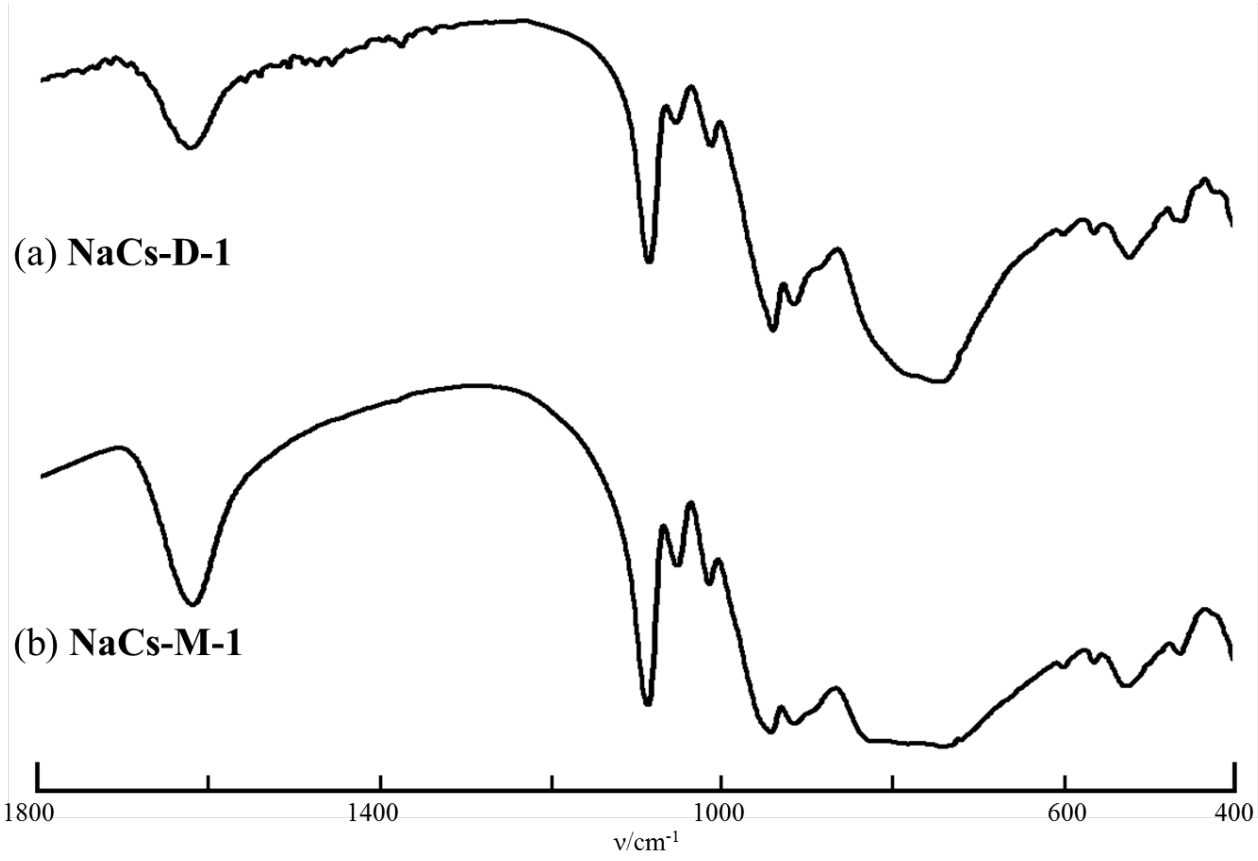

Fig. 1.

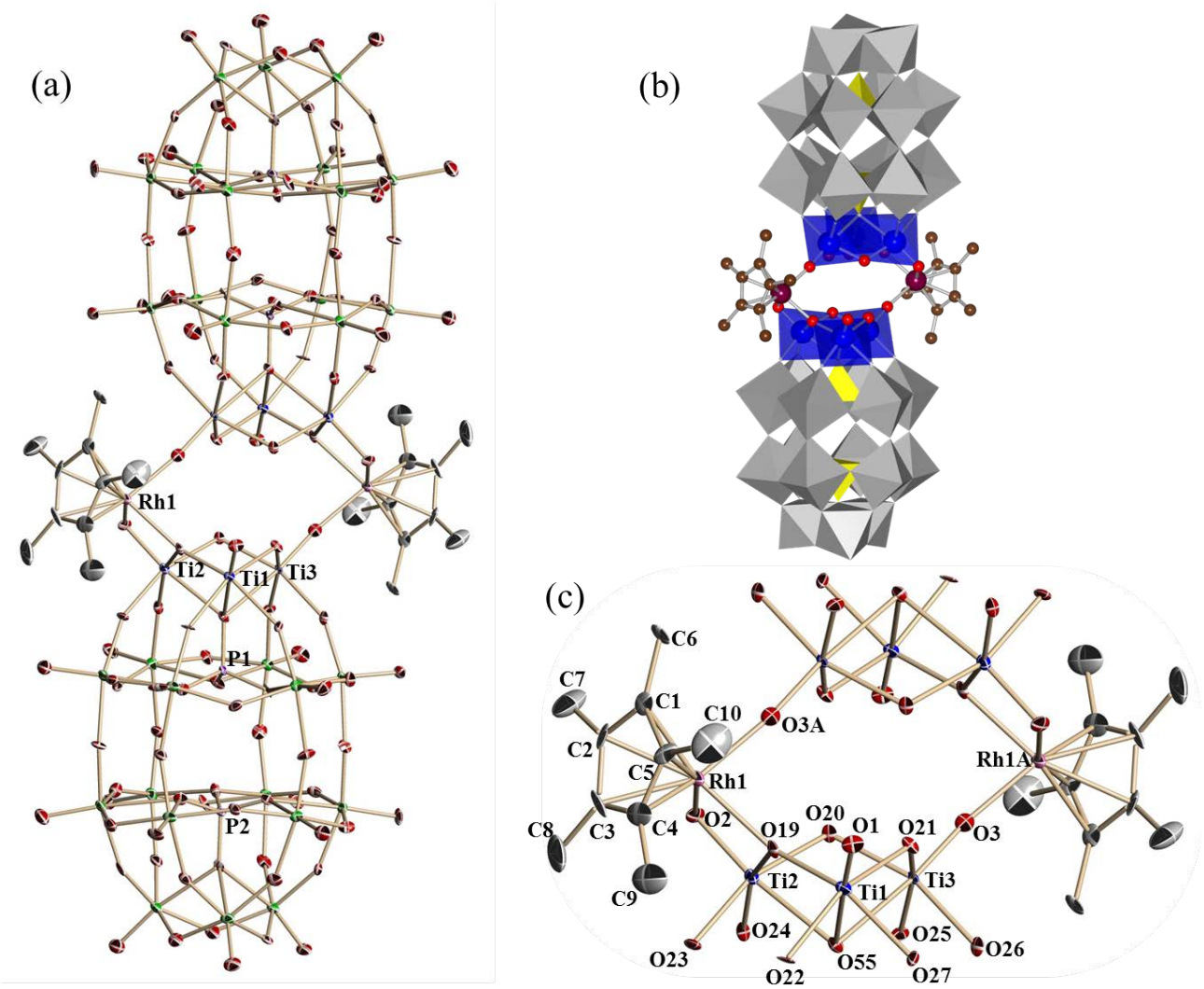
(a)
Rh1
Ti2
Ti1
Ti3
P1
P2
(b)
(c)
C6
C7
C1
C10
O3A
C2
C5
Rh1
Rh1A
C8
C3
C4
O2
O19
O20
O1
O21
O3
C9
Ti2
Ti1
Ti3
O24
O25
O26
O23
O22
O55
O27

Fig. 2.

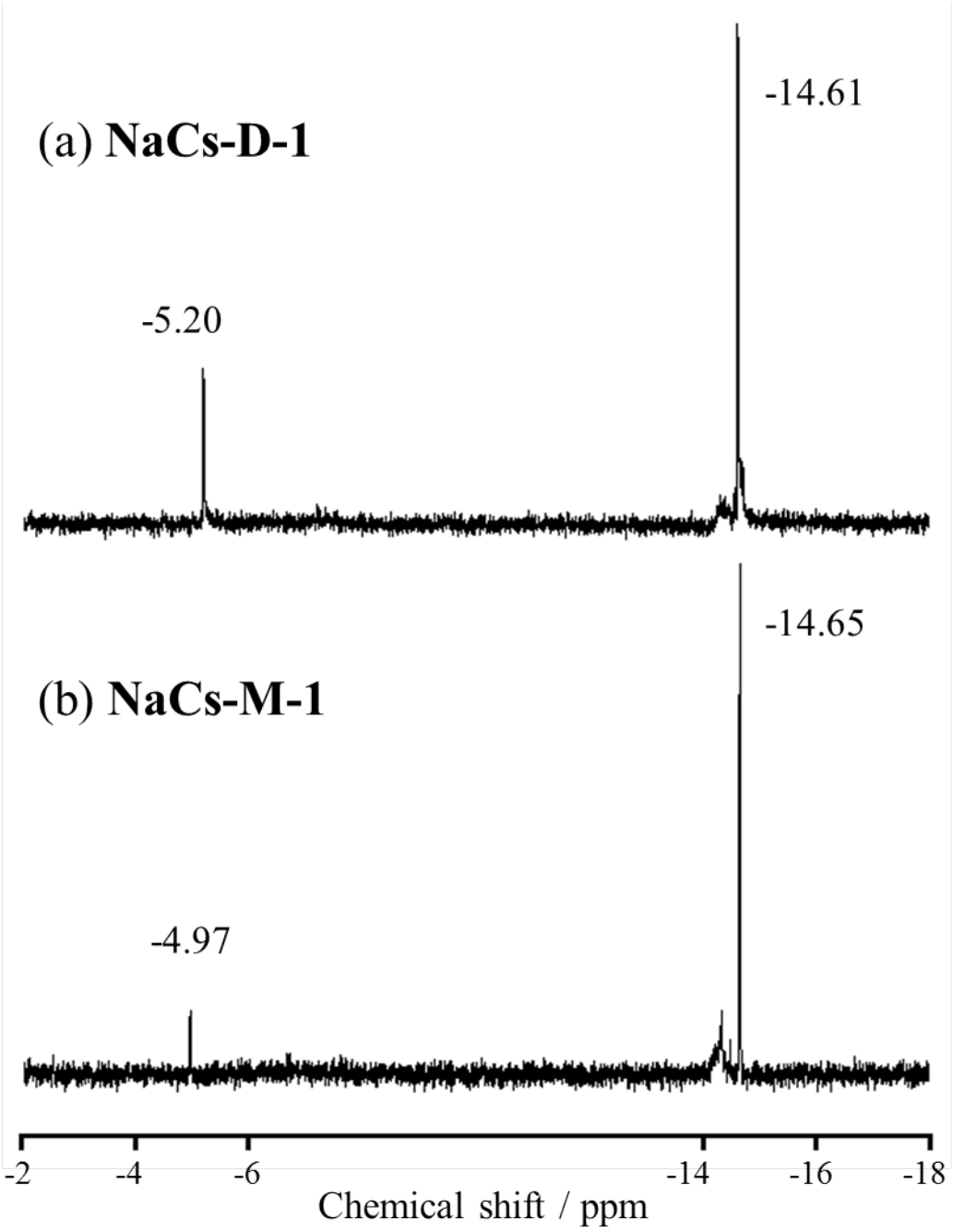
(a) NaCs-D-1
-14.61
-5.20
(b) NaCs-M-1
-14.65
-4.97
-2
-4
-6
-14
-16
-18
Chemical shift / ppm

Fig. 3.

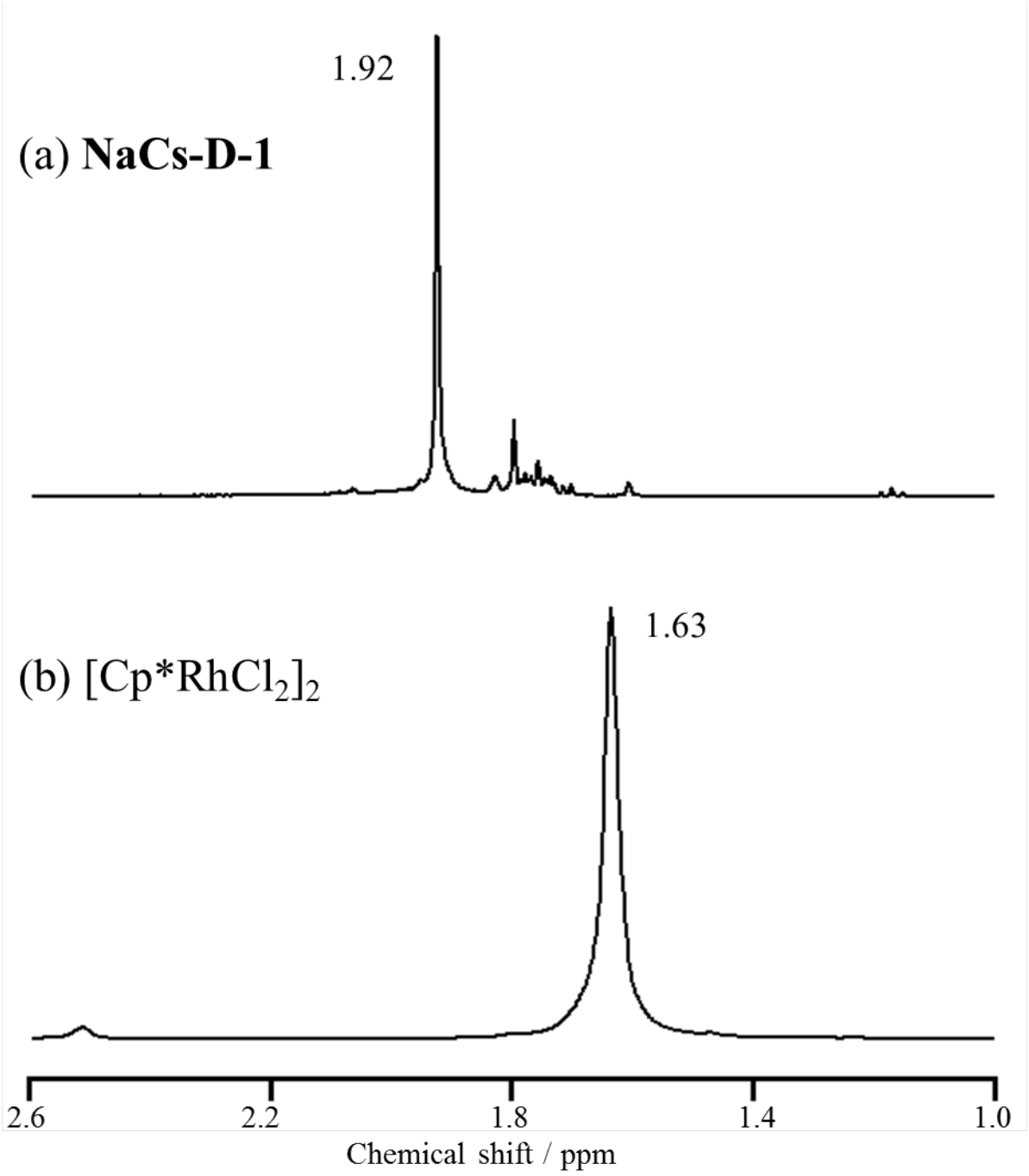

Fig. 4.

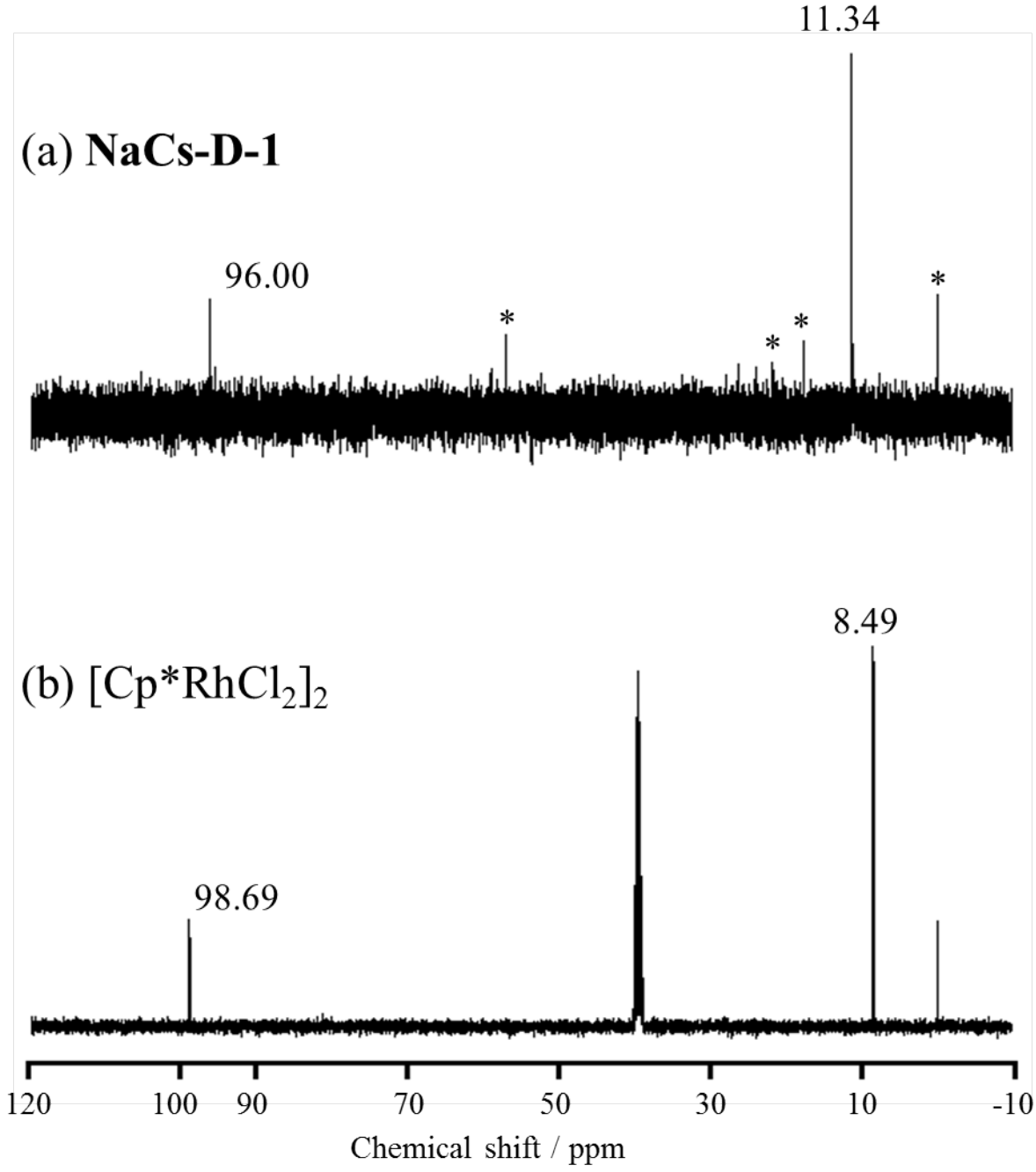
11.34
(a) NaCs-D-1
96.00
*
*
*
*
8.49
(b) [Cp*RhCl2]2
98.69
120
100
90
70
50
30
10
-10
Chemical shift / ppm

Fig. 5.

Supporting Information Ver. 1.01 (14-12-14)

Synthesis and molecular structure of dimeric tri-titanium(IV)-substituted Dawson polyoxometalate bridged by two Cp^*Rh^{2+} groups

Yusuke Matsuki, Shoko Takaku, Takahiro Hoshino, Satoshi Matsunaga and Kenji Nomiya*

Department of Chemistry, Faculty of Science, Kanagawa University, Hiratsuka, Kanagawa 259-1293, Japan

Contents:

Table S1. Selected bond lengths (Å) around the atom (P, W) center for

$[\{\alpha\text{-}1,2,3\text{-}P_2W_{15}Ti_3O_{60}(OH)_2\}_2(Cp^*Rh)_2]^{16-}$ (**D-1)**

W-Ot (Ot : termnal oxygen)		W-Oa (Oa : oxygen coordinating to P atom)	
W(1)-O(4)	1.726(13)	W(1)-O(56)	2.343(12)
W(2)-O(5)	1.718(14)	W(2)-O(56)	2.359(13)
W(3)-O(6)	1.731(14)	W(3)-O(57)	2.361(13)
W(4)-O(7)	1.730(13)	W(4)-O(57)	2.327(12)
W(5)-O(8)	1.735(12)	W(5)-O(58)	2.339(11)
W(6)-O(9)	1.726(13)	W(6)-O(58)	2.344(11)
W(7)-O(10)	1.710(13)	W(7)-O(59)	2.349(12)
W(8)-O(11)	1.733(14)	W(8)-O(59)	2.352(13)
W(9)-O(12)	1.724(13)	W(9)-O(60)	2.341(12)
W(10)-O(13)	1.726(12)	W(10)-O(60)	2.373(12)
W(11)-O(14)	1.723(12)	W(11)-O(61)	2.361(13)
W(12)-O(15)	1.707(14)	W(12)-O(61)	2.346(12)
W(13)-O(16)	1.741(14)	W(13)-O(62)	2.387(12)
W(14)-O(17)	1.706(14)	W(14)-O(62)	2.341(12)
W(15)-O(18)	1.720(12)	W(15)-O(62)	2.365(11)
W-Oe (Oe : edge-sharing oxygen)		P-O	
W(1)-O(29)	1.919(14)	P(1)-O(55)	1.561(12)
W(2)-O(29)	1.920(14)	P(1)-O(56)	1.527(12)
W(3)-O(31)	1.936(12)	P(1)-O(57)	1.533(13)
W(4)-O(31)	1.912(12)	P(1)-O(58)	1.526(12)
W(5)-O(33)	1.945(12)	P(2)-O(59)	1.527(13)
W(6)-O(33)	1.936(12)	P(2)-O(60)	1.527(13)
W(7)-O(41)	1.933(14)	P(2)-O(61)	1.528(13)
W(8)-O(41)	1.889(14)	P(2)-O(62)	1.579(12)
W(9)-O(43)	1.900(13)		
W(10)-O(43)	1.929(12)		
W(11)-O(45)	1.903(12)		
W(12)-O(45)	1.938(12)		
W(13)-O(52)	1.964(14)		
W(13)-O(54)	1.941(12)		
W(14)-O(52)	1.923(14)		
W(14)-O(53)	1.941(13)		

W(15)-O(53)	1.922(14)
W(15)-O(54)	1.904(13)

~~Table S1. Selected bond lengths (Å) around the atom (P, W) center for~~

~~$[\{\alpha\text{-}1,2,3\text{-}P_2W_{15}Ti_3O_{60}(OH)_2\}_2(Cp^*Rh)_2]^{16-}$ (D-1)~~

W-Oc (Oc : corner-sharing oxygen)

W(1)-O(22)	1.780(11)	W(8)-O(35)	1.817(12)
W(1)-O(28)	1.904(13)	W(8)-O(42)	1.888(14)
W(1)-O(34)	2.024(12)	W(8)-O(47)	1.970(13)
W(2)-O(23)	1.803(11)	W(9)-O(36)	1.815(12)
W(2)-O(30)	1.922(12)	W(9)-O(42)	1.904(13)
W(2)-O(35)	2.024(12)	W(9)-O(48)	1.985(13)
W(3)-O(24)	1.820(12)	W(10)-O(37)	1.846(13)
W(3)-O(30)	1.875(13)	W(10)-O(44)	1.892(13)
W(3)-O(36)	2.029(12)	W(10)-O(49)	1.978(13)
W(4)-O(25)	1.796(11)	W(11)-O(38)	1.837(12)
W(4)-O(32)	1.912(13)	W(11)-O(44)	1.902(13)
W(4)-O(37)	1.992(13)	W(11)-O(50)	1.957(12)
W(5)-O(26)	1.793(12)	W(12)-O(39)	1.809(13)
W(5)-O(32)	1.907(12)	W(12)-O(40)	1.894(12)
W(5)-O(38)	1.992(12)	W(12)-O(51)	2.003(13)
W(6)-O(27)	1.793(12)	W(13)-O(46)	1.886(12)
W(6)-O(28)	1.903(13)	W(13)-O(51)	1.859(13)
W(6)-O(39)	2.046(12)	W(14)-O(47)	1.878(12)
W(7)-O(34)	1.825(12)	W(14)-O(48)	1.858(13)
W(7)-O(40)	1.897(12)	W(15)-O(49)	1.883(13)
W(7)-O(46)	1.959(12)	W(15)-O(50)	1.881(12)

Table S2. Bond valence sum (BVS) calculations of W, Ti, P and O atoms

for[{α-1,2,3-$P_2W_{15}Ti_3O_{60}(OH)_2\}_2(Cp^*Rh)_2]^{16-}$ (**D-1)**

Ti(1)	4.140	O(9)	1.676	O(36)	2.056
Ti(2)	4.197	O(10)	1.750	O(37)	2.028
Ti(3)	4.241	O(11)	1.644	O(38)	2.058
W(1)	6.219	O(12)	1.685	O(39)	2.045
W(2)	6.103	O(13)	1.676	O(40)	2.120
W(3)	6.063	O(14)	1.689	O(41)	2.036
W(4)	6.218	O(15)	1.764	O(42)	2.117
W(5)	6.124	O(16)	1.609	O(43)	2.015
W(6)	6.083	O(17)	1.769	O(44)	2.111
W(7)	6.249	O(18)	1.703	O(45)	1.983
W(8)	6.290	O(19)	2.044	O(46)	1.980
W(9)	6.235	O(20)	1.230	O(47)	1.978
W(10)	6.065	O(21)	1.173	O(48)	2.005
W(11)	6.209	O(22)	2.061	O(49)	1.944
W(12)	6.218	O(23)	2.020	O(50)	2.000
W(13)	5.965	O(24)	1.882	O(51)	1.962
W(14)	6.292	O(25)	1.995	O(52)	1.865
W(15)	6.222	O(26)	2.037	O(53)	1.924
P(1)	4.972	O(27)	1.937	O(54)	1.973
P(2)	4.931	O(28)	2.074	O(55)	1.911
O(1)	1.391	O(29)	1.987	O(56)	1.894
O(2)	1.534	O(30)	2.107	O(57)	1.886
O(3)	1.936	O(31)	1.964	O(58)	1.914
O(4)	1.676	O(32)	2.041	O(59)	1.895
O(5)	1.712	O(33)	1.877	O(60)	1.885
O(6)	1.653	O(34)	2.031	O(61)	1.887
O(7)	1.658	O(35)	2.059	O(62)	2.005
O(8)	1.635				

Polyhedron 52 (2013) 389–397

Contents lists available at SciVerse ScienceDirect

Polyhedron

journal homepage: www.elsevier.com/locate/poly

2:2-Type complexes of zirconium(IV)/hafnium(IV) centers with mono-lacunary Keggin polyoxometalates: Syntheses and molecular structures of $[(\alpha\text{-}SiW_{11}O_{39}M)_2(\mu\text{-}OH)_2]^{10-}$ (M = Zr, Hf) with edge-sharing octahedral units and $[(\alpha\text{-}SiW_{11}O_{39}M)_2(\mu\text{-}OH)_3]^{11-}$ with face-sharing octahedral units

Hironori Osada, Akio Ishikawa, Yoshio Saku, Yoshitaka Sakai, Yusuke Matsuki, Satoshi Matsunaga, Kenji Nomiya *

Department of Chemistry, Faculty of Science, Kanagawa University, Hiratsuka, Kanagawa 259-1293, Japan

ARTICLE INFO

Article history:
Available online 1 September 2012

We dedicate this paper to Professor Alfred Werner on the 100th anniversary of his Nobel Prize in Chemistry.

Keywords:
Polyoxometalates (POMs)
Zr^{IV} and Hf^{IV} atoms
Sandwiched structure
Face-sharing
X-ray structure analysis

ABSTRACT

This paper describes the syntheses and crystal structures of a set of novel 2:2-type Zr^{IV}/Hf^{IV}-containing Keggin complexes with edge-sharing and face-sharing linkages prepared under different pH conditions, each consisting of di-Zr^{IV}/Hf^{IV} cluster cations sandwiched between two mono-lacunary α-Keggin polyoxometalates (POMs) with an Si heteroatom, i.e., $(Et_2NH_2)_{10}[(\alpha\text{-}SiW_{11}O_{39}M)_2(\mu\text{-}OH)_2]\cdot 4H_2O$ (M = Zr, **Zr-edge**; Hf, **Hf-edge**) and $(Et_2NH_2)_{11}[(\alpha\text{-}SiW_{11}O_{39}M)_2(\mu\text{-}OH)_3]\cdot 15H_2O$ (M = Zr, **Zr-face**; Hf, **Hf-face**). The two central Zr and Hf atoms of the **Zr-edge** and **Hf-edge** are linked by two μ-OH groups, i.e., an edge-sharing linkage, whereas those of the **Zr-face** and **Hf-face** are linked by three μ-OH groups, i.e., a face-sharing linkage. Previously reported Zr/Hf-containing POM dimers were generally linked by edge-sharing $M(OH)_2M$ (M = Zr, Hf) bonds. Therefore, the present **Zr-face** and **Hf-face** are the first examples of Zr/Hf-containing POM dimers linked in a face-sharing fashion.

1. Introduction

The coordination chemistry of polyoxometalates (POMs) with d^0 transition metals has been particularly well documented in the past few decades. Indeed, the d^0 transition metal derivatives of polyoxoanions have attracted considerable attention in the fields of catalysis, surface science, and materials science because POMs are often considered as molecular analogs of oxides in terms of structure [1–19]. In the Group IV (d^0) metal ion-containing POMs, the Zr/Hf atoms function very similarly to each other but show quite different behavior from the Ti atom [20]. The Zr and Hf atoms in the group IV metals, compared with the Ti atom (ionic radius 0.75 Å and a maximum coordination number of 6 in POMs), have larger ionic radii (approximately 0.85 Å) and show higher coordination numbers (6, 7, and 8). Therefore, if they are incorporated into the POMs, a wide variety of molecular structures are anticipated. Furthermore, Lewis acid catalysis in the coordinatively unsaturated complexes of Zr and Hf atoms is also anticipated.

Following the development of Ti^{IV}-containing POMs, there has been a dramatic advance in recent years in studies on various types of Zr^{IV}/Hf^{IV} complexes in combination with several lacunary POMs [21–54]. For example, the following have been reported as Zr^{IV}/Hf^{IV} sandwich-structured complexes with the same compositions and formulas: mono-nuclear, 8-coordinate metal complexes sandwiched between two mono-lacunary α-Keggin- and α_2-Dawson-type POMs, i.e., $[M(\alpha\text{-}PW_{11}O_{39})_2]^{10-}$ (M = Hf, Zr; the Keggin 1:2 complexes) and $[M(\alpha_2\text{-}P_2W_{17}O_{61})_2]^{16-}$ (the Dawson 1:2-type complexes), respectively [34,46]; di- and tetra-nuclear 7-coordinate metal complexes sandwiched between two γ-Keggin silicotungstates, i.e., $[\{M(H_2O)\}_2(\mu\text{-}OH)_2(\gamma\text{-}SiW_{10}O_{36})_2]^{10-}$ and $[\{M(H_2O)\}_4(\mu_4\text{-}O)(\mu\text{-}OH)_6(\gamma\text{-}SiW_{10}O_{36})_2]^{8-}$ (M = Hf, Zr), respectively [38]; tetra-nuclear two 7-coordinate and two 8-coordinate metal complexes with two β-Keggin silicotungstates, i.e., $[Zr_4(\mu_3\text{-}O)_2(OH)_2(H_2O)_4(\beta\text{-}SiW_{10}O_{37})_2]^{10-}$ [31]; hexa-nuclear three 7-coordinate and three 8-coordinate metal complexes formed with three β-Keggin silicotungstates, i.e., $[Zr_6O_2(OH)_4(H_2O)_3(\beta\text{-}SiW_{10}O_{37})_3]^{14-}$ [31]; tetra-nuclear 7-coordinate metal complexes with acetate ligands sandwiched between two di-lacunary Keggin-type POMs, i.e., $[Zr_4(OH)_6(CH_3CO_2)_2(\alpha\text{-}PW_{10}O_{37})_2]^{10-}$ [51] and $[Hf_4(OH)_6(CH_3CO_2)_2(x\text{-}PW_{10}O_{37})_2]^{12-}$ (x = α, β) [52], respectively; and hexa-nuclear 6-peroxo metal complexes formed with three γ-Keggin silicotungstates, i.e., $[M_6(O_2)_6(\mu\text{-}OH)_6(\gamma\text{-}SiW_{10}O_{36})_3]^{18-}$ (M = Hf, Zr) [40,45]. Recently, three 6-coordinate prismatic Hf^{IV} and Zr^{IV} ions, i.e., the $[M_3(\mu\text{-}OH)_3]^{9+}$ cluster cations (M = Hf, Zr) sandwiched between two tri-lacunary α-Keggin POMs, or $[M_3(\mu\text{-}OH)_3$

* Corresponding author.
E-mail address: nomiya@kanagawa-u.ac.jp (K. Nomiya).

0277-5387/$ - see front matter © 2012 Elsevier Ltd. All rights reserved.
http://dx.doi.org/10.1016/j.poly.2012.08.062

$(A\text{-}\alpha\text{-}PW_9O_{34})_2]^{9-}$ (the Keggin 3:2 complexes), were reported [47]; the analogous tri-nuclear 6-coordinate Zr^{IV} cluster compound $[Zr_3(\mu\text{-}OH)_3(A\text{-}\beta\text{-}SiW_9O_{34})_2]^{11-}$ has previously been reported [24]. The di-nuclear, 7-coordinate Hf and Zr cluster cations sandwiched between two mono-lacunary α-Keggin POMs and between two mono-lacunary α-Dawson POMs, i.e., $[\{\alpha\text{-}PW_{11}O_{39}M(H_2O)\}_2(\mu\text{-}OH)_2]^{8-}$ (M = Hf, Zr; the Keggin 2:2 complexes) [48,53] and $[\{\alpha_2\text{-}P_2W_{17}O_{61}M(H_2O)\}_2(\mu\text{-}OH)_2]^{14-}$ (the Dawson 2:2 complexes) [50,53], respectively, and the tetra-nuclear 7-coordinate metal cluster cation species $[M_4(\mu_3\text{-}O)_2(\mu\text{-}OH)_2(H_2O)_4]^{10+}$ (M = Zr [27], Hf [49]) sandwiched between two di-lacunary Dawson POMs, i.e., $[M_4(\mu_3\text{-}O)_2(\mu\text{-}OH)_2(H_2O)_4(P_2W_{16}O_{59})_2]^{14-}$ (the Dawson 4:2 complexes), have also been reported. As a molybdo-POM, the 8-coordinate Hf complex, i.e., $\{Hf[PMo_{12}O_{40}][(NH_4)PMo_{11}O_{39}]\}^{5-}$, has also recently been reported [41].

Most Ti-substituted Keggin POMs are isolated as oligomers formed by corner-sharing Ti–O–Ti bonds. Meanwhile, Zr/Hf-containing α-Keggin/α-Dawson POMs are usually isolated as di-, tri-, tetra-Zr/Hf cluster cations sandwiched between two lacunary POMs, the cluster cations of which are formed by edge-sharing $M(OH)_2M$ (M = Zr, Hf) bonds [20]. For example, the Keggin 2:2 and the Dawson 2:2 complexes, i.e., $[\{\alpha\text{-}PW_{11}O_{39}M(H_2O)\}_2(\mu\text{-}OH)_2]^{8-}$ and $[\{\alpha_2\text{-}P_2W_{17}O_{61}M(H_2O)\}_2(\mu\text{-}OH)_2]^{14-}$ (M = Zr, Hf), respectively, are composed of two mono-Zr- and Hf-substituted POM units $[\alpha\text{-}PW_{11}O_{39}M]$ and $[\alpha_2\text{-}P_2W_{17}O_{61}M]$ linked via two μ-OH groups [48,50].

In this work, we prepared a set of novel 2:2-type Zr^{IV}/Hf^{IV}-containing Keggin complexes with edge-sharing and face-sharing linkages under different pH conditions, each consisting of di-Zr^{IV}/Hf^{IV} cluster cations sandwiched between two mono-lacunary α-Keggin POMs with an Si heteroatom, i.e., $(Et_2NH_2)_{10}[(\alpha\text{-}SiW_{11}O_{39}M)_2(\mu\text{-}OH)_2]\cdot 4H_2O$ (M = Zr, **Zr-edge**; Hf, **Hf-edge**) and $(Et_2NH_2)_{11}[(\alpha\text{-}SiW_{11}O_{39}M)_2(\mu\text{-}OH)_3]\cdot 15H_2O$ (M = Zr, **Zr-face**; Hf, **Hf-face**). We successfully determined their molecular structures by X-ray crystallography. Two central Zr and Hf atoms of the **Zr-edge** and the **Hf-edge** were linked by two μ-OH groups, i.e., an edge-sharing linkage, whereas those of the **Zr-face** and the **Hf-face** were linked by three μ-OH groups, i.e., a face-sharing linkage. The Zr/Hf-containing POM dimers reported so far are usually linked by edge-sharing $M(OH)_2M$ (M = Zr, Hf) bonds [20]. Therefore, the **Zr-face** and the **Hf-face** are the first examples of Zr/Hf-containing POM dimers linked in a face-sharing fashion.

2. Experimental

2.1. Synthesis

2.1.1. Materials

The following reactants were used as received: 1 M aqueous HCl solutions (quantitative analysis grade), 0.1 and 1 M aqueous KOH solutions (quantitative analysis grade), EtOH, Et_2O, Et_2NH_2Cl, zirconium(IV) dichloride oxide octahydrate, hafnium(IV) dichloride oxide octahydrate (Wako), and D_2O (Isotec). The precursor or mono-lacunary α-Keggin POM with heteroatom Si and the 2:2-type Zr^{IV}-containing Keggin POM, $K_8[\alpha\text{-}SiW_{11}O_{39}]\cdot 15H_2O$ [55] and $(Et_2NH_2)_8[\{\alpha\text{-}PW_{11}O_{39}Zr(H_2O)\}_2(\mu\text{-}OH)_2]\cdot 9H_2O$ [48], respectively, were prepared according to the literature and identified by FTIR, thermogravimetric (TG)/differential thermal analyses (DTA), ^{29}Si NMR, and ^{31}P NMR.

2.1.2. Preparation of sample mixture of *Zr-edge* and *Zr-face*

$ZrCl_2O\cdot 8H_2O$ (0.258 g, 0.80 mmol) was dissolved in 20 mL of water, and the solution was stirred vigorously in a water bath at >90 °C for 1 min. To the hot solution was added 2.61 g (0.80 mmol) of solid $K_8[\alpha\text{-}SiW_{11}O_{39}]\cdot 15H_2O$, followed by stirring for 30 min. This solution was stirred at >90 °C (pH 7.3). To the colorless solution was added 2.0 g (18.2 mmol) of Et_2NH_2Cl, followed by stirring for 1 min. The colorless solution was slowly evaporated at r.t. After 2 days, colorless, clear needle crystals formed, which were collected on a membrane filter (JG 0.2 μm), washed with EtOH (30 mL × 3) and Et_2O (50 mL × 3), and dried *in vacuo* for 2 h. This crystalline sample was a mixture of **Zr-edge** and **Zr-face** and the obtained yield was 1.45 g.

2.1.3. Synthesis of $(Et_2NH_2)_{10}[(\alpha\text{-}SiW_{11}O_{39}Zr)_2(\mu\text{-}OH)_2]\cdot 4H_2O$ (*Zr-edge*)

The sample mixture (2.5 g) was dissolved in 10 mL of water. This solution (pH 7.1) was slowly adjusted to pH 4.5 with a 1 M aqueous HCl solution and slowly evaporated at r.t. After 1 day, colorless, clear prismatic crystals formed, which were collected on a membrane filter (JG 0.2 μm), washed with EtOH (30 mL × 3) and Et_2O (50 mL × 3), and dried *in vacuo* for 2 h. The yield was 1.83 g (47.5% based on $K_8[\alpha\text{-}SiW_{11}O_{39}]\cdot 15H_2O$).

The crystalline samples were soluble in water and DMSO but insoluble in diethyl ether and ethanol. *Anal.* Calc. for $C_{40}H_{130}N_{10}O_{84}Si_2W_{22}Zr_2$ or $(Et_2NH_2)_{10}[(\alpha\text{-}SiW_{11}O_{39}Zr)_2(\mu\text{-}OH)_2]\cdot 4H_2O$: C, 7.53; H, 2.05; N, 2.20. Found: C, 7.60; H, 1.61; N, 2.33%.

TG/DTA under atmospheric conditions: a weight loss of 1.25% due to dehydration was observed at below 166.9 °C; calc. 1.13% for a total of four water molecules. A weight loss of 11.44% was observed between 166.9 and 500.0 °C with an exothermic peak at 381.2 °C; calc. 11.62% for a total of 10 $Et_2NH_2^+$ cations. Selected IR (KBr): 1624 w, 1471 w, 1454 w, 1433 w, 1387 w, 1363 vw, 1198 vw, 1159 vw, 1061 w, 1045 w, 1001 w, 957 m, 906 vs, 877 m, 789 vs, 692 m, 663 m, 642 m, 540 m, 525 m, 507 m cm^{-1}. Solution ^{29}Si NMR (22.2 °C, D_2O): δ −85.47 ppm. Solid-state ^{29}Si CPMAS NMR (r.t.): δ −83.89 ppm.

2.1.4. Synthesis of $(Et_2NH_2)_{11}[(\alpha\text{-}SiW_{11}O_{39}Zr)_2(\mu\text{-}OH)_3]\cdot 15H_2O$ (*Zr-face*)

The sample mixture (2.5 g) was dissolved in 10 mL of water. This solution was slowly adjusted to pH 9.5 with a 1 M aqueous KOH solution and slowly evaporated at r.t. After 7 days, colorless, clear prismatic crystals formed, which were collected on a membrane filter (JG 0.2 μm), washed with EtOH (30 mL × 3) and Et_2O (50 mL × 3), and dried *in vacuo* for 2 h. The yield was 1.85 g (45.9% based on $K_8[\alpha\text{-}SiW_{11}O_{39}]\cdot 15H_2O$).

The crystalline samples were soluble in water and DMSO but insoluble in diethyl ether and ethanol. *Anal.* Calc. for $C_{44}H_{165}N_{11}O_{96}Si_2W_{22}Zr_2$ or $(Et_2NH_2)_{11}[(\alpha\text{-}SiW_{11}O_{39}Zr)_2(\mu\text{-}OH)_3]\cdot 15H_2O$: C, 7.93; H, 2.49; N, 2.31. Found: C, 7.86; H, 2.18; N, 2.37%.

TG/DTA under atmospheric conditions: a weight loss of 3.94% due to dehydration was observed at below 169.8 °C; calc. 4.05% for a total of fifteen water molecules. A weight loss of 11.57% was observed between 169.8 and 500.0 °C with an exothermic peak at 374.4 °C; calc. 12.23% for a total of eleven $Et_2NH_2^+$ cations. Selected IR (KBr): 1620 w, 1471 w, 1454 w, 1390 w, 1362 vw, 1312 vw, 1275 vw, 1196 vw, 1159 vw, 1062 w, 1047 w, 1000 m, 956 m, 903 s, 786 vs, 586 w, 541 m, 526 m, 504 m, 478 w, 461 w, 403 w cm^{-1}. Solution ^{29}Si NMR (25.9 °C, D_2O) δ −85.51 ppm. Solid-state ^{29}Si CPMAS NMR (r.t.): δ −84.09 ppm.

2.1.5. Preparation of sample mixture of *Hf-edge* and *Hf-face*

In the synthesis of the sample mixture of **Hf-edge** and **Hf-face**, $HfCl_2O\cdot 8H_2O$ was used in place of $ZrCl_2O\cdot 8H_2O$ with almost the same work-up. A sample mixture of **Hf-edge** and **Hf-face** was obtained as a yield of 1.67 g.

*2.1.6. Synthesis of $(Et_2NH_2)_{10}[(\alpha\text{-}SiW_{11}O_{39}Hf)_2(\mu\text{-}OH)_2]\cdot 4H_2O$ (**Hf-edge**)*

The sample mixture (2.5 g) was dissolved in 10 mL of water. This solution was slowly adjusted to pH 4.5 with a 1 M aqueous HCl solution and slowly evaporated at r.t. After 1 day, colorless, clear prismatic crystals formed, which were collected on a membrane filter (JG 0.2 μm), washed with EtOH (30 mL × 3) and Et_2O (50 mL × 3), and dried *in vacuo* for 2 h. Yield 1.98 g (56.1% based on $K_8[\alpha\text{-}SiW_{11}O_{39}]\cdot 15H_2O$).

The crystalline samples were soluble in water and DMSO but insoluble in diethyl ether and ethanol. *Anal.* Calc. for $C_{40}H_{130}N_{10}O_{84}Si_2W_{22}Hf_2$ or $(Et_2NH_2)_{10}[(\alpha\text{-}SiW_{11}O_{39}Hf)_2(\mu\text{-}OH)_2]\cdot 4H_2O$: C, 7.33; H, 2.00; N, 2.14. Found: C, 7.37; H, 1.54; N, 2.28%.

TG/DTA under atmospheric conditions: a weight loss of 1.11% due to dehydration was observed at below 168.6 °C; calc. 1.10% for a total of four water molecules. A weight loss of 11.04% was observed between 168.6 and 500.0 °C with an exothermic peak at 381.5 °C; calc. 11.31% for a total of 10 $Et_2NH_2^+$ cations. Selected IR (KBr): 1622 w, 1471 w, 1452 w, 1430 w, 1390 w, 1363 vw, 1198 vw, 1159 vw, 1061 w, 1045 w, 1001 w, 957 m, 906 vs, 877 m, 791 vs, 702 m, 671 w, 646 w, 542 m, 523 m, 509 m cm^{-1}. Solution ^{29}Si NMR (21.4 °C, D_2O): δ −85.69 ppm. Solid-state ^{29}Si CPMAS NMR (r.t.): δ −84.09 ppm.

*2.1.7. Synthesis of $(Et_2NH_2)_{11}[(\alpha\text{-}SiW_{11}O_{39}Hf)_2(\mu\text{-}OH)_3]\cdot 15H_2O$ (**Hf-face**)*

The sample mixture (2.5 g) was dissolved in 10 mL of water. This solution was slowly adjusted to pH 9.5 with a 1 M aqueous KOH solution and slowly evaporated at r.t. After 7 days, colorless, clear prismatic crystals formed, which were collected on a membrane filter (JG 0.2 μm), washed with EtOH (30 mL × 3) and Et_2O (50 mL × 3), and dried *in vacuo* for 2 h. Yield 1.91 g (54.2% based on $K_8[\alpha\text{-}SiW_{11}O_{39}]\cdot 15H_2O$).

The crystalline samples were soluble in water and DMSO but insoluble in diethyl ether and ethanol. *Anal.* Calc. for $C_{44}H_{165}N_{11}O_{96}Si_2W_{22}Hf_2$ or $(Et_2NH_2)_{11}[(\alpha\text{-}SiW_{11}O_{39}Hf)_2(\mu\text{-}OH)_3]\cdot 15H_2O$: C, 7.72; H, 2.43; N, 2.25. Found: C, 7.76; H, 1.83; N, 2.42%.

TG/DTA under atmospheric conditions: a weight loss of 3.93% due to dehydration was observed at below 197.3 °C; calc. 3.95% for a total of fifteen water molecules. A weight loss of 9.78% was observed between 197.3 and 500.0 °C with an exothermic peak at 361.6 °C; calc. 11.92% for a total of eleven $Et_2NH_2^+$ cations. Selected IR (KBr): 1626 m, 1471 w, 1456 w, 1390 w, 1363 vw, 1198 vw, 1159 vw, 1063 w, 1045 w, 1003 w, 957 m, 906 vs, 877 m, 791 vs, 700 m, 665 m, 644 m, 542 m, 523 m, 509 m cm^{-1}. Solution ^{29}Si NMR (21.2 °C, D_2O) δ −85.69 ppm. Solid-state ^{29}Si CPMAS NMR (r.t.): δ −84.28 ppm.

2.1.8. Control experiment: attempting to prepare the phosphotungstate Keggin 2:2-type complex linked in a face-sharing fashion

The pH of the solution (pH 4.2) containing the Keggin 2:2-type complex with heteroatom P, i.e., $(Et_2NH_2)_8[\{\alpha\text{-}PW_{11}O_{39}Zr(H_2O)\}_2(\mu\text{-}OH)_2]\cdot 9H_2O$, (0.75 g, 0.12 mmol) dissolved in 15 mL water at 70 °C, was adjusted to 4.5, 5.5, 6.5, 7.5, 8.5 and finally 9.5. ^{31}P NMR spectra were measured (Fig. 6): pH 4.2 (−13.55 ppm), pH 4.5 (−13.51, −14.52, −14.61 ppm), pH 5.5 (−13.46, −14.53, −14.61 ppm), pH 6.5 (−13.41, −14.52, −14.62 ppm), pH 7.5 (−13.40, −14.51, −14.60 ppm), pH 8.5 (2.67 ppm), pH 9.5 (2.76 ppm).

2.2. Instrumentation/analytical procedures

CHN elemental analyses were carried out with a Perkin Elmer 2400 CHNS Elemental Analyzer II. Infrared spectra were recorded on a JASCO 4100 FTIR spectrometer in KBr disks at room temperature. TG and DTA were acquired using a Rigaku Thermo Plus 2 series TG/DTA TG 8120 instrument. ^{29}Si NMR (78.0 MHz) spectra in D_2O solution were recorded in 5-mm outer diameter tubes on a JEOL JNM ECA 400 FT-NMR spectrometer with a JEOL ECA-400 NMR data-processing system and on a JEOL JNM ECP 500 FT-NMR spectrometer with a JEOL ECP-500 NMR data-processing system. The ^{29}Si NMR spectra were referenced to an internal standard of DSS. ^{31}P NMR (160.0 MHz) spectra in a D_2O solution were recorded in 5-mm outer diameter tubes on a JEOL JNM-ECA-400 FT-NMR spectrometer with a JEOL ECA-400 NMR data-processing system. The ^{31}P NMR spectra were referenced to an external standard of 25% H_3PO_4 in H_2O in a sealed capillary. The ^{31}P NMR signals with the usual 85% H_3PO_4 were shifted to +0.544 ppm from our data with 25% H_3PO_4. Solid-state ^{29}Si CPMAS NMR (59.0 MHz) spectra were recorded in 6-mm outer diameter rotors on a JEOL JNM-ECP-300 FT-NMR spectrometer with a JEOL ECP-300 NMR data-processing system and were referenced to an external standard of polydimethylsilane (δ = −34.0 ppm). Powder X-ray diffraction (PXRD) was carried out on a RIGAKU Ultima IV and characterization instrument using Cu Kα radiation.

Table 1
Crystallographic data for **Zr-edge**, **Zr-face**, **Hf-edge**, and **Hf-face**.

	Zr-edge	Zr-face	Hf-edge	Hf-face
Formula	$C_{40}H_{120}N_{10}O_{86}Si_2W_{22}Zr_2$	$C_{44}H_{132}N_{11}O_{94}Si_2W_{22}Zr_2$	$C_{40}H_{120}Hf_2N_{10}O_{86}Si_2W_{22}$	$C_{44}H_{132}Hf_2N_{11}O_{93}Si_2W_{22}$
Formula weight	6400.78	6602.93	6575.32	6761.47
Color, shape	colorless, prismatic	colorless, prismatic	colorless, prismatic	colorless, prismatic
Crystal system	triclinic	monoclinic	triclinic	monoclinic
Space group	$P\bar{1}$	$P2(1)/c$	$P\bar{1}$	$P2(1)/c$
T (K)	120	90	120	120
a (Å)	12.2571(9)	13.5533(8)	12.2527(11)	13.6619(5)
b (Å)	13.5084(10)	45.823(3)	13.4995(12)	45.6954(17)
c (Å)	20.1586(15)	21.5559(13)	20.1314(18)	21.5558(8)
α (°)	79.7940(10)	90	79.7620(10)	90
β (°)	86.3960(10)	99.7050(10)	86.3360(10)	99.6130(10)
γ (°)	65.7590(10)	90	65.7310(10)	90
V (Å^3)	2995.1(4)	13195.8(14)	2987.1(5)	13268.0(8)
Z	1	4	1	4
D_{calc} (g cm^{-3})	3.549	3.324	3.655	3.385
F_{000}	2854	11844	2918	12068
GOF	0.956	1.064	1.059	1.050
R_1 ($I > 2.00\sigma(I)$))	0.0443	0.0457	0.0592	0.0503
R (all data)	0.0636	0.0599	0.0623	0.0700
wR_2 (all data)	0.1288	0.1024	0.1747	0.1448

2.3. X-ray crystallography

Single crystals with dimensions of $0.15 \times 0.08 \times 0.04\ mm^3$ for **Zr-edge**, $0.28 \times 0.08 \times 0.04\ mm^3$ for **Zr-face**, $0.20 \times 0.19 \times 0.03\ mm^3$ for **Hf-edge**, $0.29 \times 0.10 \times 0.07\ mm^3$ for **Hf-face** were mounted on cryoloops using liquid paraffin (Paratone-N) and cooled by a stream of cooled N_2 gas. All measurements were made on a Bruker SMART APEX CCD diffractometer at 90 K with a graphite monochromated Mo Kα radiation ($\lambda = 0.71073$ Å). The intensity data were automatically collected for Lorentz and polarization effects during integration. The structures were solved by direct methods (SHELXS-97) [56] followed by a subsequent difference Fourier calculation and refined by a full-matrix, least-squares procedure on F^2 (SHELXL-97) [57]. Absorption corrections were performed with SADABS (empirical absorption correction) [58]. The compositions and formulae of the POM containing many countercations and many hydrated water molecules were determined by CHN elemental analysis and TG analysis. As with other structural investigations of crystals of highly hydrated large polyoxometalate complexes, it was not possible to locate every diethylammonium countercation and hydrated water molecule for all the complexes. This frequently encountered situation is attributed to extensive disorder of the cations and many of the hydrated water molecules. The details of the crystallographic data for **Zr-edge**, **Zr-face**, **Hf-edge**, and **Hf-face** are listed in Table 1.

3. Results and discussion

3.1. Synthesis and compositional characterization

The diethylammonium salts of the di-zirconium(IV) and di-hafnium(IV) cluster cations sandwiched between the two mono-lacunary Keggin POMs with heteroatom Si linked in an edge-sharing fashion and a face-sharing fashion, $(Et_2NH_2)_{10}[(\alpha\text{-}SiW_{11}O_{39}Zr)_2(\mu\text{-}OH)_2]\cdot 4H_2O$ (**Zr-edge**) and $(Et_2NH_2)_{11}[(\alpha\text{-}SiW_{11}O_{39}Zr)_2(\mu\text{-}OH)_3]\cdot 15H_2O$ (**Zr-face**), were obtained in 47.5% and 45.9% yields, respectively. First, the mixed sample of **Zr-edge** and **Zr-face** was obtained by a 1:1-M ratio reaction of the separately prepared $K_8[\alpha\text{-}SiW_{11}O_{39}]\cdot 15H_2O$ with $ZrCl_2O\cdot 8H_2O$ in water without pH adjustment (pH 7.3), following by stirring the solution at 90 °C. From this solution, two types of crystals having different shapes were formed. This mixed sample of **Zr-edge** and **Zr-face** was dissolved in water (pH 7.1). When the solution was adjusted to pH 4.5 with a 1 M aqueous HCl solution and evaporated slowly, the crystalline sample of **Zr-edge** was obtained. On the other hand, from the solution adjusted to pH 9.5 with a 1 M aqueous KOH solution, the crystals of **Zr-face** were formed. The Hf analogs, **Hf-edge** and **Hf-face**, were obtained by procedures and conditions similar to the **Zr-edge** and **Zr-face** syntheses. Each crystalline sample was characterized by CHN elemental analysis, FTIR, TG/DTA, solution and solid-state ^{29}Si NMR, and X-ray crystallography.

The formation of the mixtures of **M-edge** and **M-face** (M = Zr, Hf) can be represented by the sum of Eqs. (1) and (2).

$$2[\alpha\text{-}SiW_{11}O_{39}]^{8-} + 2MCl_2O + 2H^+ \rightarrow [(\alpha\text{-}SiW_{11}O_{39}M)_2(\mu\text{-}OH)_2]^{10-} + 4Cl^- \quad (1)$$

$$2[\alpha\text{-}SiW_{11}O_{39}]^{8-} + 2MCl_2O + 2H_2O \rightarrow [(\alpha\text{-}SiW_{11}O_{39}M)_2(\mu\text{-}OH)_3]^{11-} + 4Cl^- + OH^- \quad (2)$$

When the sample mixture solution was adjusted to pH 4.5, **M-face** in the solution was converted into **M-edge** by the reaction with H^+ (Eq. (3)). In this way a pure sample of M-edge can be obtained.

$$[(\alpha\text{-}SiW_{11}O_{39}M)_2(\mu\text{-}OH)_3]^{11-} + H^+ \rightarrow [(\alpha\text{-}SiW_{11}O_{39}M)_2(\mu\text{-}OH)_2]^{10-} + H_2O \quad (3)$$

On the other hand, adjusting to pH 9.5 using a 1 M KOH solution, **M-edge** in the solution was converted into **M-face** by the insertion of OH^- for the $M(\mu\text{-}OH)_2M$ bonds (Eq. (4)).

$$[(\alpha\text{-}SiW_{11}O_{39}M)_2(\mu\text{-}OH)_2]^{10-} + OH^- \rightarrow [(\alpha\text{-}SiW_{11}O_{39}M)_2(\mu\text{-}OH)_3]^{11-} \quad (4)$$

M-edge and **M-face** (M = Zr, Hf) have different charges, i.e., **M-edge** is 10− and **M-face** is 11−, due to the difference in the number of bridged $\mu\text{-}OH^-$ groups. Therefore, the number of counter cations is also different, and the CHN elemental analyses of these compounds showed a clear difference. The data we found were in good accord with the calculated values for the formulae with 10 Et_2NH_2 cations, two μ-OH groups, and four crystalline water molecules for **M-edge**, and for the formulae with eleven Et_2NH_2 cations, three μ-OH groups and fifteen crystalline water molecules for **M-face**.

In the TG/DTA measurements carried out under atmospheric conditions, the weight losses of 1.25% observed at below 166.9 °C for **Zr-edge** (Fig. S8) and 1.11% observed at below 168.6 °C for **Hf-edge** (Fig. S10) corresponded to ca. four water molecules for both, and the weight losses of 3.94% observed at below 169.8 °C for **Zr-face** (Fig. S9) and 3.93% observed at below 197.3 °C for **Hf-face** (Fig. S11) corresponded to ca. 15 water molecules for both, all of which were consistent with the elemental analyses data.

The four FTIR spectra of **Zr-edge**, **Zr-face** (Fig. 1 and Fig. S1), **Hf-edge**, and **Hf-face** (Figs. S2 and S3), measured in KBr disks, showed the characteristic bands of the Keggin POM framework (1500–750 cm^{-1}). The bands were very similar to each other and almost coincident within the experimental error.

The powder X-ray diffractions (PXRD) of **Zr-edge**, **Zr-face** (Fig. S12), **Hf-edge**, and **Hf-face** (Fig. S13) were measured. The PXRD patterns did not agree with the PXRD patterns simulated from the respective single-crystal X-ray data, because several hydrated water molecules were lost during the measurement of PXRD and the crystal structures were changed. In the meantime, clear difference in the PXRD patterns of **M-edge** and **M-face**

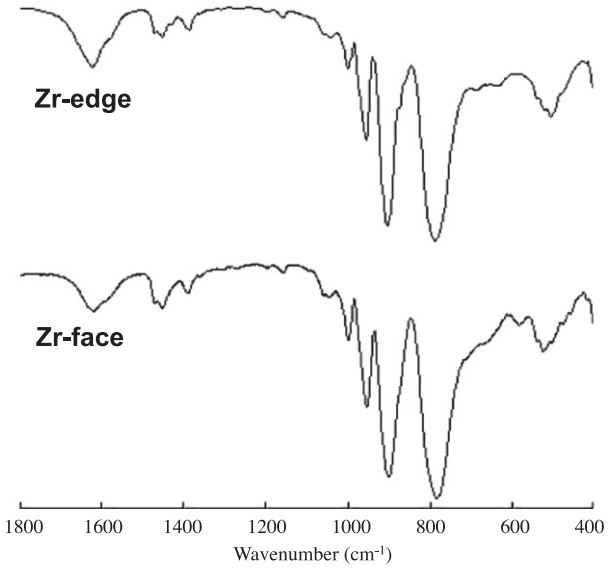

Fig. 1. The FTIR spectra in the polyoxoanion region (1200–400 cm^{-1}), measured in KBr disks, of $(Et_2NH_2)_{10}[(\alpha\text{-}SiW_{11}O_{39}Zr)_2(\mu\text{-}OH)_2]\cdot 4H_2O$ (**Zr-edge**) and $(Et_2NH_2)_{11}[(\alpha\text{-}SiW_{11}O_{39}Zr)_2(\mu\text{-}OH)_3]\cdot 15H_2O$ (**Zr-face**).

appeared. Thus, **M-edge** and **M-face** can be distinguished and purity of the bulk materials was confirmed.

3.2. Structural analyses

3.2.1. Molecular structures of M-edge (M = Zr and Hf)

The molecular structure of polyoxoanion **Zr-edge**, its polyhedral representation, and the partial structure around the Zr_2 centers are shown in Fig. 2a, b, and c, respectively. Selected bond lengths (Å) and angles (°) around the Zr_2 centers in **Zr-edge** are given in Table 2.

The composition and formula of **Zr-edge**, which contains 10 diethylammonium countercations and four hydrated water molecules, were determined by CHN elemental analysis and TG/DTA analysis. In X-ray crystallography, one polyoxoanion, five diethylammonium cations, and three hydrated water molecules per formula unit were identified in the crystal structure.

X-ray crystallography of **Zr-edge** revealed that two polyhedral Zr units were linked in an edge-sharing fashion, i.e., two mono-Zr-substituted α-Keggin POM units [α-$SiW_{11}O_{39}Zr$] were linked via two μ-OH groups (O1M) [Zr–O average 2.130 Å] (Fig. 2a, b, and c). Bond valence sum (BVS) calculations [59–62] have strongly suggested that the oxygen atoms (O1M) are protonated, i.e., they are ascribed to the OH^- groups (the BVS value of O1M is 1.160). Each Zr atom is bonded to four oxygen atoms (O(16), O(22), O(23), O(28)) of the lacunary site in each $SiW_{11}O_{39}$ unit (Fig. 2c) [Zr–O average 2.086 Å]. Thus, two Zr atoms can be considered as 6-coodinate and the whole symmetry of the molecule is shown with approximate C_i symmetry. The Zr–Zr distance is 3.577 Å.

The 2:2-type Zr^{IV}-containing Keggin POMs related to the present **Zr-edge**, a di-zirconium(IV) cation species sandwiched between two mono-lacunary Keggin POMs with heteroatom P, i.e., $(Et_2NH_2)_8[\{\alpha\text{-}PW_{11}O_{39}Zr(H_2O)\}_2(\mu\text{-}OH)_2]\cdot 7H_2O$ (**Et_2NH_2-2**) and (n-$Bu_4N)_8[(\alpha\text{-}PW_{11}O_{39}Zr)_2(\mu\text{-}OH)_2]$ (**OK-2**), have been reported by our group [48] and Kholdeeva's group [32], respectively. Both of these 2:2-type POMs were also linked in an edge-sharing fashion; however, the coordination environment around the Zr center in the previous **Et_2NH_2-2** was different from that of the present **Zr-edge** and Kholdeeva's **OK-2**. In the case of **Zr-edge** and **OK-2**, the 6-coordinate geometry around the Zr center was accomplished by bonding with two bridging μ-OH and four terminal oxygen atoms in the mono-lacunary site of the Keggin POM and without any coordinating water molecules. The **Et_2NH_2-2** which was previously reported by us contained one water molecule coordinating to each Zr atom, resulting in the 7-coordination environment around the Zr center. On the other hand, the orientation of the two lacunary Keggin units of **Zr-edge** was similar to that of **Et_2NH_2-2**; however, it was different from that of **OK-2**. The two lacunary Keggin units of **Zr-edge** and **Et_2NH_2-2** oriented in the opposite direction; therefore, the whole symmetry of these molecules is shown with approximate C_i symmetry. **OK-2** had two lacunary Keggin units oriented in the same direction, resulting in the approximate C_{2h} symmetry. [*Note:* It has been erroneously described in the text to be C_s symmetry. We have checked it using the CIF file downloaded from the ESI of Ref. [32]].

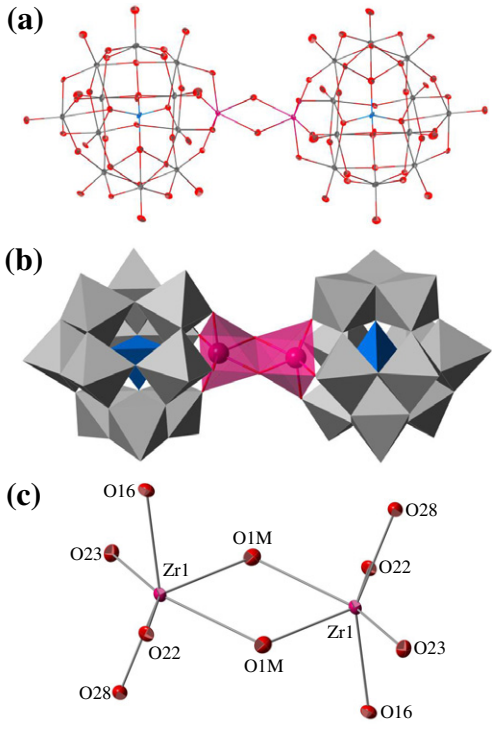

Fig. 2. (a) Molecular structure of the polyoxoanion $[(\alpha\text{-}SiW_{11}O_{39}Zr)_2(\mu\text{-}OH)_2]^{10-}$ in **Zr-edge**, (b) its polyhedral representation, and (c) the partial structure around the Zr_2 center.

Table 2
Selected bond lengths (Å) and angles (°) around the Zr^{IV} center in **Zr-edge**.

Lengths			
Zr(1)–O(1M)	2.137(10)	Zr(1)–O(16)	2.073(10)
Zr(1)–O(1M)$^{\#}$	2.123(11)	Zr(1)–O(22)	2.084(9)
Average	2.130	Zr(1)–O(23)	2.113(9)
		Zr(1)–O(28)	2.073(10)
		average	2.086
Angles			
Zr(1)–O(1M)–Zr(1)$^{\#}$	114.2(4)	O(1M)–Zr(1)–Zr(1)$^{\#}$	32.8(3)
		O(1M)$^{\#}$–Zr(1)–Zr(1)$^{\#}$	33.0(3)
O(1M)–Zr(1)–O(1M)$^{\#}$	65.8(4)	average	32.9

$^{\#}$ Symmetry operators: $-x+2, -y+1, -z$.

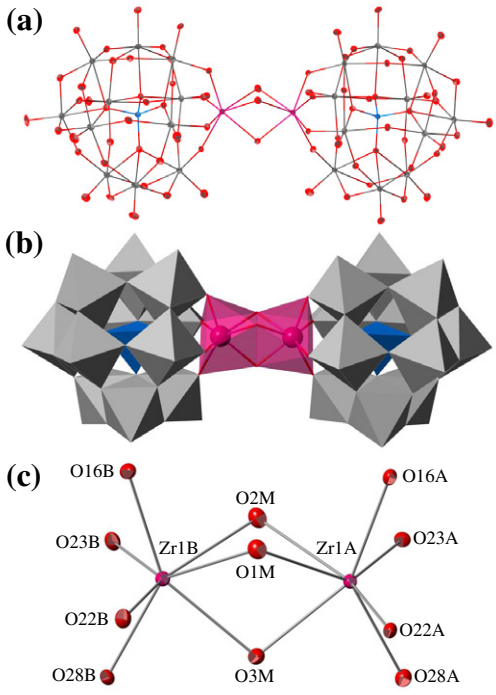

Fig. 3. (a) Molecular structure of the polyoxoanion $[(\alpha\text{-}SiW_{11}O_{39}Zr)_2(\mu\text{-}OH)_3]^{11-}$ in **Zr-face**, (b) its polyhedral representation, and (c) the partial structure around the Zr_2 center.

X-ray crystallography revealed that the molecular structure of **Hf-edge** was isostructural with that of **Zr-edge** (see Fig. S4 and Table S1).

3.2.2. Molecular structures of M-face (M = Zr and Hf)

The molecular structure of polyoxoanion **Zr-face**, its polyhedral representation, and the partial structure around the Zr_2 centers are shown in Fig. 3a, b, and c, respectively. Selected bond lengths (Å) and angles (°) around the Zr_2 centers in **Zr-face** are given in Table 3.

The composition and formula of **Zr-face**, which contains 11 diethylammonium countercations and fifteen hydrated water molecules, were determined by CHN elemental analysis and TG/DTA analysis. In X-ray crystallography, one polyoxoanion, eleven diethylammonium cations and thirteen hydrated water molecules per formula unit were identified in the crystal structure.

X-ray crystallography of **Zr-face** revealed that two polyhedral Zr units were linked in a face-sharing fashion, i.e., two mono-Zr-substituted α-Keggin POM units [α-$SiW_{11}O_{39}Zr$] were linked via three μ-OH groups (O1M, O2M, O3M) [Zr-O average 2.188 Å] (Fig. 3a, b, and c). To the best of our knowledge, it is the first example of a sandwiched compound of POMs containing group IV metals with a face-sharing linkage. BVS calculations have strongly suggested that the oxygen atoms (O1M, O2M, O3M) are protonated, i.e., they are ascribed to the OH^- groups (the BVS value of O1M is 0.876, O2M 0.947, and O3M 1.175). Each Zr atom (Zr1A, Zr1B) is bonded to four oxygen atoms (O16A, O22A, O23A, O28A; O16B, O22B, O23B, O28B) of the lacunary site in each $SiW_{11}O_{39}$ unit (Fig. 3c) [Zr–O average 2.126 Å]. Thus, two Zr atoms can be considered as 7-coordinate.

Two $SiW_{11}O_{39}Zr$ units were slightly twisted away from each other (torsion angle between O16A–Zr1A–Zr1B plane and Zr1A–Zr1B–O16B plane, 3.579°; O22A–Zr1A–Zr1B plane and Zr1A–Zr1B–O22B plane, 4.323°; O23A–Zr1A–Zr1B plane and Zr1A–Zr1B–O23B, 3.445°; O28A–Zr1A–Zr1B plane and Zr1A–Zr1B–O28B plane, 3.621°; average 3.742°), and the two enantiomers of the $[(\alpha\text{-}SiW_{11}O_{39}Zr)_2(\mu\text{-}OH)_3]^{11-}$ anion were defined by the relative twist direction. Therefore, the whole symmetry of **Zr-face** is shown with approximate C_1 symmetry. The $[(\alpha\text{-}SiW_{11}O_{39}Zr)_2(\mu\text{-}OH)_3]^{11-}$ anions of **Zr-face** were detected as two sets of enantiomeric pairs of two different units in the unit cell. The Zr–Zr distance of **Zr-face** was much shorter than that of **Zr-edge** due to the effect of the face-sharing connection (**Zr-face**, 3.282 Å; **Zr-edge**, 3.577 Å). Unlike the edge-sharing analogs **Zr-** and **Hf-edge**, the two mono-lacunary Keggin units oriented in the same direction. This orientation mode was similar to that of Kholdeeva's **OK-2**.

X-ray crystallography revealed that the molecular structure of **Hf-face** was isostructural with that of **Zr-face** (see Fig. S5 and Table S2).

Table 3
Selected bond lengths (Å) and angles (°) around the Zr^{IV} center in **Zr-face**.

Lengths			
Zr(1A)–O(1M)	2.252(7)	Zr(1A)–O(16A)	2.134(7)
Zr(1A)–O(2M)	2.186(7)	Zr(1A)–O(22A)	2.120(7)
Zr(1A)–O(3M)	2.109(7)	Zr(1A)–O(23A)	2.136(7)
Zr(1B)–O(1M)	2.216(7)	Zr(1A)–O(28A)	2.133(7)
Zr(1B)–O(2M)	2.224(7)	Zr(1B)–O(16B)	2.124(7)
Zr(1B)–O(3M)	2.141(7)	Zr(1B)–O(22B)	2.130(7)
Average	2.188	Zr(1B)–O(23B)	2.114(7)
		Zr(1B)–O(28B)	2.120(7)
		average	2.126
Angles			
Zr(1A)–O(1M)–Zr(1B)	94.5(2)	O(1M)–Zr(1A)–O(2M)	67.4(3)
Zr(1A)–O(2M)–Zr(1B)	96.2(3)	O(1M)–Zr(1A)–O(3M)	68.2(3)
Zr(1A)–O(3M)–Zr(1B)	101.1(3)	O(2M)–Zr(1A)–O(3M)	73.7(3)
Average	97.3	O(1M)–Zr(1B)–O(2M)	67.4(3)
		O(1M)–Zr(1B)–O(3M)	68.3(3)
		O(2M)–Zr(1B)–O(3M)	72.4(3)
		average	69.6

3.3. Solution ^{29}Si NMR and solid-state ^{29}Si CPMAS NMR

The solution ^{29}Si NMR spectra of **Zr-edge** and **Zr-face** in D_2O showed only one resonance for each at −85.47 and −85.51 ppm, respectively (Fig. 4). The solid-state ^{29}Si CPMAS NMR spectra of the crystalline sample of **Zr-edge** and **Zr-face** showed a single broad signal for each at −83.89 and −84.09 ppm, respectively (Fig. 5). Although in both solution and solid-state ^{29}Si CPMAS NMR spectra, only one signal was observed which should correspond to one solid-state structure as determined by X-ray crystallography, these chemical shifts hardly reflect a difference in solid-state structure due to the very small difference in their

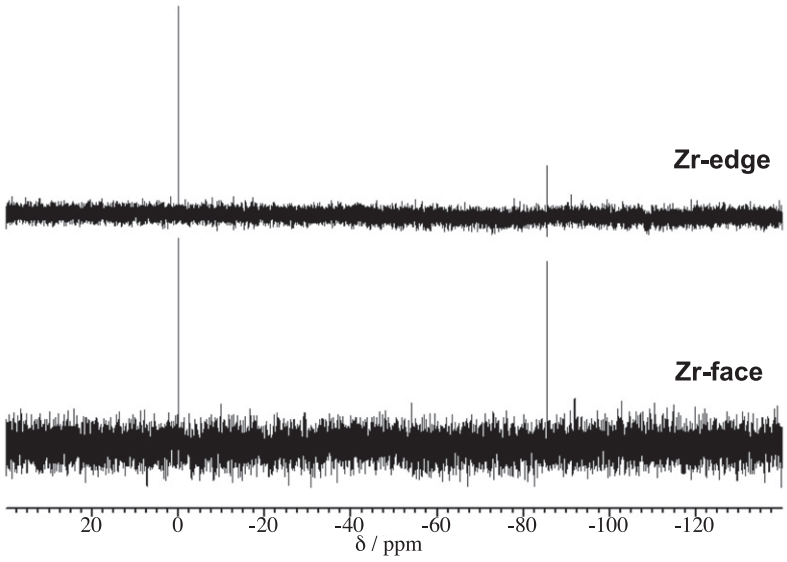

Fig. 4. Solution ^{29}Si NMR spectra of **Zr-edge** and **Zr-face** dissolved in D_2O.

molecular structures. As a matter of fact, the solid-state ^{29}Si CPMAS NMR spectrum of a 3:4 M-ratio mixed sample of **Zr-edge** and **Zr-face**, which were separately prepared and then mixed, also showed only one signal at −83.85. Therefore, **Zr-edge** and **Zr-face** were difficult to identify by solution and solid-state ^{29}Si NMR spectra.

Solution ^{29}Si NMR spectra of both **Hf-edge** and **Hf-face** in D_2O showed only one resonance at −85.69 ppm (Fig. S6). The solid-state ^{29}Si CPMAS NMR spectra of the crystalline sample of **Hf-edge** and **Hf-face** showed a single broad signal for each at −84.09 and −84.28 ppm, respectively (Fig. S7). The tendency for the ^{29}Si NMR resonances of the Hf compounds to appear in a higher field

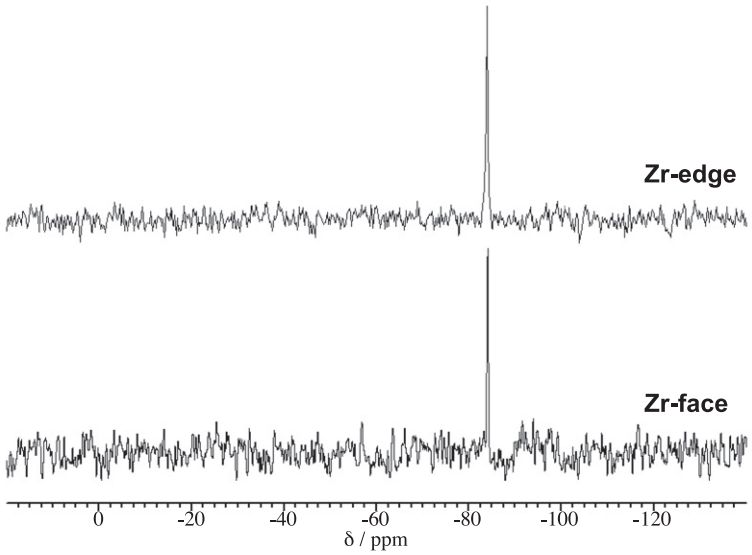

Fig. 5. Solid-state ^{29}Si CPMAS NMR spectra of **Zr-edge** and **Zr-face**.

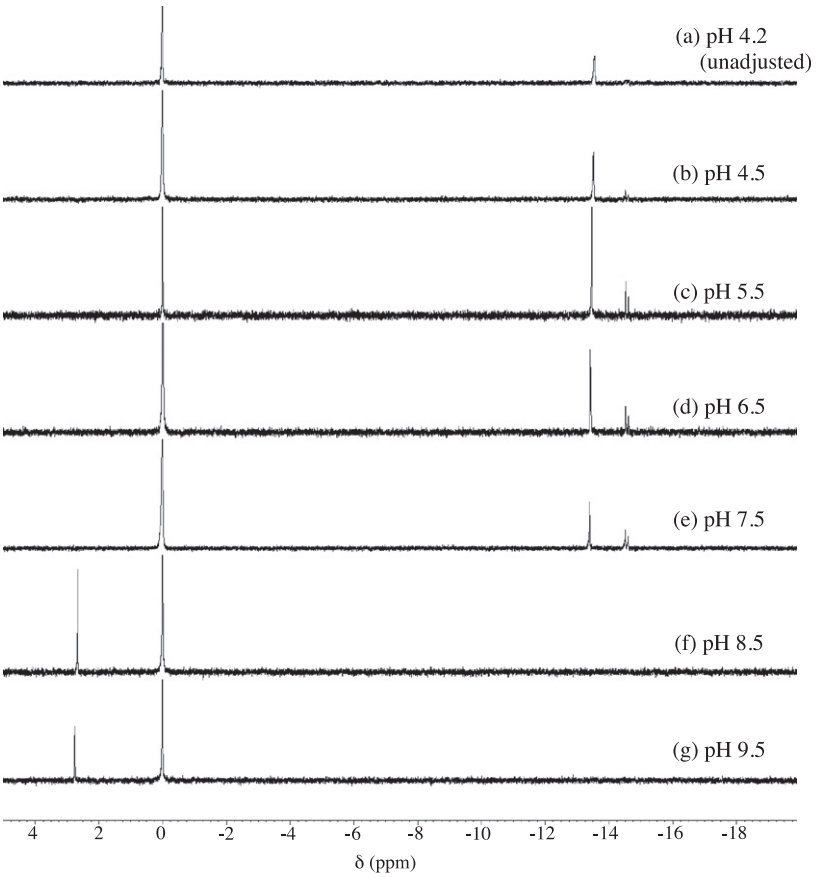

Fig. 6. ^{31}P NMR of the solutions of the Keggin 2:2-type complex with heteroatom P, $[\{\alpha\text{-}PW_{11}O_{39}Zr(H_2O)\}_2(\mu\text{-}OH)_2]^{8-}$ (**Et_2NH_2-2**), in which pH was changed: pH (a) 4.2 (unadjusted); (b) 4.5; (c) 5.5; (d) 6.5; (e) 7.5; (f) 8.5; (g) 9.5.

than those of the Zr compounds is consistent with the recently reported ^{31}P NMR resonances of Zr- and Hf-containing POMs: $[M_3(\mu\text{-}OH)_3(A\text{-}\alpha\text{-}PW_9O_{34})_2]^{9-}$ in D_2O (M = Hf, Zr) at −11.45 and −10.85 ppm, respectively [47]; $[M(\alpha\text{-}PW_{11}O_{39})_2]^{10-}$ in D_2O at −14.67 and −14.77 ppm for M = Hf and at −14.57 and −14.65 ppm for M = Zr [48]; $[M(\alpha_2\text{-}P_2W_{17}O_{61})_2]^{16-}$ in D_2O at −9.25 and −13.82 ppm for M = Hf and at −9.20 and −13.81 ppm for M = Zr [48].

3.4. Attempting to prepare the phosphotungstate Keggin 2:2-type complex linked in a face-sharing fashion, $[(\alpha\text{-}PW_{11}O_{39}Zr)_2(\mu\text{-}OH)_3]^{9-}$

The Zr/Hf cluster cations sandwiched between α-Keggin phosphotungstate POMs are usually linked with edge-sharing $M(OH)_2M$ (M = Zr, Hf) bonds. We tried to prepare the 2:2-type Zr complexes sandwiched between α-Keggin phosphotungstate in a face-sharing fashion by alkalification. Thus, we have examined the pH-dependent ^{31}P NMR of the 2:2-type Zr complex sandwiched between two α-Keggin phosphotungstates in an edge-sharing fashion. The pH of the aqueous solution (pH 4.2) of the Keggin 2:2-type complex with heteroatom P, i.e., $[\{\alpha\text{-}PW_{11}O_{39}Zr(H_2O)\}_2(\mu\text{-}OH)_2]^{8-}$ (**Et_2NH_2-2**) [48], was adjusted to 4.5, 5.5, 6.5, 7.5, 8.5 and finally 9.5, and ^{31}P NMR spectra were measured (Fig. 6). ^{31}P NMR spectra in the unadjusted sample (pH 4.2) showed a singlet signal at −13.55 ppm, which can be assigned to the Keggin 2:2-type complex in an edge-sharing fashion. In the pH range of 4.5–7.5, other signals were observed in addition to the signal of the 2:2-type complex. These signals can be tentatively assigned to the 1:2-type complex, $[M(\alpha\text{-}PW_{11}O_{39})_2]^{10-}$ and the proton-dissociation species of the coordination water molecules. We previously reported that the 2:2-type complexes $[\{\alpha\text{-}PW_{11}O_{39}M(H_2O)\}_2(\mu\text{-}OH)_2]^{8-}$ undergo a conversion to the 1:2-type complexes $[M(\alpha\text{-}PW_{11}O_{39})_2]^{10-}$ in solution under less acidic conditions [48]. However, in more basic conditions, no peaks due to POM were observed, and the peak of the decomposition product appeared in a lower field region (ca. 2.7 ppm). This fact suggests that the 2:2-type Keggin POM in a face-sharing fashion can be formed only if the heteroatom is Si because the POM with heteroatom Si is resistant to base.

4. Conclusion

We have prepared a set of novel 2:2-type Zr^{IV}/Hf^{IV}-containing Keggin complexes with edge-sharing and face-sharing linkages under different pH conditions, each consisting of di-Zr^{IV}/Hf^{IV} cluster cations sandwiched between two mono-lacunary α-Keggin POMs with heteroatom Si, i.e., $(Et_2NH_2)_{10}[(\alpha\text{-}SiW_{11}O_{39}M)_2(\mu\text{-}OH)_2]\cdot 4H_2O$ (M = Zr, **Zr-edge**; Hf, **Hf-edge**) and $(Et_2NH_2)_{11}[(\alpha\text{-}SiW_{11}O_{39}M)_2(\mu\text{-}OH)_3]\cdot 15H_2O$ (M = Zr, **Zr-face**; Hf, **Hf-face**). We successfully determined their molecular structures by X-ray crystallography. When the solution was adjusted to pH 4.5 with a 1 M aqueous HCl solution, **Zr-edge** or **Hf-edge** was crystallized. On the other hand, from a solution adjusted to pH 9.5 with a 1 M aqueous KOH solution, the crystals of **Zr-face** or **Hf-face** were formed. Two central Zr and Hf atoms of **Zr-edge** and **Hf-edge** were linked by two μ-OH groups, i.e., an edge-sharing linkage, whereas those of **Zr-face** and **Hf-face** were linked by three μ-OH groups, i.e., a face-sharing linkage. **Zr-face** and **Hf-face** are the first examples of Zr/Hf-containing POM dimers linked in a face-sharing fashion. In the case of heteroatom P, the 2:2-type Zr^{IV}-containing Keggin POM decomposed in basic conditions. Therefore, the 2:2-type Keggin POM in a face-sharing fashion can be prepared only if the heteroatom is Si due to its basic resistance. From the viewpoint of catalysis, Zr^{IV}/Hf^{IV}-containing POMs have attracted much attention [20]. Oxidation catalysis for H_2O_2-based epoxidation of olefins by the present 2:2-type Keggin POM in a face-sharing fashion is in progress.

Acknowledgments

This work was supported by a Grant-in-Aid for Scientific Research (C) No. 22550065 from the Ministry of Education, Culture, Sports, Science and Technology, Japan.

Appendix A. Supplementary data

CCDC 875058, 875059, 875060, and 875061 contain the supplementary crystallographic data for **Zr-edge**, **Zr-face**, **Hf-edge**, and **Hf-face**, respectively. These data can be obtained free of charge via http://www.ccdc.cam.ac.uk/conts/retrieving.html, or from the Cambridge Crystallographic Data Centre, 12 Union Road, Cambridge CB2 1EZ, UK; fax: (+44) 1223-336-033; or e-mail: deposit@ccdc.cam.ac.uk. Supplementary data associated with this article can be found, in the online version, at http://dx.doi.org/10.1016/j.poly.2012.08.062.

References

[1] M.T. Pope, Heteropoly and Isopoly Oxometalates, Springer-Verlag, New York, 1983.
[2] V.W. Day, W.G. Klemperer, Science 228 (1985) 533.
[3] M.T. Pope, A. Müller, Angew. Chem., Int. Ed. 30 (1991) 34.
[4] C.L. Hill, C.M. Prosser-McCartha, Coord. Chem. Rev. 143 (1995) 407.
[5] T. Okuhara, N. Mizuno, M. Misono, Adv. Catal. 41 (1996) 113.
[6] C.L. Hill, J. Mol. Catal. A: Chem. 114 (1996) 1. A series of 34 papers in a volume devoted to polyoxoanions in catalysis.
[7] C.L. Hill, Chem. Rev. 98 (1998) 1.
[8] R. Neumann, Prog. Inorg. Chem. 47 (1998) 317.
[9] M.T. Pope, A. Müller (Eds.), Polyoxometalate Chemistry from Topology via Self-Assembly to Applications, Kluwer Academic Publishers, Netherlands, 2001.
[10] T. Yamase, M.T. Pope (Eds.), Polyoxometalate Chemistry for Nano-Composite Design, Kluwer Academic Publishers, Netherlands, 2002.
[11] M.T. Pope, Polyoxoanions: synthesis and structure, Comprehensive Coordination Chemistry II, vol. 4, Elsevier Science, New York, 2004, p. 635.
[12] C.L. Hill, Polyoxometalates: reactivity, Comprehensive Coordination Chemistry II, vol. 4, Elsevier Science, New York, 2004, p. 679.
[13] C.L. Hill, J. Mol. Catal. A: Chem. 262 (2007) 1. A series of 32 recent papers in a volume devoted to polyoxometalates in catalysis.
[14] A. Proust, R. Thouvenot, P. Gouzerh, Chem. Commun. (2008) 1837.
[15] B. Hasenknopf, K. Micoine, E. Lacôte, S. Thorimbert, M. Malacria, R. Thouvenot, Eur. J. Inorg. Chem. (2008) 5001.
[16] D. Laurencin, R. Thouvenot, K. Boubekeur, F. Villain, R. Villanneau, M.-M. Rohmer, M. Benard, A. Proust, Organometallics 28 (2009) 3140.
[17] D.-L. Long, R. Tsunashima, L. Cronin, Angew. Chem., Int. Ed. 49 (2010) 1736.
[18] A. Dolbecq, E. Dumas, C.R. Mayer, P. Mialane, Chem. Rev. 110 (2010) 6009.
[19] C.P. Pradeep, D.-L. Long, L. Cronin, Dalton Trans. 39 (2010) 9443.
[20] K. Nomiya, Y. Sakai, S. Matsunaga, Eur. J. Inorg. Chem. (2011) 179.
[21] R. Villanneau, H. Carabineiro, X. Carrier, R. Thouvenot, P. Herson, F. Lemos, E.R. Ribeiro, M.J. Che, Phys. Chem. B 108 (2004) 12465.
[22] H. Carabineiro, R. Villanneau, X. Carrier, P. Herson, F. Lemos, E.R. Ribeiro, A. Proust, M. Che, Inorg. Chem. 45 (2006) 1915.
[23] R.J. Errington, S.S. Petkar, P.S. Middleton, W. McFarlane, W. Clegg, R.A. Coxall, W. Harrington, J. Am. Chem. Soc. 129 (2007) 12181.
[24] R.G. Finke, B. Rapko, T.J.R. Weakley, Inorg. Chem. 28 (1989) 1573.
[25] E.V. Radkov, V.G. Young Jr., R.H. Beer, J. Am. Chem. Soc. 121 (1999) 8953.
[26] A.J. Gaunt, I. May, D. Collison, M. Helliwell, Acta Crystallogr., Sect. C 59 (2003) i65.
[27] A.J. Gaunt, I. May, D. Collison, K.T. Holman, M.T. Pope, J. Mol. Struct. 656 (2003) 101.
[28] A.J. Gaunt, I. May, D. Collison, O.D. Fox, Inorg. Chem. 42 (2003) 5049.
[29] X. Fang, T.M. Anderson, Y. Hou, C.L. Hill, Chem. Commun. (2005) 5044.
[30] X. Fang, T.M. Anderson, C.L. Hill, Angew. Chem., Int. Ed. 44 (2005) 3540.
[31] B.S. Bassil, M.H. Dickman, U. Kortz, Inorg. Chem. 45 (2006) 2394.
[32] O.A. Kholdeeva, G.M. Maksimov, R.I. Maksimovskaya, M.P. Vanina, T.A. Trubitsina, D.Y. Naumov, B.A. Kolesov, N.S. Antonova, J.J. Carbo, J.M. Poblet, Inorg. Chem. 45 (2006) 7224.
[33] O.A. Kholdeeva, R.I. Maksimovskaya, J. Mol. Catal. A: Chem. 262 (2007) 7.
[34] M.N. Sokolov, E.V. Chubaroba, E.V. Peresypkina, A.V. Virovets, V.P. Fedin, Russ. Chem. Bull., Int. Ed. 56 (2007) 220.
[35] S. Yamaguchi, Y. Kikukawa, K. Tsuchida, Y. Nakagawa, K. Uehara, K. Yamaguchi, N. Mizuno, Inorg. Chem. 46 (2007) 8502.
[36] X. Fang, C.L. Hill, Angew. Chem., Int. Ed. 46 (2007) 3877.
[37] Y. Hou, X. Fang, C.L. Hill, Chem. Eur. J. 13 (2007) 9442.

[38] Y. Kikukawa, S. Yamaguchi, K. Tsuchida, Y. Nakagawa, K. Uehara, N. Mizuno, J. Am. Chem. Soc. 130 (2008) 5472.
[39] N. Leclerc-Laronze, J. Marrot, M. Haouas, F. Taulelle, E. Cadot, Eur. J. Inorg. Chem. (2008) 4920.
[40] B.S. Bassil, S.S. Mal, M.H. Dickman, U. Kortz, H. Oelrich, L. Walder, J. Am. Chem. Soc. 130 (2008) 6696.
[41] R. Copping, L. Jonasson, A.J. Gaunt, D. Drennan, D. Collison, M. Helliwell, R.J. Pirttijarvi, C.J. Jones, A. Huguet, D.C. Apperley, N. Kaltsoyannis, I. May, Inorg. Chem. 47 (2008) 5787.
[42] S.S. Mal, N.H. Nsouli, M. Carraro, A. Sartorel, G. Scorrano, H. Oelrich, L. Walder, M. Bonchio, U. Kortz, Inorg. Chem. 49 (2010) 7.
[43] C. Jahier, S.S. Mal, U. Kortz, S. Nlate, Eur. J. Inorg. Chem. (2010) 1559.
[44] R. Villanneau, D. Racimor, E. Messner-Henning, H. Rousselière, S. Picart, R. Thouvenot, A. Proust, Inorg. Chem. 50 (2011) 1164.
[45] M. Carraro, N. Nsouli, H. Oelrich, A. Sartorel, A. Sorarù, S.S. Mal, G. Scorrano, L. Walder, U. Kortz, M. Bonchio, Chem. Eur. J. 17 (2011) 8371.
[46] C.N. Kato, A. Shinohara, K. Hayashi, K. Nomiya, Inorg. Chem. 45 (2006) 8108.
[47] Y. Saku, Y. Sakai, A. Shinohara, K. Hayashi, S. Yoshida, C.N. Kato, K. Yoza, K. Nomiya, Dalton Trans. (2009) 805.
[48] K. Nomiya, Y. Saku, S. Yamada, W. Takahashi, H. Sekiya, A. Shinohara, M. Ishimaru, Y. Sakai, Dalton Trans. (2009) 5504.
[49] Y. Saku, Y. Sakai, K. Nomiya, Inorg. Chem. Commun. 12 (2009) 650.
[50] Y. Saku, Y. Sakai, K. Nomiya, Inorg. Chim. Acta 363 (2010) 967.
[51] W. Zhang, S.-X. Liu, C.-D. Zhang, R.-K. Tan, F.-J. Ma, S.-J. Li, Y.-Y. Zhang, Eur. J. Inorg. Chem. (2010) 3473.
[52] A.S. Assran, S.S. Mal, N.V. Izarova, A. Banerjee, A. Suchopar, M. Sadakane, U. Kortz, Dalton Trans. 40 (2011) 2920.
[53] M.N. Sokolov, N.V. Izarova, E.V. Peresypkina, A.V. Virovets, V.P. Fedin, Russ. Chem. Bull., Int. Ed. 58 (2009) 507.
[54] M.N. Sokolov, N.V. Izarova, E.V. Peresypkina, D.A. Mainichev, V.P. Fedin, Inorg. Chim. Acta 362 (2009) 3756.
[55] A. Tézé, G. Hervé, Inorg. Synth. 27 (1990) 89.
[56] G.M. Sheldrick, Acta Crystallogr., Sect. A 46 (1990) 467.
[57] G.M. Sheldrick, SHELXL-97 Program for Crystal Structure Refinement, University of Göttingen, Göttingen, Germany, 1997.
[58] G.M. Sheldrick, SADABS, University of Göttingen, Göttingen, Germany, 1996.
[59] I.D. Brown, D. Altermatt, Acta Crystallogr., Sect. B 41 (1985) 244.
[60] I.D. Brown, R.D. Shannon, Acta Crystallogr., Sect. A 29 (1973) 266.
[61] I.D. Brown, Acta Crystallogr., Sect. B 48 (1992) 553.
[62] I.D. Brown, J. Appl. Crystallogr. 29 (1996) 479.